CHAPTER-5

RESULTS AND DISCUSSIONS

This chapter contains the results and their interpretation of

(1) Adsorption-desorption studies for recovery of naringin from following three variations of kinnow peels
   a) Fresh peels
   b) Preharvest dropped peels
   c) Dry peels

   on two different resins Indion PA-500 and Indion PA-800

(2) Adsorption-desorption studies for recovery of naringin from fresh peels on regenerated resins PA-500 and PA-800

(3) Pectin extraction studies from fresh dropped, and dry kinnow peel boiled water remainig after adsorption of naringin in column

Therefore in all, the following eight systems have been encountered, for which the studies are carried out for adsorption-desorption followed by pectin extraction.

System 1 : Fresh peels with resin PA-500

System 2 : Fresh peels with resin PA-800

System 3 : Dropped peels with resin PA-500

System 4 : Dropped peels with resin PA-800

System 5 : Dry peels with resin PA-500

System 6 : Dry peels with resin PA-800

System 7 : Fresh peels with regenerated resin PA-500

System 8 : Fresh peels with regenerated resin PA-800

5.1. Adsorption-Desorption studies of naringin with fresh peels on Resin PA-500 (System 1)

The naringin content of fresh kinnow peel boiled water (extracts) from the three years (2012, 2013, and 2014) samples was determined and was found to be 0.810, 0.780, and 0.750 kg/m^3 respectively.

5.1.1. Adsorption equilibrium studies (System 1)

The adsorption equilibrium studies with kinnow peel boiled water were carried out as per the procedure described in the section 3.5.1. The amount of naringin picked up by the adsorbent was calculated by material balance. The data have been presented in Table B1.

The adsorption equilibrium experimental data were correlated by using Langmuir, Freundlich, Redlich–Peterson, Dubinin–Radushkevich, and Toth isotherms and their parameters were evaluated and presented in Table 5.1. The isotherms for adsorption of naringin from fresh KPBW on resin PA-500 for the year 2012 are shown in Figure 5.1. The charctersticts and significance of the mentioned adsorbtion isotherms are discussed in section 4.2.1. The mean free energy of adsorption was estimated using the Dubinin–Radushkevich isotherm constants. It was in the range of 2-4 (kJ mol^{-1}) signifying the occurrence of physical adsorption, which is true in our case because no chemical reaction is involved in the naringin adsorption on the non-ionic adsorbent.

Among the above mentioned isotherms the Langmuir, Freundlich and Dubinin–Radushkevich isotherms fit better than the other isotherms to the observed data as evidenced from R^2 values. The Freundlich isotherm has validity in the limited range of concentrations, Dubinin–Radushkevich is the three parameter model and requires more calculations. Langmuir adsorption isotherm is simple two parameter model and has highest R^2 values amongst these. Therefore Langmuir isotherms have been used for correlating the adsorption equilibrium data of all the systems studied.

The Langmuir isotherms for naringin adsorption from fresh KPBW on resin PA-500 for the data of the three years are presented in Figure 5.2. It was found, the maximum naringin that can be picked up by resin PA-500 from fresh KPBW (calculated from Langmuir adsorption isotherm constants) was 0.145, 0.179, and 0.138 kg per kg of dry resin respectively for the years 2012, 2013 and 2014. The amount of naringin picked up by the resin does not much depend on the concentration of naringin in peel boiled water.

Table 5.1: Different isotherm parameters for adsorption of naringin from fresh KPBW on resin PA-500

Langmuir	Year	a	b	R^2	
	2012	0.220	1.574	0.963	
	2013	0.256	1.432	0.911	
	2014	0.211	1.528	0.941	
Freundlich		K_f	1/n	R^2	
	2012	0.092	0.601	0.938	
	2013	0.107	0.586	0.881	
	2014	0.089	0.584	0.904	
Redlich-Peterson		K_R	a_R	β	R^2
	2012	2.087	21.77	0.436	0.910
	2013	1.705	13.94	0.412	0.862
	2014	0.972	10.15	0.505	0.872
Dubinin-Radushkevich		q_D	B_D	E	R^2
	2012	0.095	0.055	3.015	0.937
	2013	0.117	0.057	2.941	0.876
	2014	0.092	0.056	2.979	0.924
Toth		A	B	D	R^2
	2012	0.666	1.079	0.365	0.911
	2013	4.176	1.372	0.239	0.861
	2014	2.010	1.073	0.231	0.873

However, to know the thermodynamic parameters, the equilibrium studies were carried out at three different temperatures 303, 313 and 323 K. The results are shown in Figure 5.3 and Table B2.

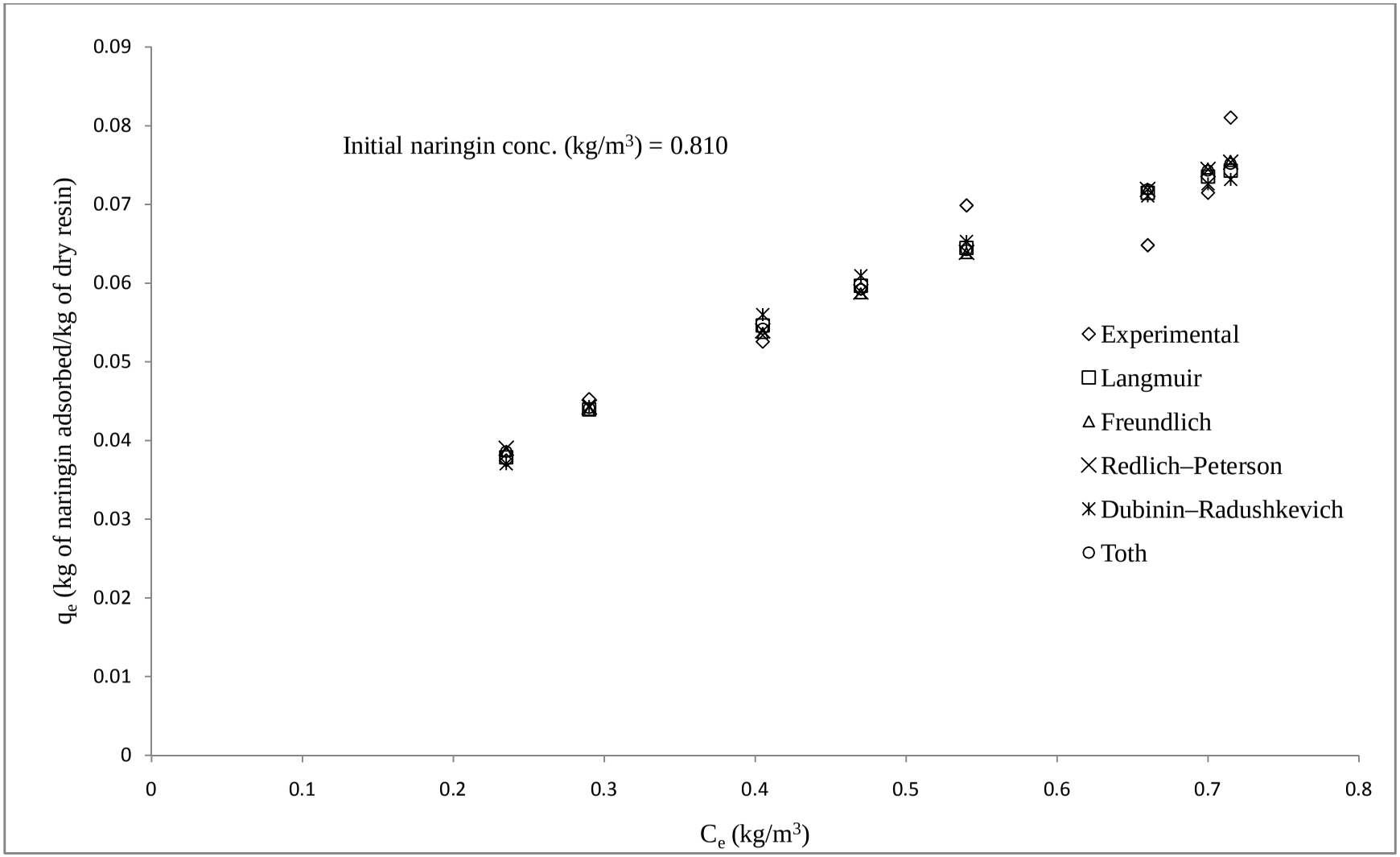

Figure 5.1: Comparison of various adsorption isotherms with experimental data for adsorption of naringin on resin PA-500 from fresh KPBW for the year 2012 (system 1)

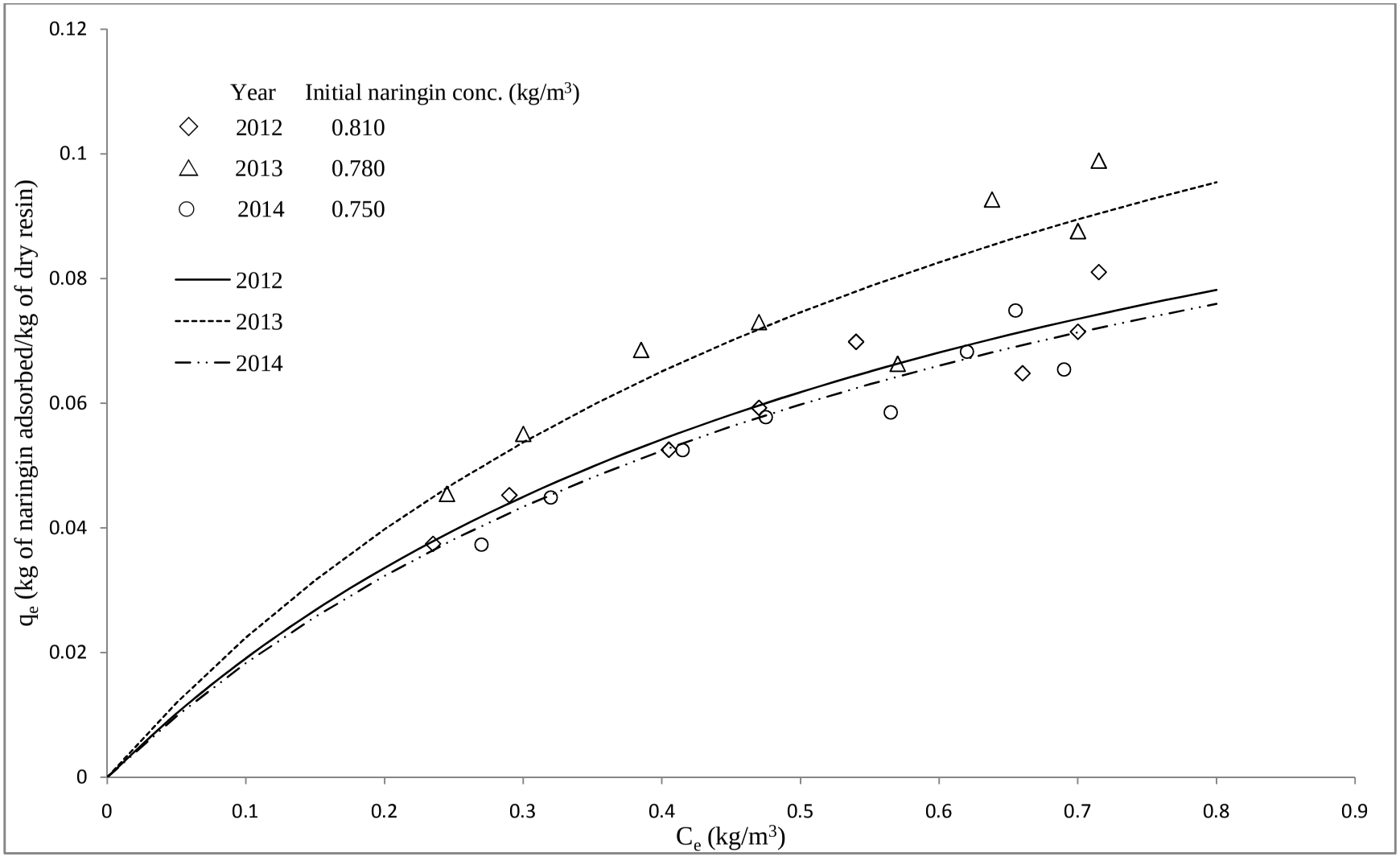

Figure 5.2: Adsorption equilibrium studies with fresh KPBW on resin PA-500 in different years (system 1)

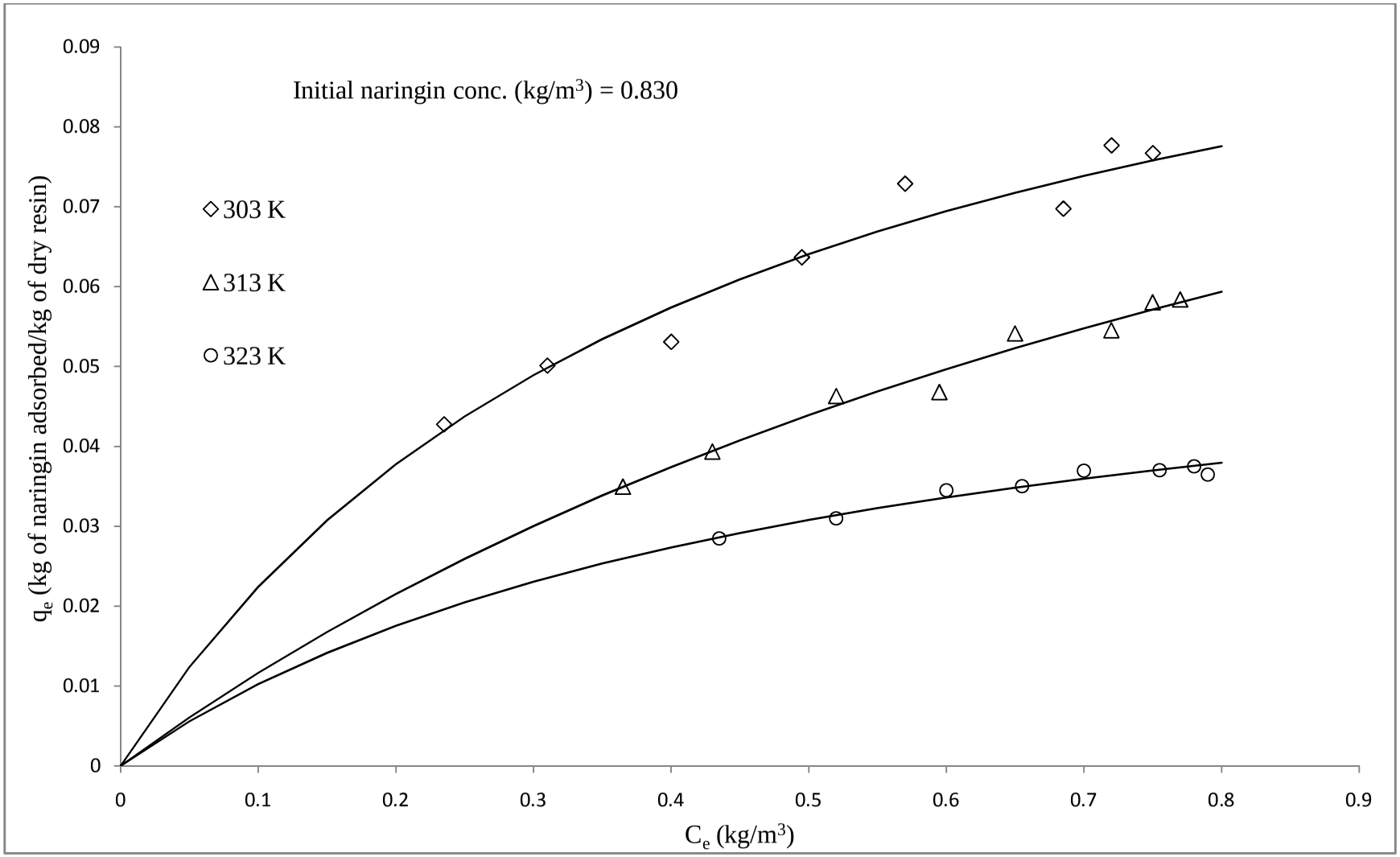

Figure 5.3: Effect of temperature on adsorption of naringin from fresh KPBW on PA-500 (system 1)

From Figure 5.3, it is evident that the adsorption of naringin on resin PA-500 decreases with the rise in temperature, due to exothermic nature of the sorption process and greater mobility of the molecules at elevated temperature.

The spontaneity of a process can be identified by thermodynamic parameters such as enthalpy change (ΔH), free energy change (ΔG) and entropy change (ΔS). The Van't Hoff plots of $\ln(K_{a/d})$ versus 1/T (Figure 5.4) are found to be linear, and ΔH and ΔS values are calculated from the intercept and slope of the plot. The values of the thermodynamic parameters for the three operating temperatures are presented in Table 5.2.

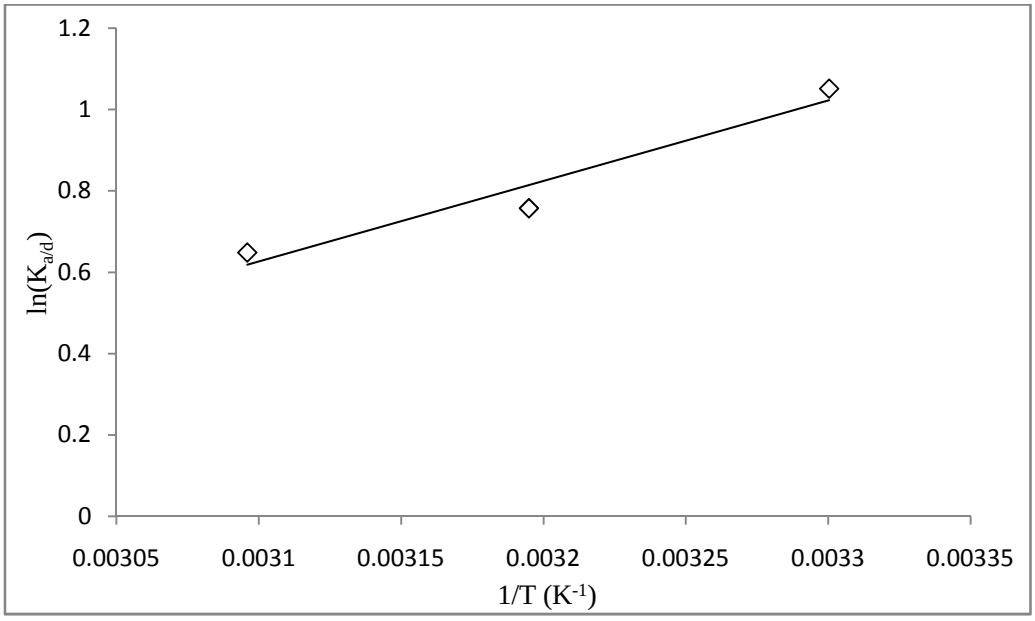

Figure 5.4: The Van't Hoff plot of $\ln(K_{a/d})$ versus 1/T for the resin PA-500 (system 1)

Table 5.2: Thermodynamic parameters for adsorption of naringin on resin PA-500 from fresh KPBW

S.No	Temp (K)	ΔS (kJ/mol K)	ΔH (kJ/mol)	ΔG (kJ/mol)	R^2 of linear plot between $\ln(K_{a/d})$ vs 1/T
1	303	-4.580	-16.453	-2.575	0.943
2	313			-2.117	
3	323			-1.652	

The negative values of ΔH confirmed the exothermic nature of adsorption process. Since ΔH and ΔS both are negative and temperatures involved are low; therefore the process of adsorption of naringin on the resin PA 500 is spontaneous.

The change in free energy for physical adsorption is typically in the range of -20 to 0 kJ mol^{-1} (Jaycock, 1981). The changes in free energy of adsorption for the resin PA-500 was estimated to be less than 0 kJ/mol, indicating an occurrence of the physical adsorption process. The lower values of the free energy also indicate the feasibility of the adsorption process. The values obtained in our case are in the same range as reported for Ginsenoside adsorption on XAD-16 (Barkakati *et al.* 2010).

5.1.2. Adsorption kinetic studies (System 1)

The adsorption kinetic studies were carried out as per the procedure described in the section 3.5.2.

Reproducibility test:

A set of two kinetic runs (1a, 1b) under almost similar conditions was carried out to establish reproducibility. The kinetic data for reproducibility test are given in Table B3 and shown in Figure 5.5. From the Figure 5.5, It is evident the data are reproducible within experimental limitations.

In adsorption kinetic studies four to five runs were carried out every year by varying the mass of the resin. The concentration of naringin in the solution (KPBW) as a function of time during adsorption for various amounts of resin is presented in Figures 5.6-5.8 for the years 2012, 2013, and 2014. The data obtained in these experiments are given in Tables B4 (a-c). It may be observed that the rate of change in concentration of a solution is more when the mass of the resin used is more. It is as expected; this is due to increase of surface area of adsorbent per unit volume of KPBW solution. Almost more than 80% adsorption takes place in first 6 h in all runs. Adsorption of naringin increased with contact time.

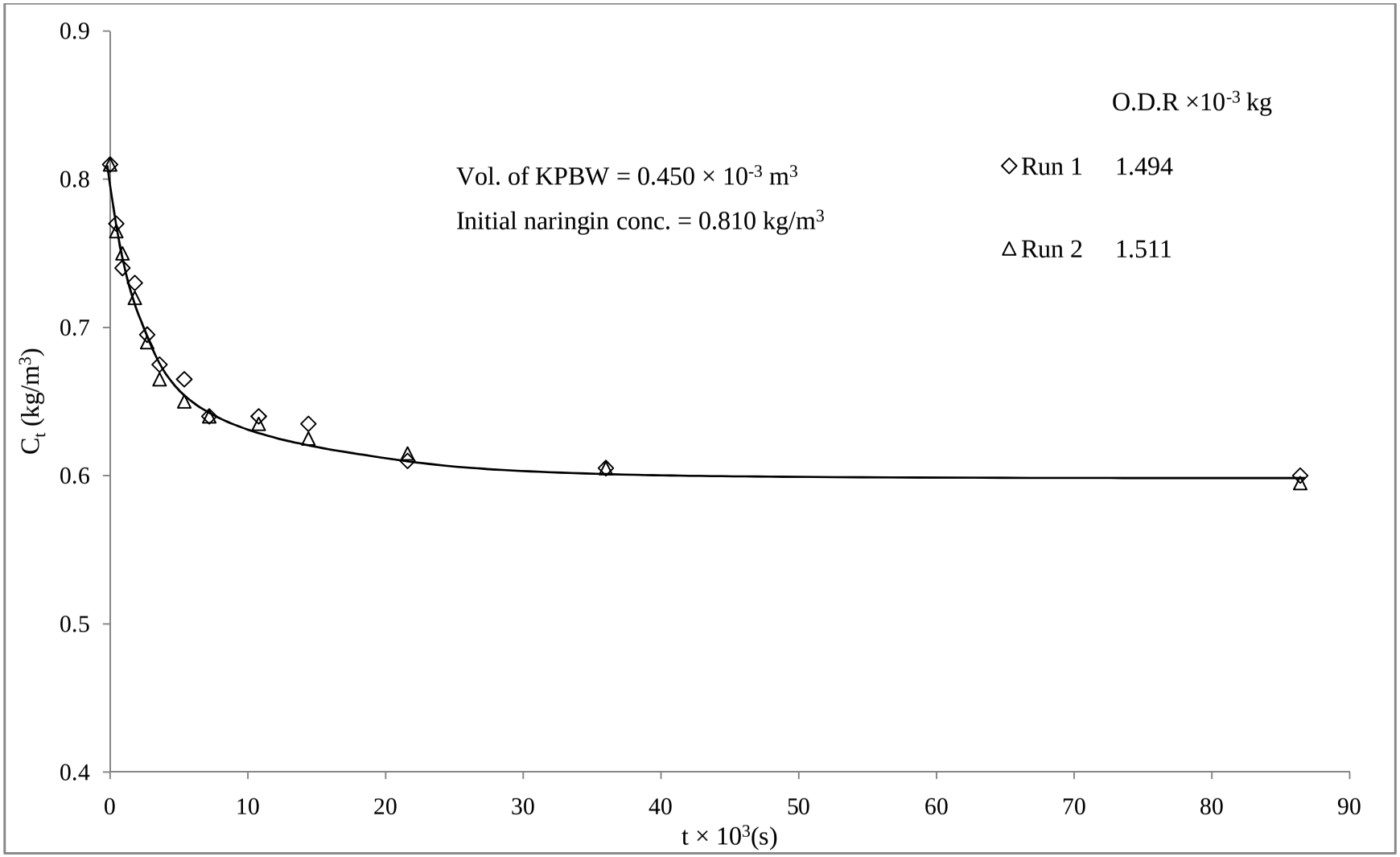

Figure 5.5: Adsorption of naringin on adsorbent PA-500 from fresh KPBW: kinetic studies, for reproducibility test (system 1)

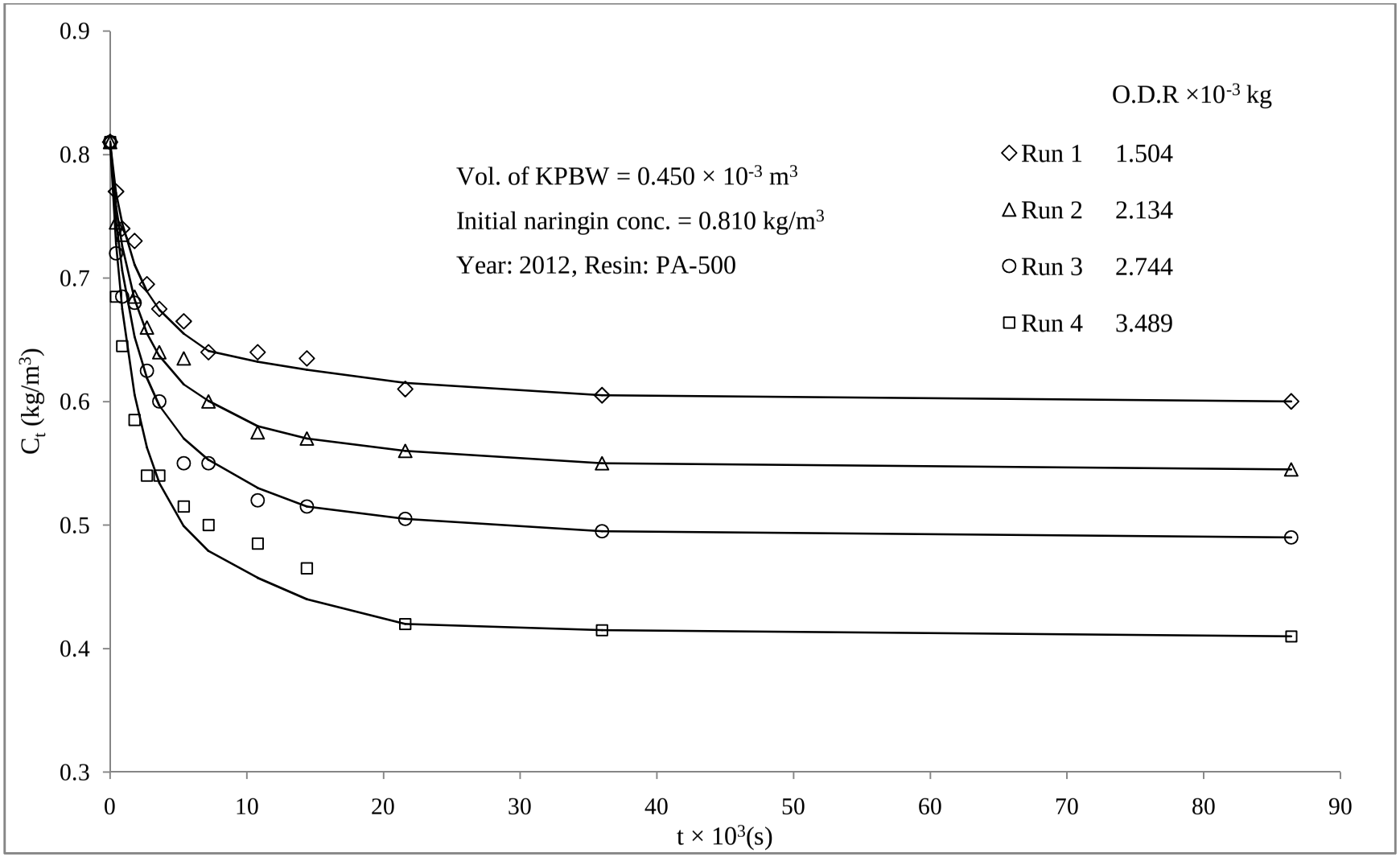

Figure 5.6: Kinetic studies for adsorption of naringin on the resin PA-500 from fresh KPBW for the year 2012, C_t *vs* t (system 1)

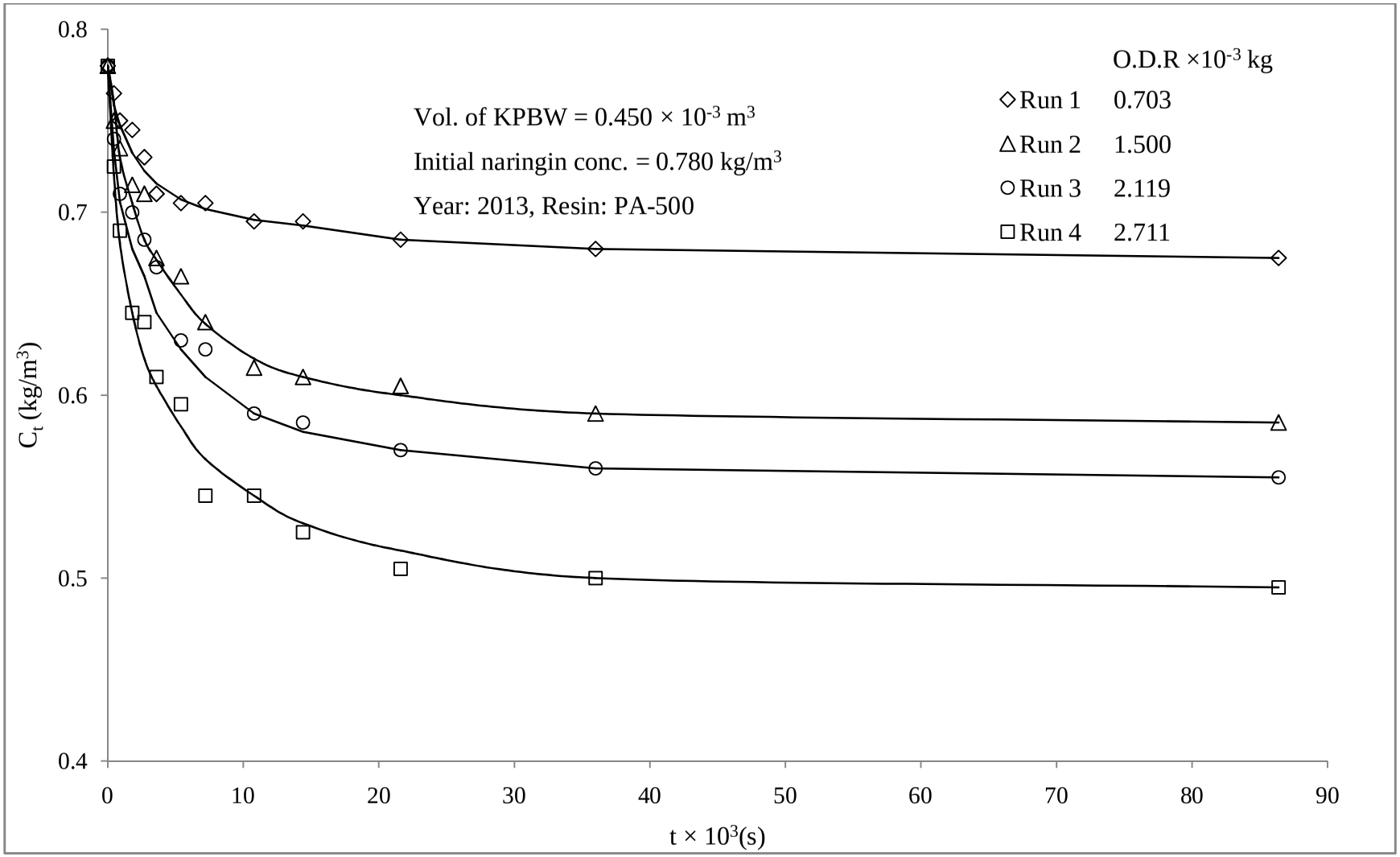

Figure 5.7: Kinetic studies for adsorption of naringin on the resin PA-500 from fresh KPBW for the year 2013, C_t *vs* t (system 1)

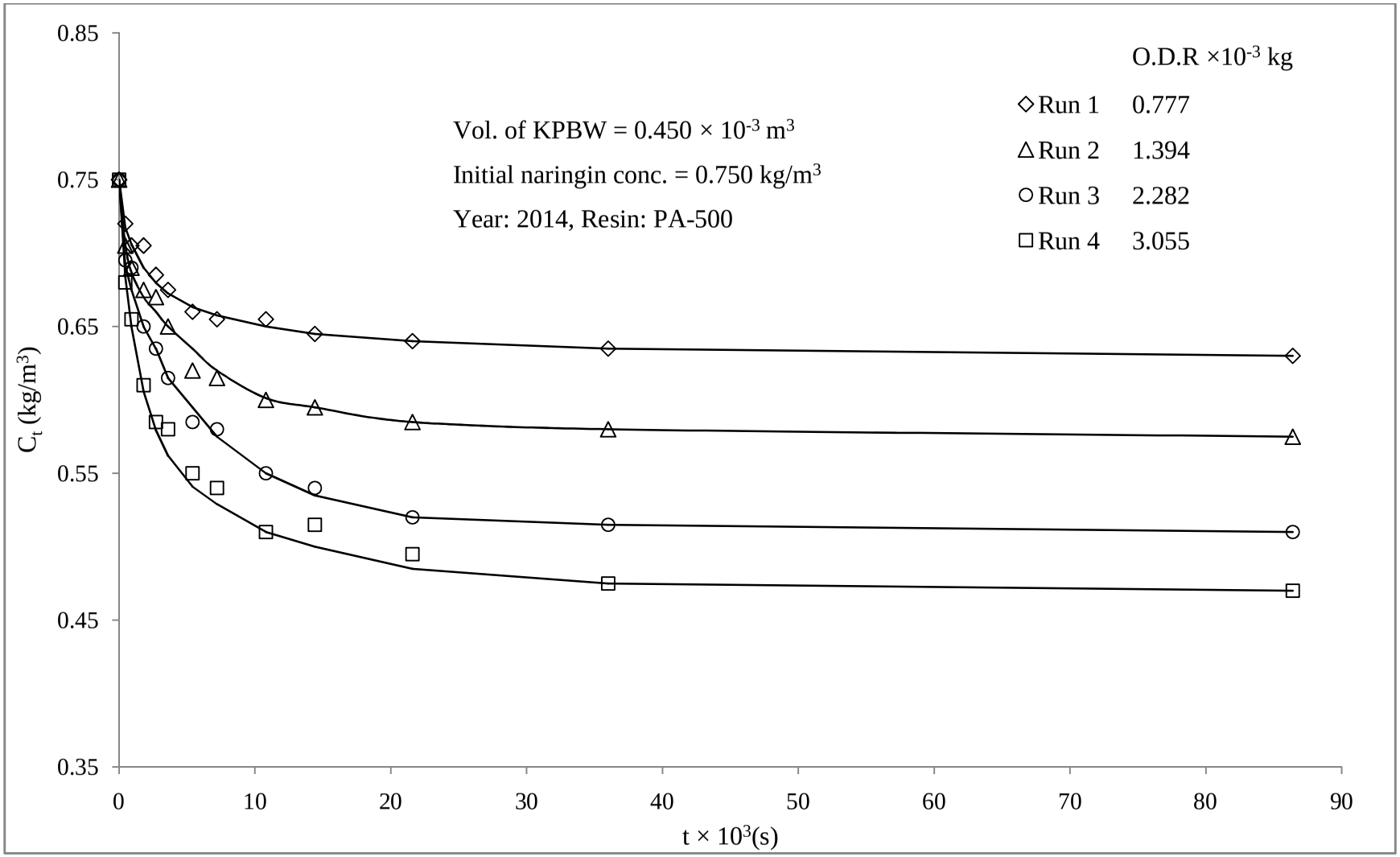

Figure 5.8: Kinetic studies for adsorption of naringin on the resin PA-500 from fresh KPBW for the year 2014, C_t *vs* t (system 1)

Modelling of kinetic data:

The adsorption kinetics was analysed using a series of rate equations like first-order rate equation (Lagergren, 1898), second-order rate equation (Ho and McKay, 1998), Bangham's model (Aharoni *et al.* 1979), Elovich kinetic equation (Roginsky and Zeldovich, 1934), Weber's kinetic diffusion model or the intra-particle diffusion kinetic equation (Weber and Morris, 1963), Boyd's Diffusivity model (Boyd *et al.* 1947) and Modified adsorption shell model (Singh *et al.* 2008) as per the procedure described in the section 4.3.1.

Lagergren plot is drawn between $\ln(q_e - q_t)$ vs time (t) for adsorption data of the resin PA-500 with fresh peels (system 1) of the year 2012 and shown in Figure 5.9. The values of the first order rate constant k_f, naringin picked up by resin at equilibrium (q_e) calculated from intercept are tabulated in Table 5.3. The calculated q_e and experimental q_e values are widely different, so the adsorption of naringin on PA-500 resin does not fit this equation.

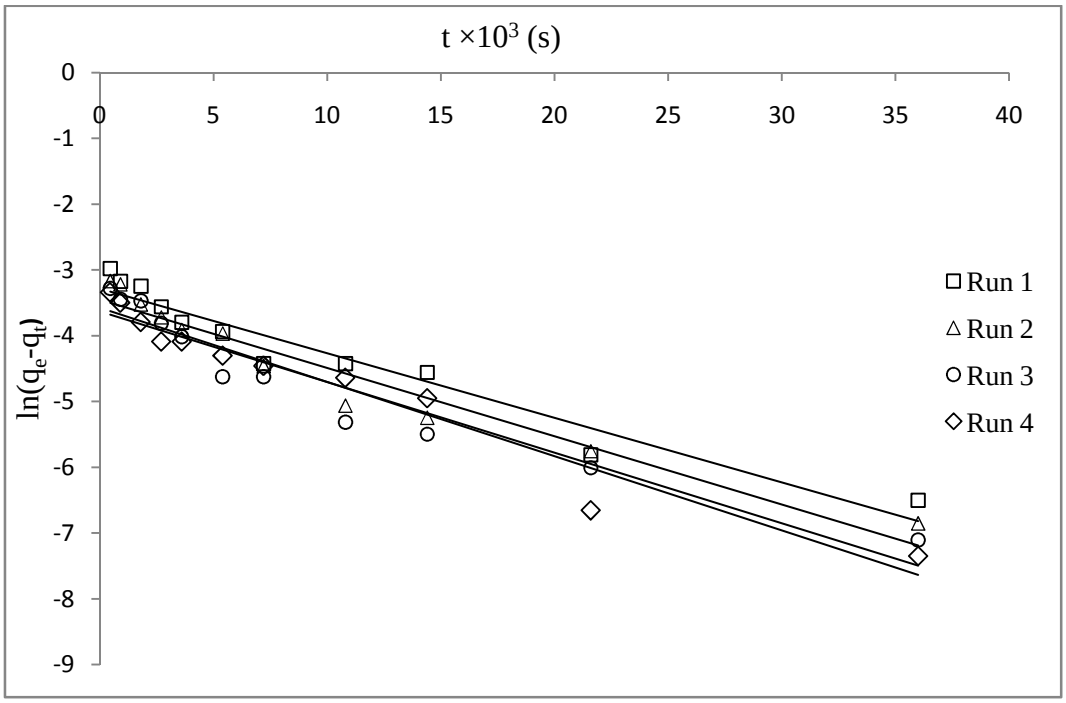

Figure 5.9: Lagergren plot $\ln(q_e - q_t)$ *vs time*(t) for adsorption of naringin from fresh KPBW on resin PA-500 (year 2012) (system 1)

Table 5.3: Pseudo first and Pseudo second order kinetic parameters of adsorption of naringin on resin PA-500 from fresh peels for the year 2012

S. No	Run	q_e (kg/kg) (experimental)	Pseudo-first order			Pseudo-second order		
			k_f × 10^{-3} (s^{-1})	q_e (kg/kg) (calculated)	R^2	$k_s \times 10^{-2}$ ($kgkg^{-1}s^{-1}$)	q_e (kg/kg) (calculated)	R^2
1	1	0.062	0.098	0.037	0.940	0.650	0.064	0.999
2	2	0.055	0.103	0.031	0.944	0.841	0.057	0.999
3	3	0.052	0.107	0.026	0.924	1.091	0.053	0.999
4	4	0.051	0.113	0.028	0.951	1.092	0.052	0.999

The values of the second order rate constant k_s and the calculated values of the amount of naringin adsorbed per kg/ kg of dry resin at equilibrium (q_e) estimated using linear plots of t/q against time (t) are shown in Figure 5.10 Table 5.3 (for the year 2012) along with experimental q_e values for all runs.

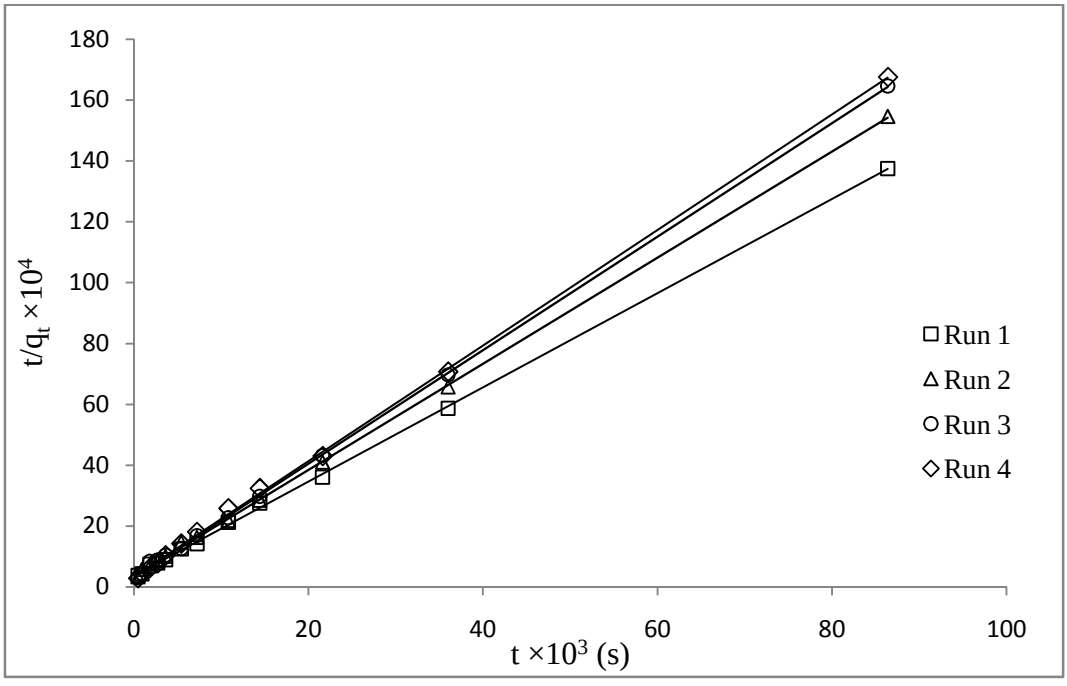

Figure 5.10: Pseudo second order plot t/q vs time (t) for adsorption of naringin from fresh KPBW on resin PA-500 (year 2012)

The values of the amount of naringin adsorbed by the resins calculated and experimental are very close to each other for the pseudo second order kinetic model, but k_s values are varying widely, which should be same for all runs. Hence, naringin adsorption on resin does not follow the pseudo-second-order kinetic model.

The adsorption kinetic data (for the year 2012) were analysed using the Bangham's equation. The non-linear plot (Figure 5.11) shows that the diffusion of the naringin into the pores of the adsorbents is not the only rate controlling step. The values of the Bangham equation parameters σ and k_o, and the correlation coefficients are given in Table 5.4. The correlation coefficients given by the Bangham's equation verified that the model did not fit the experimental data.

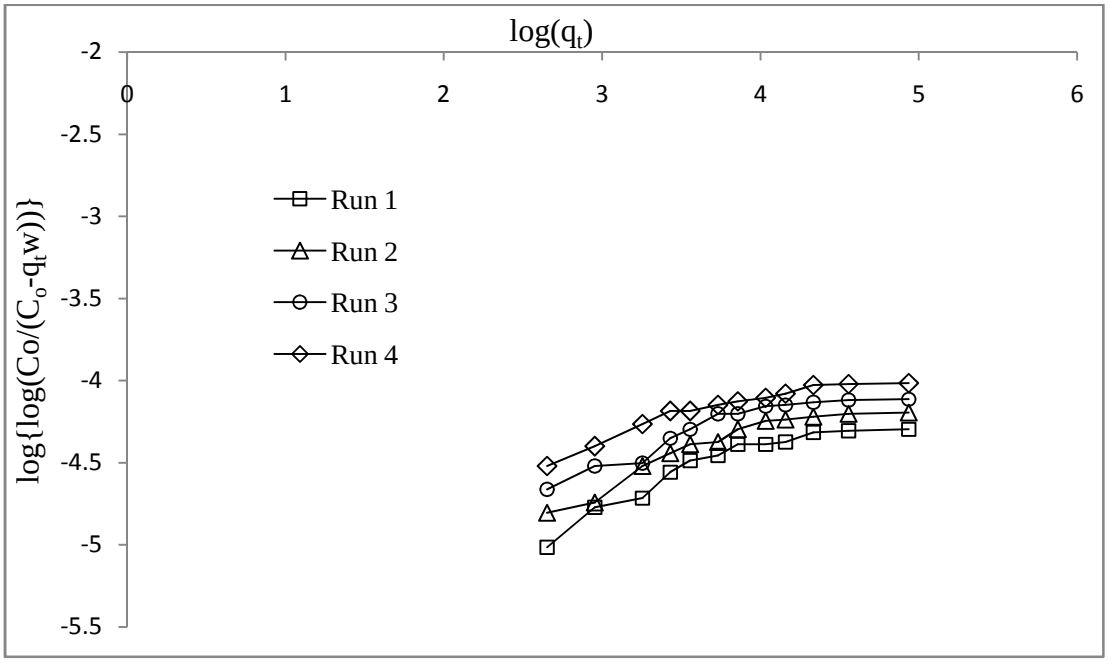

Figure 5.11: Bangham's plot for adsorption of naringin from fresh KPBW on resin PA-500 (year 2012)

Experimental data (for the year 2012) of naringin adsorption were analysed with the Elovich equation. Model parameters were determined using a linear plot drawn between C_t vs ln (t), shown in Figure 5.12 and are given Table 5.4. Although values of R^2 are quite high and the

Elovich equation applies to chemisorptions cases, it does not represent the physical situation. Therefore the equation is not suitable to our system.

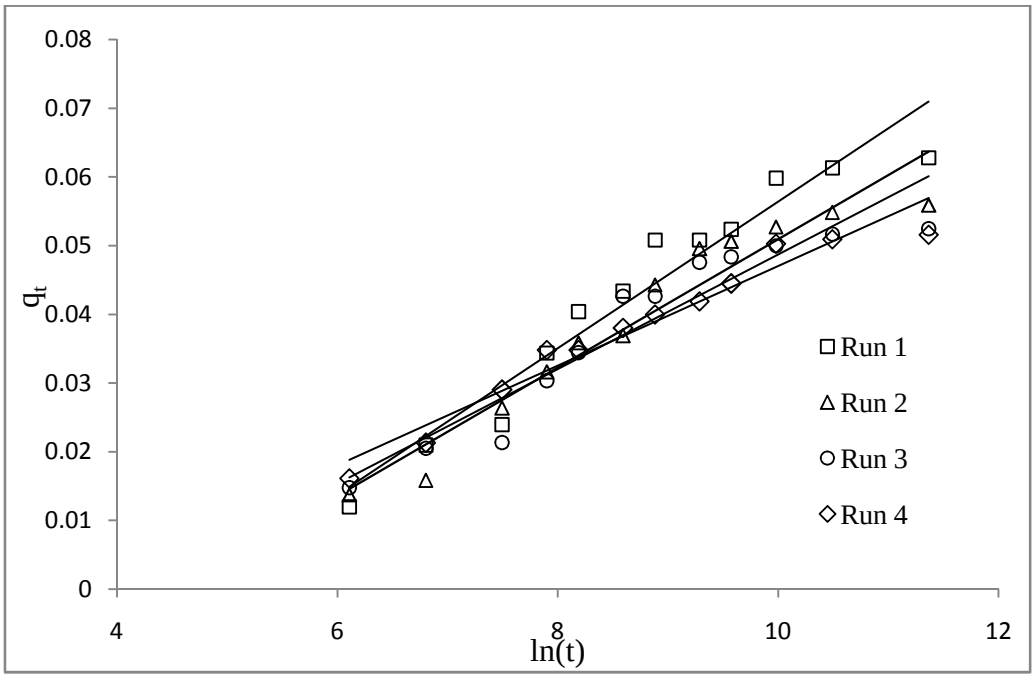

Figure 5.12: Elovich model plot for adsorption of naringin from fresh KPBW on resin PA-500 (year 2012)

Table 5.4: Bangham and Elovich model parameters for adsorption of naringin on resin PA-500 from fresh peels for the year 2012

S.No	Run	Bangham model			Elovich model		
		σ	k_o (m^3kg^{-1})	R^2	ω	α × 10^{-5}	R^2
1	1	0.310	0.005	0.857	93.74	9.56	0.941
2	2	0.290	0.005	0.868	107.0	9.91	0.935
3	3	0.259	0.005	0.859	119.9	13.2	0.906
4	4	0.220	0.007	0.885	137.8	21.5	0.952

The adsorption kinetic data were analysed by Weber's kinetic diffusion model (the intra-particle diffusion kinetic equation). If a biporous solid is considered to a homogeneous sphere, then for mass transfer micropore resistance will be negligible and Intra-particle

diffusion mechanism will be dominating. The plot q_t vs $t^{-1/2}$ is presented in Figure 5.13 for adsorption of naringin on the resin. It is observed that the lines do not pass through the origin, and multi-linear plots are depicting the influence of two or more rate controlling steps in the adsorption process. The positive value of intercept is indicative of some degree of boundary layer control. The first linear portion is for macropore or inter-particle diffusion and the second portion representing the micropore or intra-particle diffusion. The values of the intra-particle diffusion k_d and thickness of the boundary layer (I) were calculated and tabulated in Table 5.5. The values of R^2 are very small; therefore Weber kinetic diffusion model does not describe our system.

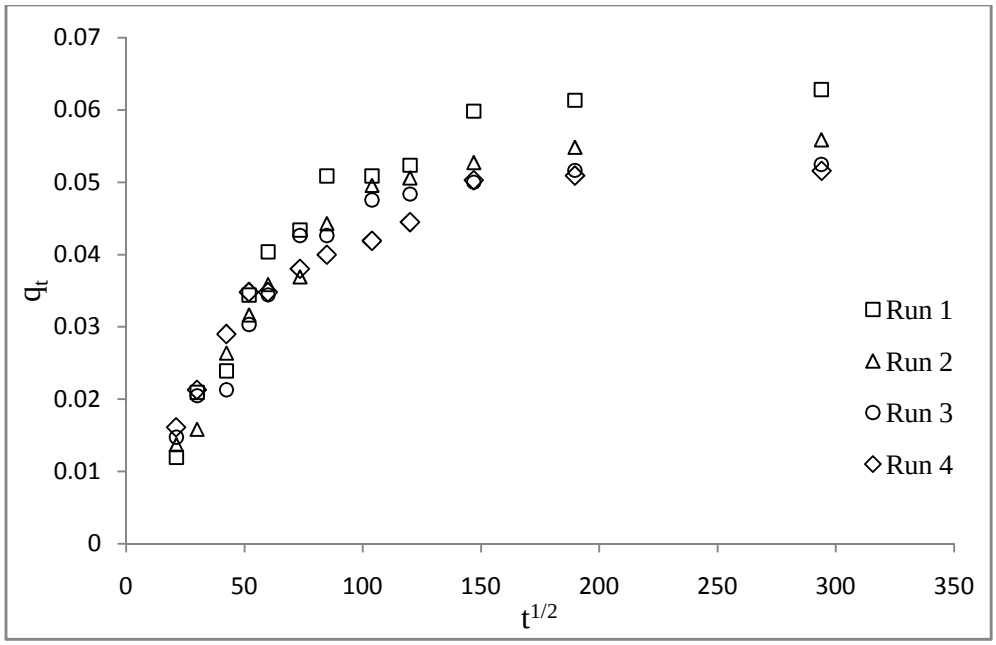

Figure 5.13: Weber's kinetic diffusion model plot for adsorption of naringin from fresh KPBW on resin PA-500 (year 2012)

The kinetic data were also analysed by using Boyd's Diffusivity model which is based on diffusion through the boundary liquid film, considering adsorption kinetics as a chemical phenomenon. The macropores may put negligible resistance to the solute diffusion in the pores and therefore micropore resistance will be controlling and hence the Boyds diffusivity model will be applicable to such cases, since size of the micropores is very small (1-10 μm

diameter each). A linear plot of $\left(1/1-u_t^2\right)$ vs time (t) is drawn and shown in Figure 5.14, where $u_t = q_t / q_e$. The pore diffusivities were calculated and in the range of 1.33-1.59×10^{-12} m^2/ s and tabulated in Table 5.5. This model takes into consideration only one pore diffusion. However, in macroporous bead, it is likely that micropore and macropore both diffusional resistances are present. Therefore this model does not useful in our case although it gives the almost same value of D_e.

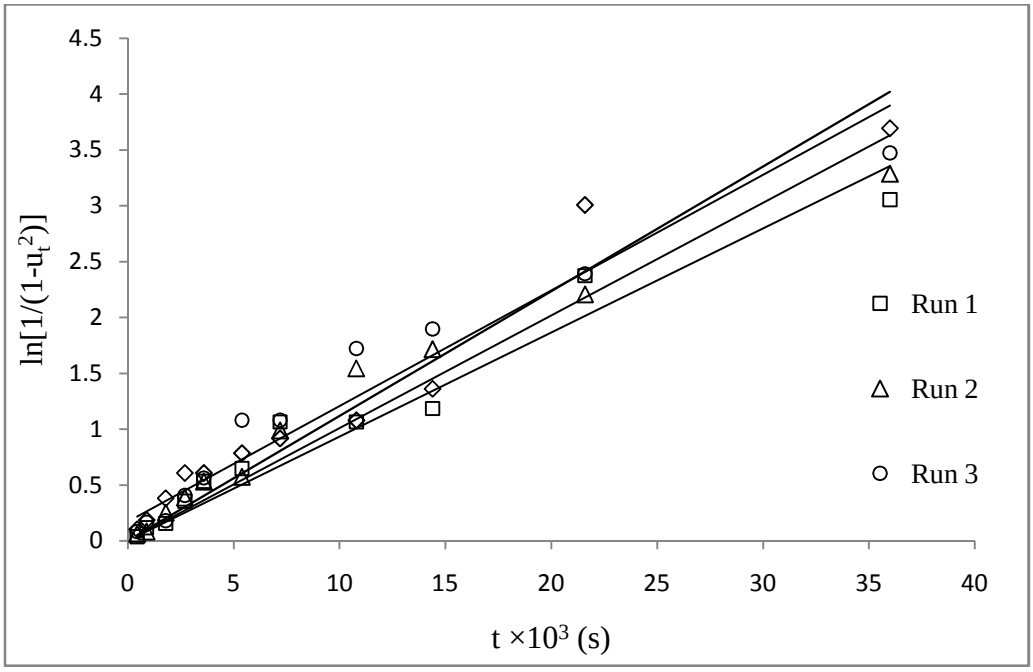

Figure 5.14: Boyd's Diffusivity model plot for adsorption of naringin from fresh KPBW on resin PA-500 (year 2012)

Table 5.5: Intra-particle diffusion and Boyd's diffusivity model parameters for adsorption of naringin on PA 500 with fresh peels for the year 2012

S.No	Run	Intra-particle diffusion model			Boyd's diffusivity model	
		I (kg/kg)	k_d × 10^{-3} (kg/kg $s^{-1/2}$)	R^2	D_e × 10^{-12} (m^2s^{-1})	R^2
1	1	0.024	0.177	0.681	1.33	0.948
2	2	0.023	0.154	0.667	1.44	0.951
3	3	0.024	0.135	0.630	1.56	0.916
4	4	0.025	0.121	0.696	1.59	0.943

Modified adsorption shell model:

As mentioned in the theory chapter in the section 4.3.1, the experimental kinetic data was analysed by modified adsorption shell model by Singh *et al.* (2008) and Singh *et al.* (2015). For this model correlating the equation is

$$\left[\frac{1}{(1-u_t)^{2/3}}-1\right] = \frac{2K\,D_P\,\varepsilon\,C_0}{5(1-\varepsilon)q_e R_P^2}t \qquad (4.26)$$

where the left-handed side is termed as $F_n(t)$

When both micropore and macropore resistances are comparable then the above equation will be applicable. The fractional saturation values obtained from Figures 5.6 to 5.8 were employed to calculate $F_n(t)$, and these were plotted against time (Figure 5.15). It was found that the data were lying on the straight line in most of the cases. Straight line passing through the origin should be obtained, and the slope would be $\frac{2K\,D_P\,\varepsilon\,C_0}{5(1-\varepsilon)q_e R_P^2}$

The slope for run1 (in the year 2012) was found to be 2.51×10^{-4} s.

Singh *et al.* (2008) estimated the diffusivity of naringin in aqueous solution using group contribution method (Perry and Green, 1984) and its numerical value was found to be 3.09×10^{-10} m^2/ s. The diffusivity of naringin in macropores of the resin (D_P), was taken to be one-third of the above value to consider the tortuosity of macropores in the resin using Wheeler equation (Helfferich, 1962). The same diffusivity value ($D_P = 1.032\times10^{-10} m^2/s$) has been used for diffusivity of naringin in KPBW. Although, it is likely to be lesser.

R_p the radius of the particle (bead) was taken from an average diameter of a number of particles. It was found to 0.375×10^{-3} m (for PA-500). The overall porosity ϵ has been taken equal to 0.39, as mentioned by the manufacturer.

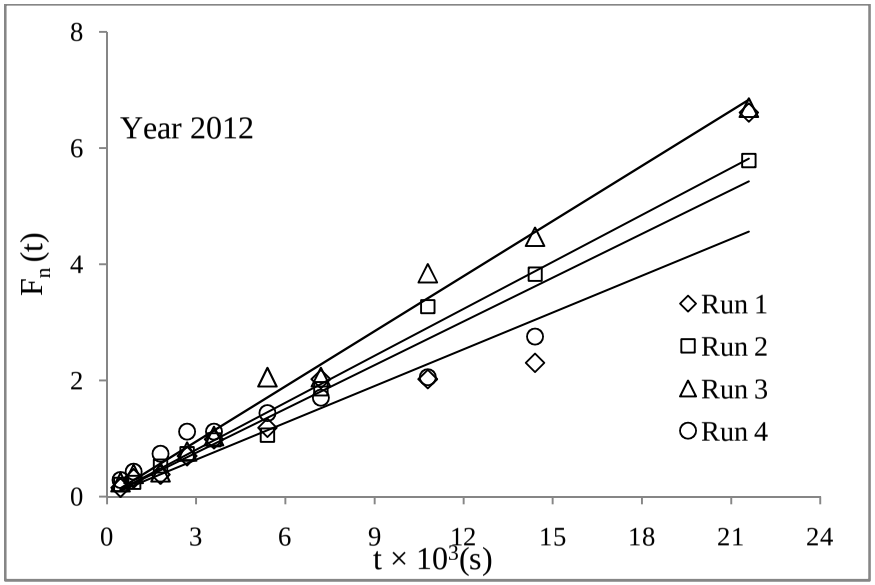

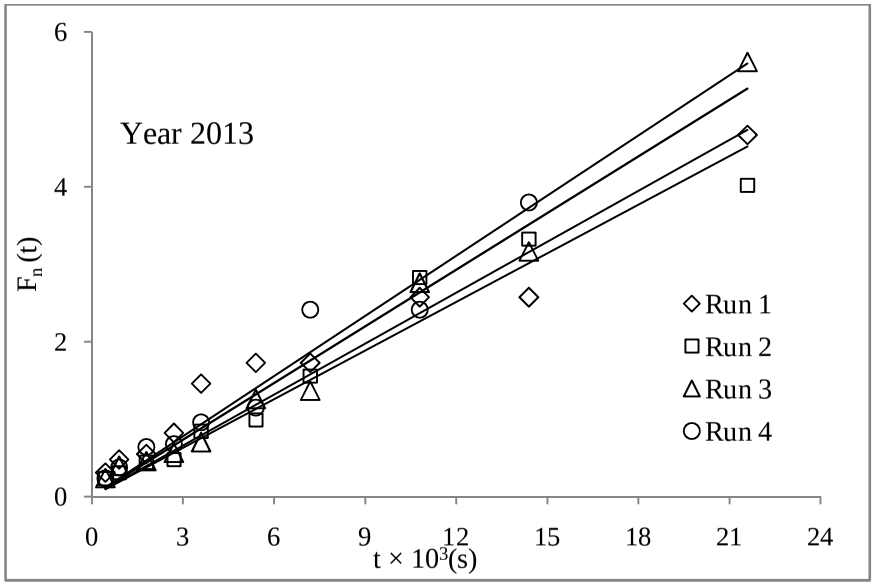

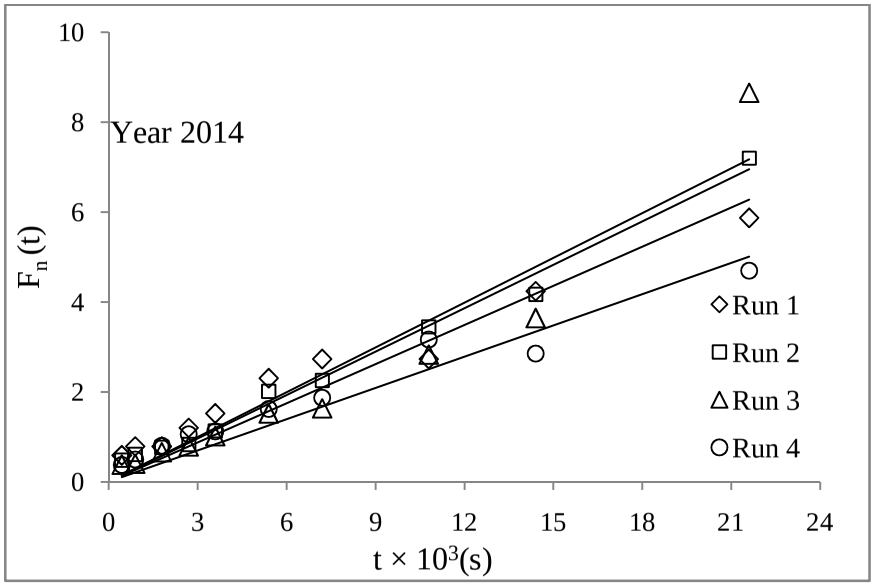

Fig. 5.15: Adsorption of naringin on adsorbent PA-500 from fresh KPBW: Kinetic Studies, F_n (t) vs t (system 1)

Substituting for the slope, $D_P = 1.032 \times 10^{-10} m^2/s$, ϵ = 0.39, C_o = 0.810 kg/m^3, q_e = 62.81 kg/m^3, and R_p = 0.375×10^{-3} m; the value of parameter K was determined and found to be equal to 103.84.

From this value of K, the value of β was obtained using the expression

$$\log_{10} K = 1.357 \exp (0.207 \log_{10} \beta) \tag{4.25}$$

The value of β was found to be 81.8. The sample calculations are given in Appendix-I. It is notable that

$$\beta = \frac{3(1-\varepsilon) q_e D_c / r_c^2}{\varepsilon C_0 D_P / R_P^2} \tag{4.27}$$

$$\beta = \psi \frac{q_e}{C_0} \tag{4.28}$$

where $$\psi = \frac{3(1-\varepsilon) D_c / r_c^2}{\varepsilon D_P / R_P^2} \tag{4.29}$$

From the above value of β, the value of ψ was calculated by substituting the values of C_o and q_e in equation 4.28.

The value of ψ is 1.055. The value of D_c / r_c^2 calculated from this value of ψ is 1.65×10^{-4}/s. The detailed calculations are given in Appendix I.

Similar analysis and calculations were done for all runs, and the values of various parameters are tabulated in Table 5.6.

The value of ψ can be used to generate the kinetic data. The values of ψ are different in all runs although ψ should be same as it is characteristic of the absorbent-adsorbate system. The difference observed in the ψ values may be attributed for following reasons.

The initial experimental conditions are different for all the runs. During adsorption, solution concentration decreases and the kinetics of adsorption at the later period is likely to be different from the earlier period.

Table 5.6: Modified adsorption shell model parameters for system 1

$D_P = 1.032\times10^{-10}\, m^2/s, \varepsilon = 0.39,\ R_p = 0.375\times10^{-3}$ m

Year	Run	C_o kg/m^3	q_e kg/m^3	Slope × 10^{-4} (s^{-1})	K	β	ψ	$\frac{D_c}{r_c^2}$ × 10^{-4} (s^{-1})
2012	1	0.810	62.81	2.51	103.8	81.88	1.05	1.65
	2	0.810	55.87	2.69	98.94	72.88	1.05	1.65
	3	0.810	52.46	3.16	109.1	92.20	1.42	2.22
	4	0.810	51.57	3.59	121.8	119.2	1.87	2.92
2013	1	0.780	67.13	2.19	100.5	75.75	0.88	1.37
	2	0.780	58.47	2.09	83.54	48.01	0.64	1.00
	3	0.780	47.76	2.44	79.59	42.47	0.69	1.08
	4	0.780	46.27	3.40	107.5	89.09	1.50	2.34
2014	1	0.750	63.67	2.91	133.3	146.6	1.70	2.66
	2	0.750	53.25	3.22	123.4	123.0	1.70	2.67
	3	0.750	45.34	3.32	108.4	90.72	1.48	2.31
	4	0.750	39.76	2.32	66.42	26.57	0.49	0.77

As mentioned earlier that the function F_n considers three well-defined zones. In practical situations zones develops only after particular time. When the resin loading is higher, the microspheres of outer layers of the bead are exposed to the solution of initial composition, and there is a sharper drop in concentration. Also, it is likely the q_e values will be somewhat different for different layers.

It is also notable that the assumptions of infinite solution volume and rectangle boundary condition do not exactly hold, for which the equation (4.26) was developed.

The function $F_n(t)$ is calculated from u_t which is itself calculated from q_t and q_e, furthur these are calculated from solution concentration. The sensitivity of $F_n(t)$ is high to the values of u_t, for the value of $u_t >$ 0.75, function $F_n(t)$ becomes highly sensitive to even small changes in value of u_t. The wide variation of D_c / r_c^2 and ψ otherwise these should be same for a particular system, may be due to the above probable reasons. However, C_t vs t was generated in the following manner. Although the generation of kinetic data is discussed in the section 4.3.1. It is reproduced again here.

Generation of kinetic data

The experimental change in concentration for any run may be generated with following steps:

1. From the value of ψ, the value of β is calculated, $\beta = \psi \frac{q_e}{C_0}$, the experimental values of C_0 and q_e of that run need to be used.
2. From value of β, the value of K is calculated by relation

$$\log_{10} K = 1.357 \exp (0.207 \log_{10} \beta) \tag{4.25}$$

3. The value of K obtained in step (ii) is used to calculate the value of u_t by relation

$$u_t = 1 - \frac{1}{\left(1 + \frac{2}{5} \frac{K D_p \varepsilon C_0}{(1-\varepsilon) q_e R_p^2} t\right)^{3/2}} \tag{4.30}$$

4. From u_t, C_t was calculated by formula

$$C_t = C_o^{\mathrm{I}} - u_t (C_o^{\mathrm{I}} - C_e) \tag{4.31}$$

The concentration of naringin at the start of three distinct zones C_o^{I} (i.e. Modified adsorption shell model) is given by $C_o^{\mathrm{I}} = C_o - \frac{k q_e w}{V}$ (4.34)

where V is the volume of solution (KPBW).

The volume fraction of the shell is k = 0.064 for PA-500 as mentioned in the section 4.3.1.

The generated C_t (with a representative value of ψ = 1.578), as well as experimental data for run 1 are given in Table 5.7. The data were tested for significance of the mean difference, paired observation by t -test at a 5% level of significance, and it was found that the experimental and predicted data of the run do not differ significantly.

For all the runs of the system 1 the generated data C_t (with a representative value of ψ = 1.578) are shown by smooth curves, and experimental data are given for comparison in Figures 5.16 to 5.18.

It was observed that when predicted (generated) vs experimental values were drawn on the graph, straight lines were passing through the origin having slope near to 1.00. The data were tested for significance of the mean difference, paired observation by t -test at a 5% level of significance, and it was found that the experimental and predicted data for almost all the runs do not differ significantly. The summary of the statistics analysis values is given in Table 5.8.

Table 5.7: Adsorption kinetic data: C_t generated vs. C_t experimental (system 1), Run 1

t (sec)	C_t experimental	C_t generated
0	0.81	0.81
7.5	0.77	0.768
15	0.74	0.744
30	0.73	0.710
45	0.695	0.689
60	0.675	0.674
90	0.665	0.655
120	0.64	0.644
180	0.64	0.632
240	0.635	0.625
360	0.61	0.619
600	0.605	0.614
1440	0.6	0.611

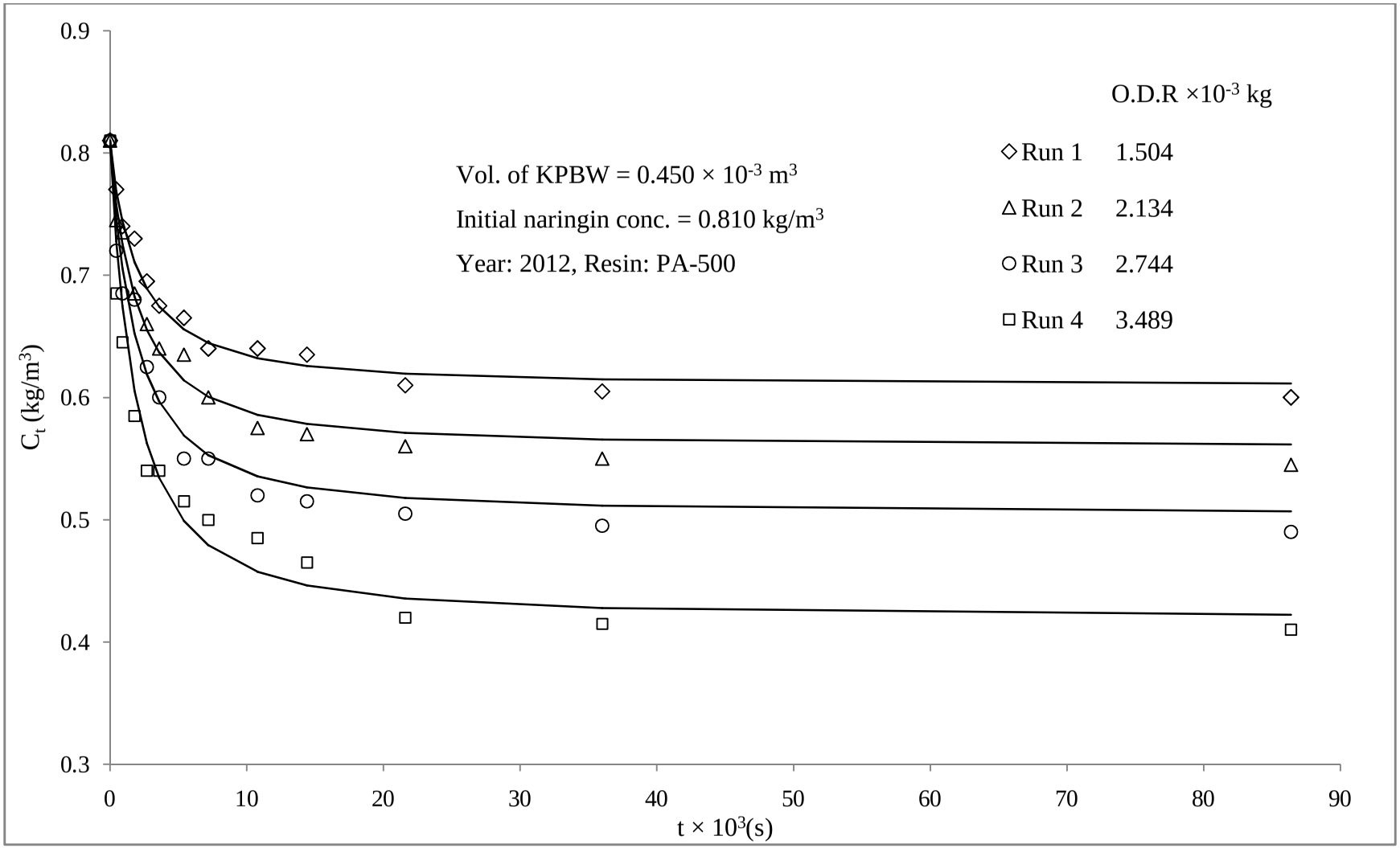

Figure 5.16: Adsorption of naringin on adsorbent PA-500 from fresh KPBW: kinetic studies, correlation of experimental data, C_t *vs t* (system 1, year 2012)

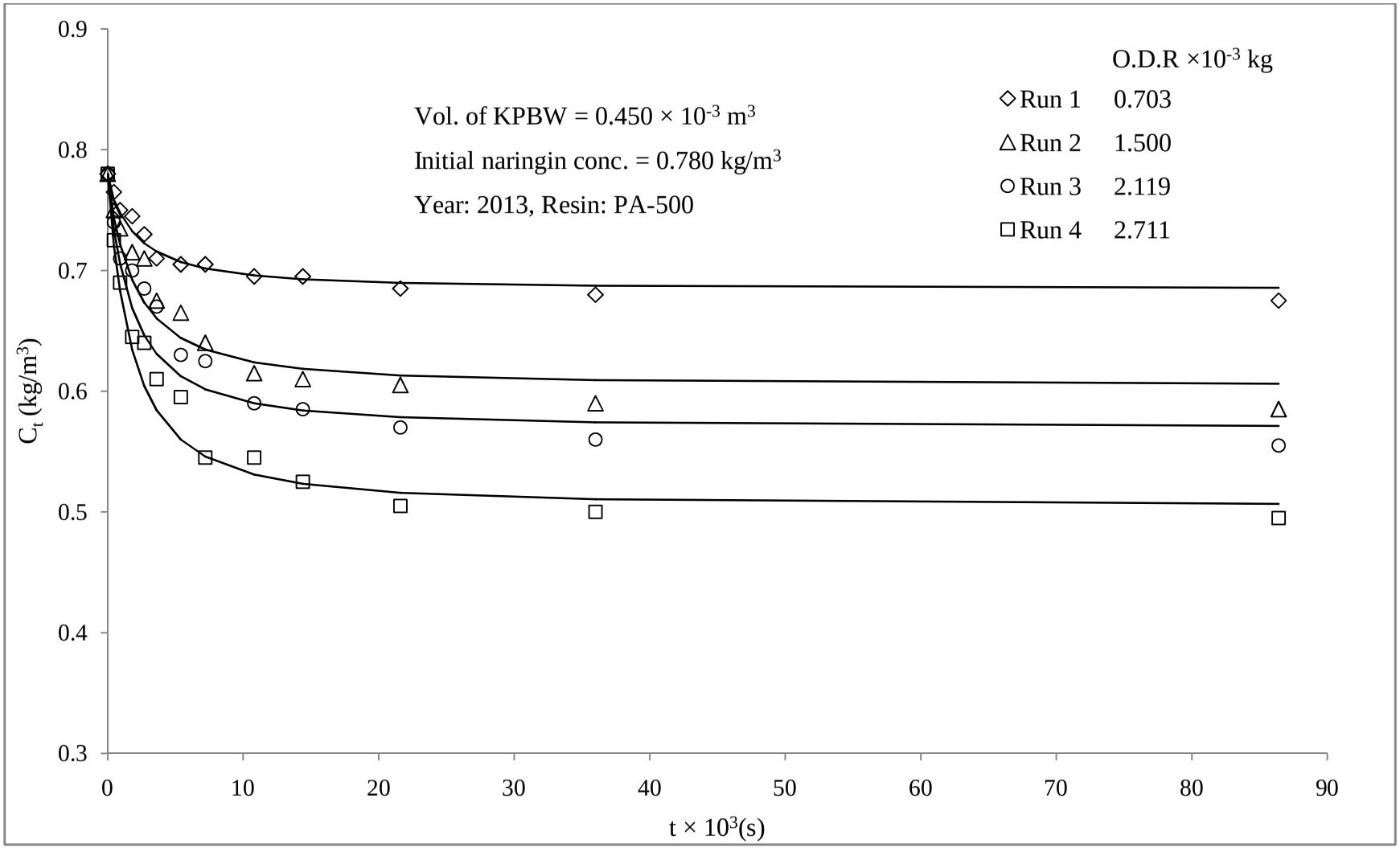

Figure 5.17: Adsorption of naringin on adsorbent PA-500 from fresh KPBW: kinetic studies, correlation of experimental data, C_t *vs t* (system 1, year 2013)

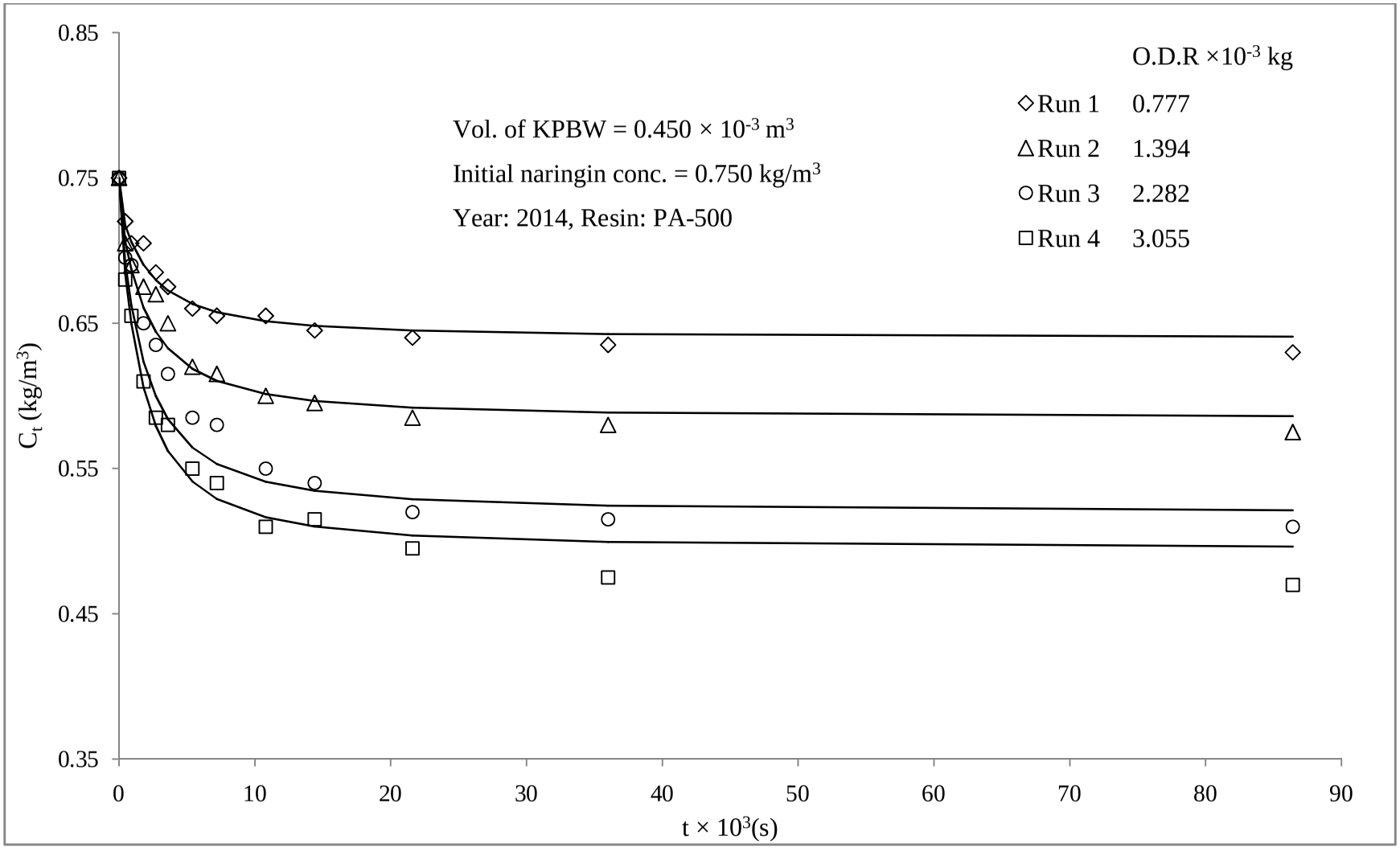

Figure 5.18: Adsorption of naringin on adsorbent PA-500 from fresh KPBW/: kinetic studies, correlation of experimental data, C_t *vs t* (system 1, year 2014)

Table 5.8: Statistical analysis for predicted and experimental values of C_t (system 1)

Year	Run	Slope C_{trep} vs. $C_{t\exp}$ passing through origin	R^2	t-Cri	t-Cal	Inference
2012	1	0.997	0.968	2.2009	0.4314	NSD
	2	1.003	0.968	2.2009	-0.8768	NSD
	3	1.014	0.963	2.2009	-2.0260	NSD
	4	1.013	0.952	2.2009	-0.8577	NSD
2013	1	0.999	0.923	2.2009	0.1316	NSD
	2	0.991	0.852	2.2009	0.8785	NSD
	3	0.982	0.899	2.2009	1.8155	NSD
	4	0.984	0.948	2.2009	1.7523	NSD
2014	1	1.000	0.93	2.2009	-0.1635	NSD
	2	0.994	0.926	2.2009	0.9528	NSD
	3	0.976	0.918	2.2009	0.9528	NSD
	4	1.000	0.951	2.2009	-4.8167	SD

*NSD- No Significance difference, SD- Significance difference

From the above, it is evident that observed kinetic data of all runs for system 1 could be correlated well by modified adsorption shell model. The same approach that is modified adsorption shell model has been used to correlate the kinetic data of all other systems studied because it represents more realistic picture than the other approaches mentioned earlier.

Comparison of adsorption kinetic studies:

The kinetics of adsorption of naringin from kinnow peel boiled water for different years with the almost same weight of resin have been compared, and it is shown in Figure 5.19. Although initial concentrations of naringin are different in all three years also KPBW is a multi-component system and composition of peel varies with time of harvest, the storage time of fruit, place and other climate conditions and hence the composition of KPBW also vary; therefore comparison has limited validity.

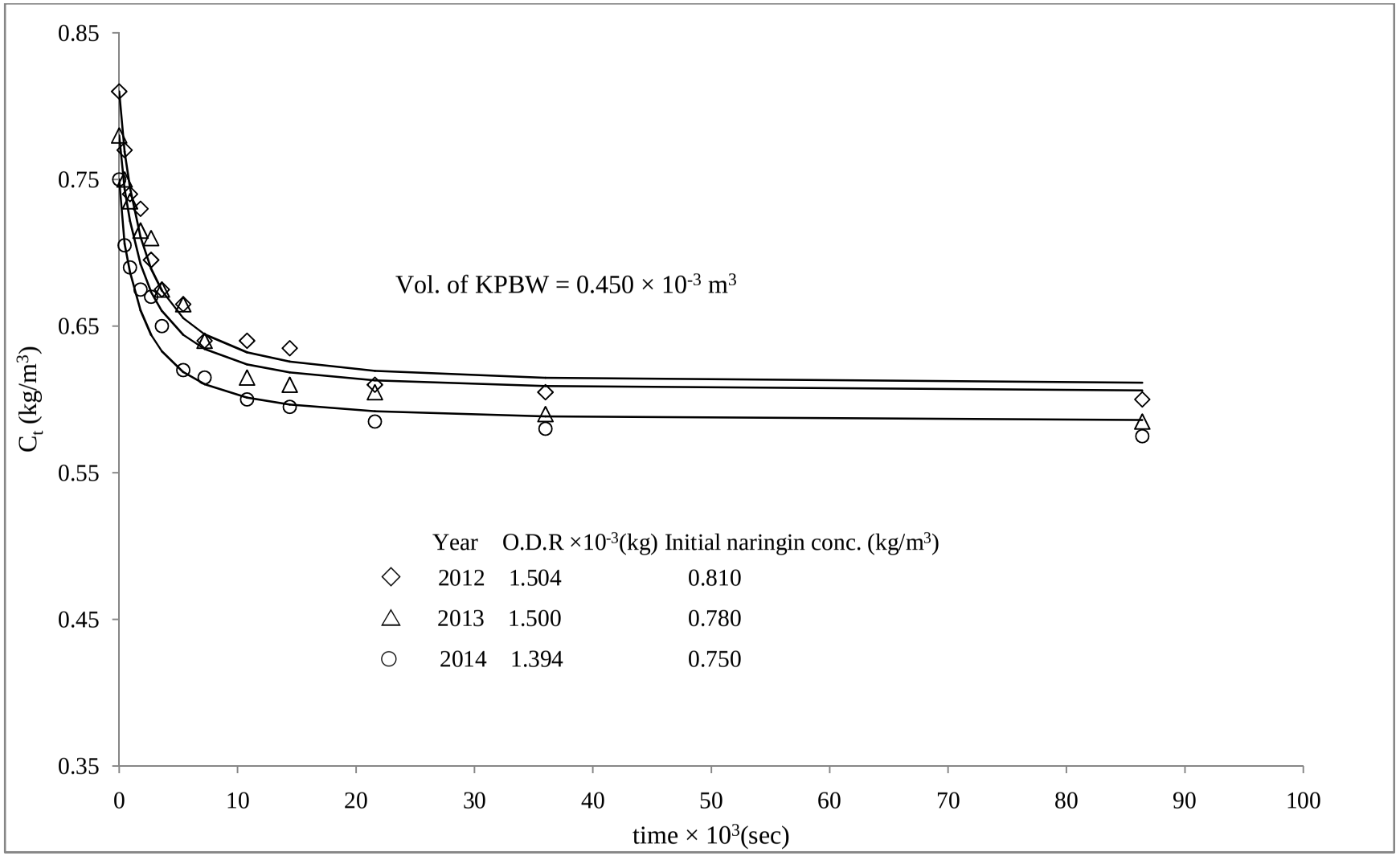

Figure 5.19: Comparison of naringin adsorption kinetic studies on the resin PA-500 from fresh KPBW with year (system 1), C_t *vs t*

From Figure 5.9, it is observed in 2013 and 2014 data when initial concentrations are similar the data are almost same. So the year of collection of peels has little effect on the kinetics of adsorption of naringin from KPBW.

5.1.3. Fixed bed column adsorption studies (System 1)

The adsorption column studies were carried out as per the procedure described in the section 3.5.3. Column studies are performed to make a breakthrough curve and helpful in scale up because these give realistic situation.

Breakthrough curves can explain the efficiency of the column. A breakthrough curve is obtained by plotting column effluent concentration versus time of treatment.

Influence of operating parameters on adsorption

The effect of parameters adsorbent bed height and effluent flow rate were investigated to evaluate adsorption capacity, H_{UNB} and MTZ of the column.

(a) Effect of adsorbate solution flow rate

Flow rate significantly affects the performance of the column in a continuous mode of study, and this is an important parameter for evaluating the efficiency of adsorbent in a continuous treatment process in the pilot or industrial scale. The effect of the flow rate of the adsorption of naringin on resin PA-500 was investigated by varying the outlet flow rate 2, 4, and 6 ml/min (3.3×10^{-8}, 6.6×10^{-8}, and 10×10^{-8} m^3/s) with a constant bed height of 1.20 m and inlet naringin concentration of 0.810 kg/m^3. The column study data are shown in Figure 5.20 and Table B5 (a).

From the Figure 5.20, initially the adsorption was very rapid for all the three flow rates (3.3×10^{-8}, 6.6×10^{-8}, and 10×10^{-8} m^3/s) because of the availability of adsorption sites. The breakthrough curves became steeper when the flow rate was increased, with which the breakpoint time and amount of naringin adsorbed decreased. The reason behind this is that

when the residence time of KPBW in the column was not long enough for adsorption equilibrium to be reached at that flow rate, the front of the adsorption zone quickly come to the bottom of the column, which saturated the column early. When at a low rate, KPBW had more time to contact the resin PA-500, resulting the higher amount of naringin adsorbed in the column and it was found that the maximum amount of naringin was achieved at a flow rate of 3.3×10^{-8} m^3/s. The parameters of the three breakthrough curves are presented in Table 5.9.

(b) Effect of adsorbent bed height

The accumulation of adsorbate in a fixed-bed column is dependent on the quantity of adsorbent inside the column and is a function of bed height. To find out the effect of bed height on the breakthrough curves, KPBW concentration 0.810 kg/m^3 at an effluent flow rate 3.3×10^{-8} m^3/s was passed through the column by varying the bed height (0.90 and 1.20 m). The column study data are shown in Figure 5.21 and Table B5 (b).

The results revealed that the breakthrough time increased with increasing the bed height from 0.90 to 1.20 m. The bed capacity also increased with increasing bed height. As the bed height increased, the residence time of KPBW solution inside the column increased, allowing the naringin molecules to diffuse deeper into the resin PA-500 and resulting in the higher amount of naringin adsorbed in a column. The parameters of the two breakthrough curves are given in Table 5.9.

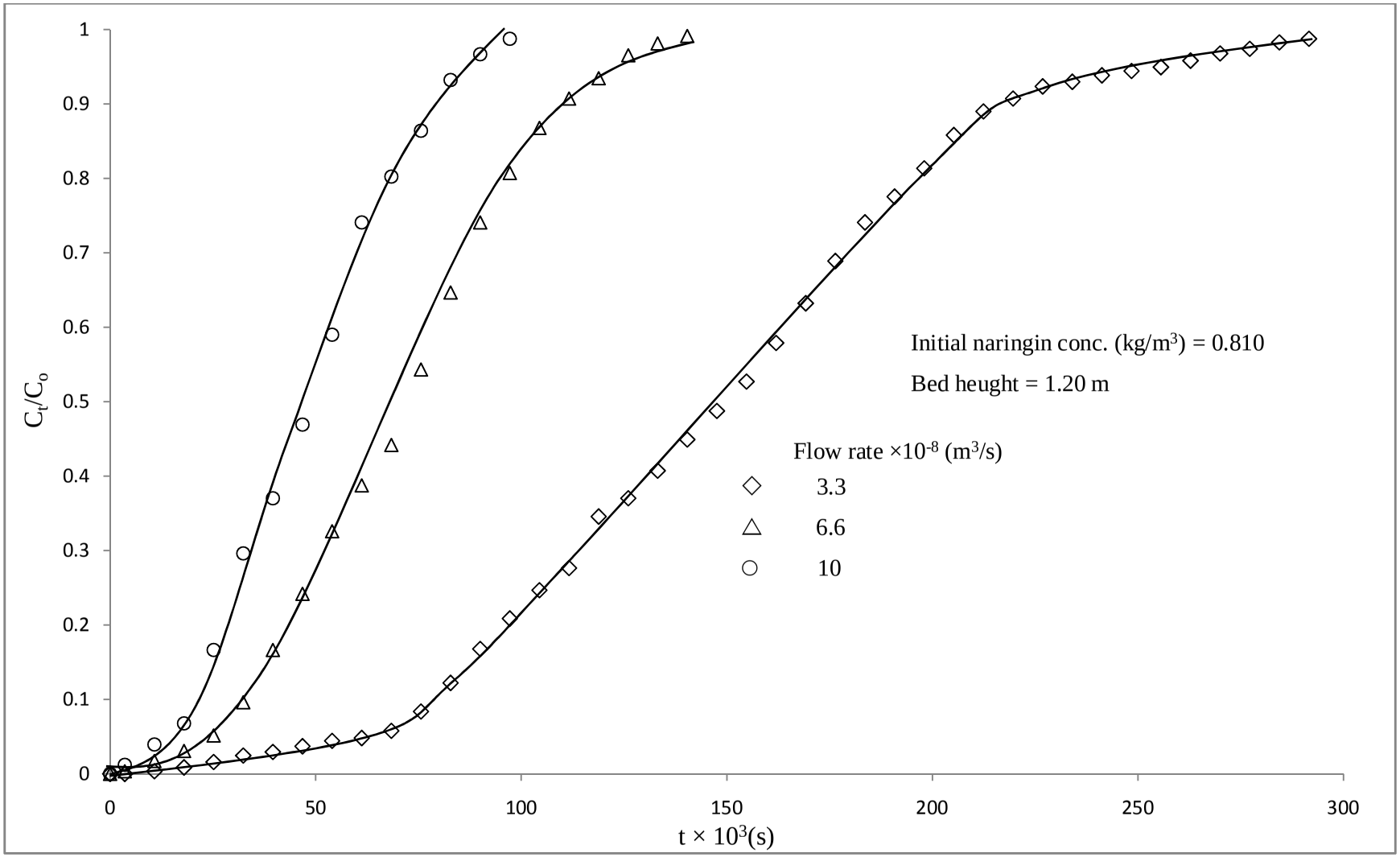

Figure 5.20: Adsorption of naringin on adsorbent PA-500 from fresh KPBW (column studies): Effect of flow rate (system 1)

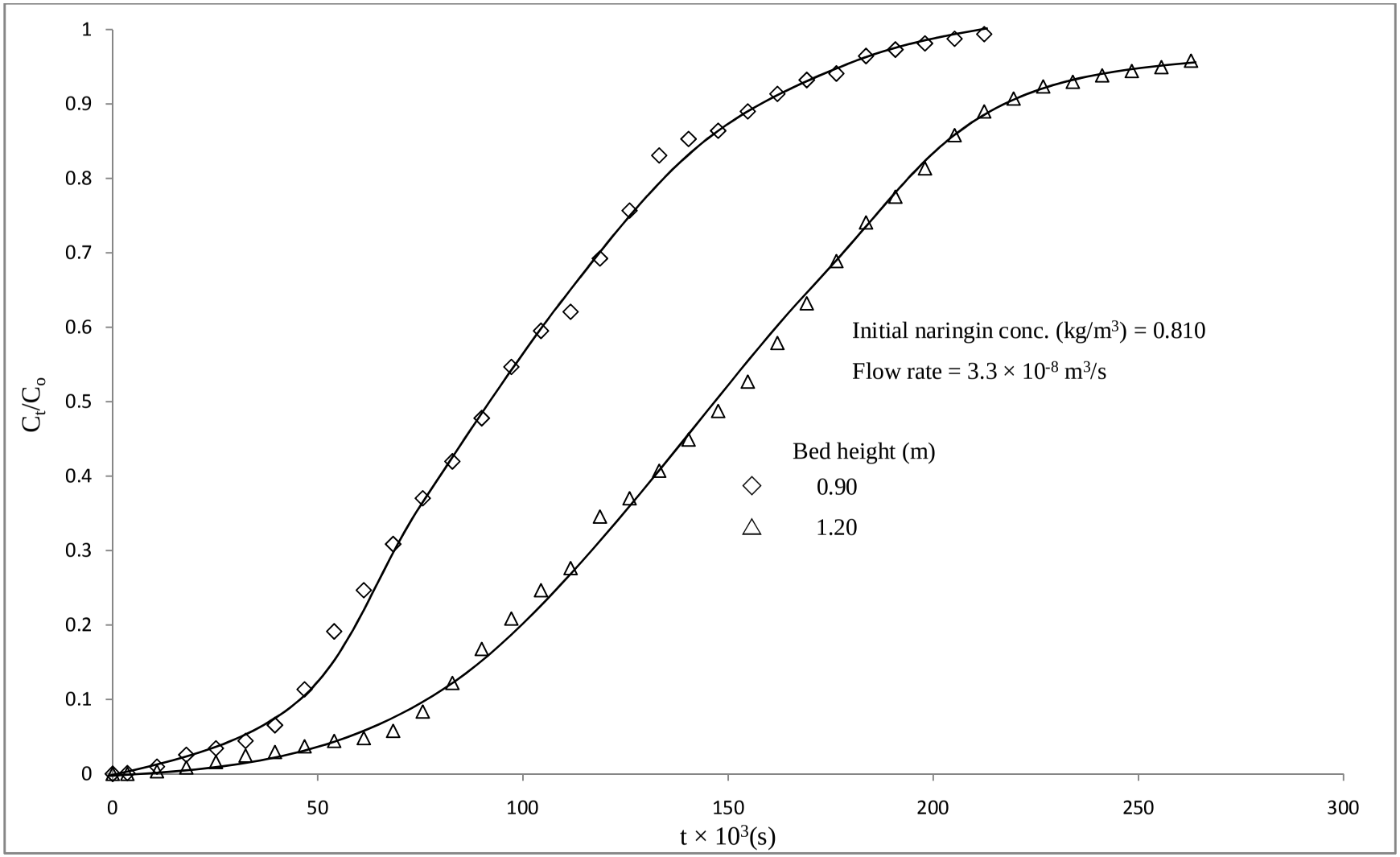

Figure 5.21: Adsorption of naringin on adsorbent PA-500 from fresh KPBW (column studies): Effect of height (system 1)

Table 5.9: Parameters of breakthrough curves for adsorption of naringin on resin PA-500 from fresh KPBW in a fixed-bed column at different process conditions

Z (m)	Q $\times 10^{-8}$ (m^3/s)	$t_b \times 10^3$ (s)	$t_t \times 10^3$ (s)	q_{total} g	q_s kg/kg	H_{UNB} (m)	MTZ (m)
1.20	3.3	66.6	157.6	4.25	0.077	0.692	0.711
	6.6	25.2	73.15	3.91	0.074	0.786	0.812
	10	18.0	46.80	3.73	0.069	0.738	0.775
1.20	3.3	66.6	157.6	4.26	0.077	0.692	0.711
0.90		36.0	119.5	3.28	0.067	0.629	0.635

Column studies were carried out with resin bed height 1.20 m and flow rate 3.3×10^{-8} m^3/s in different years (2012, 2013 and 2014) samples of KPBW which had concentrations of 0.810, 0.780 and 0.750 kg/m^3 respectively. The data obtained is shown in Figure 5.22.

From the Figure 5.22, it was observed that the first 7200 sec the concentration of naringin in outgoing solution was almost zero. The adsorption column data are given in Tables B6 (a-c). The parameters of breakthrough curves are presented for the three years in Table 5.10.

Table 5.10: Parameters of breakthrough curves for adsorption of naringin on resin PA-500 from fresh KPBW in a fixed-bed column for different years

Bed height = 1.20 m, Flow rate = 3.3×10^{-8} m^3/s

S.No	Year	C_o (kg/m^3)	$t_b \times 10^3$ (s)	$t_t \times 10^3$ (s)	q_{total} g	q_s kg/kg	H_{UNB} (m)	*MTZ* (m)
1	2012	0.800	66.6	157.6	4.25	0.077	0.692	0.711
2	2013	0.780	64.0	161.8	4.20	0.076	0.725	0.734
3	2014	0.750	63.3	151.3	3.53	0.070	0.697	0.717

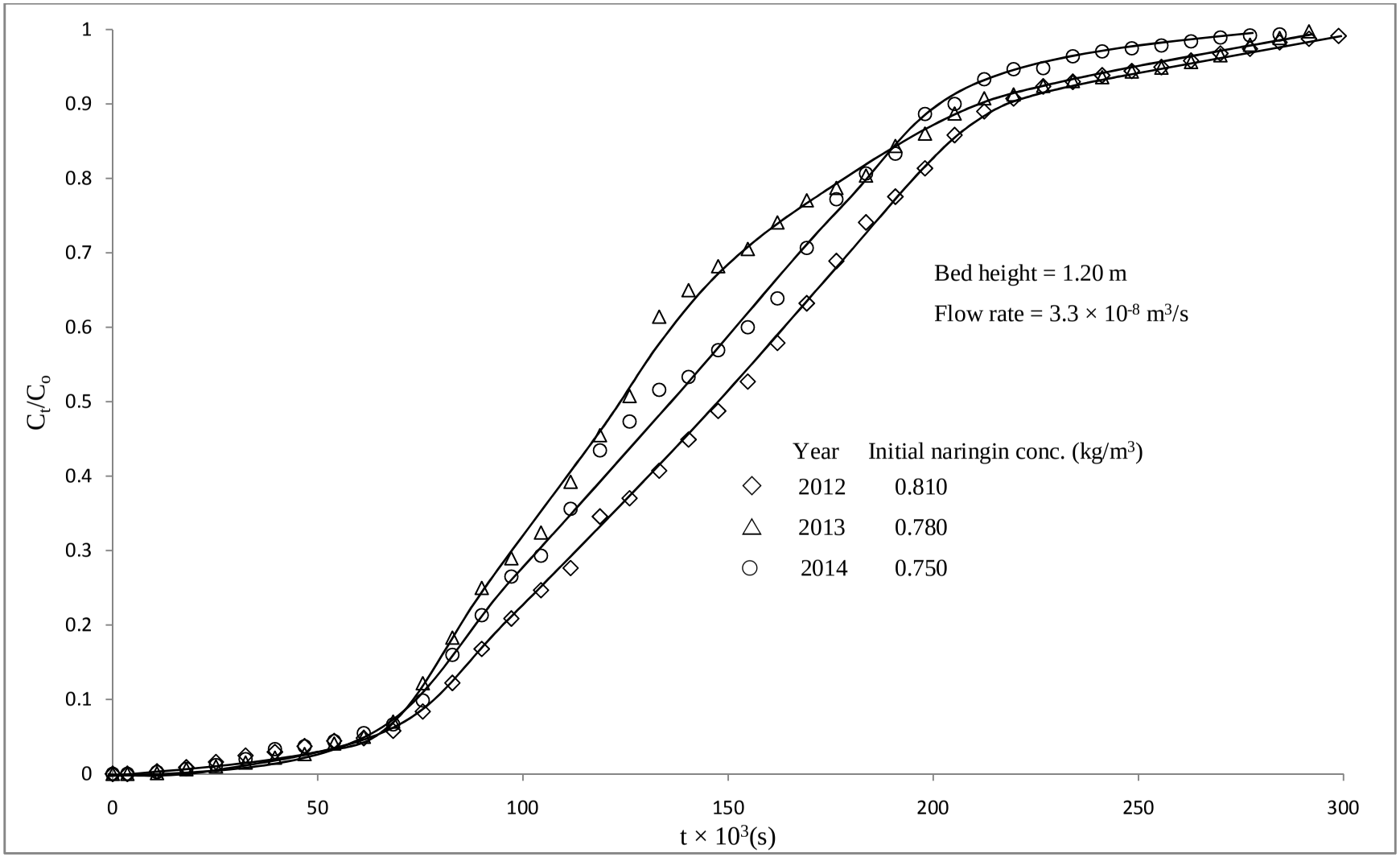

Figure 5.22: Adsorption of naringin on adsorbent PA-500 from fresh KPBW: fixed bed column study (system 1)

5.1.4. Desorption equilibrium studies (System 1)

The desorption equilibrium studies with ethanol from naringin saturated resin were carried out as per the procedure described in the section 3.6.1.

The data have been presented in Table B7 and Fig. 5.23. The desorption equilibrium curves Figure 5.23 shows a trend as expected and desorption is favourable (as it data shows the unfavourable adsorption equilibrium) with ethanol but does not approach completion. It indicates that at an equilibrium below the concentration 0.025 kg/m^3 of ethanol naringin solution, the change in the value of q_{ed} is very less and the curve almost flatten. Hence, approximately 0.025 to 0.03 kg of naringin/kg resin will be retained on resin even for a small concentration of the naringin-ethanol solution. Although, it is expected that naringin desorption equilibrium curves should be same for all years. The reason for observing different desorption curves is that resin had adsorbed some other constituents like limonin, essentials oils and other big molecules. These molecules compete for desorption also when they block sites, does not allow the naringin molecules to come out. The desorption equilibrium experimental data could be correlated with Freundlich adsorption isotherm equation (4.42), and its parameters were evaluated and are presented in Table 5.11.

Table 5.11: Freundlich isotherm constants for desorption of naringin from naringin saturated resin PA-500 (fresh peels)

S.No	Year	Freundlich constants		
		K_{fd}	n_d	R^2
1	2012	0.088	1.58	0.945
2	2013	0.099	1.42	0.970
3	2014	0.110	1.43	0.911

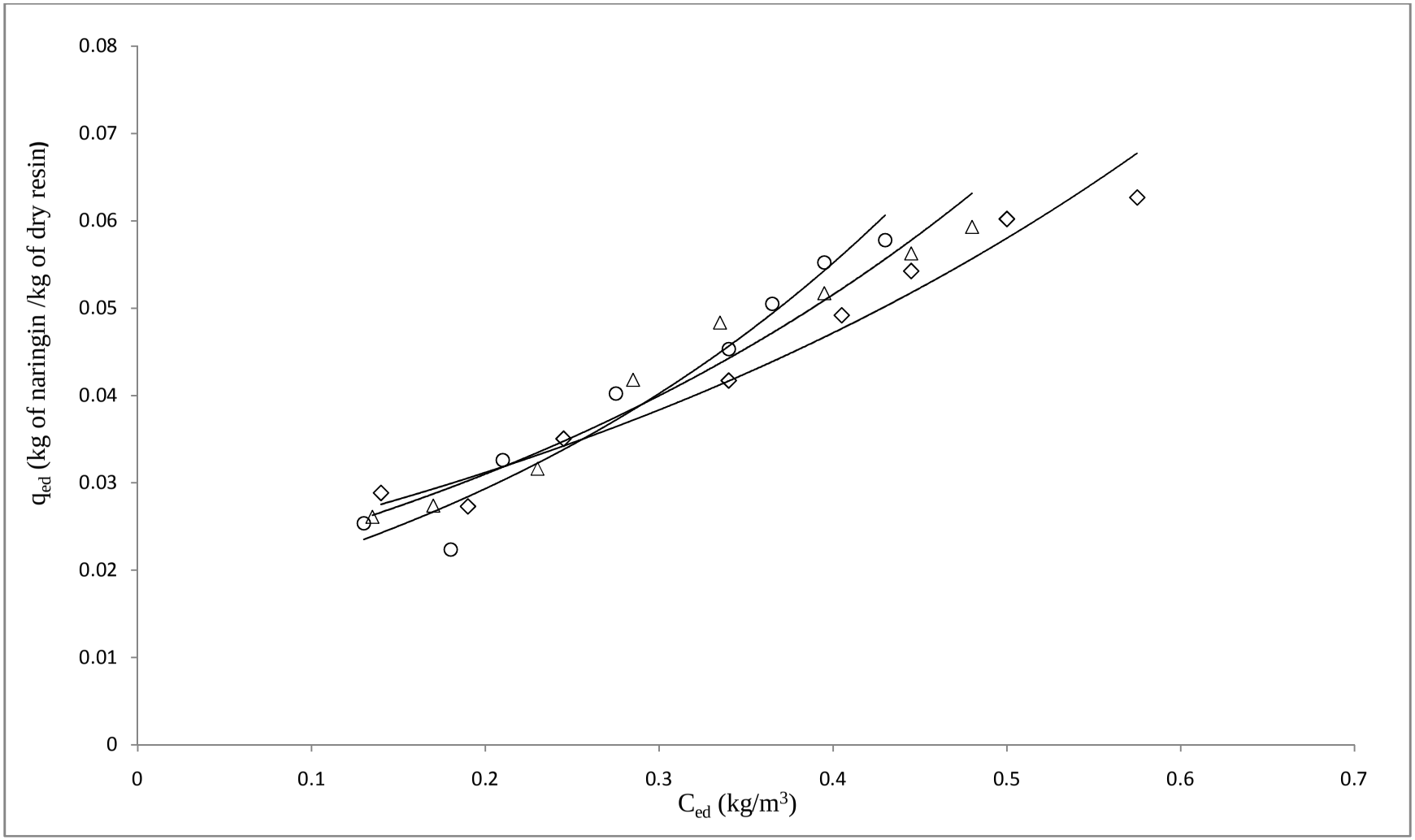

Figure 5.23: Desoption equilibrium studies from naringin saturated resin PA-500 to ethanol solution (system 1)

5.1.5. Desorption kinetic studies (System 1)

The Desorption kinetic studies with ethanol from naringin saturated resin were carried out as per the procedure described in the section 3.6.2 and are data presented in Table B8 (a-c) and Figures 5.24 to 5.26. From Figures 5.24 to 5.26, it is notable that initially concentration of naringin in ethanol rises sharply then slowly, the rate of concentration change decline which is as per expectation because the driving force reduces with time. Almost 90% desorption of naringin (from saturated resin obtained after passing KPBW through resin) is completed in first 11000 s.

Modelling of desorption kinetic data

The desorption kinetics was analysed using Boyd's diffusivity model (Boyd *et al.* 1947) equation, as per the procedure described in section 4.7. The value of Boyd's effective diffusivity constant D_{ed}, was estimated using linear plots of $\ln\left(1/1-u_d^2(t)\right)$ against time (t) which are shown in Figure 5.27 and Table 5.12. The average value of Boyd's diffusivity rate constant D_{ed} was found to be $9.75\times10^{-13}\,m^2s^{-1}$. The values of correlation coefficient R^2 of plot between $\ln\left(1/1-u_d^2(t)\right)$ vs time (t) are quite high; therefore Boyd's diffusivity model equation could be used to represent the observed data.

Table 5.12: Boyd's diffusivity model parameters for desorption of naringin from naringin saturated resin PA-500 (system 1)

S.No	Run	Year					
		2012		2013		2014	
		$D_{ed}\times10^{-13}$ (m^2s^{-1})	R^2	$D_{ed}\times10^{-13}$ (m^2s^{-1})	R^2	$D_{ed}\times10^{-13}$ (m^2s^{-1})	R^2
1	1	9.60	0.973	10.9	0.948	9.41	0.988
2	2	11.2	0.985	8.89	0.995	8.83	0.990
3	3	10.9	0.968	8.93	0.979	9.05	0.986

Generation of desorption kinetic data

(i) The concentration of naringin desorbed in ethanol at any time C_{td} for any run can be generated by the Boyd's diffusivity model equation using average value of $D_{ed}(m^2 s^{-1})$.

(ii) From the value of D_{ed}, the value of $u_d(t)$ is calculated by relation (4.43).

(iii) From value of $u_d(t)$, the value of C_{td} is calculated by relation (4.44).

The generated C_{td} (with the representative value of D_{ed} = $9.75\times10^{-13}\ m^2 s^{-1}$), as well as experimental data for run 1, are given in Table 5.13. The data were tested for significance of the mean difference, paired observation by t -test at a 5% level of significance, and it was found that the experimental and predicted data do not differ significantly.

Table 5.13: Desorption kinetic data: C_{td} generated and C_{td} experimental: Run 1

t (s)	C_{td} experimental	C_{td} generated
0	0	0
450	0.01	0.017
900	0.025	0.024
1800	0.030	0.033
2700	0.045	0.041
3600	0.050	0.047
5400	0.050	0.057
7200	0.075	0.065
10800	0.080	0.079
14400	0.095	0.089
21600	0.100	0.106

For all runs, the generated C_{td} (with a representative value of D_{ed} = $9.75\times10^{-13}m^2s^{-1}$) are shown by the smooth curve, and experimental data are given for comparison in Figures 5.24 to 5.26.

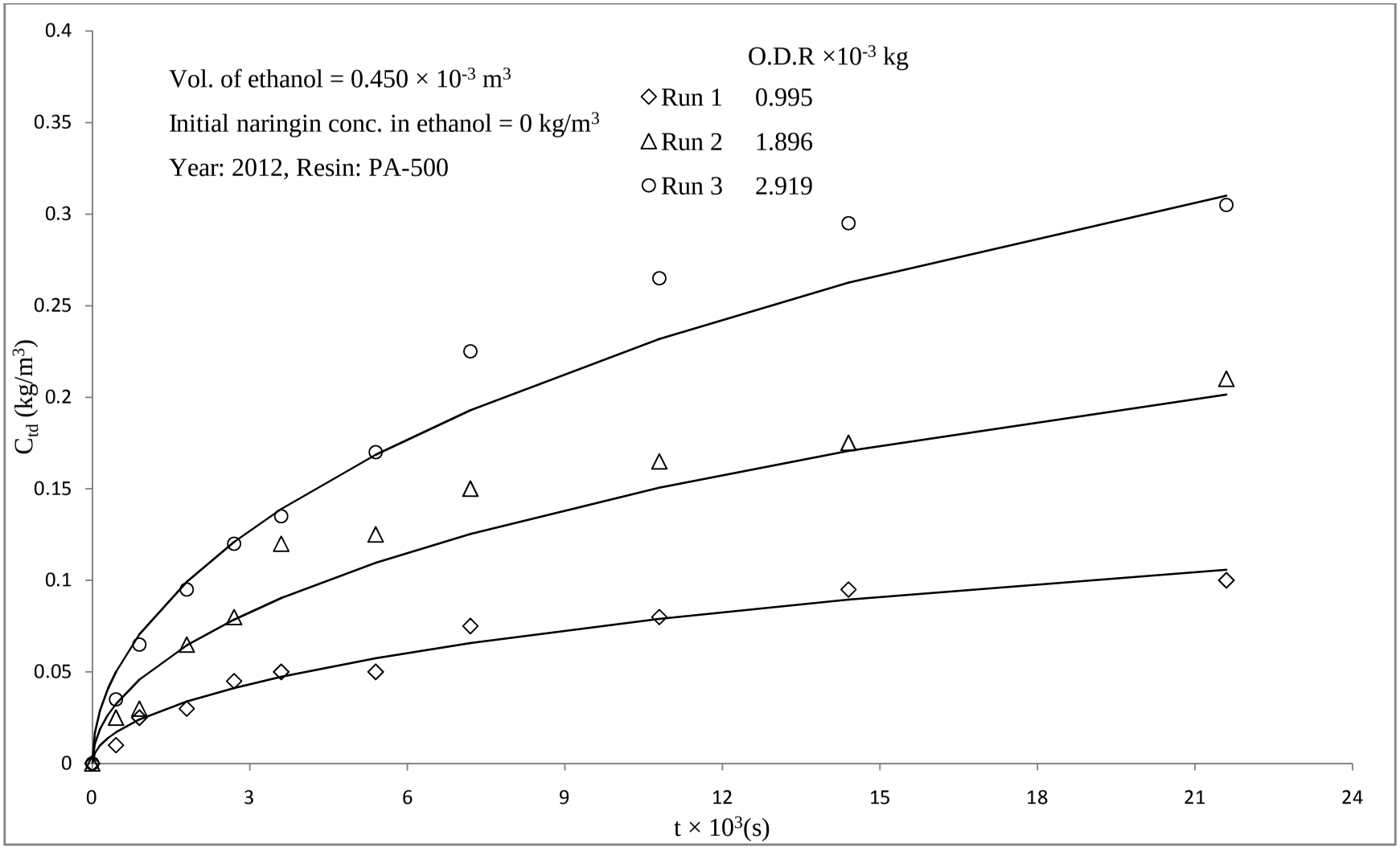

Figure 5.24: Desorption kinetic studies with naringin saturated resin PA-500 in ethanol: correlation of experimental data C_{td} *vs t* (system 1, year 2012)

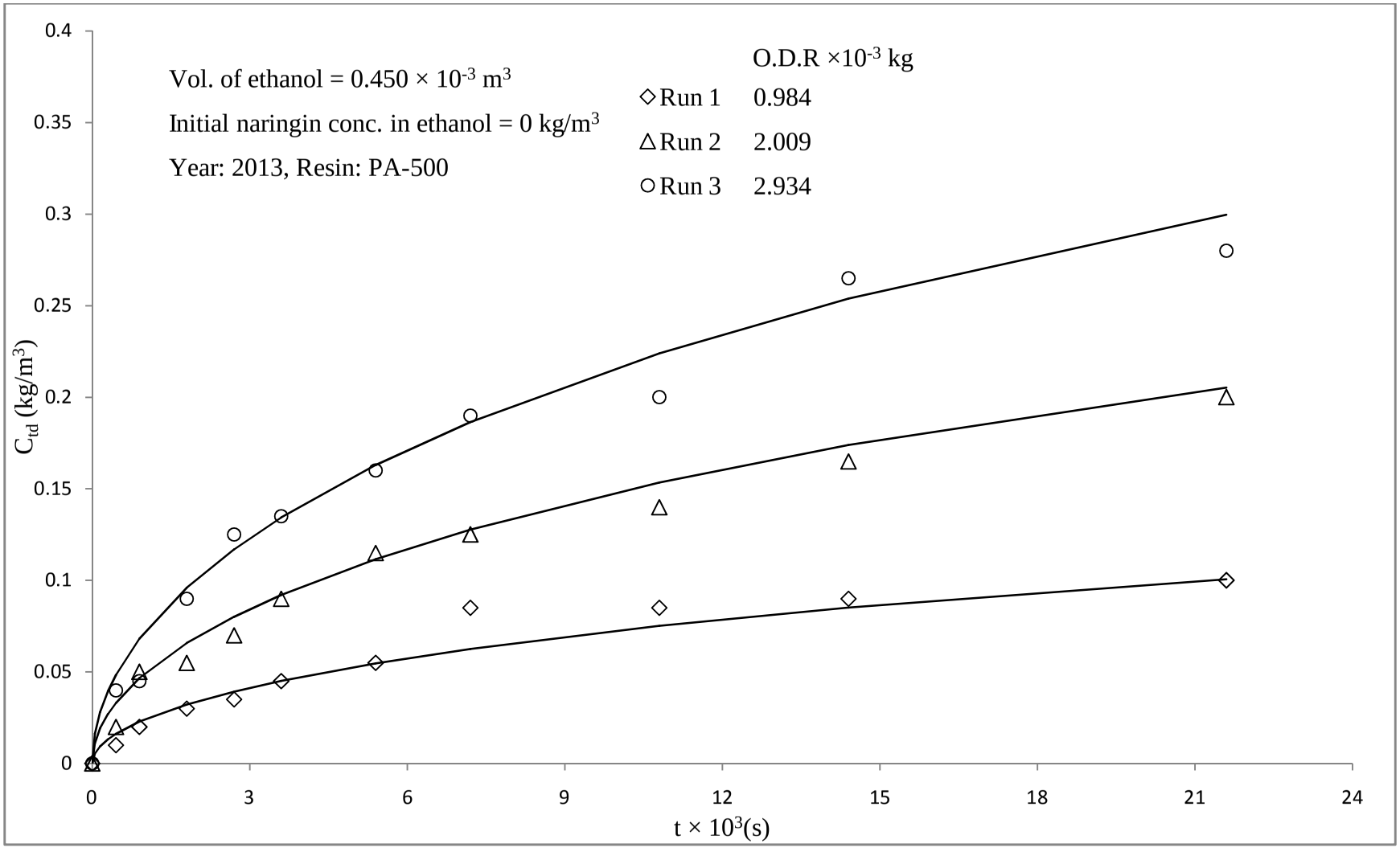

Figure 5.25: Desorption kinetic studies with naringin saturated resin PA-500 in ethanol: correlation of experimental data C_{td} *vs t* (system 1, year 2013)

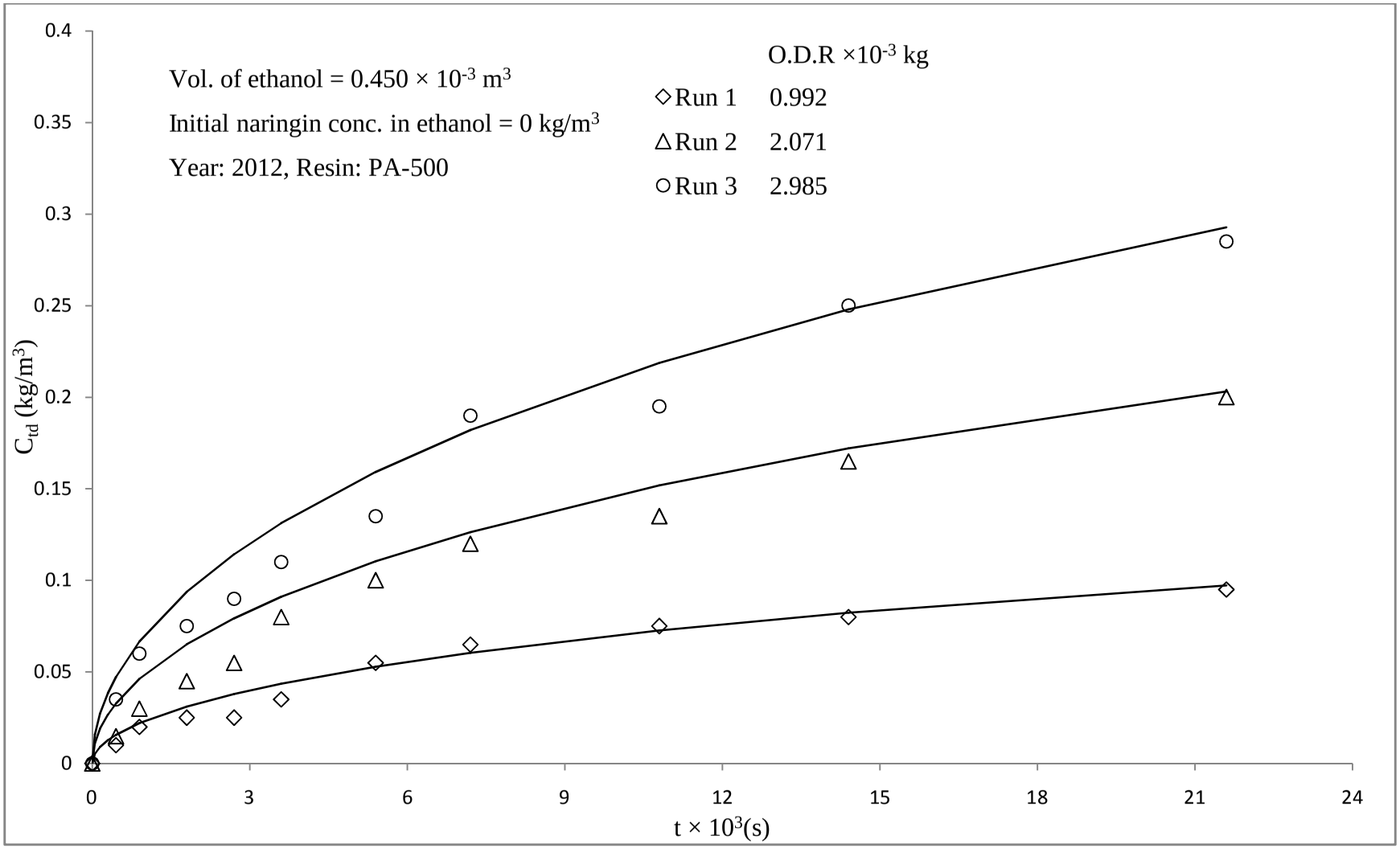

Figure 5.26: Desorption kinetic studies with naringin saturated resin PA-500 in ethanol: correlation of experimental data C_{td} *vs t* (system 1, year 2014)

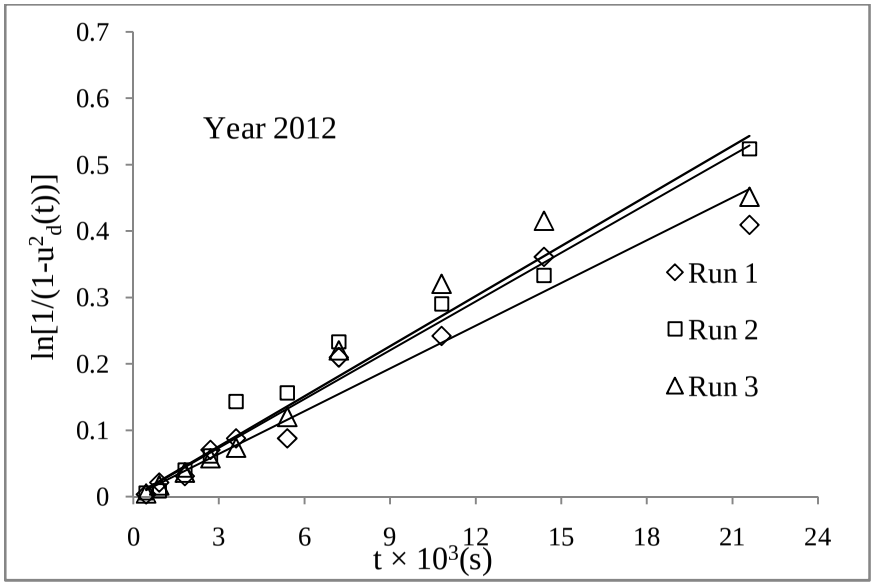

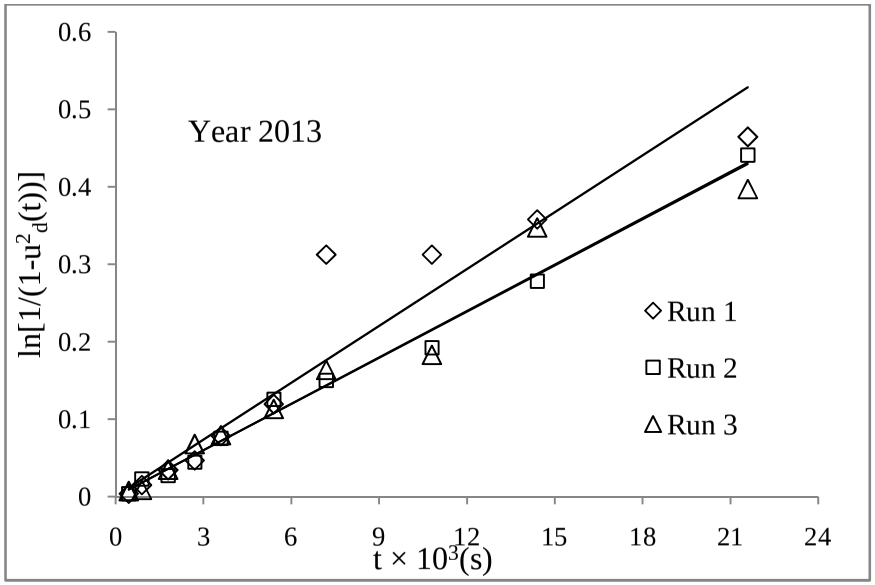

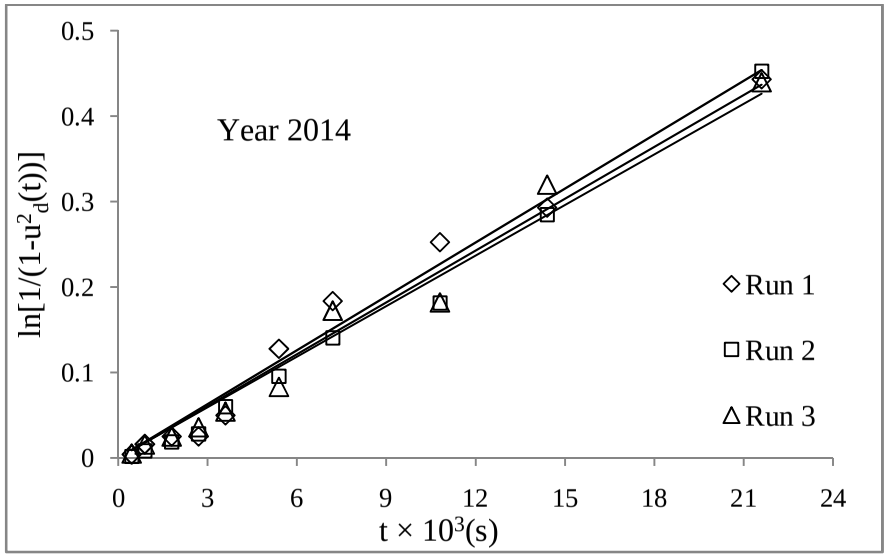

Figure 5.27: Boyd's plot for desorption of naringin from adsorbed resin PA-500 to ethanol solution (system 1)

The summary of the statistics analysis of the predicted values from the model and experimental values is given in Table 5.14. The data were tested for significance of the mean difference, paired observation by t -test at a 5% level of significance, and it was found that the experimental and predicted data for almost all the runs do not differ significantly.

Table 5.14: Statistical analysis for predicted and experimental values of C_{td} (system 1)

Year	Run	Slope	R^2 C_{trep} vs. $C_{t\exp}$	t-Crit	t-Cal	Inference
2012	1	0.988	0.962	2.262	-0.069	NSD
	2	0.918	0.955	2.262	1.707	NSD
	3	0.940	0.966	2.262	1.097	NSD
2013	1	0.930	0.926	2.262	0.792	NSD
	2	1.044	0.984	2.262	-3.000	SD
	3	1.027	0.973	2.262	-1.512	NSD
2014	1	1.022	0.946	2.262	-1.843	NSD
	2	1.079	0.949	2.262	-6.248	SD
	3	1.055	0.964	2.262	-3.524	SD

*NSD- No Significance difference, SD- Significance difference

From the above it is evident that observed kinetic data studied, could be correlated reasonably using Boyd's diffusivity model equation. The same approach has been used to correlate the desorption kinetic data of all the other systems.

Comparison of desorption kinetics:

The kinetics of desorption of naringin from resin saturated with naringin to ethanol for different years with the same weight of resin have been compared, and it is shown in Figure 5.28. The rate of desorption of naringin into ethanol solution was almost same in all three years.

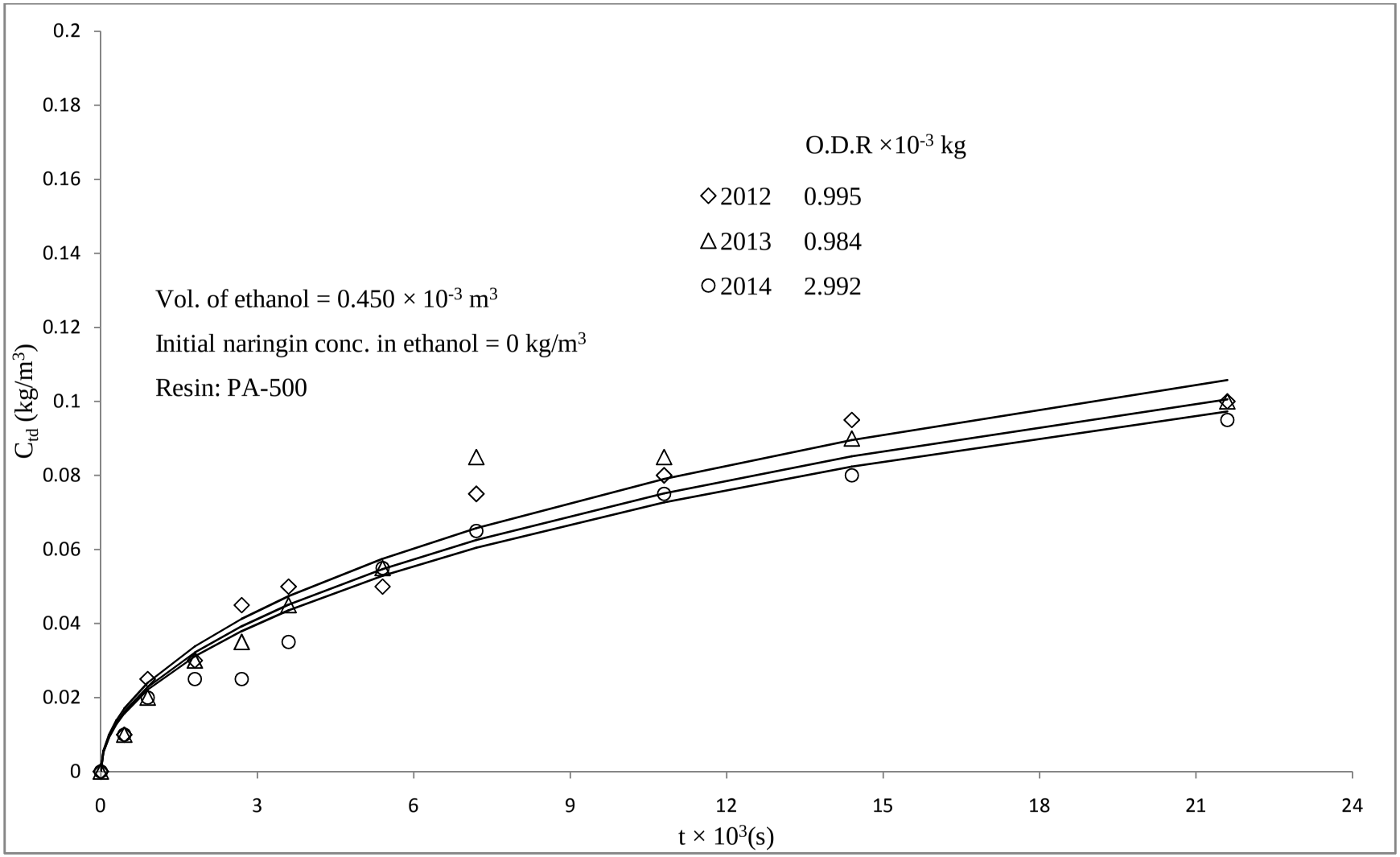

Figure 5.28: Comparison of desorption kinetic studies of naringin saturated resin PA-500 in ethanol with year (system 1), C_{td} *vs t*

5.1.6. Desorption fixed bed column studies (System 1)

The desorption column studies were carried out in glass column as per the procedure described in the section 3.6.3 and presented in Figure 5.29. From the Figure 5.29, it is evident that the amount of naringin desorbed in ethanol from resin saturated with naringin (obtained from adsorption column studies) decreases with time. The rate of desorption is different in all three years due to KPBW is a multi-component system; it contains components like limonin, pectin, essential oils etc. The data of column studies for naringin desorption with ethanol to recover naringin are given in Table B9.

From these desorption study, it can be concluded that about 2100 ml of ethanol is sufficient for almost all the possible recoverable desorption of naringin from the resin PA-500 in a glass column of 14 mm ID filled up to the height 0.95 m (about 120 g naringin saturated resin (wet)).

The amount of naringin desorbed into ethanol in the column was found to be 2.88, 2.58 and 2.49 g for the years 2012, 2013, and 2014 respectively.

5.1.7. Purity and recovery of Naringin and Pectin (System 1)

(A) Recovery of naringin

Recovery and purity of naringin were calculated as per the procedure described in section 3.9 and are tabulated in Table 5.15 for the years 2012, 2013, 2014 respectively. The photograph of obtained naringin sample is shown in Figure 5.30.

Table 5.15: Recovery of naringin from fresh peels with resin PA-500

S.No	Year	Naringin Conc. in KPBW (kg/m^3)	Naringin obtained (g)	Purity (%)	Recovery (%)
1	2012	0.810	3.1	91.2	49.4
2	2013	0.780	2.6	94.4	48.2
3	2014	0.750	2.5	93.0	48.1

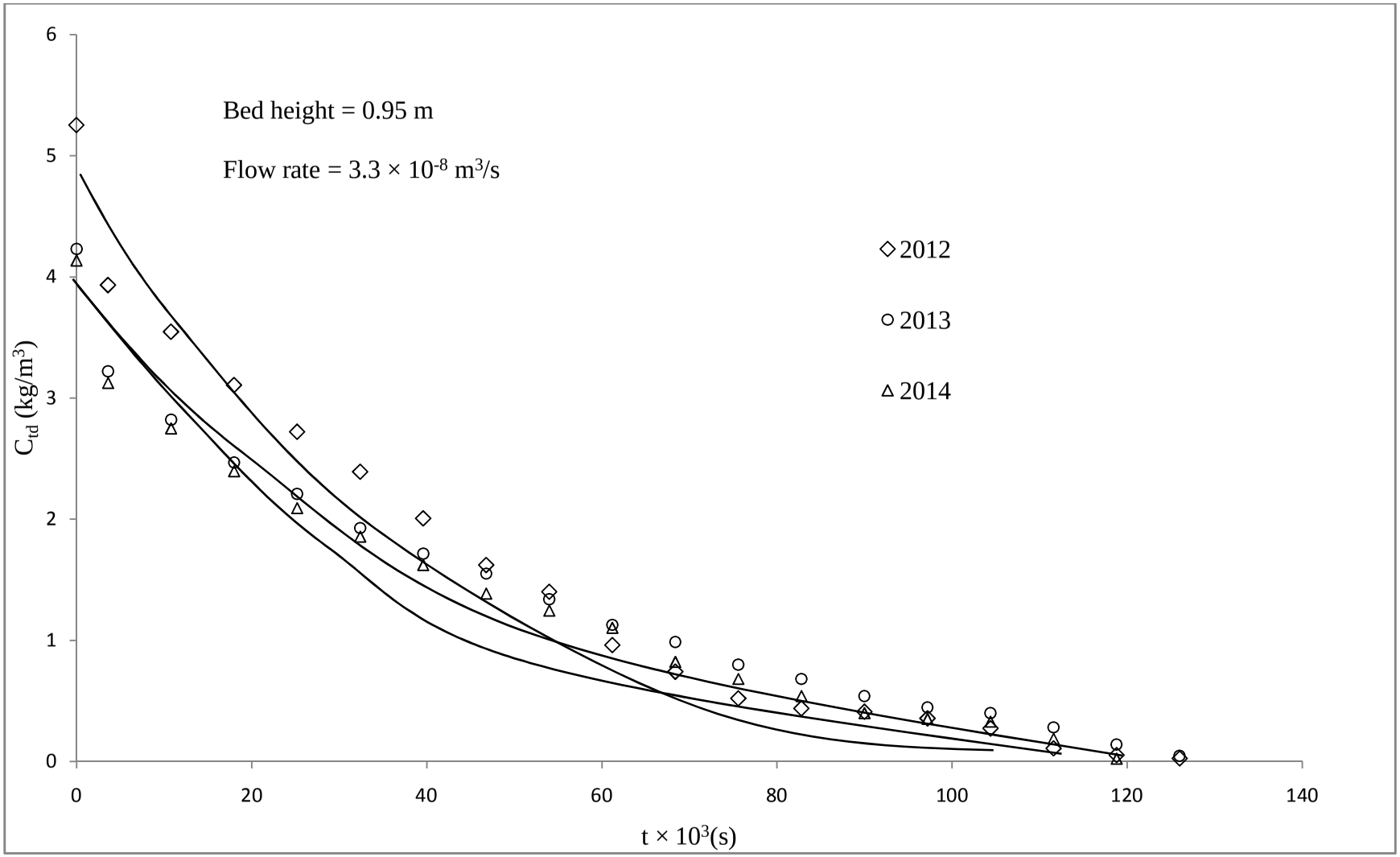

Figure 5.29: Column desorption studies from naringin saturated resin PA-500 into ethanol, C_{td} *vs t* (system 1)

Figure 5.30: Photograph of Naringin sample

(B) Recovery of pectin characterization

The obtained pectin is a light brown powder solid, and the photograph of pectin sample is shown in Figure 5.31. The recovery of pectin was calculated as per the procedure described in section 3.9. The obtained pectin was characterised, the values of different parameters determined are tabulated in Table 5.16.

Table 5.15: Recovery of naringin from fresh peels with resin PA-500

S.No	Year	Naringin Conc. in KPBW (kg/m^3)	Naringin obtained (g)	Purity (%)	Recovery (%)
1	2012	0.810	3.1	91.2	49.4
2	2013	0.780	2.6	94.4	48.2
3	2014	0.750	2.5	93.0	48.1

Figure 5.31: Photograph of Pectin sample

Table 5.16: Recovery of pectin from fresh peels with resin PA-500

S.No	Year	Recovey (%)	Moisture (%)	Ash (%)	Equivalent weigh (mg/ml)	Methoxyl content (%)	Anhdrouronic acid (%)	DE (%)
1	2012	62.0	8.5	6.9	601.1	6.74	69.5	55.1
2	2013	59.0	7.0	7.5	641.0	5.95	66.9	50.4
3	2014	67.2	8.7	6.8	631.2	5.82	72.2	45.7

5.2. Adsorption-Desorption studies of naringin with fresh peels on Resin PA-800 (system 2)

5.2.1. Adsorption equilibrium studies (System 2)

Adsorption equilibrium studies were carried out as per the procedure described in the section 3.5.1. The experimental data are shown in Table C1 and Figure 5.32.

The adsorption equilibrium experimental data could be correlated by using Langmuir adsorption isotherm and its parameters were evaluated and are presented in Table 5.17. It may be noted that the naringin concentration in solution (KPBW) was 0.810, 0.780, and 0.750 kg/m^3, respectively in the years 2012, 2013 and 2014. The maximum amount of naringin that can be picked up by resin PA-800 from fresh KPBW (calculated from Langmuir adsorption isotherm constants) was found to be 0.168, 0.155, and 0.131 kg per kg of dry resin respectively for the years 2012, 2013 and 2014. The amount of naringin adsorption is different in all three years because kinnow peel boiled water contains several compounds. During adsorption, all compounds reach the surface where they are competing to the active site.

Table 5.17: Langmuir isotherm parameters for adsorption of naringin on resin PA-800 from fresh KPBW

S.No	Year	Langmuir constants		
		a	b	R^2
1	2012	0.260	1.548	0.942
2	2013	0.409	2.639	0.937
3	2014	0.411	3.135	0.904

However, to know the thermodynamic parameters, the equilibrium studies were carried out at three different temperatures 303, 313 and 323 K. The results are shown in the Figure 5.33 in Table C2.

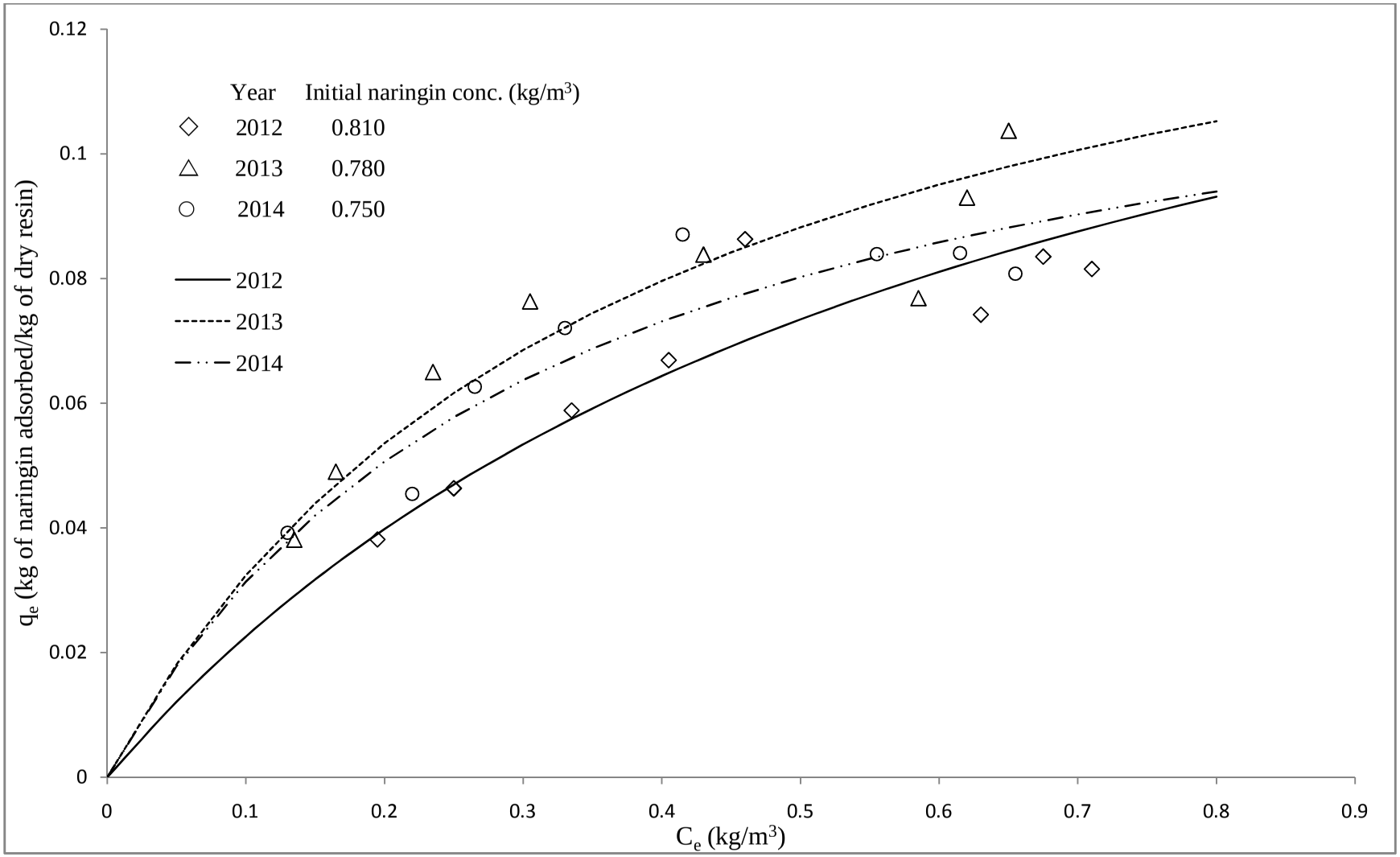

Figure 5.32: Adsorption equilibrium studies with fresh KPBW on resin PA-800 in different years (system 2)

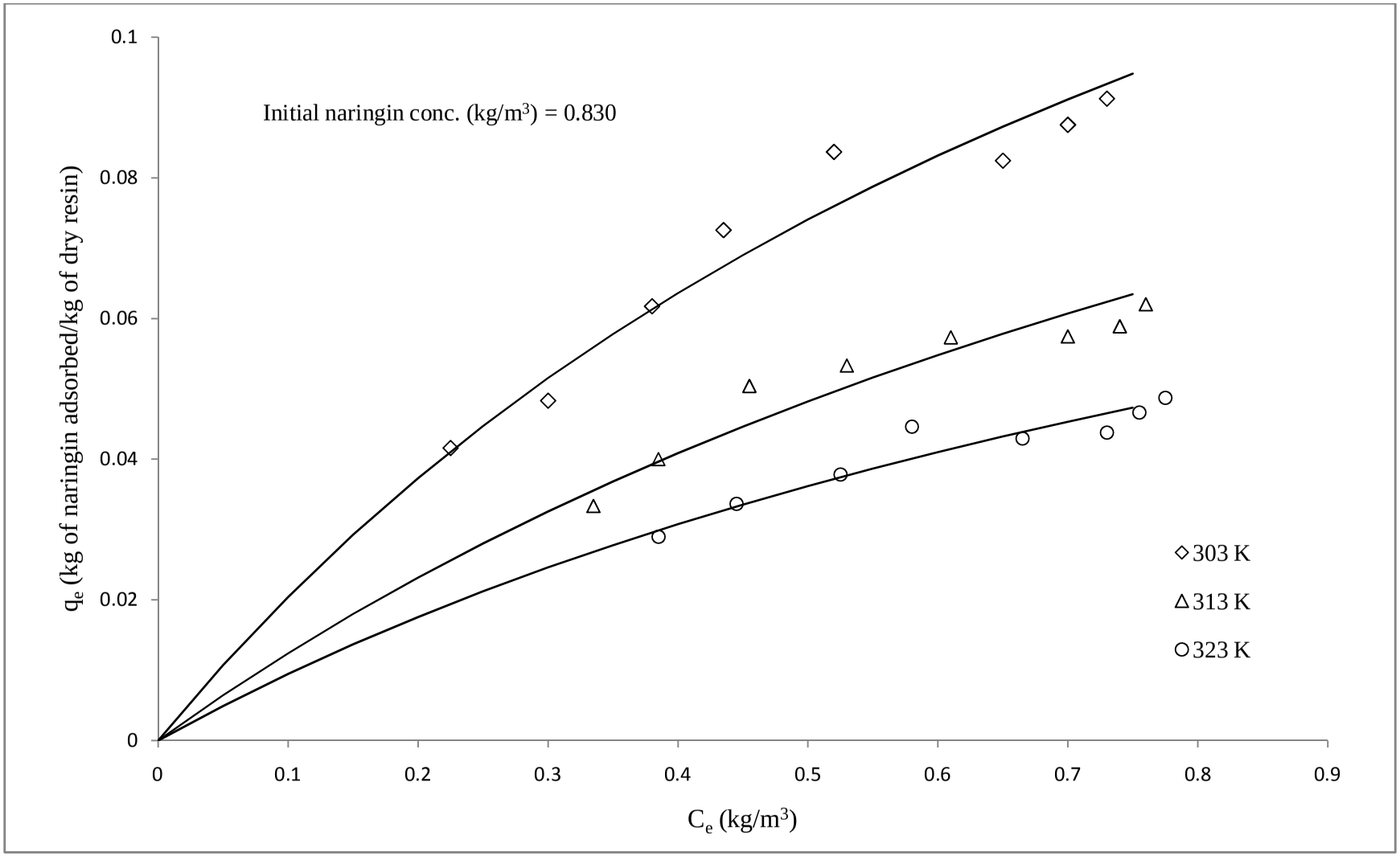

Figure 5.33: Effect of temperature on adsorption of naringin from fresh KPBW on PA-800 (system 2)

It is evident that the adsorption of naringin on resin PA-800 decreases with the rise in temperature. Observations are similar to as in the case of system 1. The Van't Hoff plots of $\ln(K_{a/d})$ versus 1/T (Figure 5.34) are found to be linear, and ΔH and ΔS values are calculated from the intercept and slope of the plot. The estimated values of the thermodynamic parameters for the three operating temperatures are presented in Table 5.18.

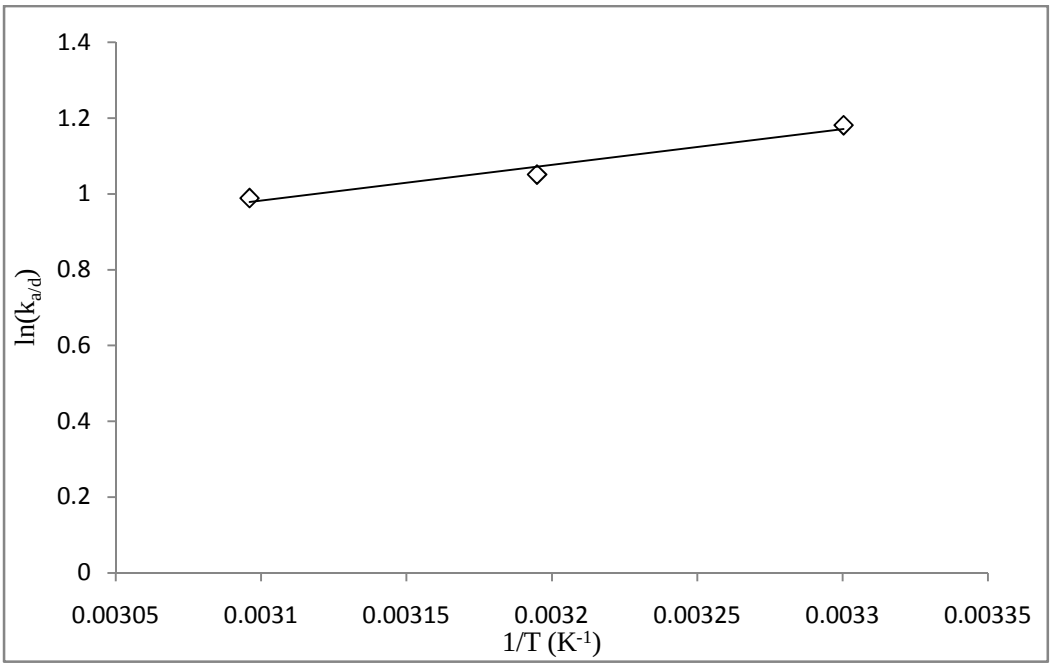

Figure 5.34: The Van't Hoff plot of $\ln(K_{a/d})$ versus 1/T for the resin PA-800 (system 2)

Table 5.18: Thermodynamic parameters for adsorption of naringin on resiPA-800 from fresh KPBW

S.No	Temp (K)	ΔS (kJ/mol K)	ΔH (kJ/mol)	ΔG (kJ/mol)	R^2 of linear plot between $\ln(K_{a/d})$ vs 1/T
1	303	-4.875	-19.653	-3.562	0.987
2	313			-2.984	
3	323			-2.571	

The negative ΔG value indicates the feasibility of the adsorption of naringin onto PA-800 surface. The negative values of ΔH confirmed the exothermic nature of adsorption process. Since ΔH and ΔS both are negative and temperatures involved are low; therefore the process of adsorption of naringin on the resin PA-800 is spontaneous.

5.2.2. Adsorption kinetic studies (System 2)

The adsorption kinetic studies were carried out as per the procedure described in the section 3.5.2

The concentration of naringin in the solution (KPBW) as a function of time during adsorption for various amounts of oven dried resin is presented in Figures 5.35-5.37 for the years 2012, 2013 and 2014. The data obtained in these experiments are given in Tables C3 (a-c). It is evident that the change in concentration is faster with the larger amount of adsorbent.

Modelling of kinetic data:

The above data have been analysed with the same approach as done for system 1, i.e., using modified adsorption shell model. It may be notable that average radius of the particle (bead) for resin PA-800 was 0.48×10^{-3} m. Also, as mentioned earlier in the section 4.3.1, the mass or volume fraction of adsorbent bead occupied by adsorbate initially (k) is 0.50 for resin PA-800. The C_t values read from the curve were used to calculate F_n values. The values of different parameters viz. slopes of $F_n(t)$ vs t plots, K, β and ψ are tabulated in Table 5.19 for all the runs of all three years.

Table 5.19: Modified adsorption shell model parameters for system 2

$D_P = 1.032\times10^{-10} m^2/s, \varepsilon = 0.39,\ R_p = 0.48\times10^{-3}$ m

Year	Run	C_o kg/m^3	q_e kg/m^3	Slope × 10^{-4} (s^{-1})	K	β	ψ	$\frac{D_c}{r_c^2}$ × 10^{-4} (s^{-1})
2012	1	0.810	85.09	2.04	187.0	308.7	2.93	2.81
	2	0.810	71.79	1.58	122.5	120.9	1.36	1.30
	3	0.810	51.10	4.37	240.9	522.5	8.28	7.91
	4	0.810	40.44	3.62	157.8	213.9	4.28	4.09
	5	0.810	38.46	4.41	183.0	294.7	6.20	5.92
2013	1	0.780	81.88	1.58	144.8	176.8	1.68	1.60
	2	0.780	59.72	2.71	181.2	288.8	3.77	3.60
	3	0.780	51.19	2.23	127.5	132.6	2.02	1.93
	4	0.780	46.77	3.92	204.9	374.5	6.24	5.96
2014	1	0.750	73.94	1.83	159.8	219.9	2.20	2.10
	2	0.750	48.84	2.17	125.0	126.7	1.92	1.83
	3	0.750	41.67	1.67	81.97	45.75	0.81	0.75

The generated (with a representative value of = 3.447) for all the runs are shown by smooth curves, and experimental data are given for comparison in Figures 5.35 to 5.37.

The data were tested for significance of the mean difference, paired observation by t -test at a 5% level of significance, and it was found that the experimental and predicted data for almost all the runs does not differ significantly. The summary of the statistical analysis values is given in Table 5.20.

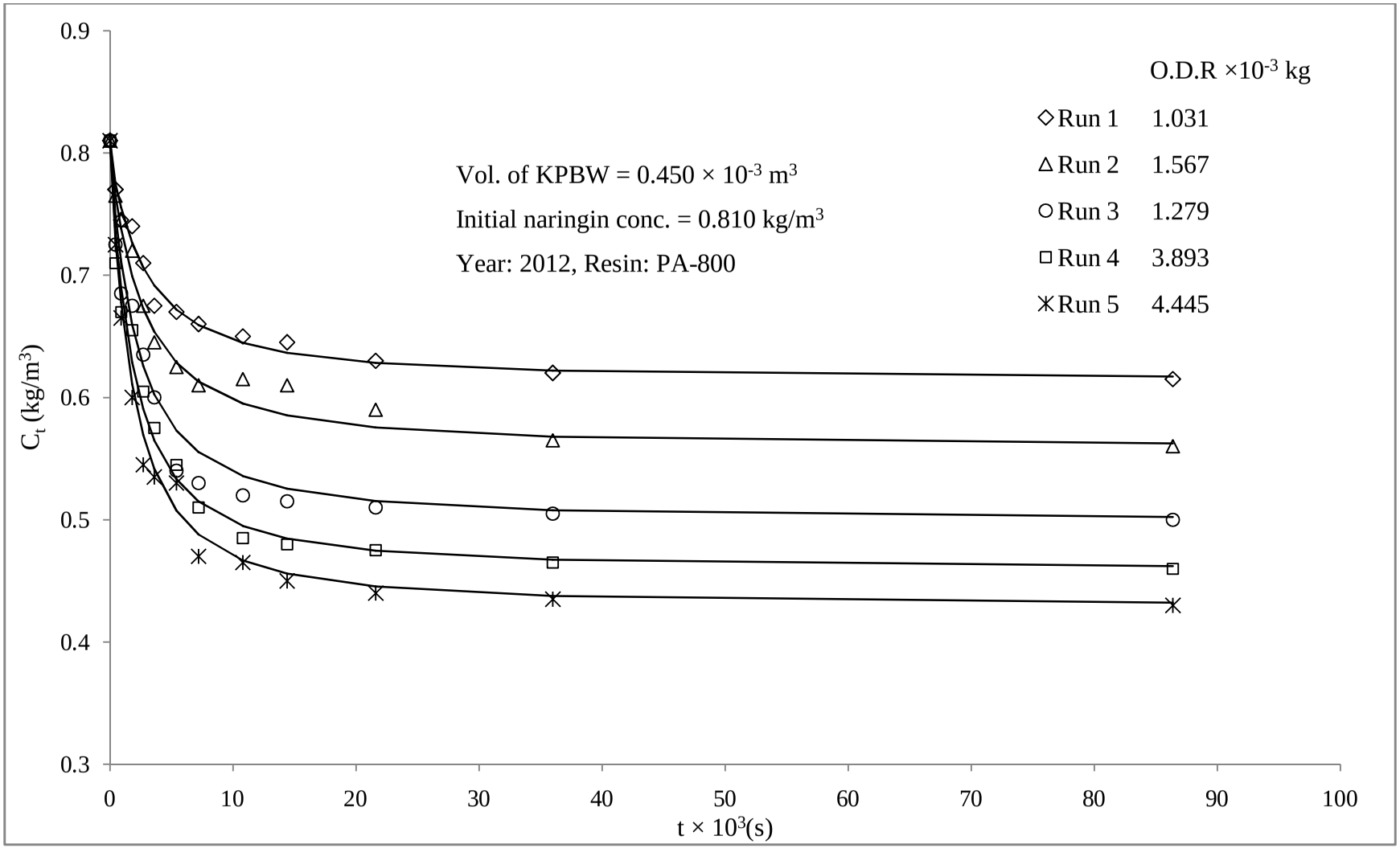

Figure 5.35: Adsorption of naringin on adsorbent PA-800 from fresh KPBW: kinetic studies, correlation of experimental data, C_t *vs t* (system 2, year 2012)

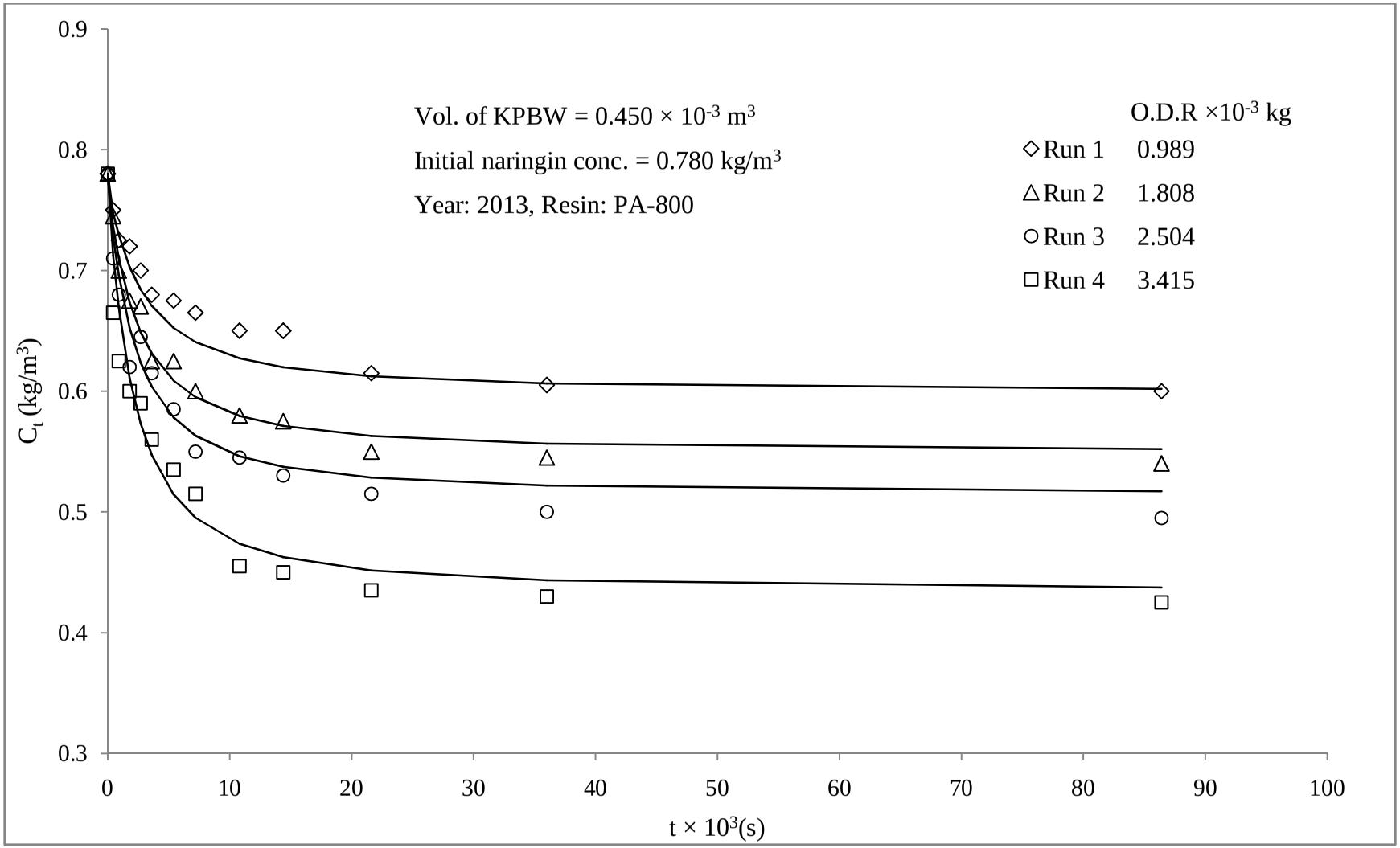

Figure 5.36: Adsorption of naringin on adsorbent PA-800 from fresh KPBW: kinetic studies, correlation of experimental data, C_t *vs* t (system 2, year 2013)

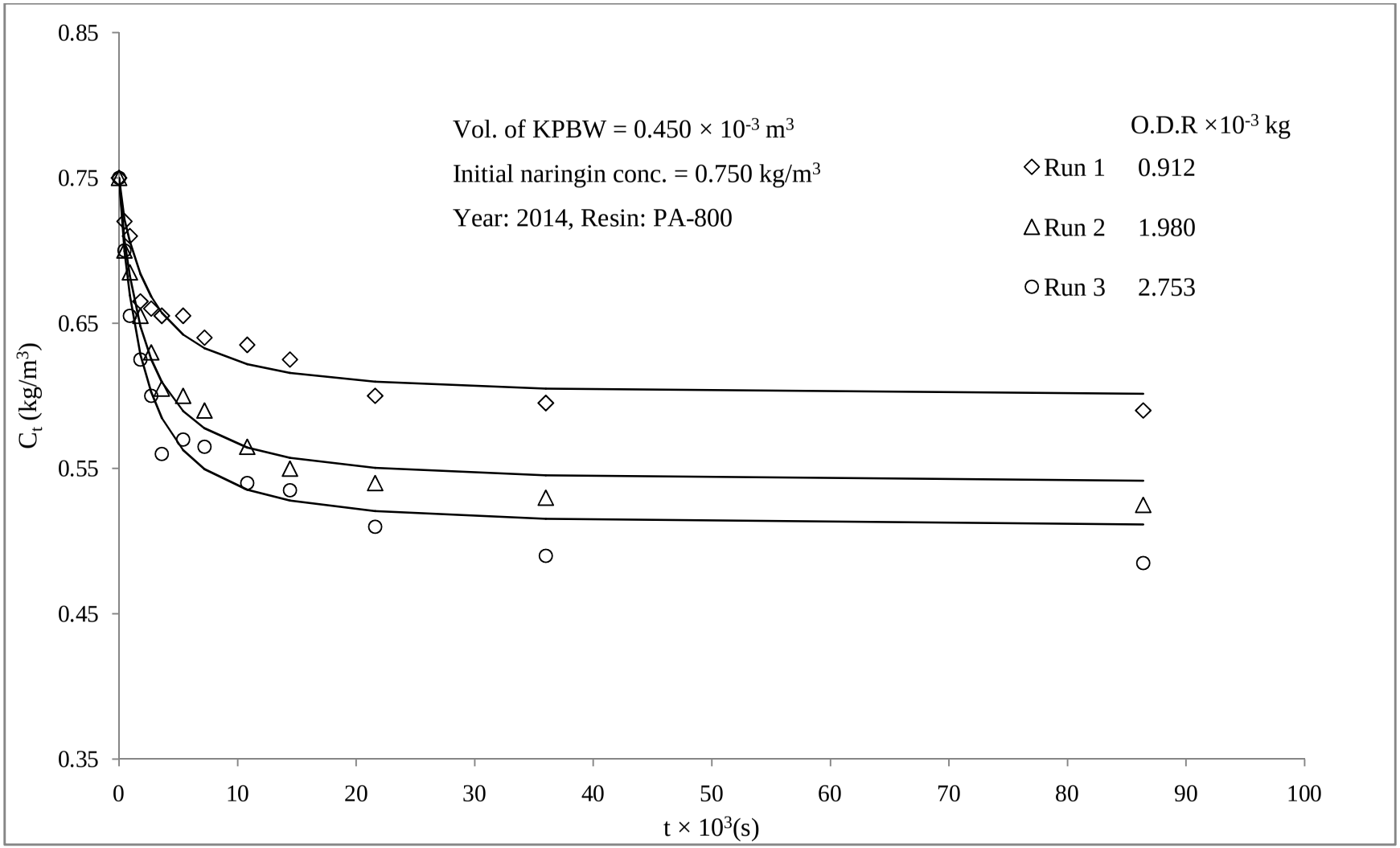

Figure 5.37: Adsorption of naringin on adsorbent PA-800 from fresh KPBW: kinetic studies, correlation of experimental data, C_t *vs* t (system 2, year 2014)

Table 5.20: Statistical analysis for predicted and experimental values of C_t (system 2)

Year	Run	Slope C_{trep} vs. $C_{t\exp}$ passing through origin	R^2	t-Cri	t-Cal	Inference
2012	1	1.000	0.977	2.200	-0.157	NSD
	2	0.991	0.972	2.200	1.753	NSD
	3	1.071	0.966	2.200	-2.364	NSD
	4	1.001	0.974	2.200	-0.131	NSD
	5	1.011	0.987	2.200	-1.826	NSD
2013	6	0.982	0.941	2.200	0.501	NSD
	7	0.998	0.966	2.200	0.101	NSD
	8	1.014	0.949	2.200	-1.959	NSD
	9	1.017	0.939	2.200	-1.338	NSD
2014	10	1.001	0.931	2.200	-0.428	NSD
	11	1.002	0.968	2.200	-0.701	NSD
	12	1.009	0.946	2.200	-1.476	NSD

*NSD- No Significance difference, SD- Significance difference

From the above, it is evident that observed kinetic data could be correlated reasonably using modified adsorption shell model.

The kinetics of adsorption of naringin from kinnow peel boiled water for different years with the same weight of resin have been compared, and it is shown in Figure 5.38. The kinetics of adsorption of naringin from KPBW is almost same in all the years.

5.2.3. Fixed bed column adsorption studies (System 2)

The adsorption column studies were carried out as per the procedure described in the section 3.5.3.

The column studies of the three years samples of KPBW are shown in Figure 5.39. From the Figure 5.39, it was observed that the first 10800 s the concentration of naringin in outgoing solution was almost zero for the year 2012.

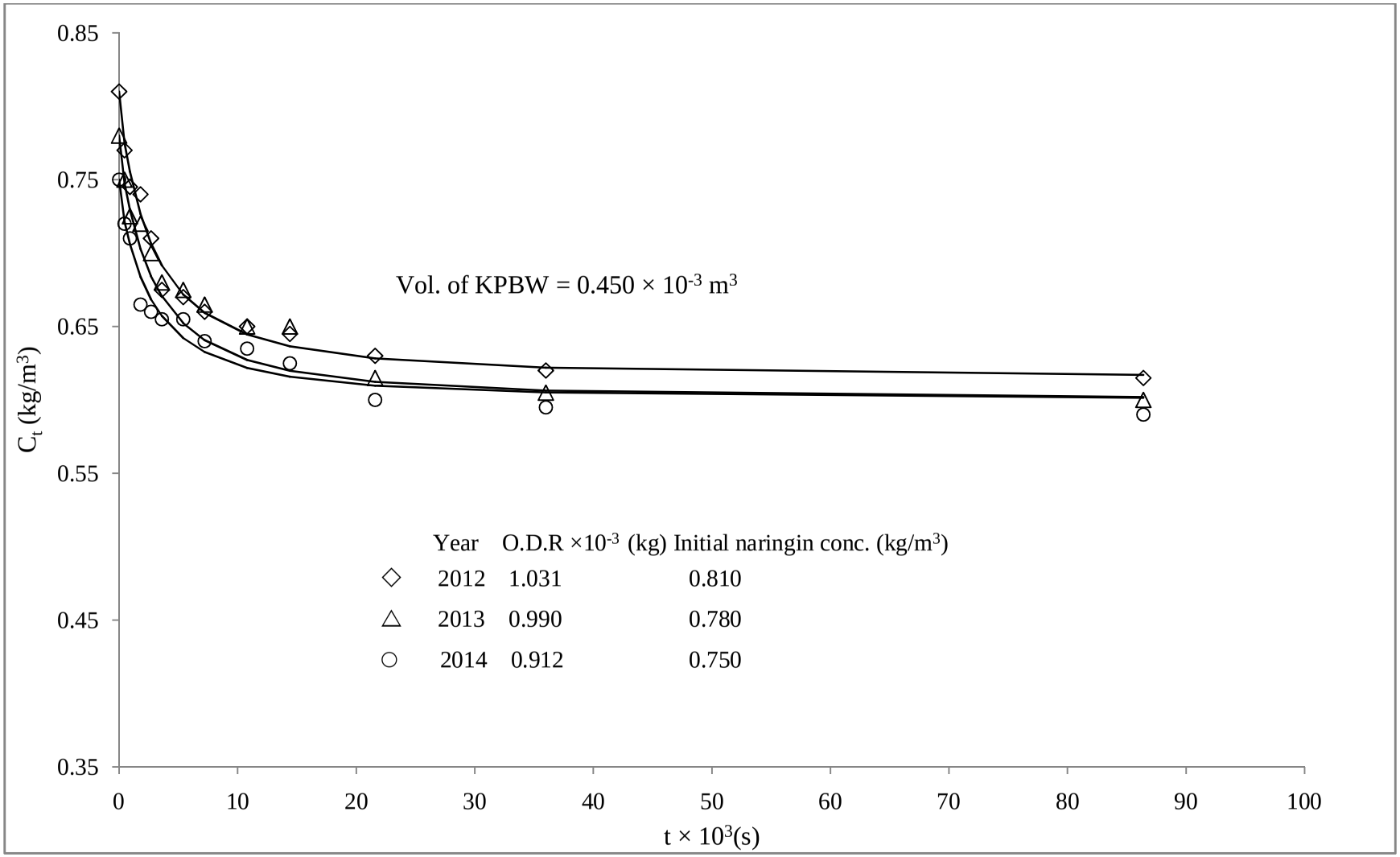

Figure 5.38: Comparison of naringin adsorption kinetic studies on the resin PA-800 from fresh KPBW with year (system 2), C_t *vs t*

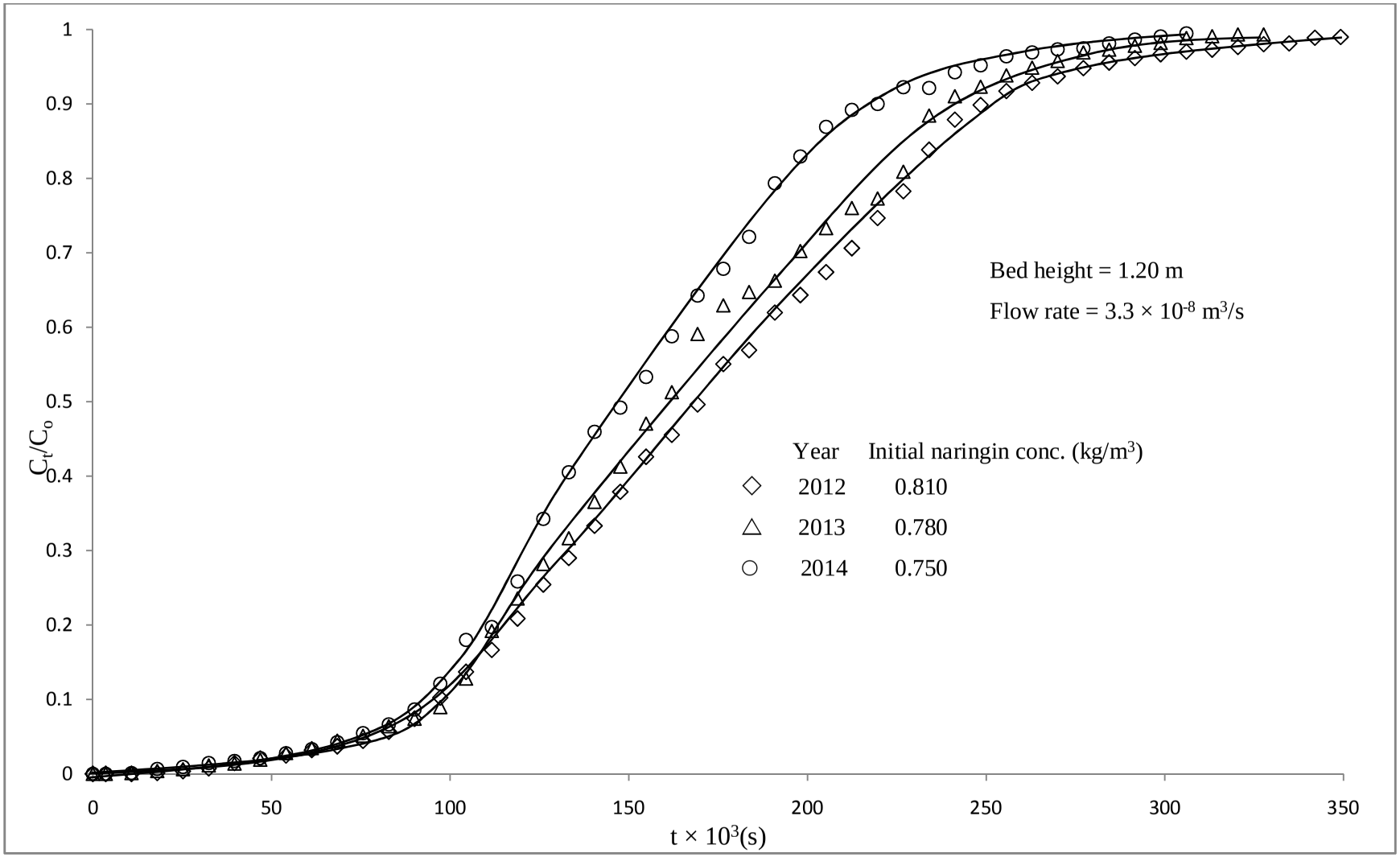

Figure 5.39: Adsorption of naringin on adsorbent PA-800 from fresh KPBW: fixed bed column study (system 2)

The adsorption column data are given in Tables C4 (a-c). The various breakthrough curves parameters are presented for the three years in Table 5.21.

Table 5.21: Parameters of breakthrough curves for adsorption of naringin on resin PA-800 from fresh KPBW in a fixed-bed column for different years

Bed height = 1.20 m, Flow rate = 3.3×10^{-8} m^3/s

S.No	Year	C_o (kg/m^3)	$t_{b\ \times 10^3}$ (s)	$t_{t\ \times 10^3}$ (s)	q_{total} g	q_s kg/kg	H_{UNB} (m)	MTZ (m)
1	2012	0.800	82.8	176.0	4.75	0.087	0.635	0.657
2	2013	0.780	79.2	163.9	4.26	0.106	0.620	0.642
3	2014	0.750	72.0	157.5	3.93	0.088	0.651	0.676

5.2.4. Desorption equilibrium studies (System 2)

The equilibrium studies of desorption of naringin into ethanol from naringin saturated resin were carried out as per the procedure described in the section 3.6.1. The data have been presented in Table C5 and Figure 5.40. Figure 5.40 shows a trend that the desorption is favourable with ethanol but does not approach completion.

The desorption equilibrium experimental data could be correlated with Freundlich adsorption isotherm and its parameters were evaluated and are presented in Table 5.22.

Table 5.22: Freundlich isotherm constants for desorption of naringin from naringin saturated resin PA-800 (fresh peels)

S.No	Year	Freundlich constants		
		K_{fd}	n_d	R^2
1	2012	0.092	1.755	0.919
2	2013	0.117	1.360	0.958
3	2014	0.130	1.219	0.955

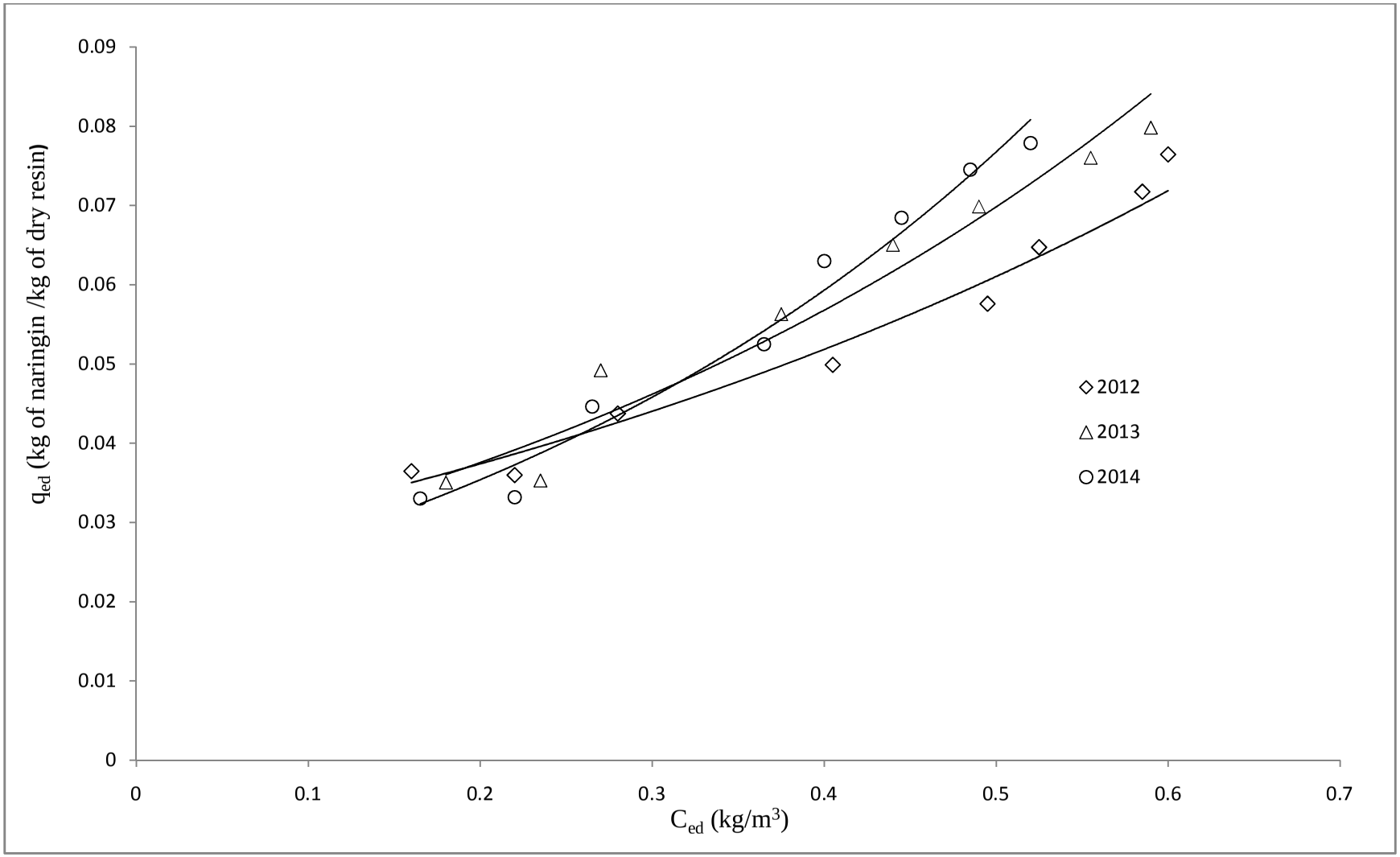

Figure 5.40: Desoption equilibrium studies from naringin saturated resin PA-800 to ethanol solution (system 2)

5.2.5. Desorption kinetic studies (System 2)

The kinetic studies of desorption of naringin into ethanol from naringin saturated resin were carried out as per the procedure described in the section 3.6.2 and data are given in Table C6 (a-c) and Figures 5.41 to 5.43.

Modelling of desorption kinetic data

The above data have been analysed with the same approach as done for System 1 (i.e., Boyd's diffusivity model equation). The values of effective diffusivity D_{ed}, were estimated using linear plots of $\ln\left(1/1-u_d^2(t)\right)$ vs time (t) and presented in Table 5.23. The average value of effective diffusivity D_{ed} was found to be 9.99 $\times 10^{-13}$ ($m^2 s^{-1}$).

Table 5.23: Boyd's diffusivity model parameters for desorption of naringin from naringin saturated resin PA-800 (system 2)

S.No	Run	Year					
		2012		2013		2014	
		$D_{ed} \times 10^{-13}$ $(m^2 s^{-1})$	R^2	$D_{ed} \times 10^{-13}$ $(m^2 s^{-1})$	R^2	$D_{ed} \times 10^{-13}$ $(m^2 s^{-1})$	R^2
1	1	11.3	0.972	11.2	0.958	11.3	0.963
2	2	9.99	0.972	10.6	0.991	9.03	0.975
3	3	9.44	0.977	7.84	0.970	9.07	0.968

The generated C_{td} (with a representative value of D_{ed} = 9.99 $\times 10^{-13}$ $m^2 s^{-1}$) for all the runs are shown by smooth curves as well as experimental data are given for comparison in Figures 5.41 to 5.43.

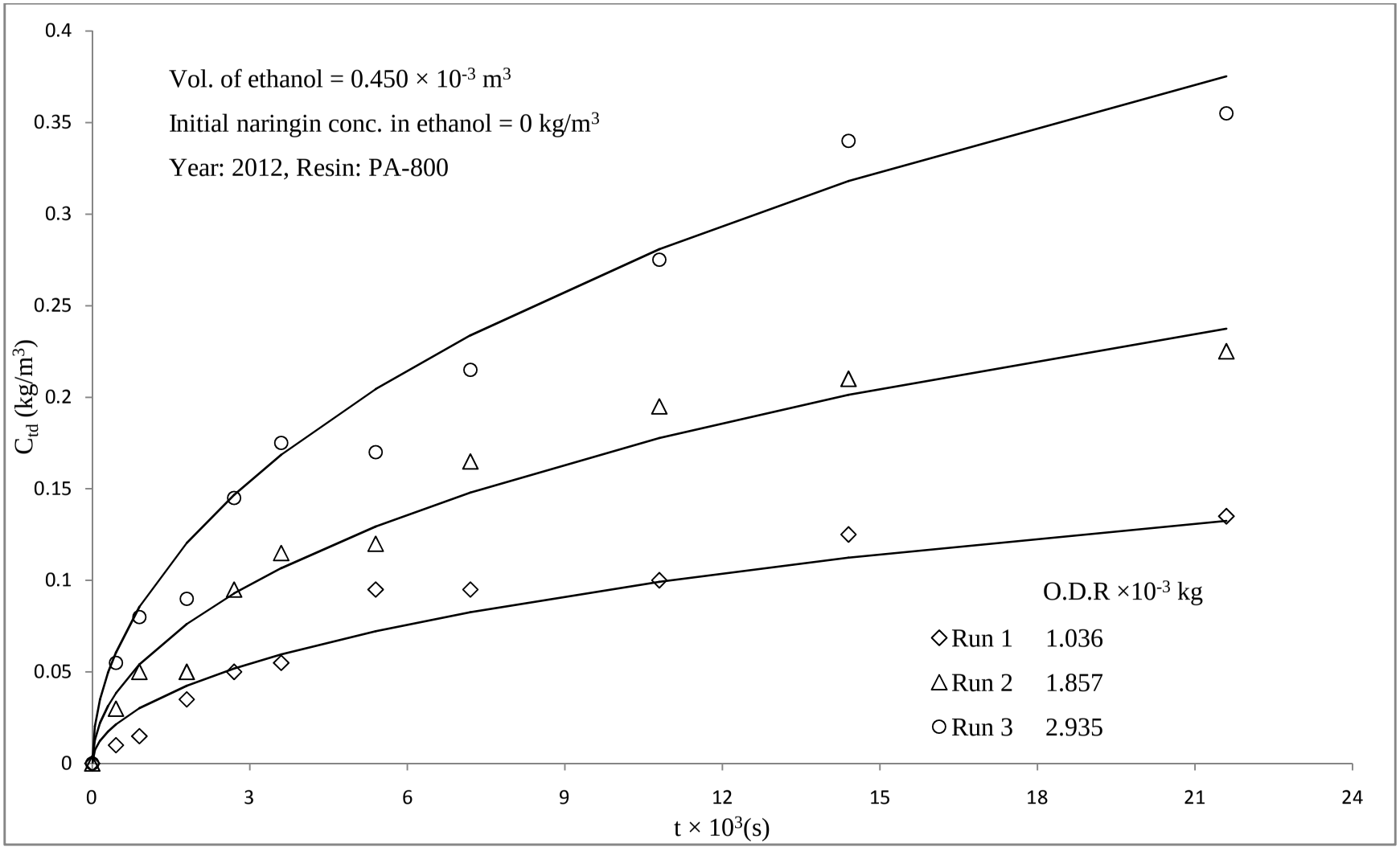

Figure 5.41: Desorption kinetic studies with naringin saturated resin PA-800 in ethanol: correlation of experimental data C_{td} *vs t* (system 2, year 2012)

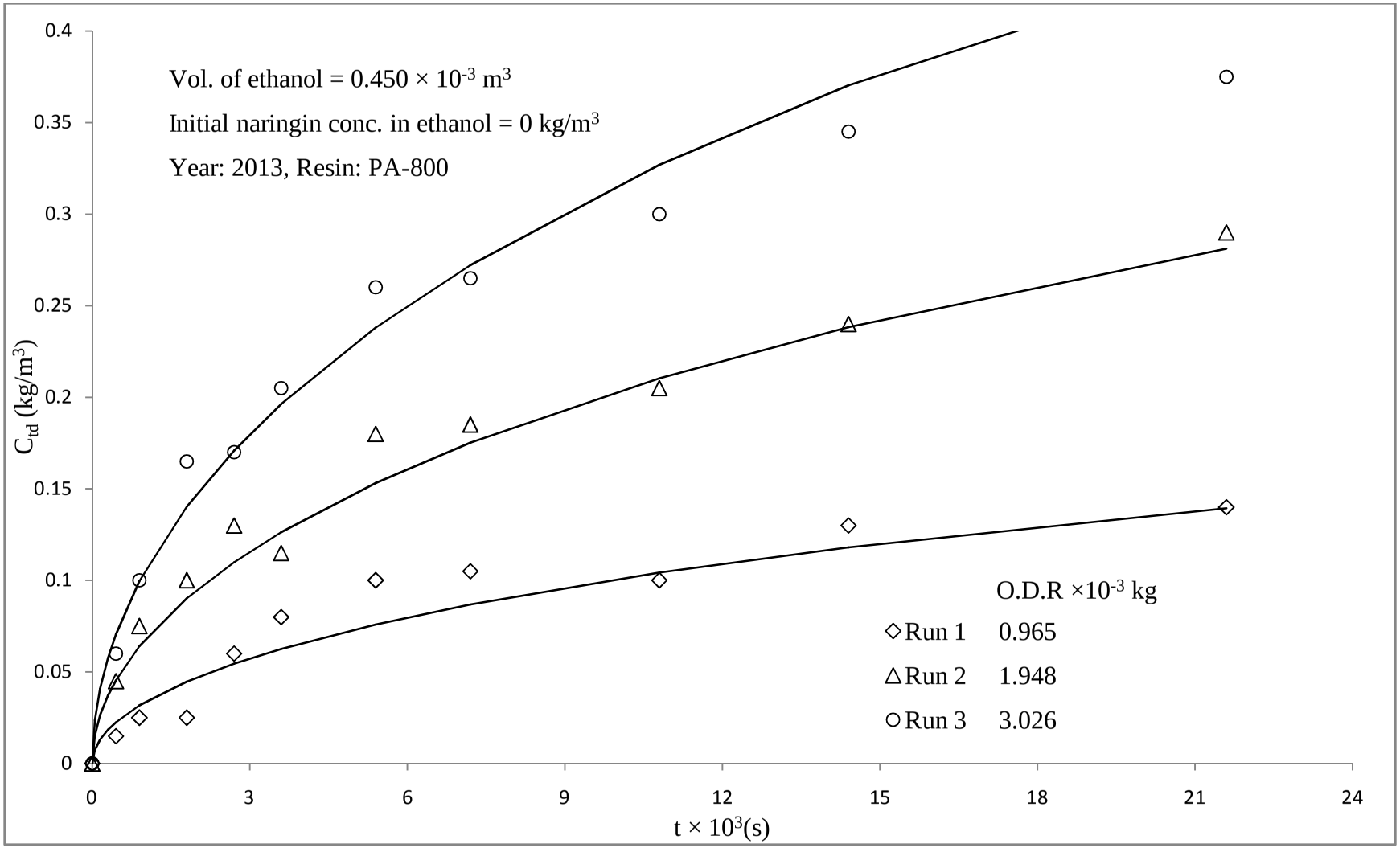

Figure 5.42: Desorption kinetic studies with naringin saturated resin PA-800 in ethanol: correlation of experimental data C_{td} *vs t* (system 2, year 2013)

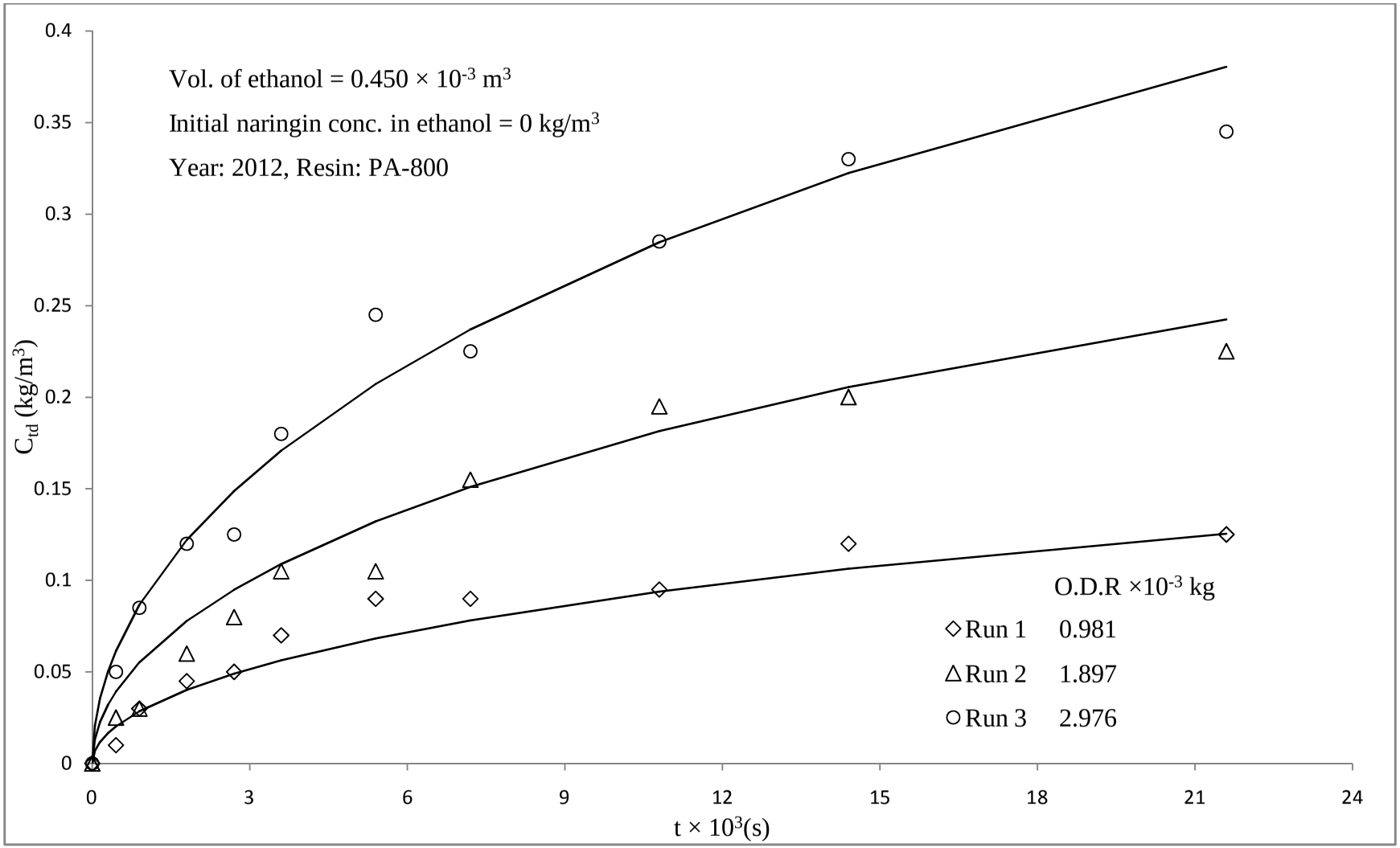

Figure 5.43: Desorption kinetic studies with naringin saturated resin PA-800 in ethanol: correlation of experimental data C_{td} *vs* t (system 2, year 2014)

The data were tested for significance of the mean difference, paired observation by t -test at a 5% level of significance, and it was found that the experimental and predicted data does not differ significantly for almost all the runs. The summary of the statistical analysis of the predicted values from the model and experimental values is given in Table 5.24.

Table 5.24: Statistical analysis for predicted and experimental values of C_{td} (system 2)

Year	Run	Slope	R^2 C_{trep} vs. $C_{t\exp}$	t-Cri	t-Cal	Inference
2012	1	0.936	0.915	2.262	0.282	NSD
	2	0.982	0.955	2.262	-0.156	NSD
	3	1.029	0.967	2.262	6.137	SD
2013	1	0.917	0.895	2.262	0.900	NSD
	2	0.961	0.977	2.262	1.966	NSD
	3	1.051	0.961	2.262	-0.942	NSD
2014	1	0.911	0.944	2.262	1.981	NSD
	2	1.045	0.942	2.262	-2.688	SD
	3	1.01	0.963	2.262	-0.502	NSD

*NSD- No Significance difference, SD- Significance difference

From the above, it is evident that observed kinetic data could be correlated reasonably using Boyd's diffusivity model equation.

Comparison of desorption kinetics:

The naringin desorption kinetics into ethanol from naringin saturated resin for different years with the same mass of resin have been compared, and it is shown in Figure 5.44. The change in concentration of naringin in ethanol is more in the year 2014 when compared to 2012 and 2013. This is due to the composition of peel varies from season to season as well as with place.

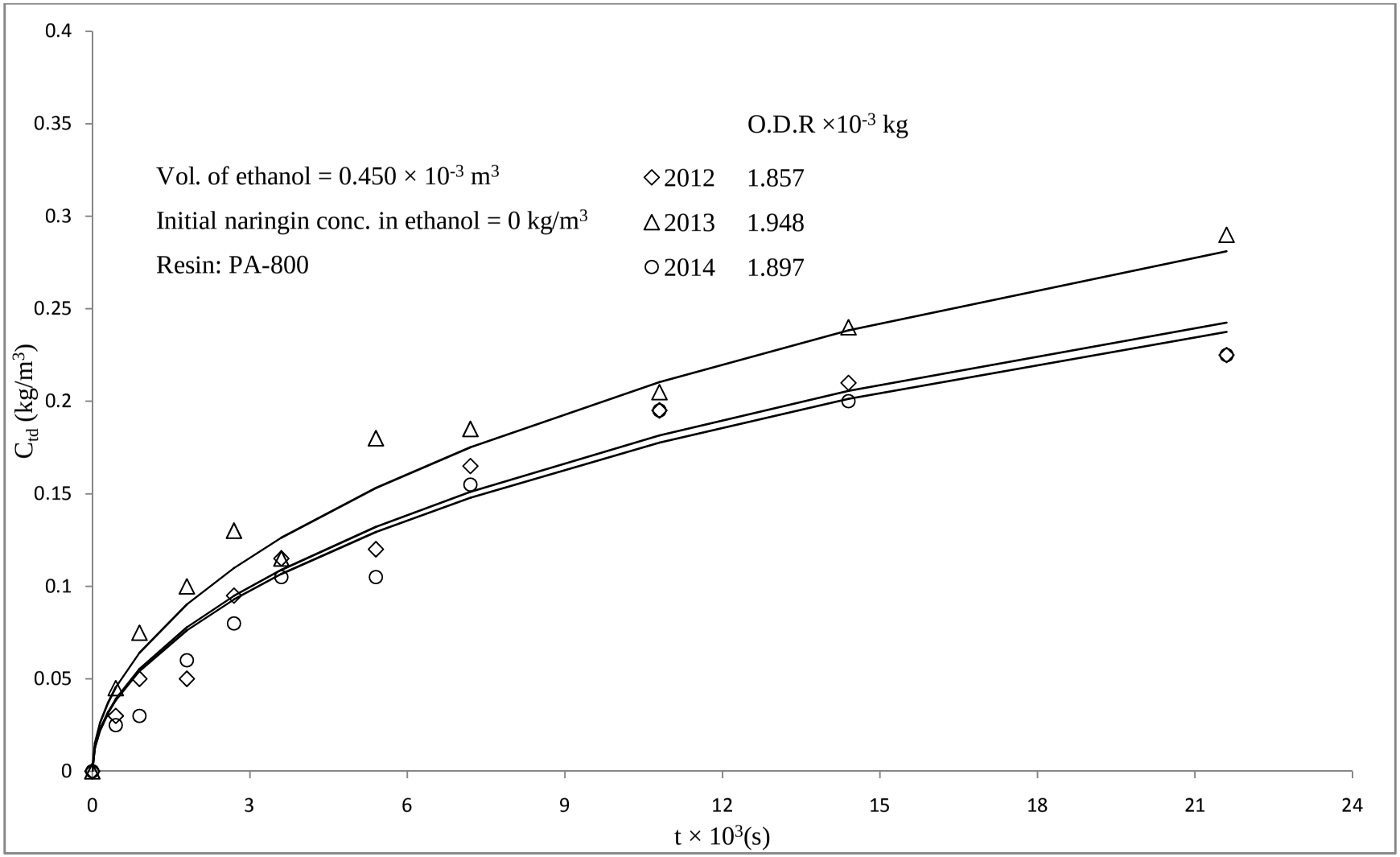

Figure 5.44: Comparison of desorption kinetic studies of naringin saturated resin PA-800 in ethanol with year (system 2), C_{td} *vs t*

5.2.6. Desorption fixed bed column studies (System 2)

The desorption column studies were carried out in glass column as per the procedure described in the section 3.6.3 and presented in Figure 5.45. From the Figure 5.45, it is evident that the amount of naringin desorbed from resin saturated with naringin, obtained from adsorption column studies, in ethanol solution decreases with time. The data of column studies for naringin desorption with ethanol to recover naringin are given in Table C7.

From these desorption study, it can be concluded that about 2100 ml of ethanol is sufficient for almost all the possible recoverable desorption of naringin from the resin PA-800 in a glass column of 14 mm ID filled up to the height 0.95 m (about 120 g naringin saturated resin (wet)).

The amount of naringin desorbed in the column was found to be 3.24, 2.95 and 2.73 g respectively for the years 2012, 2013 and 2014.

5.2.7. Purity and recovery of obtained Naringin and Pectin (System 2)

(A) Naringin recovery

Recovery and purity of naringin were calculated as per the procedure described in section 3.9 and are tabulated in Table 5.25 for the years 2012, 2013 and 2014 respectively.

Table 5.25: Recovery of naringin from fresh peels with resin PA-800

S.No	Year	Naringin Conc. in KPBW (kg/m^3)	Naringin obtained (g)	Purity (%)	Recovery (%)
1	2012	0.810	3.5	92.3	51.9
2	2013	0.780	3.2	90.9	51.3
3	2014	0.750	3.0	88.6	49.2

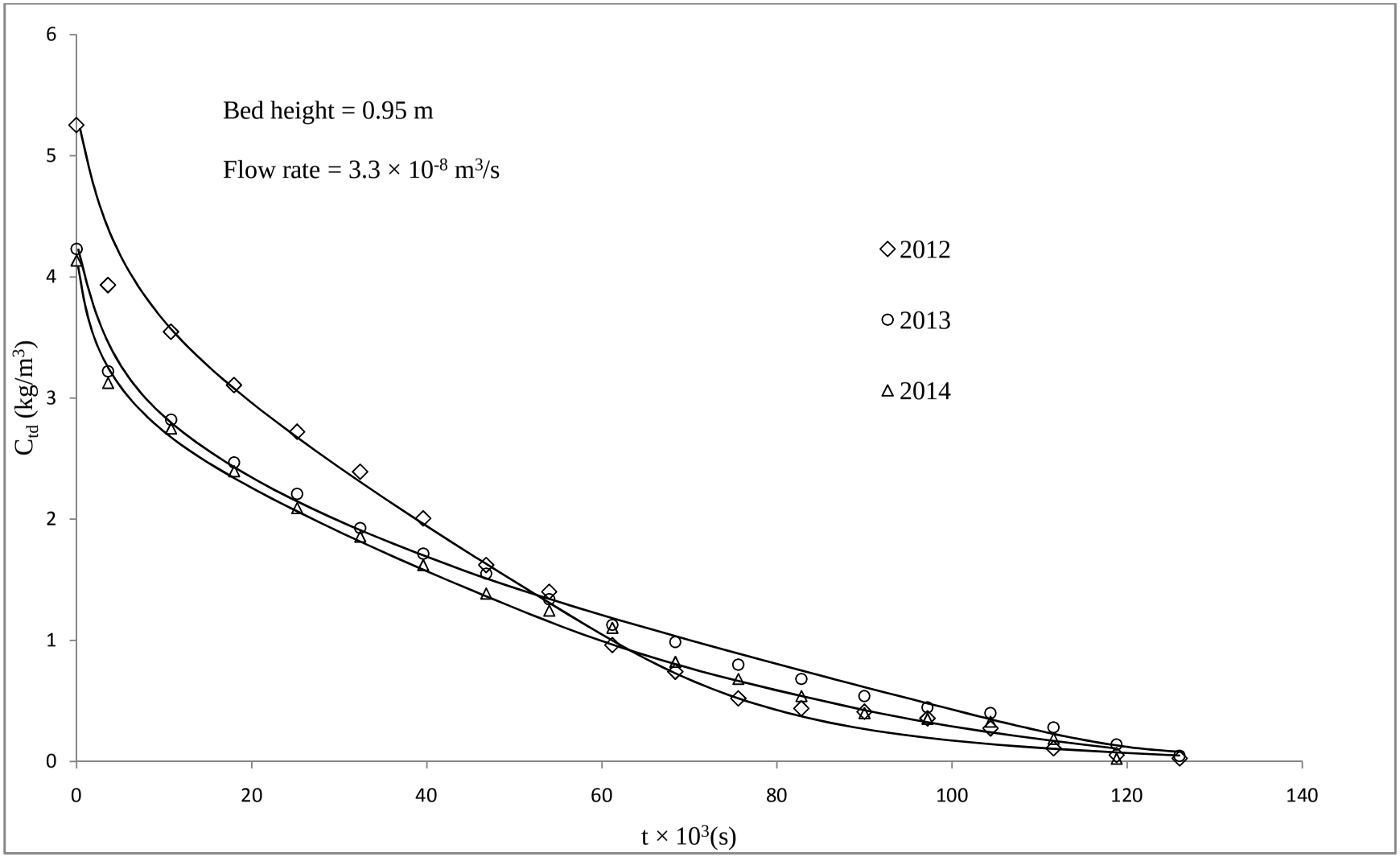

Figure 5.45: Column desorption studies from naringin saturated resin PA-800 into ethanol, C_{td} *vs* t (system 2)

(B) Recovery of pectin and characterization

The recovery of pectin was calculated as per the procedure described in section 3.9. The obtained pectin was characterised, the values of different parameters determined are tabulated in Table 5.26.

Table 5.26: Recovery of pectin from fresh peels with resin PA-800

S.No	Year	Recovey (%)	Moisture (%)	Ash (%)	Equivalent weigh (mg/ml)	Methoxyl content (%)	Anhdrouronic acid (%)	DE (%)
1	2012	60.2	7.6	8.1	658.4	5.94	56.4	59.7
2	2013	61.0	8.4	7.5	626.2	6.55	68.7	54.1
3	2014	60.9	7.9	8.2	634.5	6.42	62.5	58.2

5.3. Adsorption-Desorption studies of naringin with dropped peels on Resin PA-500 (System 3)

The naringin content of dropped kinnow peel boiled water (extracts) from the two years (2012 and 2013) samples was determined and was found to be 0.890 and 0.935 kg/m^3 respectively.

5.3.1. Adsorption equilibrium studies (System 3)

The adsorption equilibrium studies with kinnow peel boiled water were carried out as per the procedure described in the section 3.5.1. The data have been presented in Table D1 and Figure 5.46. The adsorption equilibrium experimental data could be correlated by using Langmuir adsorption isotherm and its parameters were evaluated and are given in Table 5.27. It was found that the maximum naringin that can be picked up by resin PA-500 from the dropped KPBW (calculated from Langmuir adsorption isotherm constants) was 0.180 and 0.149 kg per kg of dry resin respectively for the years 2012 and 2013.

Table 5.27: Langmuir isotherm parameters for adsorption of naringin on resin PA-500 from dropped KPBW

S.No	Year	Langmuir constants		
		a	b	R^2
1	2012	0.232	1.287	0.954
2	2013	0.392	2.630	0.969

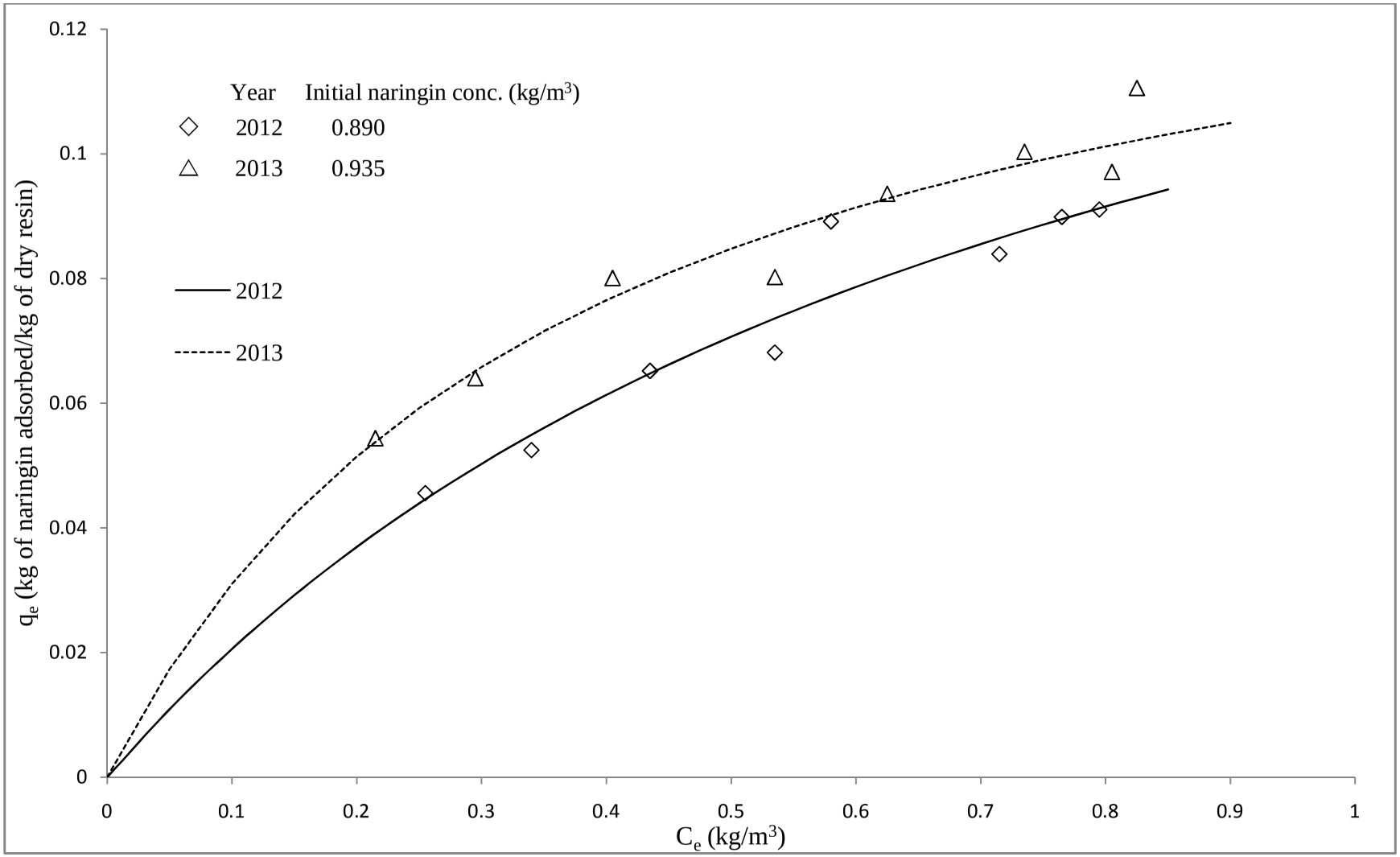

Figure 5.46: Adsorption equilibrium studies with dropped KPBW on resin PA-500 in two years (system 3)

5.3.2. Adsorption kinetic studies (System 3)

The adsorption kinetic studies were carried out as per the procedure described in the section 3.5.2. The concentration of naringin in the solution (KPBW) as a function of time during adsorption for various amounts of resin is presented in Figures 5.47 and 5.48 for the years 2012 and 2013 respectively. The data obtained in these experiments are given in Tables D2 (a-b). It may be observed that the rate of change in concentration of a solution is more when the weight of the resin used is more. The observations are similar to as in the case of system 1.

Modelling of adsorption kinetic data

The above data have been analysed with the same approach (modified adsorption shell model) as discussed in the earlier for system 1. The values of different parameters viz. slopes of $F_n(t)$ vs. t plots, K, β and ψ are tabulated below (Table 5.28) for all the runs of both the years.

Table 5.28: Modified adsorption shell model parameters for system 3

$D_P = 1.032\times10^{-10}\, m^2/s$, $\varepsilon = 0.39$, $R_p = 0.375\times10^{-3}$ m

Year	Run	C_o kg/m^3	q_e kg/m^3	Slope × 10^{-4} (s^{-1})	K	β	ψ	$\frac{D_c}{r_c^2}$ × 10^{-4} (s^{-1})
2012	1	0.890	110.5	2.80	184.9	301.5	2.42	3.80
	2	0.890	69.23	2.81	116.6	107.9	1.38	2.17
	3	0.890	56.43	3.72	125.6	128.2	2.02	3.16
	4	0.890	40.45	3.26	78.94	41.61	0.91	1.43
2013	1	0.935	100.4	2.65	151.6	195.8	1.82	2.85
	2	0.935	69.41	3.06	120.9	117.3	1.58	2.47
	3	0.935	54.15	3.77	116.1	106.8	1.84	2.89
	4	0.935	49.05	4.00	111.8	97.79	1.86	2.92

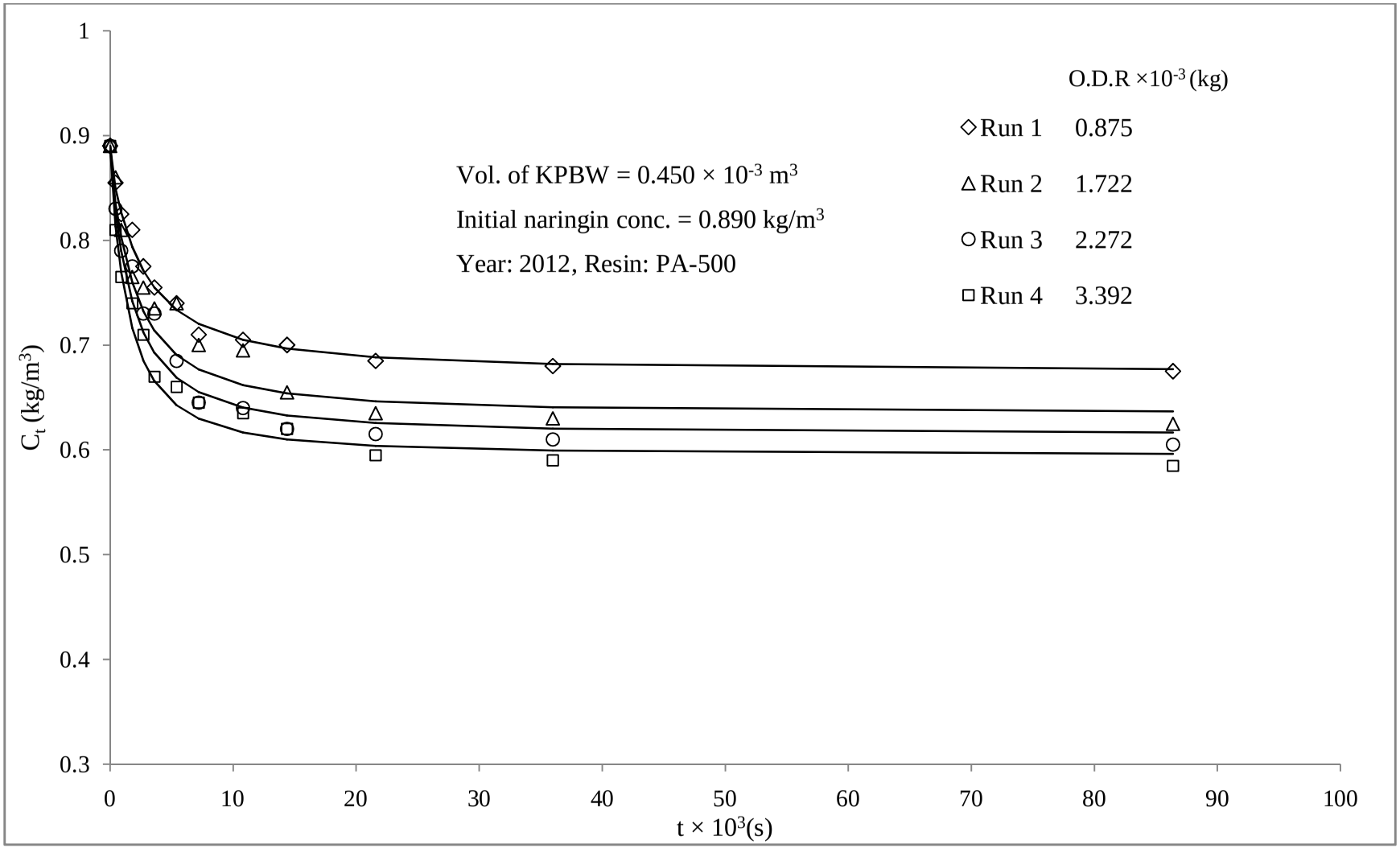

Figure 5.47: Adsorption of naringin on adsorbent PA-500 from dropped KPBW: kinetic studies, correlation of experimental data, C_t *vs t* (system 3, year 2012)

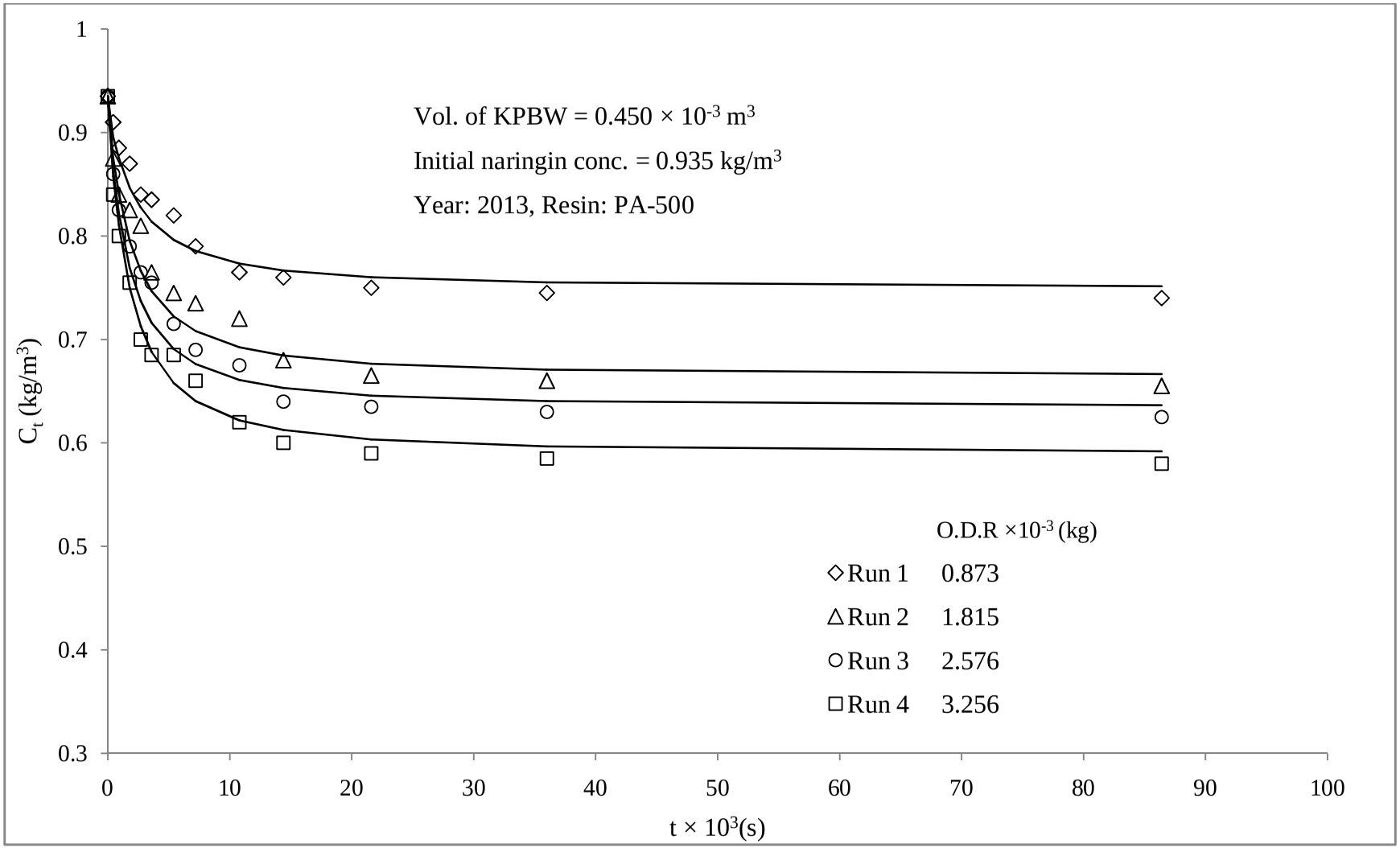

Figure 5.48: Adsorption of naringin on adsorbent PA-500 from dropped KPBW: kinetic studies, correlation of experimental data, C_t *vs t* (system 3, year 2013)

The generated C_t (with a representative value of ψ = 1.733) for all the runs are shown by smooth curves as well as experimental data are given for comparison in Figures 5.47 and 5.48.

The data were tested for significance of the mean difference, paired observation by t -test at a 5% level of significance, and it was found that the experimental and predicted data for almost all the runs does not differ significantly. The summary of the statistical analysis values is given in Table 5.29.

Table 5.29: Statistical analysis for predicted and experimental values of C_t (system 3)

Year	Run	Slope C_{trep} vs. $C_{t\exp}$ passing through origin	R^2	t-Cri	t-Cal	Inference
2012	1	0.997	0.987	2.200	0.749	NSD
	2	0.981	0.919	2.200	2.281	SD
	3	0.992	0.937	2.200	0.851	NSD
	4	0.990	0.965	2.200	1.634	NSD
2013	1	0.992	0.929	2.200	1.282	NSD
	2	0.984	0.925	2.200	1.920	NSD
	3	0.988	0.945	2.200	1.510	NSD
	4	1.005	0.974	2.200	-0.884	NSD

*NSD- No Significance difference, SD- Significance difference

From the above, it is evident that observed kinetic data could be correlated reasonably using modified adsorption shell model.

Comparison of adsorption kinetics:

The kinetics of adsorption of naringin from kinnow peel boiled water for different years with the same weight of resin have been compared, and it is shown in Figure 5.49. The rate of change in concentration of naringin in solution is almost same in 2012 and 2013.

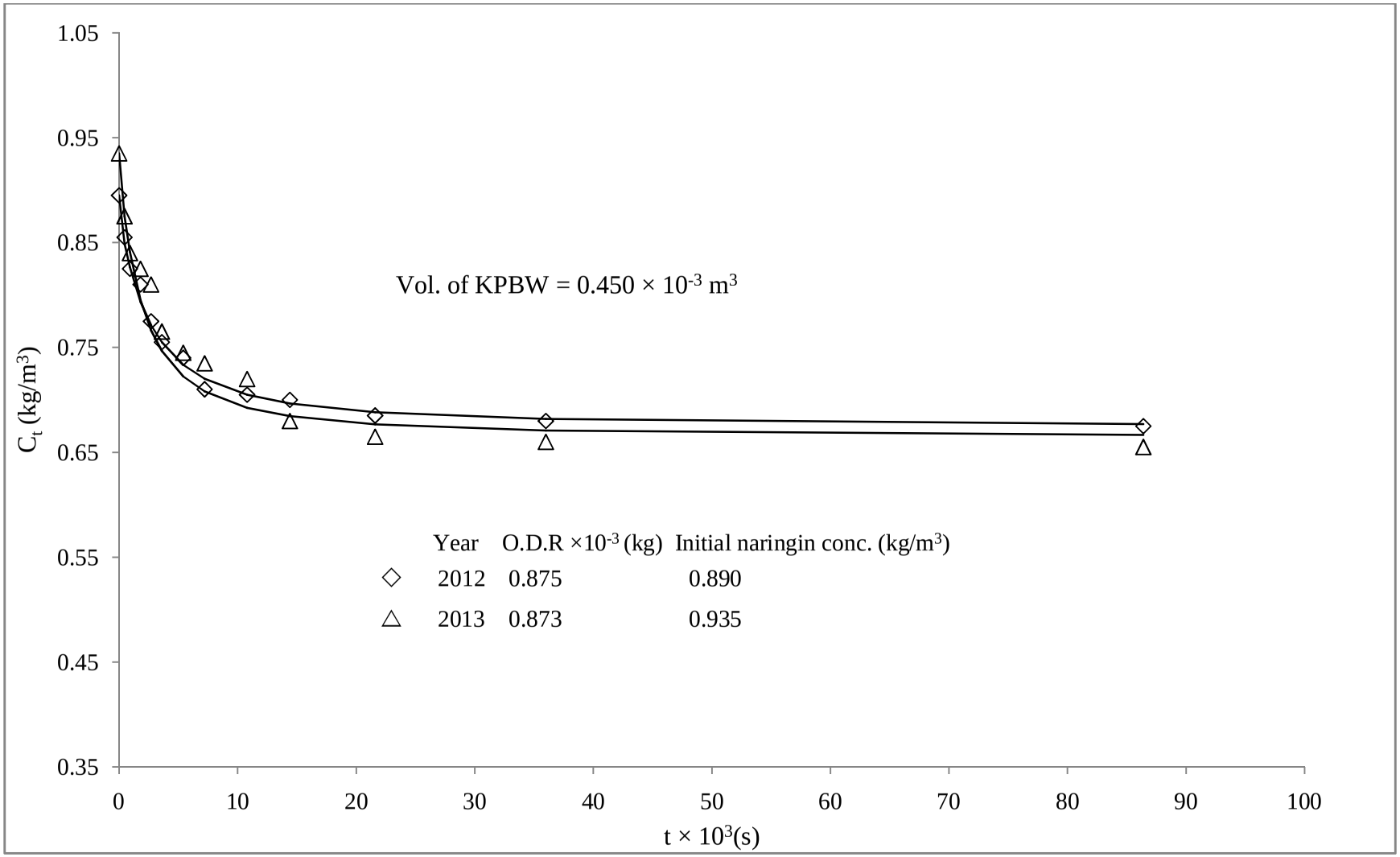

Figure 5.49: Comparison of naringin adsorption kinetic studies on the resin PA-500 from dropped KPBW with year (system 3), C_t *vs t*

5.3.3. Fixed bed column adsorption studies (System 3)

The adsorption column studies were carried out as per the procedure described in the section 3.5.3. The column studies of the different year's samples of KPBW is shown in Figure 5.50, and it was found that the first 14400 (s) the concentration of naringin in outgoing solution was almost zero for both years.

The adsorption column data are given in Tables D3 (a-b). The various parameters of breakthrough curves are presented for the two years in Table 5.30.

Table 5.30: Parameters of breakthrough curves for adsorption of naringin on resin PA-500 from dropped KPBW in a fixed-bed column for two years

Bed height = 1.20 m, Flow rate = 3.3×10^{-8} m^3/s

S.No	Year	C_o (kg/m^3)	$t_b \times 10^3$ (s)	$t_t \times 10^3$ (s)	q_{total} g	q_s kg/kg	H_{UNB} (m)	MTZ (m)
1	2012	0.890	81.0	166.7	4.97	0.094	0.617	0.648
2	2013	0.935	93.6	185.5	5.78	0.104	0.594	0.612

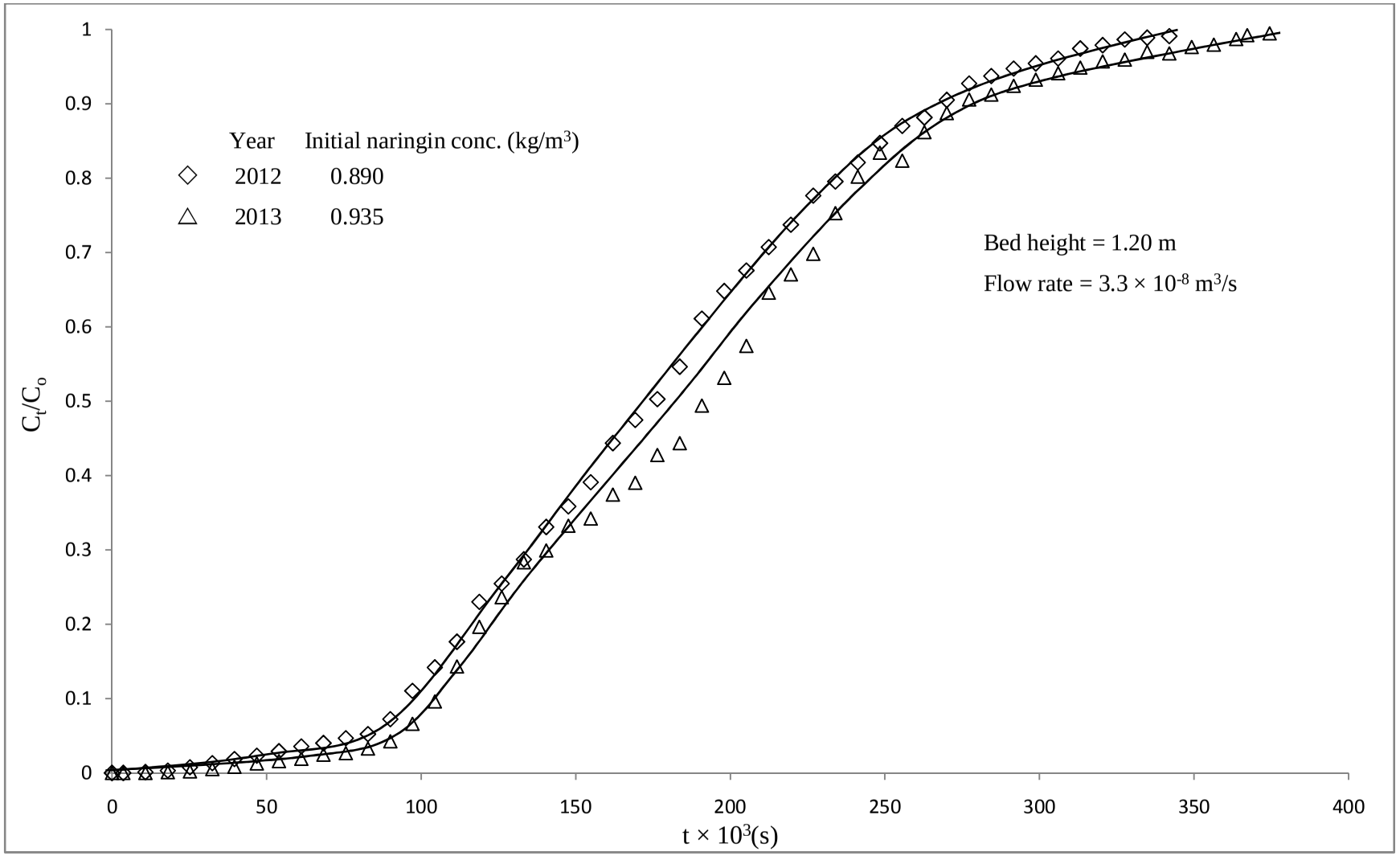

Figure 5.50: Adsorption of naringin on adsorbent PA-500 from dropped KPBW: fixed bed column study (system 3)

5.3.4. Desorption equilibrium studies (System 3)

The desorption equilibrium studies with ethanol from naringin saturated resin were carried out as per the procedure described in the section 3.6.1.

The data have been presented in Table D4 and Figure 5.51. The data show that the desorption is favourable with ethanol but does not approach completion. The desorption equilibrium experimental data could be correlated with Freundlich adsorption isotherm, and its constants are presented in Table 5.31.

Table 5.31: Freundlich isotherm constants for desorption of naringin from naringin saturated resin PA-500 (dropped peels)

S.No	Year	Freundlich constants		
		K_{fd}	n_d	R^2
1	2012	0.108	1.632	0.943
2	2013	0.155	1.139	0.981

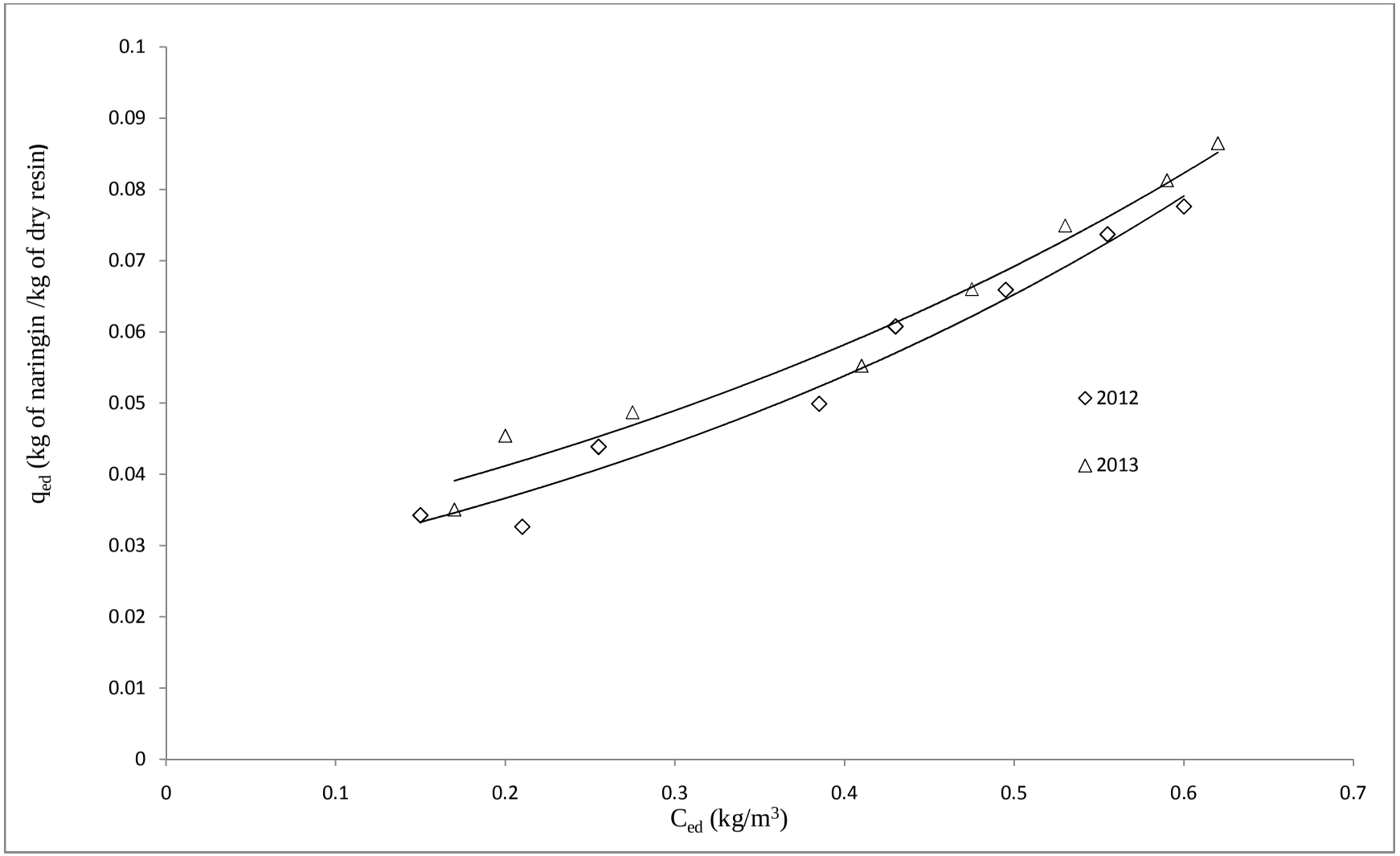

Figure 5.51: Desoption equilibrium studies from naringin saturated resin PA-500 to ethanol solution (system 3)

5.3.5. Desorption kinetic studies (System 3)

The Desorption kinetic studies with ethanol from naringin saturated resin were carried out as per the procedure described in the section 3.6.2 and data are presented in Tables D5 (a-b) in Figures 5.52 and 5.53

Modelling of desorption kinetic data

The above data have been analysed with the same approach as done for System 1 (i.e., Boyd's diffusivity model equation).

The values of effective diffusivity D_{ed}, were estimated using linear plots of $\ln\left(1/1-u_d^2(t)\right)$ vs time (t) and presented in Table 5.32. The average value of effective diffusivity D_{ed} is found to be 11.4 $\times 10^{-13}$ ($m^2 s^{-1}$).

Table 5.32: Boyd's diffusivity model parameters for desorption of naringin from naringin saturated resin PA-500 (system 3)

S.No	Run	Year			
		2012		2013	
		$D_{ed} \times 10^{-13}$ $(m^2 s^{-1})$	R^2	$D_{ed} \times 10^{-13}$ $(m^2 s^{-1})$	R^2
1	1	13.6	0.955	13.0	0.967
2	2	11.1	0.983	12.0	0.970
3	3	9.22	0.974	9.67	0.950

The generated C_{td} (with a representative value of D_{ed} = 11.4 $\times 10^{-13} m^2 s^{-1}$) for all the runs are shown by smooth curves, and experimental data are given for comparison in Figures 5.52 and 5.53.

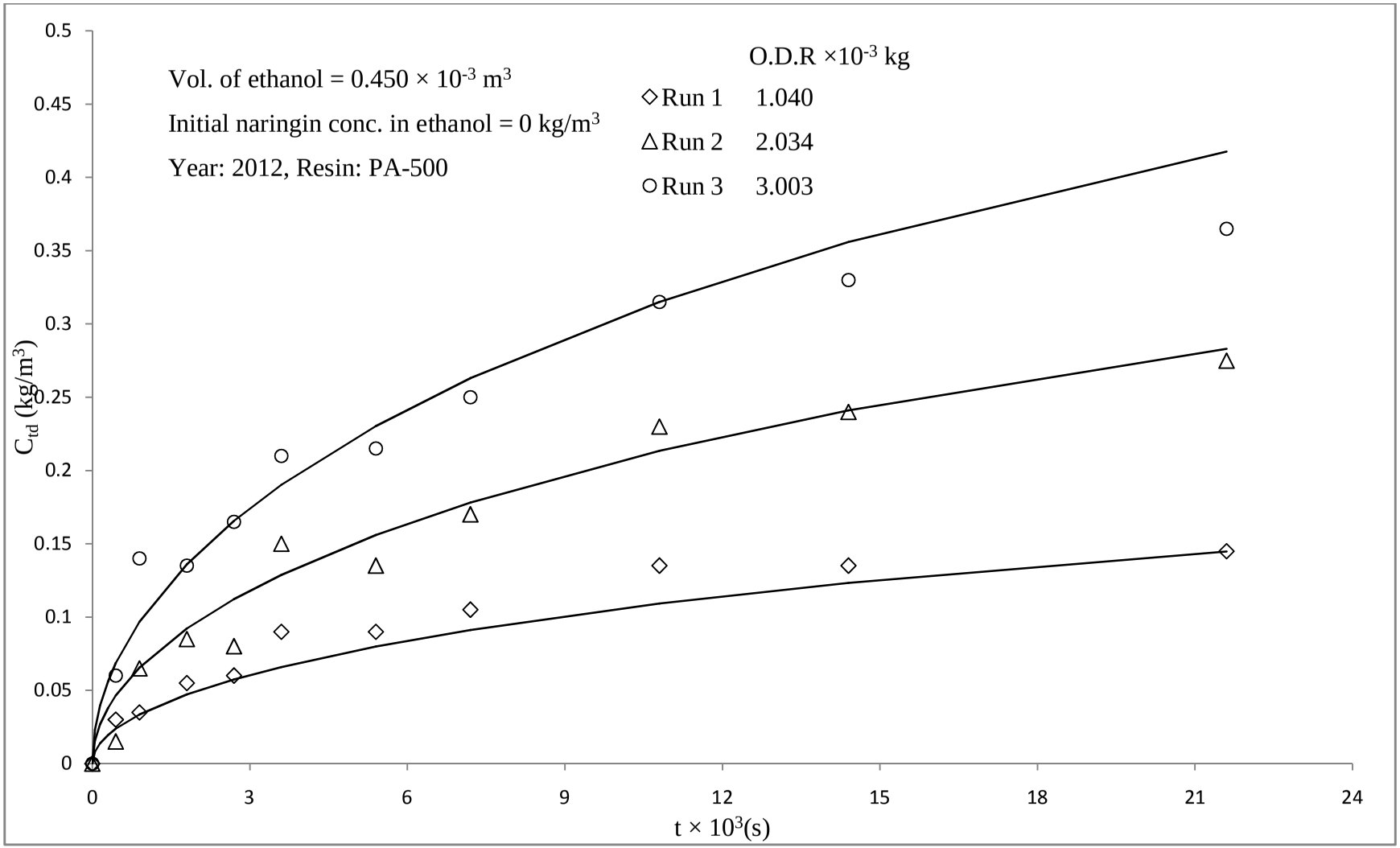

Figure 5.52: Desorption kinetic studies with naringin saturated resin PA-500 in ethanol: correlation of experimental data C_{td} *vs t* (system 3, year 2012)

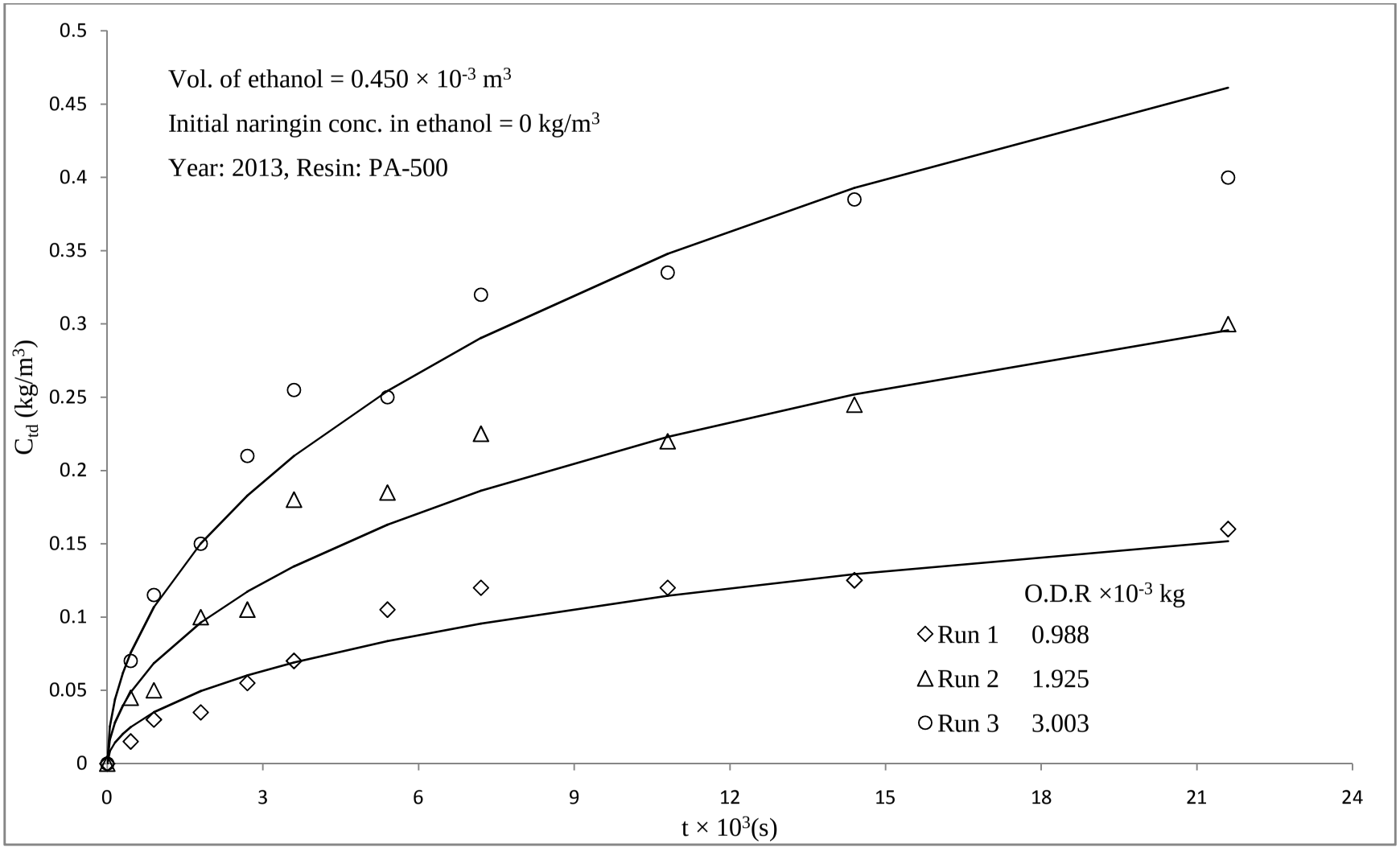

Figure 5.53: Desorption kinetic studies with naringin saturated resin PA-500 in ethanol: correlation of experimental data C_{td} *vs t* (system 3, year 2013)

The data were tested for significance of the mean difference, paired observation by t -test at a 5% level of significance, and it was found that the experimental and predicted data for almost all the runs does not differ significantly.

The summary of the statistical analysis of the predicted values from the model and experimental values is given in Table 5.33.

Table 5.33: Statistical analysis for predicted and experimental values of C_{td} (system 3)

Run	Year	Slope	R^2 C_{trep} vs. $C_{t\exp}$	t-Cri	t-Cal	Inference
1	2012	0.888	0.956	2.262	3.708	SD
2		1.012	0.938	2.262	-1.274	NSD
3		1.044	0.956	2.262	-0.669	NSD
1	2013	0.938	0.923	2.262	0.530	NSD
2		0.947	0.937	2.262	1.028	NSD
3		1.007	0.946	2.262	0.191	NSD

*NSD- No Significance difference. SD- Significance difference

From the above, It is evident that observed kinetic data could be correlated reasonably using Boyd's diffusivity model equation.

Comparison of desorption kinetics:

The kinetics of naringin desorption from resin saturated with naringin to ethanol for the two different years with the same mass of resin has been compared, and it is shown in Figure 5.54. The rate of desorption of naringin in ethanol solution is almost same in both years.

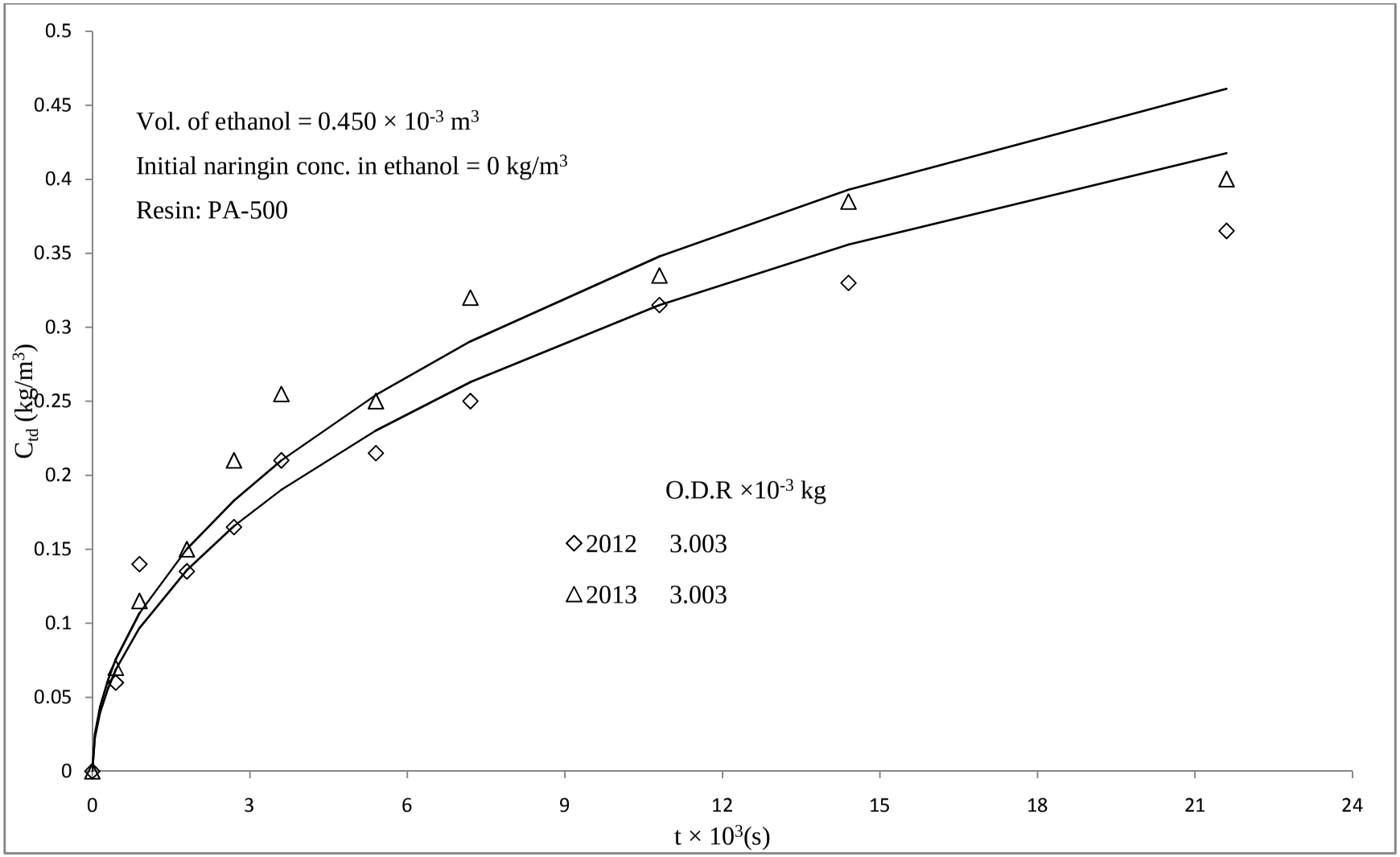

Figure 5.54: Comparison of desorption kinetic studies of naringin saturated resin PA-500 in ethanol with year (system 3), C_{td} *vs t*

5.3.6. Desorption fixed bed column studies (System 3)

The desorption column studies were carried out in glass column as per the procedure described in the section 3.6.3 and presented in Figure 5.55. From the Figure 5.55, it is evident that the amount of naringin desorbed from resin saturated with naringin, obtained from adsorption column studies, in ethanol solution decreases with time. The data of column studies for naringin desorption with ethanol to recover naringin are given in Table D6.

From these desorption studies it can be concluded that about 1700 ml of ethanol is sufficient for almost all the possible recoverable desorption of naringin from the resin PA-500 in a glass column of 14 mm ID filled up to the height 0.95 m (about 120 g naringin saturated resin (wet)). The amount of naringin desorbed in the column was found to be 3.40 and 3.69 g respectively for the years 2012 and 2013.

5.3.7. Purity and recovery of obtained Naringin and Pectin (System 3)

(A) Naringin recovery

Recovery and purity of naringin were calculated as per the procedure described in section 3.9 and are tabulated in Table 5.34 for the years 2012 and 2013 respectively.

Table 5.34: Recovery of naringin from dropped peels with resin PA-500

S.No	Year	Naringin Conc. in KPBW (kg/m^3)	Naringin obtained (g)	Purity (%)	Recovery (%)
1	2012	0.890	3.7	88.2	52.2
2	2013	0.935	3.9	91.3	51.1

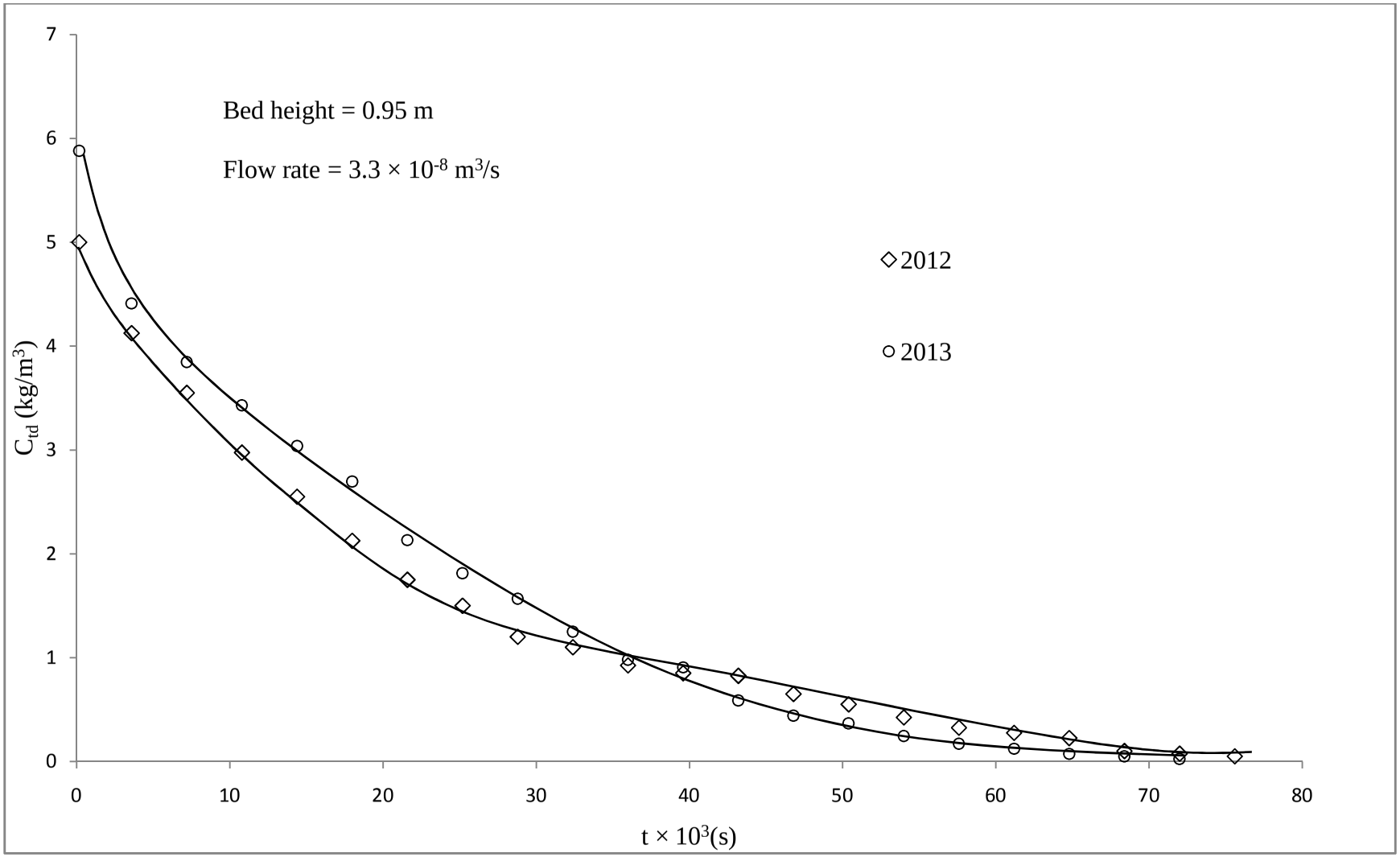

Figure 5.55: Column desorption studies from naringin saturated resin PA-500 into ethanol, C_{td} *vs* t (system 3)

(B) Recovery of pectin and characterization

The recovery of pectin was calculated as per the procedure described in section 3.10. The obtained pectin was characterised, the values of different parameters determined are tabulated in Table 5.35.

Table 5.35: Recovery of pectin from dropped peels with resin PA-500

S. No	Year	Recovey (%)	Moisture (%)	Ash (%)	Equivalent weigh (mg/ml)	Methoxyl content (%)	Anhdrouronic acid (%)	DE (%)
1	2012	53.4	8.95	9.6	551.0	6.97	69.5	56.9
2	2013	50.3	9.49	8.4	468.2	6.01	66.9	51.0

5.4. Adsorption-Desorption studies for naringin with Dropped peels on Resin PA-800 (System 4)

5.4.1. Adsorption equilibrium studies (System 4)

The adsorption equilibrium studies with kinnow peel boiled water were carried out as per the procedure described in the section 3.5.1. The data have been presented in Table E1 and Figure 5.56. The adsorption equilibrium experimental data could be correlated by using Langmuir adsorption isotherm and its parameters were evaluated and are listed in Table 5.36. It may be noted that the naringin concentration in solution (KPBW) was 0.890 and 0.935 kg/m^3 respectively in the years 2012 and 2013. The maximum amount of naringin that can be picked up by resin PA-800 (calculated from Langmuir adsorption isotherm constants) was found to be 0.175 and 0.170 kg per kg of dry resin respectively in the years 2012 and 2013.

Table 5.36: Langmuir isotherm parameters for adsorption of naringin on resin PA-800 from dropped KPBW

S.No	Year	Langmuir constants		
		a	b	R^2
1	2012	0.384	2.194	0.938
2	2013	0.584	3.423	0.947

5.4.2. Adsorption kinetic studies (System 4)

The adsorption kinetic studies were carried out as per the procedure described in the section 3.5.2. The concentration of naringin in the solution as a function of time during adsorption for various amounts of resin is presented in Figures 5.57 and 5.58 for the years 2012 and 2013.

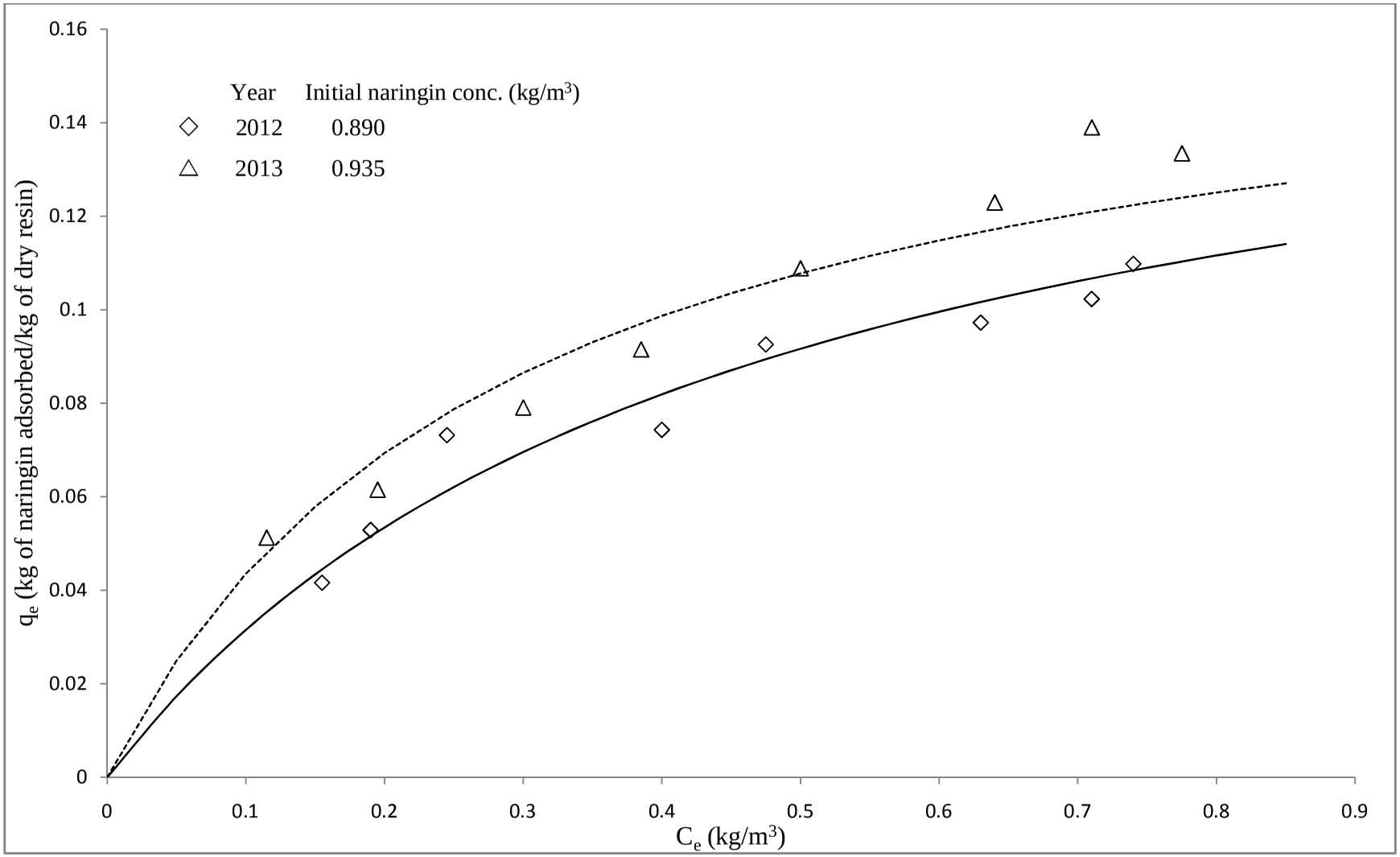

Figure 5.56: Adsorption equilibrium studies with dropped KPBW on resin PA-800 in two years (system 4)

The data obtained in these experiments are given in Tables E2 (a-b). It may be observed from the data that the rate of change in concentration of a solution is more when the mass of the resin used is more.

Modelling of adsorption kinetic data

The above data have been analyzed with the same approach (modified adsorption shell model) as discussed in the earlier for system 1. The C_t values were used to calculate F_n values. The values of different parameters viz. slopes of $F_n(t)$ vs t plots, K, β and ψ are tabulated below (Table 5.37) for all the runs of both the years.

Table 5.37: Modified adsorption shell model parameters for system 4

$D_P = 1.032\times10^{-10} m^2/s, \varepsilon = 0.39,\ R_p = 0.48\times10^{-3}$ m

Year	Run	Year	C_o kg/m^3	q_e kg/m^3	Slope × 10^{-4} (s^{-1})	K	β	ψ	$\frac{D_c}{r_c^2}$ × 10^{-4} (s^{-1})
2012	1	2012	0.890	105.2	3.13	322.7	931.0	7.87	7.51
	2		0.890	88.79	3.73	325.2	944.5	9.46	9.04
	3		0.890	69.10	3.03	205.2	375.6	4.83	4.62
	4		0.890	63.27	4.81	298.3	799.1	11.2	10.7
2013	1	2013	0.935	124.0	2.86	331.4	979.8	7.38	7.05
	2		0.935	91.72	4.17	357.0	1128.7	11.5	11.0
	3		0.935	82.51	4.07	313.7	881.3	9.98	9.53

The generated C_t (with a representative value of ψ = 8.899) for all the runs are shown by smooth curves, and experimental data are given for comparison in Figures 5.57 and 5.58.

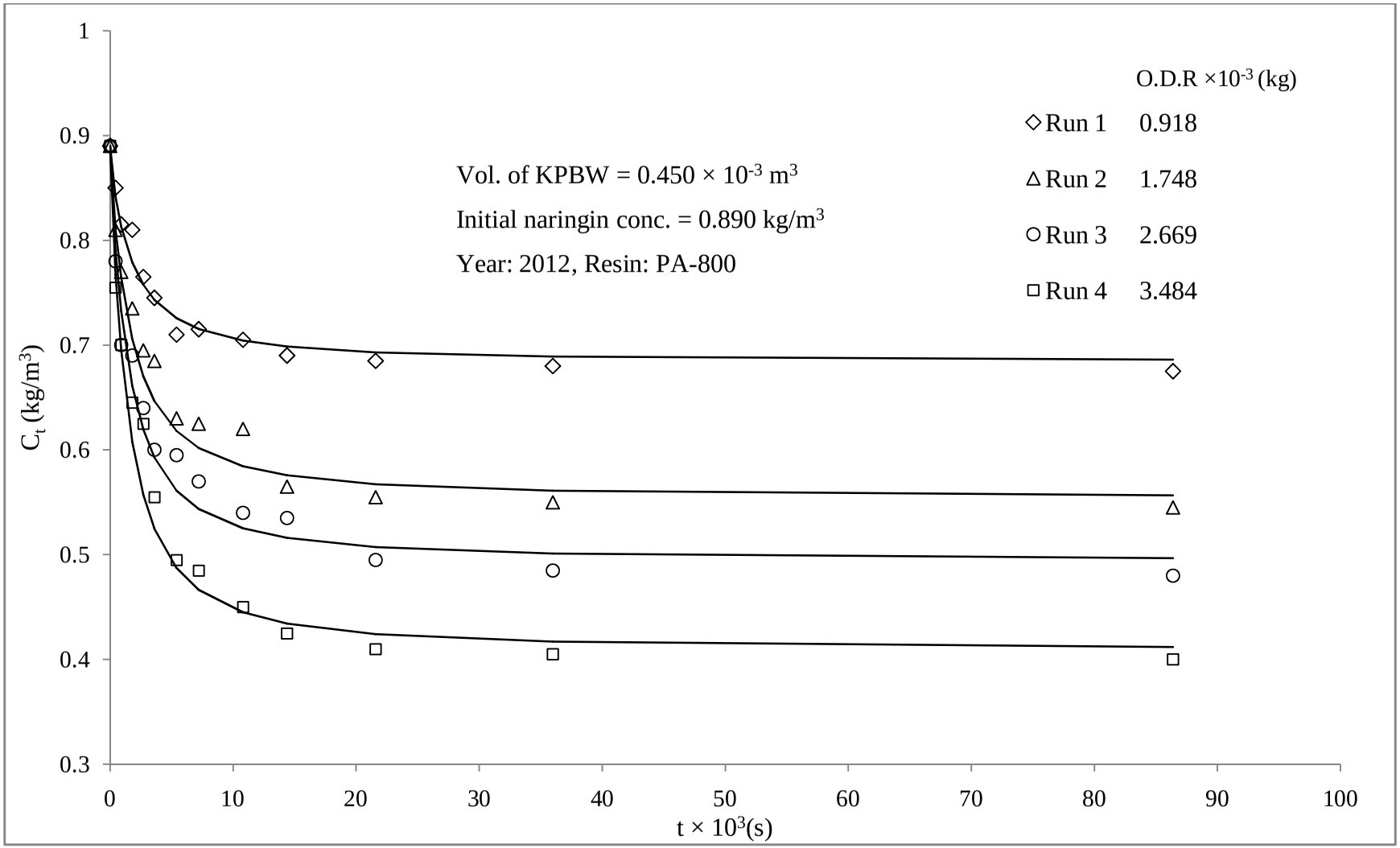

Figure 5.57: Adsorption of naringin on adsorbent PA-800 from dropped KPBW: kinetic studies, correlation of experimental data, C_t *vs t* (system 4, year 2012)

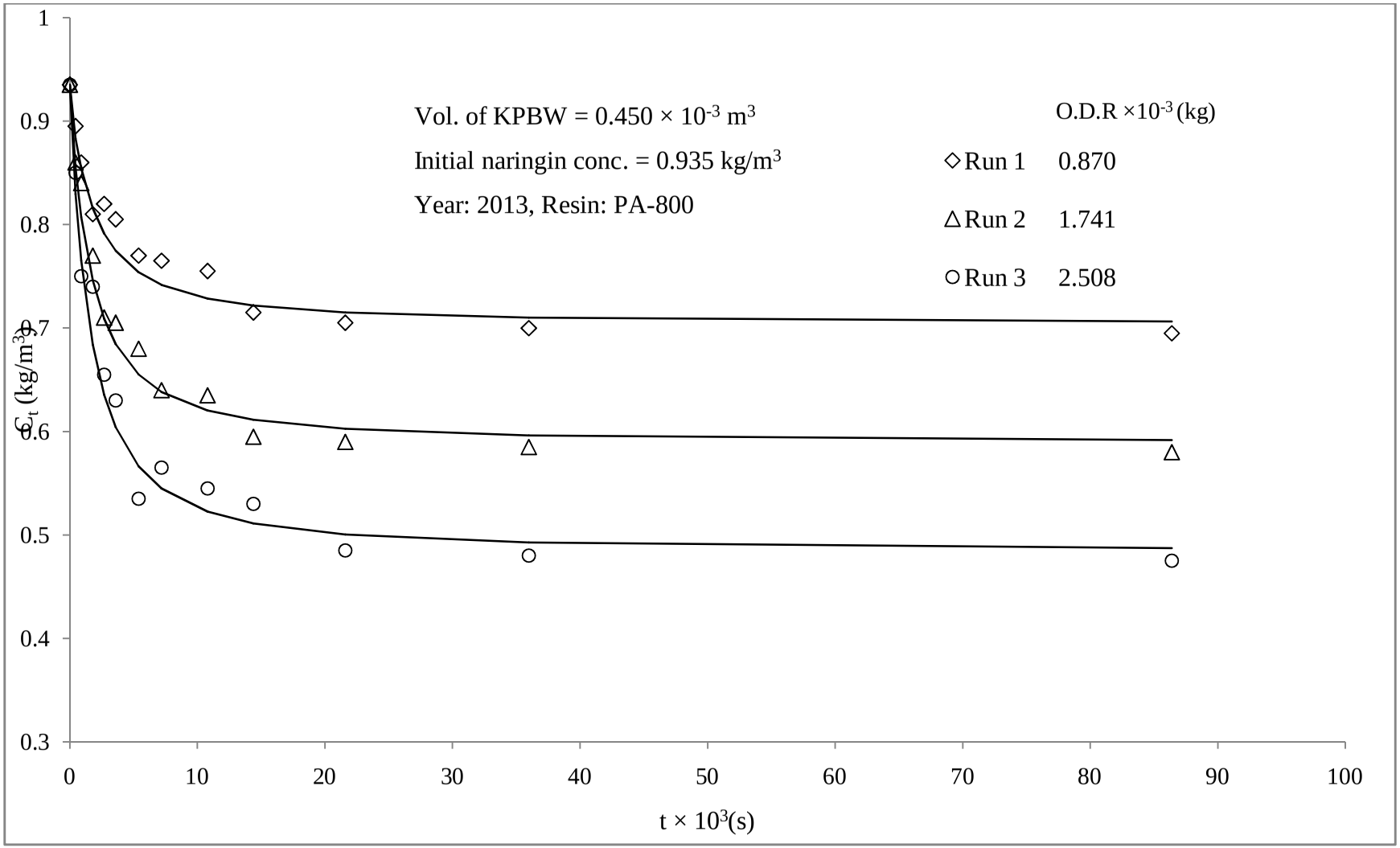

Figure 5.58: Adsorption of naringin on adsorbent PA-800 from dropped KPBW: kinetic studies, correlation of experimental data, C_t *vs t* (system 4, year 2013)

The data were tested for significance of the mean difference, paired observation by t -test at a 5% level of significance, and it was found that the experimental, as well as predicted data, does not differ significantly of almost all the runs. The summary of the statistical analysis values is given in Table 5.38,

Table 5.38: Statistical analysis for predicted and experimental values of C_t (system 4)

Year	Run	Slope C_{trep} vs. $C_{t\exp}$ passing through origin	R^2	t-Cri	t-Cal	Inference
2012	1	0.998	0.941	2.200	-0.036	NSD
	2	0.983	0.949	2.200	1.810	NSD
	3	0.991	0.948	2.200	0.832	NSD
	4	0.979	0.956	2.200	1.266	NSD
2013	1	0.988	0.924	2.200	1.715	NSD
	2	0.989	0.964	2.200	1.239	NSD
	3	0.983	0.954	2.200	1.113	NSD

*NSD- No Significance difference, SD- Significance difference

From the above, it is evident that observed kinetic data could be correlated reasonably using modified adsorption shell model.

Comparison of adsorption kinetics:

The kinetics of adsorption of naringin from kinnow peel boiled water for two years with the same mass of resin have been compared, and it is shown in Figure 5.59. Keeping in mind initial naringin concentration in KPBW of the two runs is different, the data is almost similar.

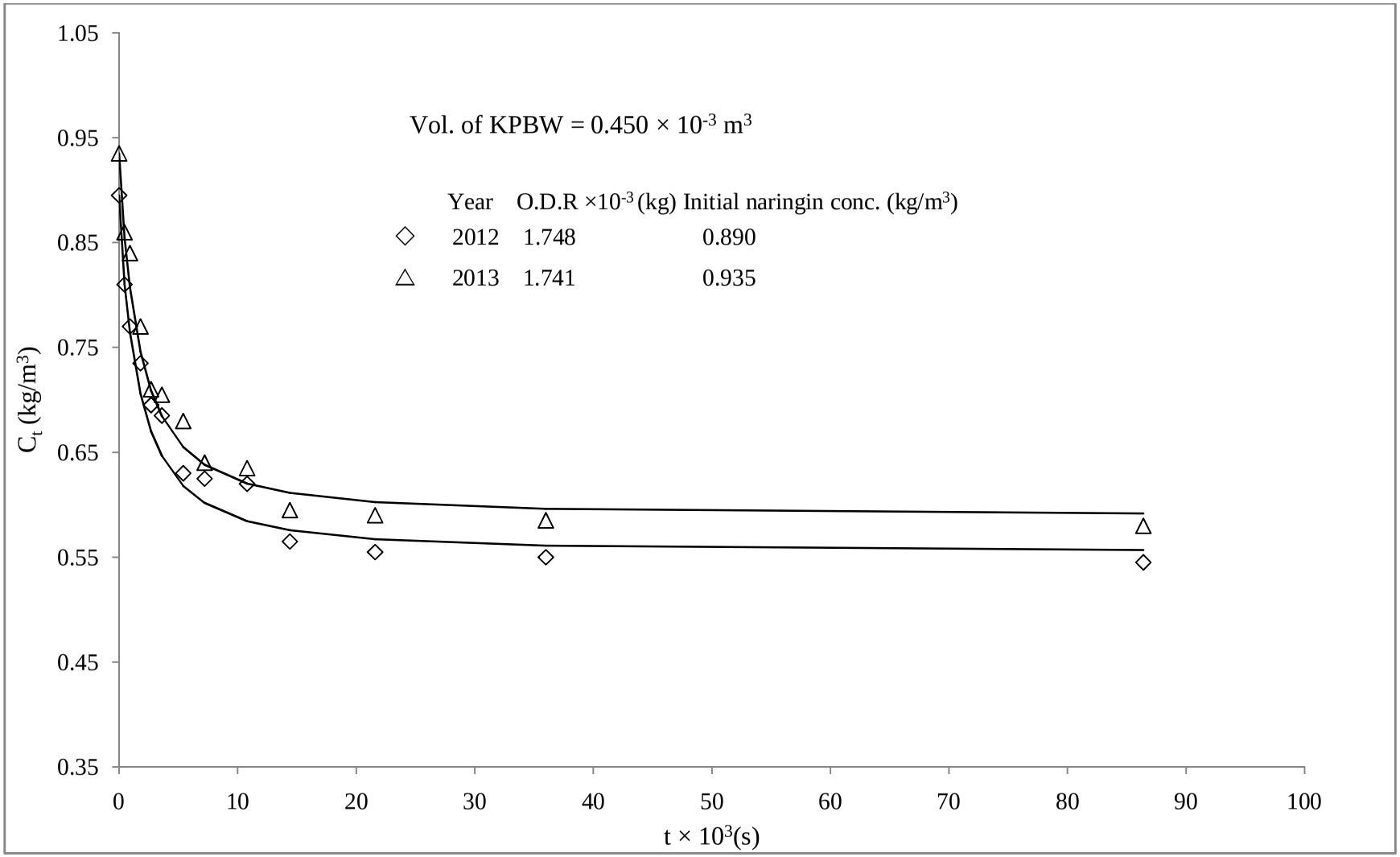

Figure 5.59: Comparison of naringin adsorption kinetic studies on the resin PA-800 from dropped KPBW with year (system 4), C_t *vs t*

5.4.3. Fixed bed column adsorption studies (System 4)

The adsorption column studies were carried out as per the procedure described in the earlier section 3.5.3. The column studies of the different year's samples of KPBW is shown in Figure 5.60. From the Figure 5.60, it was observed that the first 21600 (s) the concentration of naringin in outgoing solution was almost zero. The adsorption column data are given in Tables E3 (a-b). The various parameters of the breakthrough curve are presented for the two years in Table 5.39.

Table 5.39: Parameters of breakthrough curves for adsorption of naringin on resin PA-800 from dropped KPBW in a fixed-bed column for two years

Bed height = 1.20 m, Flow rate = 3.3×10^{-8} m^3/s

S.No	Year	C_o (kg/m^3)	$t_b \times 10^3$ (s)	$t_t \times 10^3$ (s)	q_{total} g	q_s kg/kg	H_{UNB} (m)	MTZ (m)
1	2012	0.895	111.6	204.5	6.10	0.109	0.545	0.554
2	2013	0.935	118.8	215.1	6.70	0.124	0.537	0.549

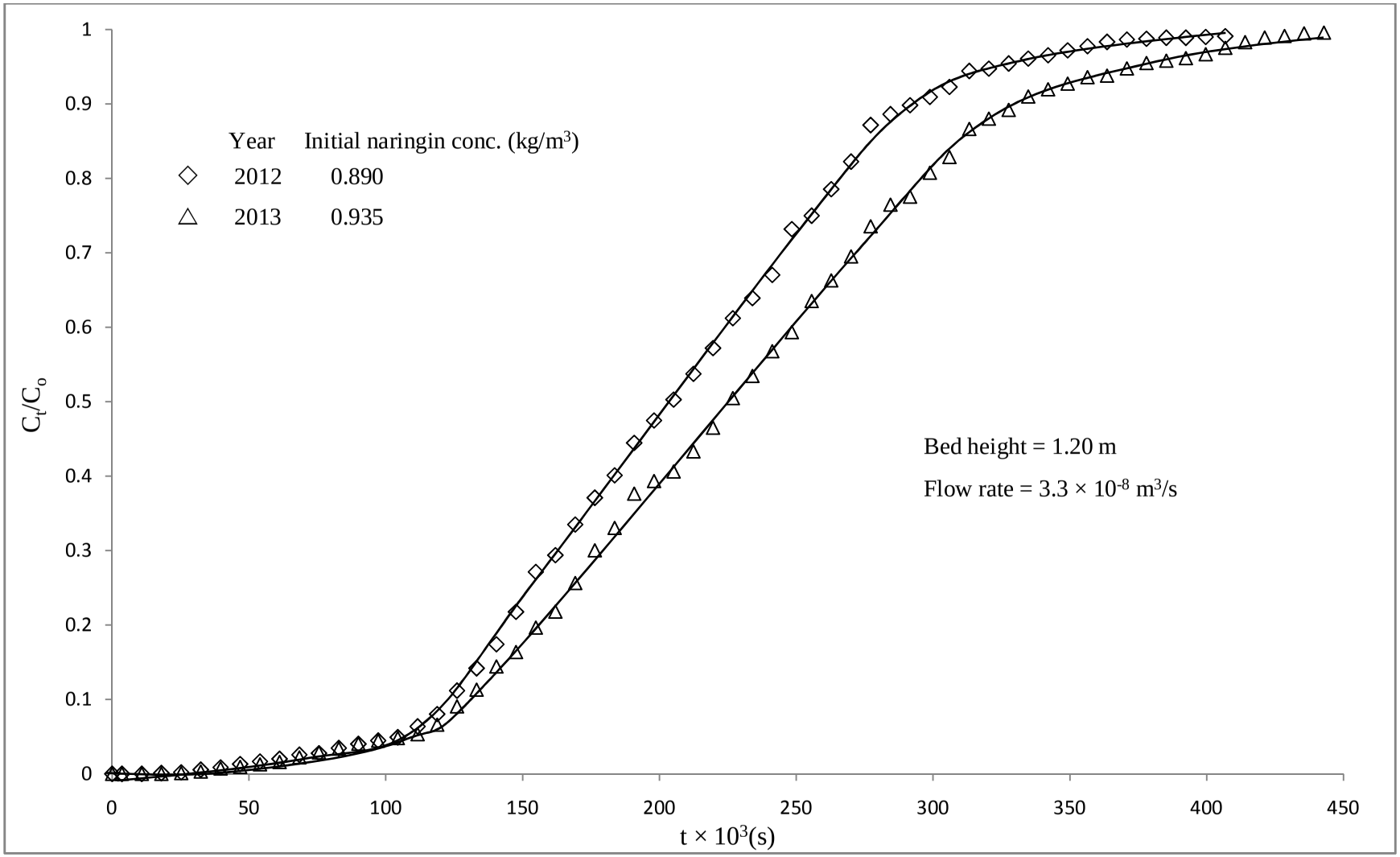

Figure 5.60: Adsorption of naringin on adsorbent PA-500 from dropped KPBW: fixed bed column study (system 4)

5.4.4. Desorption equilibrium studies (System 4)

The desorption equilibrium studies with ethanol from naringin saturated resin were carried out as per the procedure described in the section 3.6.1.

The data have been presented in Table E4 and Figure 5.61. From the Figure 5.61, it is observed that the desorption is favourable with ethanol but does not approach completion. The desorption equilibrium experimental data could be correlated with Freundlich adsorption isotherm and its parameters were evaluated and are presented in Table 5.40.

Table 5.40 Freundlich isotherm constants for desorption of naringin from naringin saturated resin PA-800 (dropped peels)

S.No	Year	Freundlich constants		
		K_{fd}	n_d	R^2
1	2012	0.155	1.139	0.981
2	2013	0.124	1.536	0.893

5.4.5. Desorption kinetic studies (System 4)

The desorption kinetic studies with ethanol from naringin saturated resin were carried out as per the procedure described in the section 3.6.2, and data are presented in Tables E5 (a-b) in Figures 5.62 and 5.63.

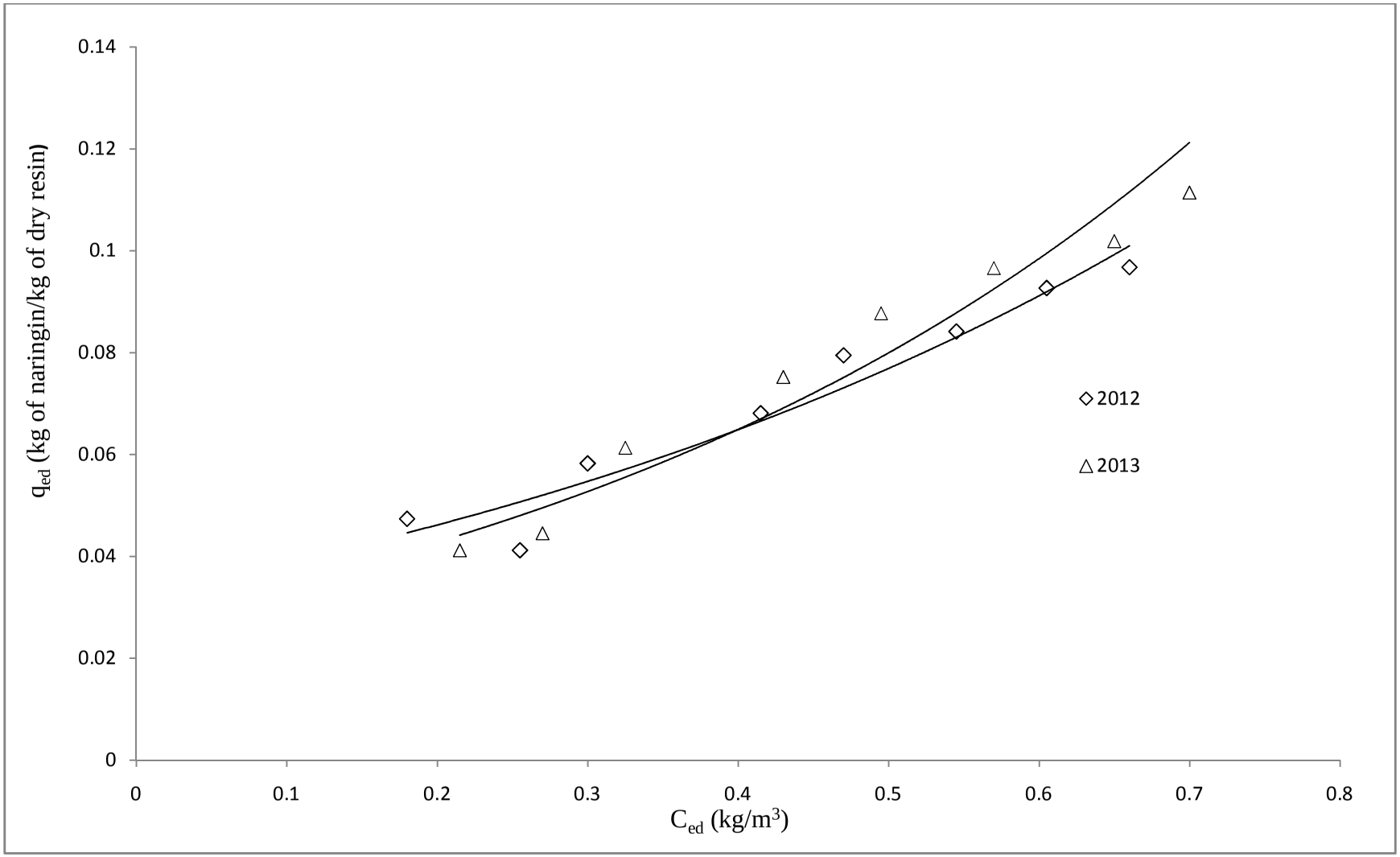

Figure 5.61: Desoption equilibrium studies from naringin saturated resin PA-800 to ethanol solution (system 4)

Modelling of desorption kinetic data

The above data have been analysed with the same approach as done for System 1 (i.e., Boyd's diffusivity model equation).

The values of effective diffusivity D_{ed}, were estimated using linear plots of $\ln\left(1/1-u_d^2(t)\right)$ vs time (t) and presented in Table 5.41. The average value of effective diffusivity D_{ed} was found to be 10.66×10^{-13} (m^2s^{-1}).

Table 5.41: Boyd's diffusivity model parameters for desorption of naringin from naringin saturated resin PA-800 (system 4)

S.No	Run	Year			
		2012		2013	
		$D_{ed}\times10^{-13}$ (m^2s^{-1})	R^2	$D_{ed}\times10^{-13}$ (m^2s^{-1})	R^2
1	1	10.6	0.951	13.6	0.939
2	2	8.86	0.972	13.0	0.969
3	3	8.46	0.974	9.54	0.981

The generated C_{td} (with a representative value of D_{ed} = $10.66\times10^{-13}\,m^2s^{-1}$) for all the runs are shown by smooth curves as well as experimental data are given for comparison in Figures 5.62 and 5.63. The data were tested for significance of the mean difference, paired observation by t -test at a 5% level of significance, and it was found that the experimental and predicted data does not differ significantly of almost all the runs. The summary of the statistical analysis of the predicted values from the model and experimental values is given in Table 5.42.

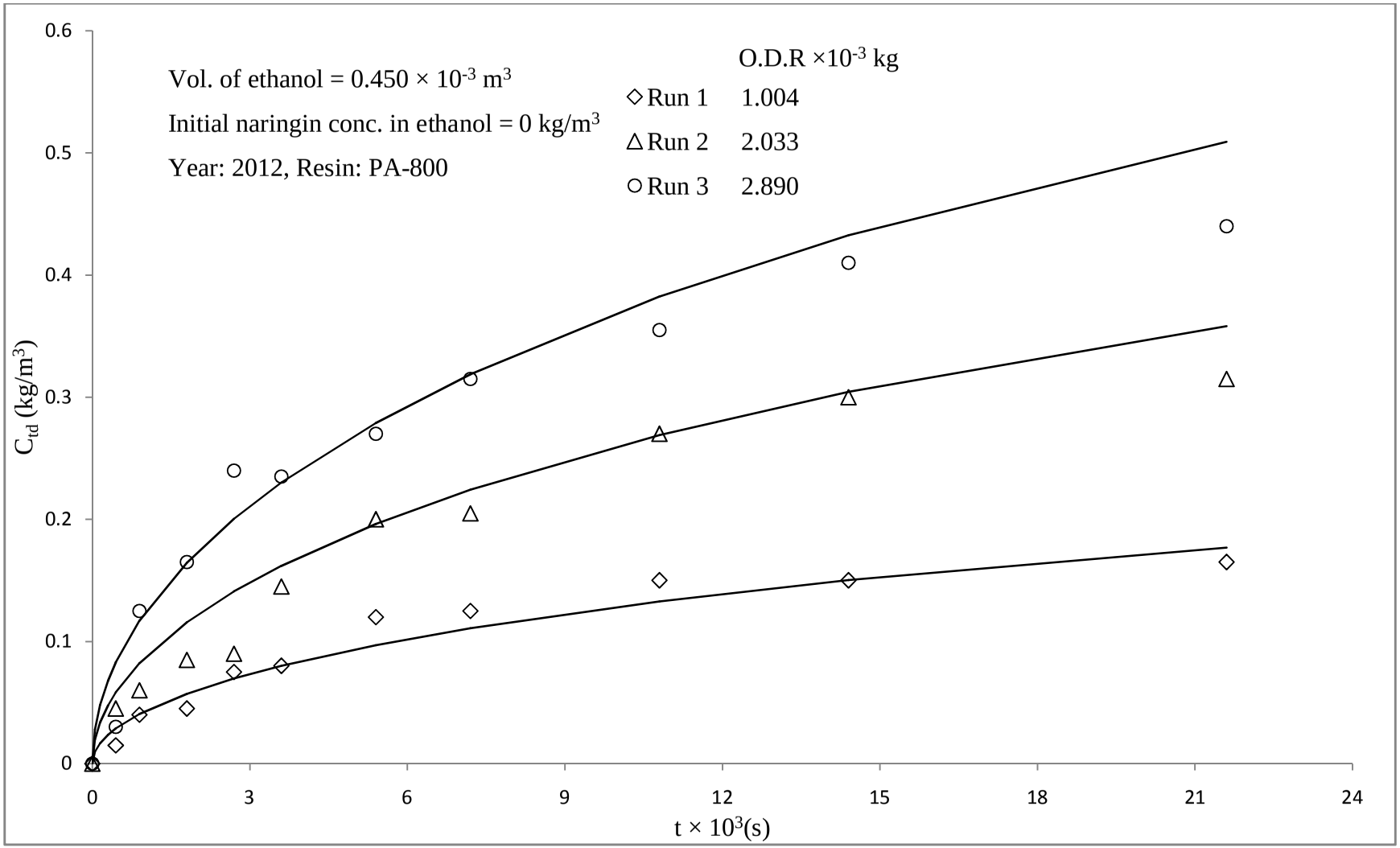

Figure 5.62: Desorption kinetic studies with naringin saturated resin PA-800 in ethanol: correlation of experimental data C_{td} *vs t* (system 4, year 2012)

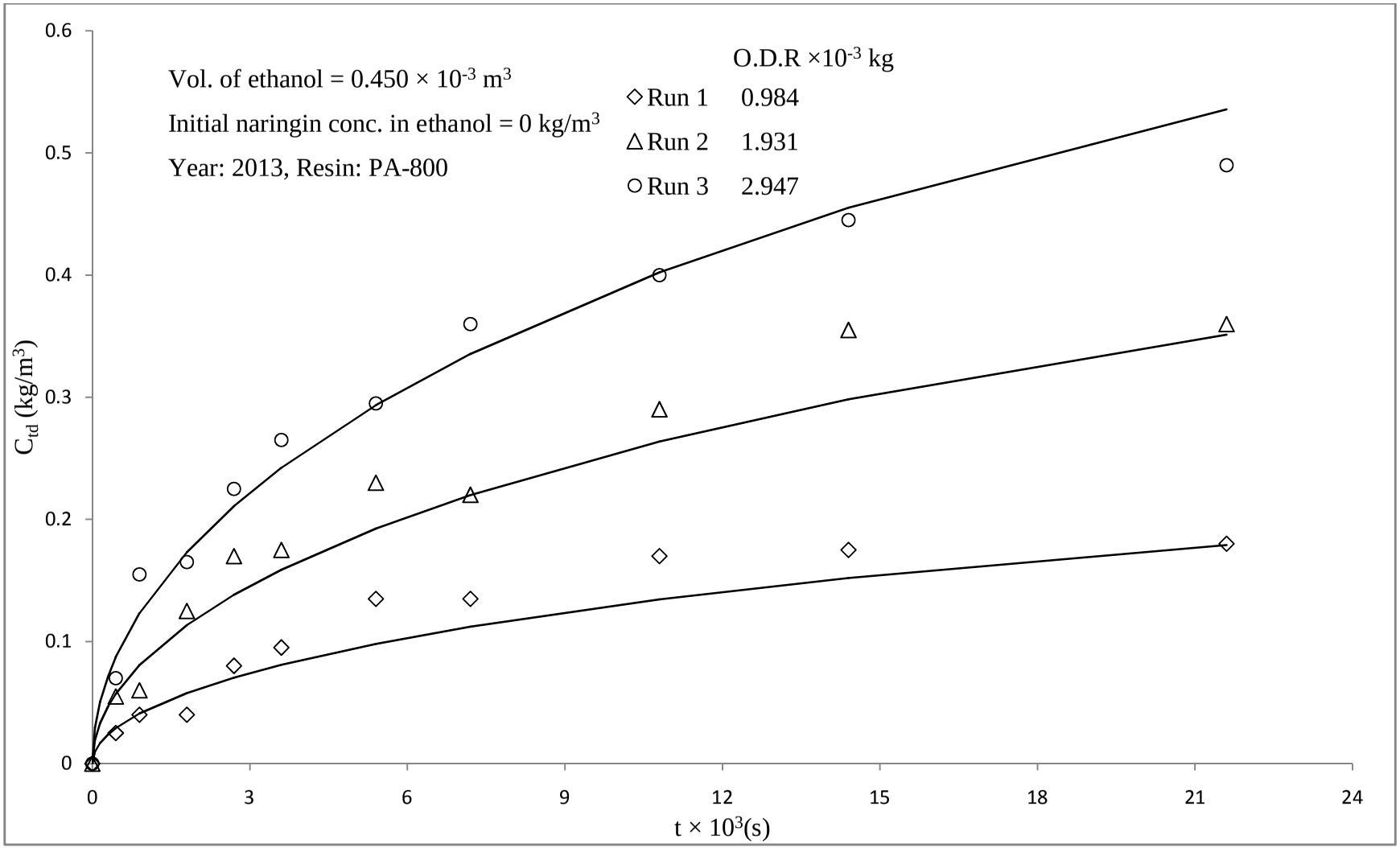

Figure 5.63: Desorption kinetic studies with naringin saturated resin PA-800 in ethanol: correlation of experimental data C_{td} *vs t* (system 4, year 2013)

Table 5.42: Statistical analysis for predicted and experimental values of C_{td} (system 4)

Run	Year	Slope	R^2 C_{trep} vs. $C_{t\exp}$	t-Cri	t-Cal	Inference
1	2012	0.96	0.936	2.262	0.514	NSD
2		1.076	0.947	2.262	-3.443	SD
3		1.052	0.952	2.262	-1.327	NSD
1	2013	0.867	0.920	2.262	2.127	NSD
2		0.908	0.965	2.262	2.362	SD
3		1.007	0.974	2.262	0.150	NSD

*NSD- No Significance difference, SD- Significance difference

From the above, it is evident that observed kinetic data studied could be correlated reasonably using Boyd's diffusivity model equation.

Comparison of desorption kinetic studies:

The kinetics of naringin desorption from resin saturated with naringin to ethanol for the two different years with the same mass of resin has been compared, and it is shown in Figure 5.64. The rate of desorption of naringin in ethanol solution is almost same in both years.

5.4.6. Desorption fixed bed column studies (System 4)

The desorption column studies were carried out in glass column as per the procedure described in the section 3.6.3 and presented in Figure 5.65. From the Figure 5.65, it is evident that the amount of naringin desorbed from resin saturated with naringin, obtained from adsorption column studies, in ethanol solution decreases with time. The data of column studies for naringin desorption with ethanol to recover naringin are given in Table E6.

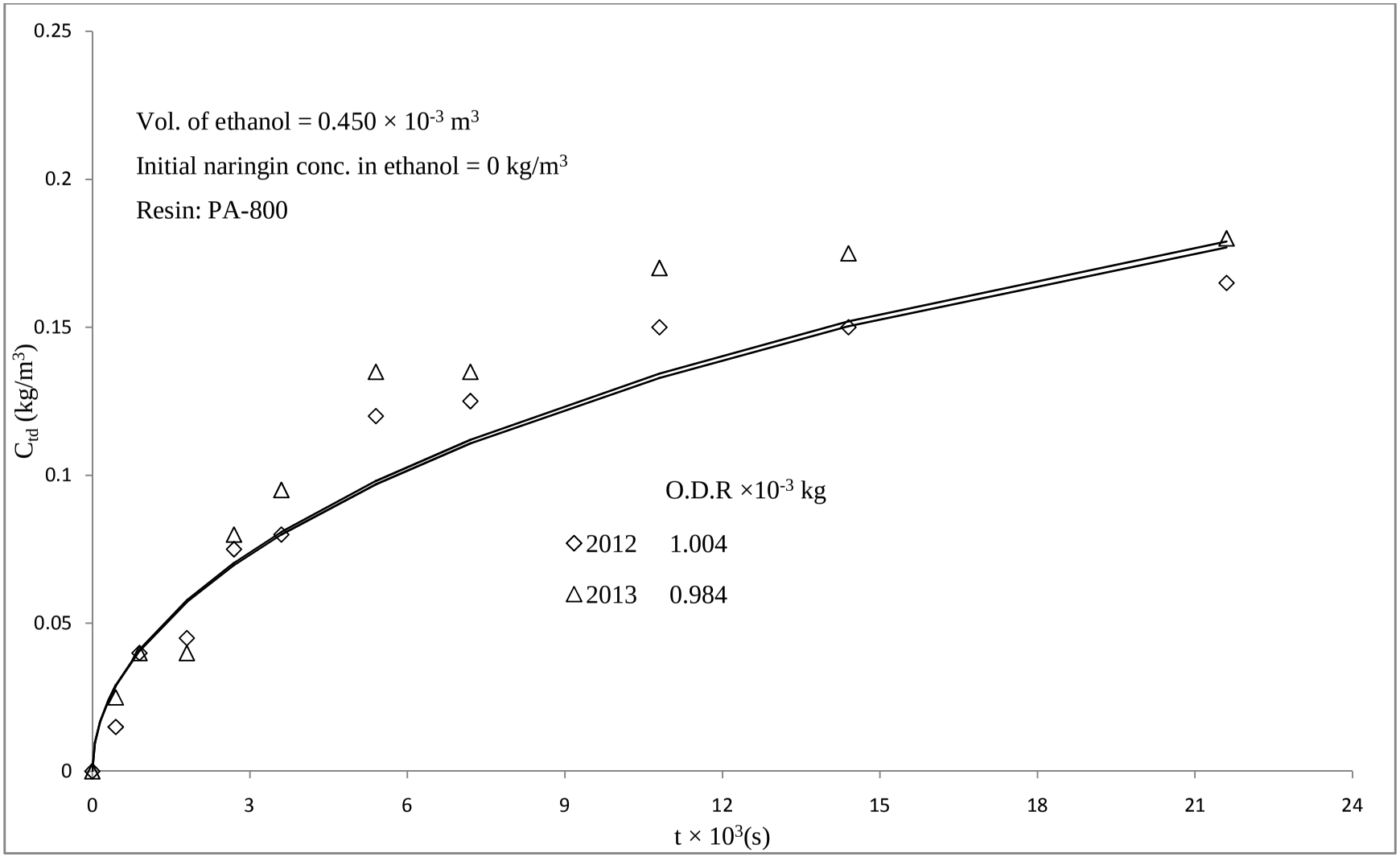

Figure 5.64: Comparison of desorption kinetic studies of naringin saturated resin PA-800 in ethanol with year (system 4), C_{td} *vs t*

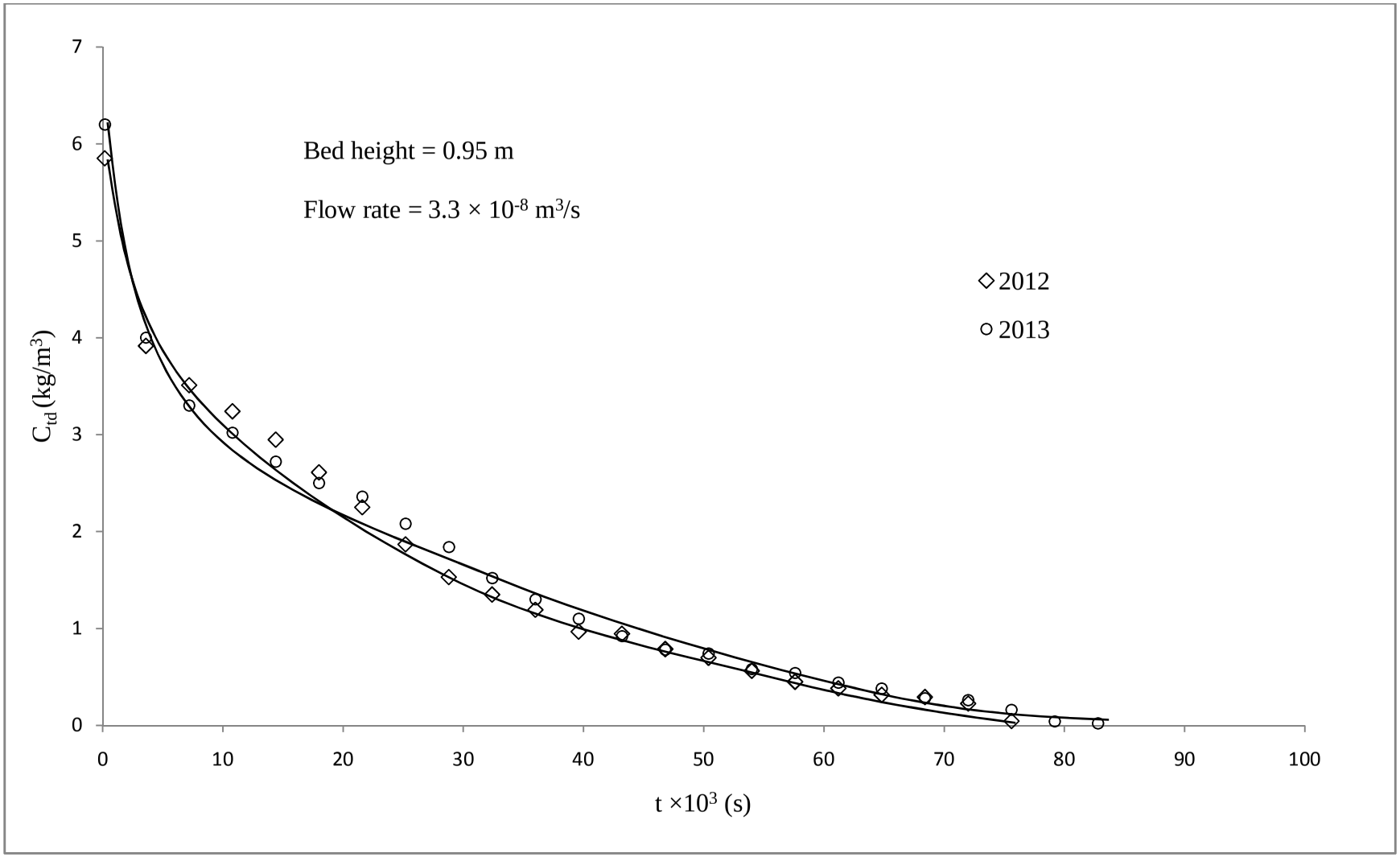

Figure 5.65: Column desorption studies from naringin saturated resin PA-800 into ethanol, C_{td} *vs t* (system 4)

From these desorption studies, it can be concluded that about 2200 ml of ethanol is sufficient for almost all the possible recoverable desorption of naringin from the resin PA-800 in a glass column of 14 mm ID filled up to the height 0.95 m (about 120 g naringin saturated resin (wet)). The amount of naringin desorbed in the column was found to be 3.92 and 4.05 g respectively for the years 2012 and 2013.

5.4.7. Purity and recovery of obtained Naringin and Pectin (System 4)

(A) Naringin recovery

Recovery and purity of naringin were calculated as per the procedure described in section 3.9 and are tabulated in Table 5.43 for the years 2012 and 2013.

Table 5.43: Recovery of naringin from dropped peels with resin PA-800

S.No	Year	Naringin Conc. in KPBW (kg/m^3)	Naringin obtained (g)	Purity (%)	Recovery (%)
1	2012	0.890	3.9	93.2	52.8
2	2013	0.935	4.3	92.5	53.7

(B) Pectin recovery and characterization

The recovery of pectin was calculated as per the procedure described in section 3.10. The obtained pectin was characterised, the values of different parameters determined are tabulated in Table 5.44.

Table 5.44: Recovery of pectin from dropped peels with resin PA-800

S. No	Year	Recovey (%)	Moisture (%)	Ash (%)	Equivalent weigh (mg/ml)	Methoxyl content (%)	Anhdrouronic acid (%)	DE (%)
1	2012	57.5	9.6	7.5	655.5	5.9	70.5	53.5
2	2013	58.0	10.1	8.1	660.1	6.1	72.5	51.2

5.5. Adsorption-Desorption studies of naringin with Dry peels on Resin PA-500 (system 5)

The naringin content of dry kinnow peel boiled water (extracts) from the two years (2012 and 2013) samples was determined and was found to be 0.700 and 0.650 kg/m^3 respectively.

5.5.1. Adsorption equilibrium studies (System 5)

The adsorption equilibrium studies with kinnow peel boiled water were carried out as per the procedure described in the section 3.5.1. The data have been presented in Table F1 and Figure 5.66. The adsorption equilibrium experimental data could be correlated by using Langmuir adsorption isotherm and its parameters were evaluated and are given in Table 5.45. The maximum amount of naringin that can be picked up by resin PA-500 from dry KPBW (calculated from Langmuir adsorption isotherm constants) was found to be 0.101 and 0.092 kg per kg of dry resin respectively for the years 2012 and 2013.

Table 5.45: Langmuir isotherm parameters for adsorption of naringin on resin PA-500 from dry KPBW

S.No	Year	Langmuir constants		
		a	b	R^2
1	2012	0.213	2.136	0.964
2	2013	0.294	3.193	0.934

5.5.2. Adsorption kinetic studies (System 5)

The adsorption kinetic studies were carried out as per the procedure described in the section 3.5.2.

The concentration of naringin in the solution as a function of time during adsorption for various amounts of resin is presented in Figures 5.67 and 5.68 for the years 2012 and 2013.

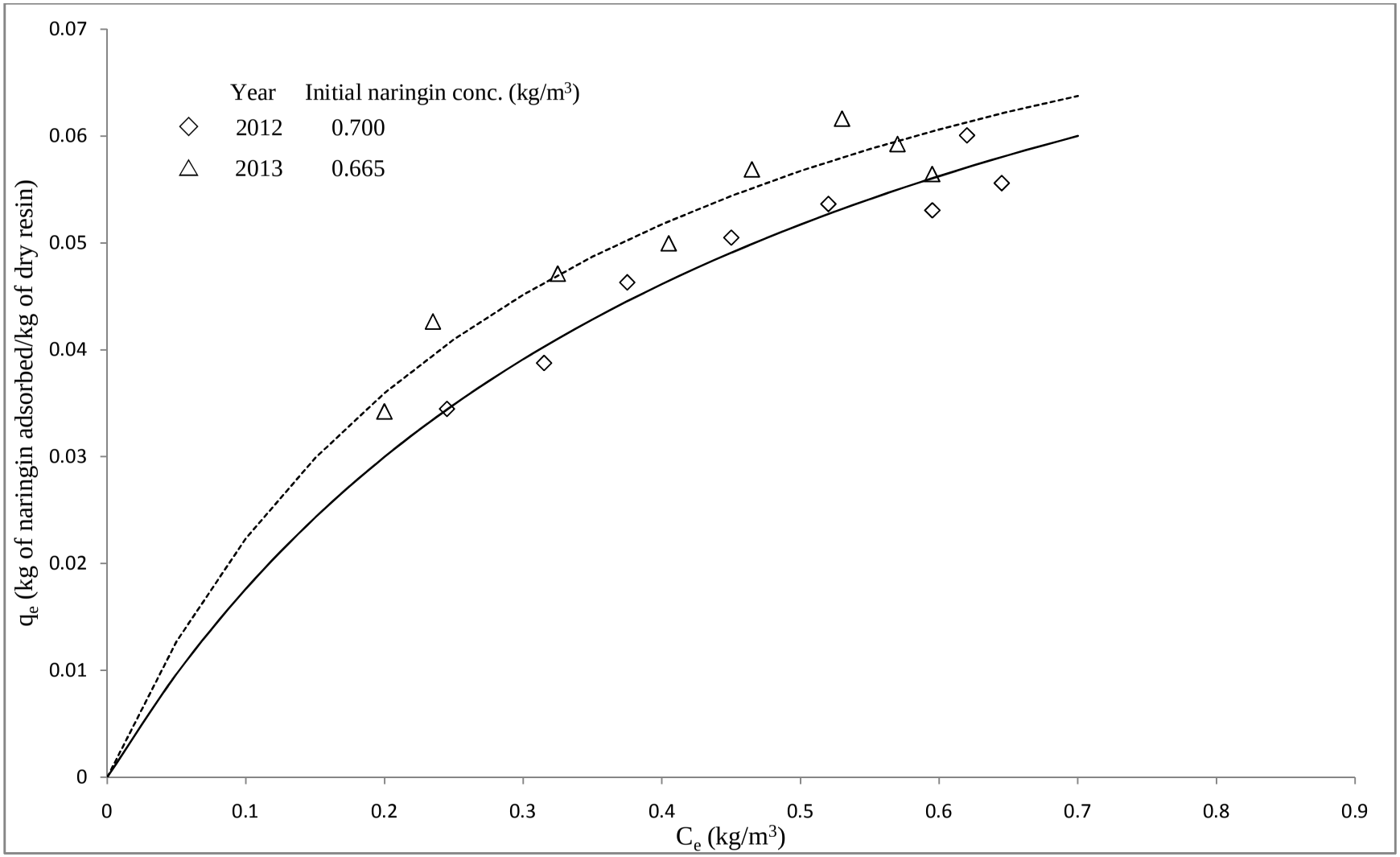

Figure 5.66: Adsorption equilibrium studies with dry KPBW on resin PA-500 in two years (system 5)

The data obtained in these experiments are given Tables F2 (a-b). It is observed that the rate of change in concentration of a solution is more when the mass of the resin used is more.

Modelling of adsorption kinetic data

The kinetic data have been analysed with the same approach (modified adsorption shell model) as discussed in the earlier for system 1. The values of different parameters viz. slopes of $F_n(t)$ vs t plots, K, β and ψ are tabulated below (Table 5.46) for all the runs of both the years.

Table 5.46: Modified adsorption shell model parameters for system 5

$D_P = 1.032\times10^{-10}\, m^2/s$, $\varepsilon = 0.39$, R_p = 0.375×10^{-3} m

Year	Run	C_o kg/m^3	q_e kg/m^3	Slope × 10^{-4} (s^{-1})	K	β	ψ	$\frac{D_c}{r_c^2}$ × 10^{-4} (s^{-1})
2012	1	0.700	65.65	1.73	86.52	52.41	0.55	0.87
	2	0.700	59.60	2.61	118.2	111.2	1.30	2.04
	3	0.700	47.05	3.30	118.0	110.8	1.64	2.58
	4	0.700	44.36	2.90	98.06	71.31	1.12	1.76
2013	1	0.650	62.49	4.36	223.2	446.8	4.64	7.27
	2	0.650	53.76	3.74	164.9	235.7	2.84	4.46
	3	0.650	49.82	3.17	129.4	137.2	1.79	2.80
	4	0.650	38.87	6.56	208.9	389.7	6.51	10.2

The generated C_t (with a representative value of ψ = 2.555) for all the runs are shown by smooth curves as well as experimental data are given for comparison in Figures 5.67 and 5.68.

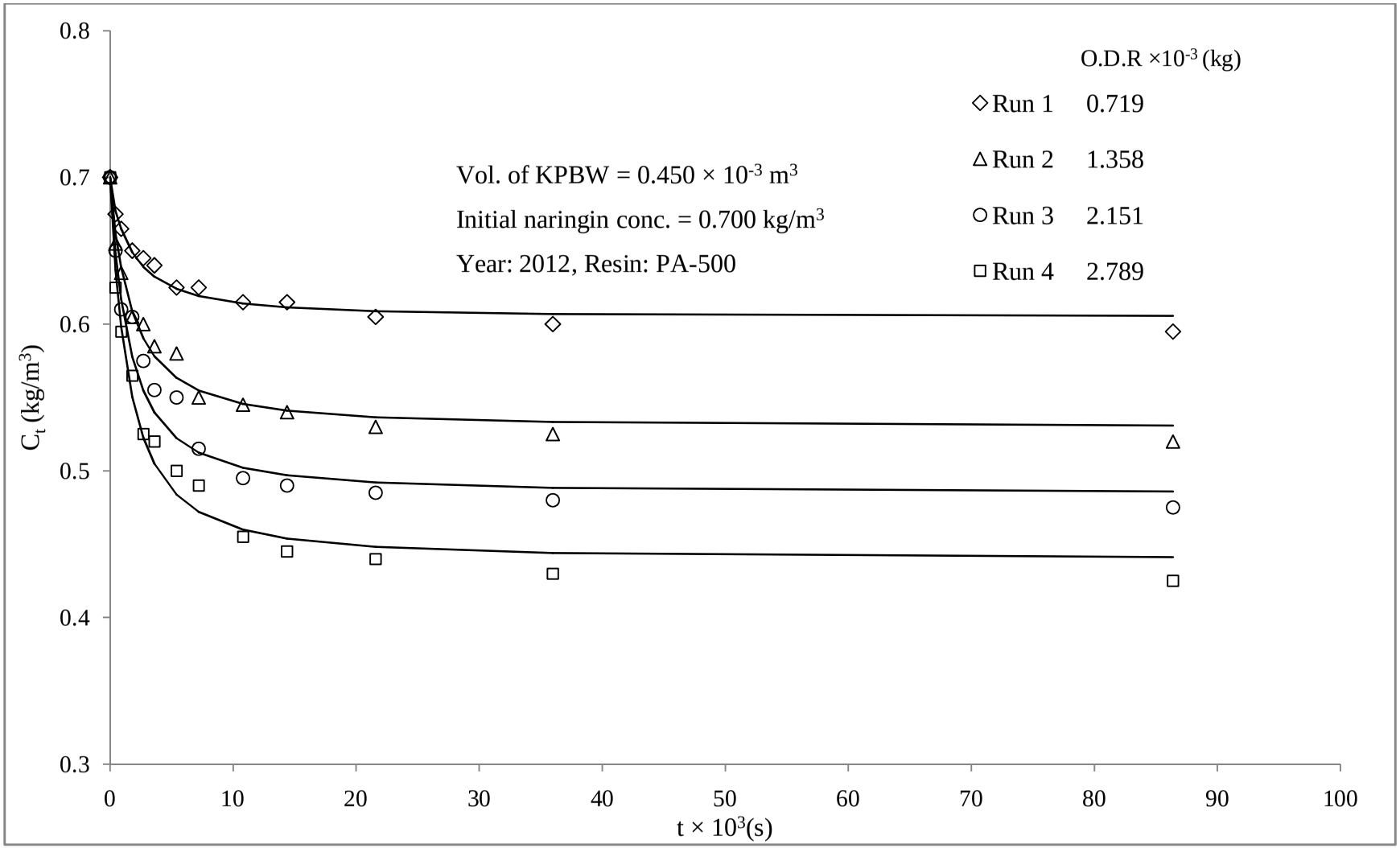

Figure 5.67: Adsorption of naringin on adsorbent PA-500 from dry KPBW: kinetic studies, correlation of experimental data, C_t *vs t* (system 5, year 2012)

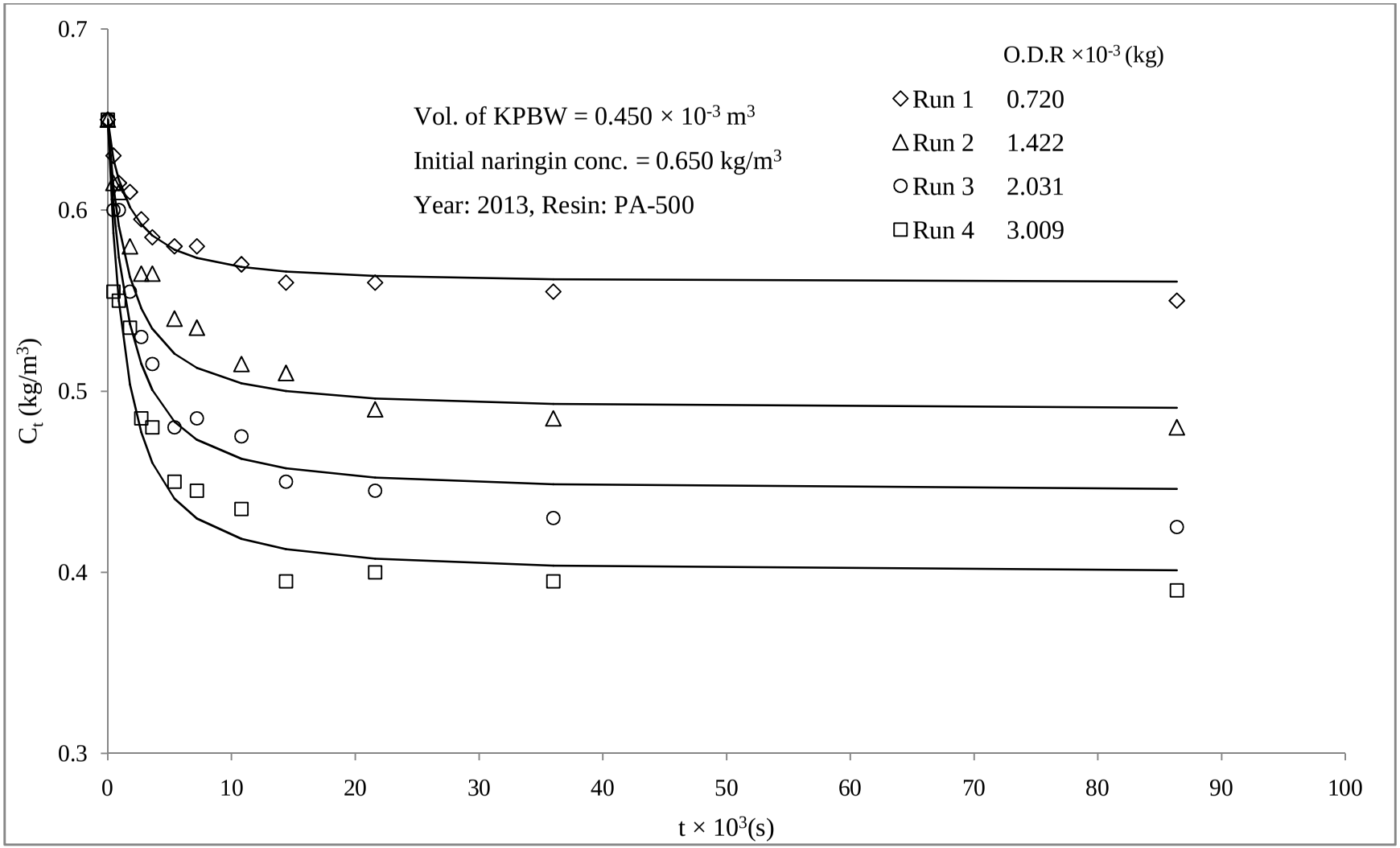

Figure 5.68: Adsorption of naringin on adsorbent PA-500 from dry KPBW: kinetic studies, correlation of experimental data, C_t *vs t* (system 5, year 2013)

The data were tested for significance of the mean difference, paired observation by t -test at a 5% level of significance, and it was found that the experimental and predicted data for almost all the runs does not differ significantly. The summary of the statistical analysis values is given in Table 5.47.

Table 5.47: Statistical analysis for predicted and experimental values of C_t (system 5)

Year	Run	Slope C_{trep} vs. $C_{t\exp}$ passing through origin	R^2	t-Cri	t-Cal	Inference
2012	1	0.999	0.948	2.200	0.152	NSD
	2	1.001	0.964	2.200	-0.452	NSD
	3	0.991	0.927	2.200	0.941	NSD
	4	0.999	0.96	2.200	-0.013	NSD
2013	1	1.000	0.939	2.200	-0.372	NSD
	2	0.979	0.900	2.200	2.705	SD
	3	0.991	0.918	2.200	0.707	NSD
	4	0.995	0.913	2.200	0.363	NSD

*NSD- No Significance difference, SD- Significance difference

From the above, it is evident that observed kinetic data could be correlated reasonably using modified adsorption shell model.

Comparison of adsorption kinetics:

The kinetics of adsorption of naringin from dry kinnow peel boiled water for two years with the same mass of resin have been compared, and it is shown in Figure 5.69. By considering different initial concentrations, it is observed that the adsorption kinetics is almost same in both years.

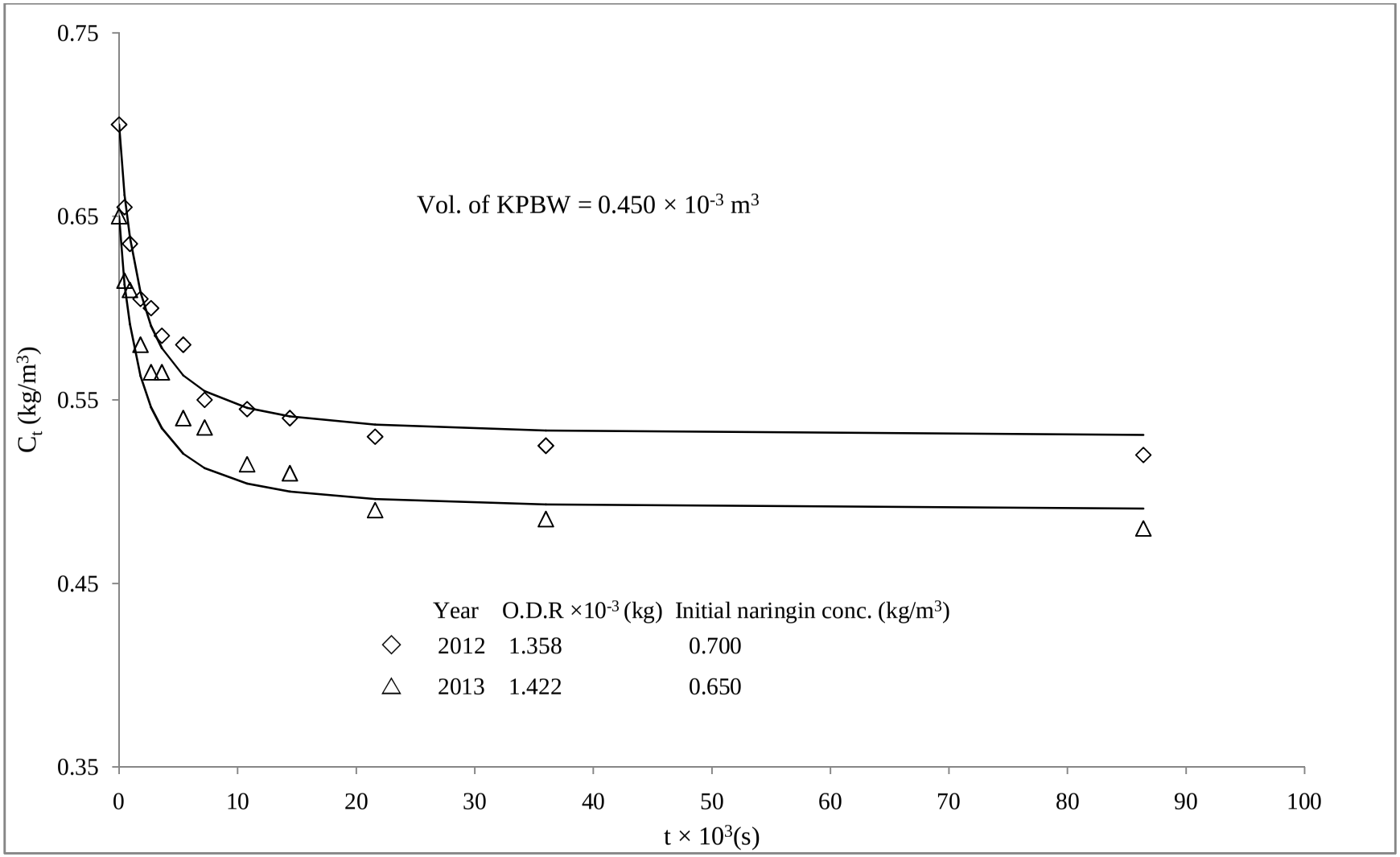

Figure 5.69: Comparison of naringin adsorption kinetic studies on the resin PA-500 from dry KPBW with year (system 5), C_t *vs t*

5.5.3. Fixed bed column adsorption studies (System 5)

The adsorption column studies were carried out as per the procedure described in the earlier section 3.5.3. The column studies of the different year's samples of KPBW is shown in Figure 5.70.

From the Figure 5.70, it was observed that the first 4000 (s) the concentration of naringin in outgoing solution was almost zero for both the years. The adsorption column data are given in Tables F3 (a-b). The various parameters of breakthrough curves are provided for the two years in Table 5.48.

Table 5.48: Parameters of breakthrough curves for adsorption of naringin on resin PA-500 from dry KPBW in a fixed-bed column for two years

Bed height = 1.20 m, Flow rate = 3.3×10^{-8} m^3/s

S.No	Year	C_o (kg/m^3)	$t_b \times 10^3$ (s)	$t_t \times 10^3$ (s)	q_{total} g	q_s kg/kg	H_{UNB} (m)	MTZ (m)
1	2012	0.700	50.4	136.1	3.17	0.058	0.755	0.795
2	2013	0.650	49.6	127.9	2.77	0.060	0.734	0.774

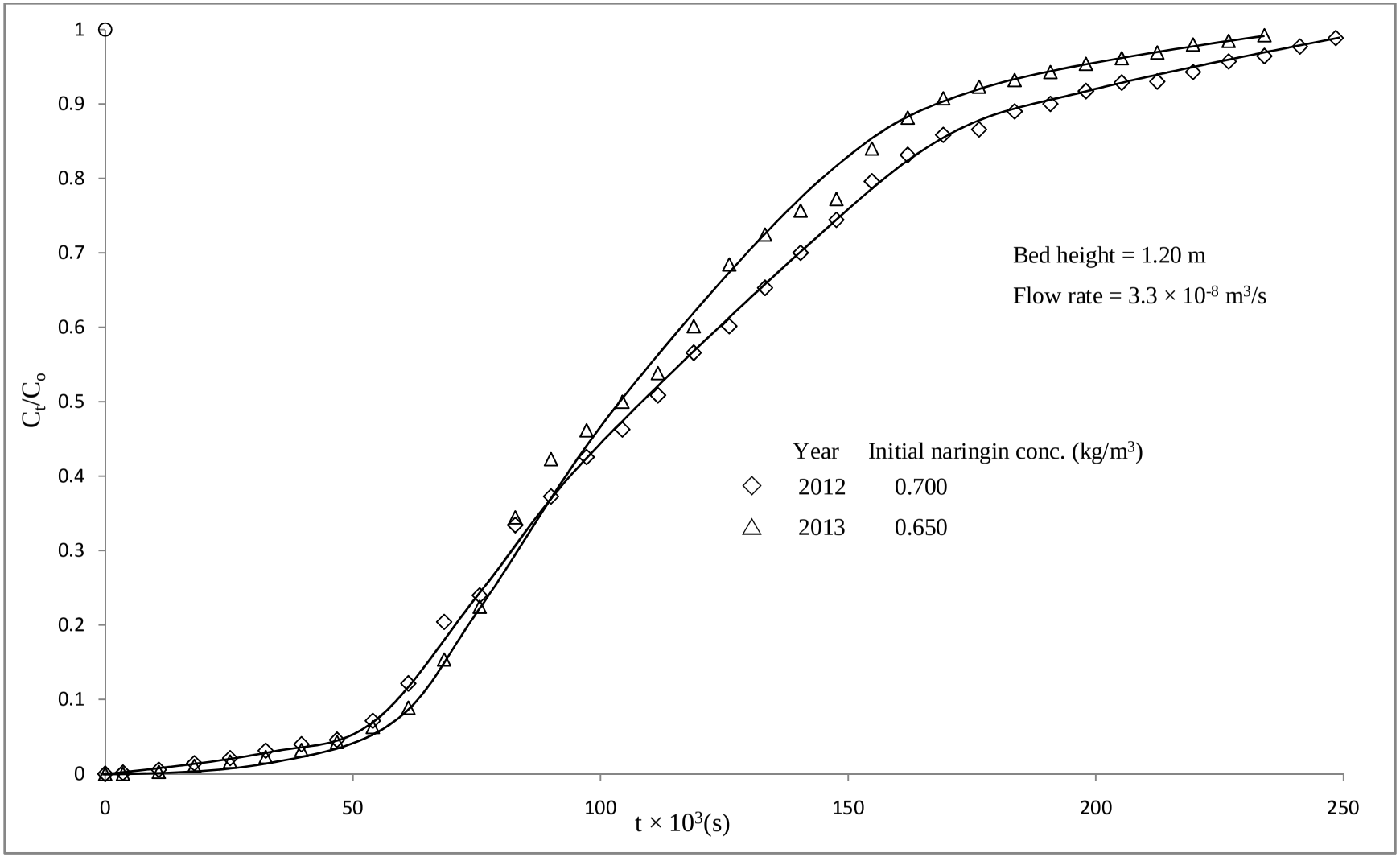

Figure 5.70: Adsorption of naringin on adsorbent PA-500 from dry KPBW: fixed bed column study (system 5)

5.5.4. Desorption equilibrium studies (System 5)

The desorption equilibrium studies with ethanol from naringin saturated resin were carried out as per the procedure described in the section 3.6.1.

The data have been presented in Table F4 and Figure 5.71. It is found that the desorption is favourable with ethanol but does not approach completion. The desorption equilibrium experimental data could be correlated with Freundlich adsorption isotherm and its parameters were evaluated and are given in Table 5.49.

Table 5.49: Freundlich isotherm constants for desorption of naringin from naringin saturated resin PA-500 (dry peels)

S.No	Year	Freundlich constants		
		K_{fd}	n_d	R^2
1	2012	0.102	1.048	0.931
2	2013	0.072	1.526	0.908

5.5.5. Desorption kinetic studies (System 5)

The desorption kinetic studies with ethanol from naringin saturated resin were carried out as per the procedure described in the section 3.6.2, and data are presented in Tables F5 (a-b) and Figures 5.72 and 5.73.

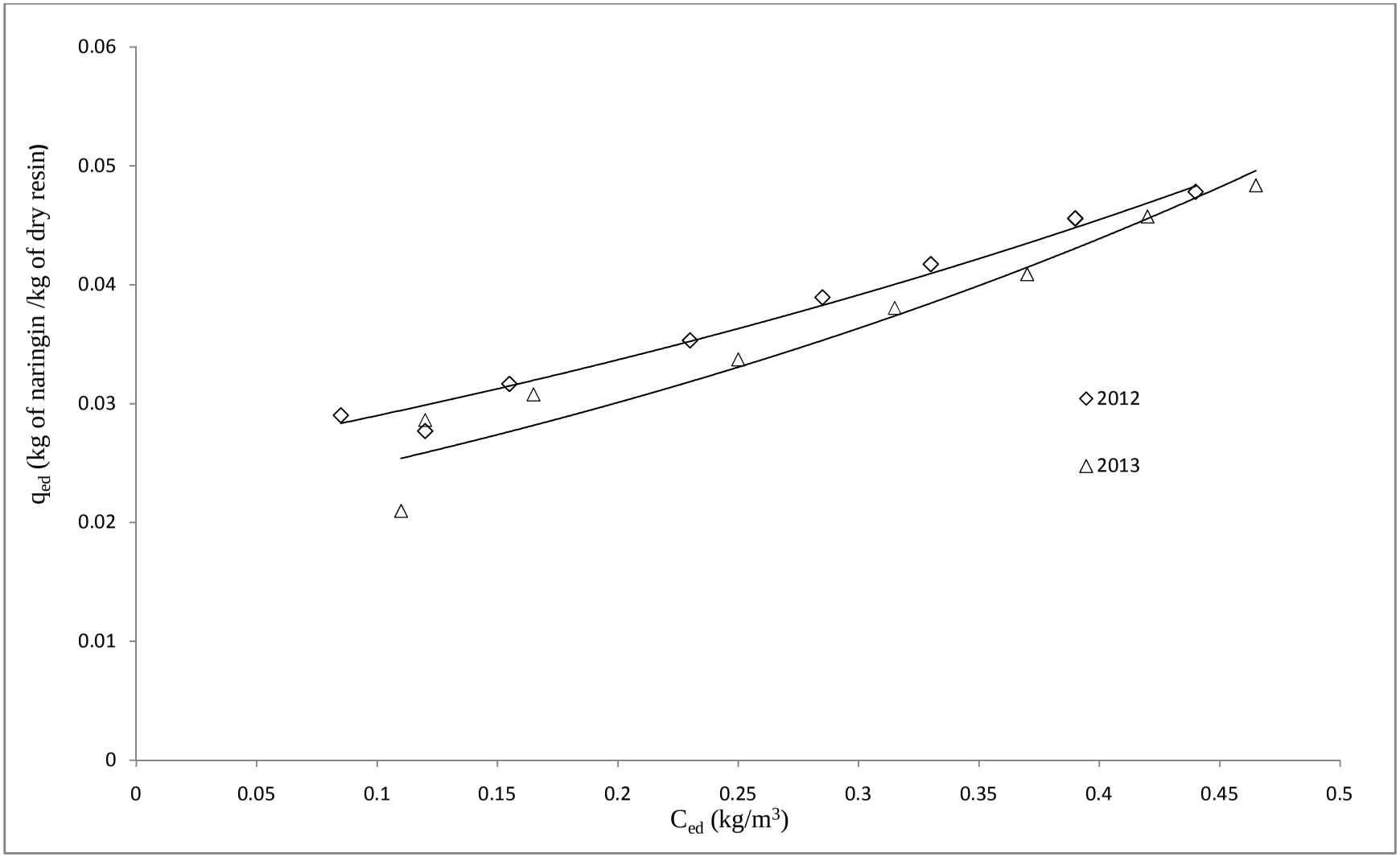

Figure 5.71: Desoption equilibrium studies from naringin saturated resin PA-500 to ethanol solution (system 5)

Modelling of desorption kinetic data

The above data have been analysed with the same approach as done for System 1 (i.e., Boyd's diffusivity model equation).

The values of effective diffusivity D_{ed}, were estimated using linear plots of $\ln\left(1/1-u_d^2(t)\right)$ vs time (t) and presented in Table 5.50. The average value of effective diffusivity D_{ed} is found to be 10.12×10^{-13} (m^2s^{-1}).

Table 5.50: Boyd's diffusivity model parameters for desorption of naringin from naringin saturated resin PA-500 (system 5)

S.No	Run	Year			
		2012		2013	
		$D_{ed}\times10^{-13}$ (m^2s^{-1})	R^2	$D_{ed}\times10^{-13}$ (m^2s^{-1})	R^2
1	1	10.1	0.986	11.5	0.977
2	2	9.23	0.983	12.2	0.985
3	3	7.67	0.975	9.91	0.962

The generated C_{td} (with a representative value of D_{ed} = $10.12\times10^{-13}m^2s^{-1}$) for all the runs are shown by smooth curves, and experimental data are given for comparison in Figures 5.72 and 5.73.

The data were tested for significance of the mean difference, paired observation by t -test at a 5% level of significance, and it was found that the experimental and predicted data for almost all the runs does not differ significantly.

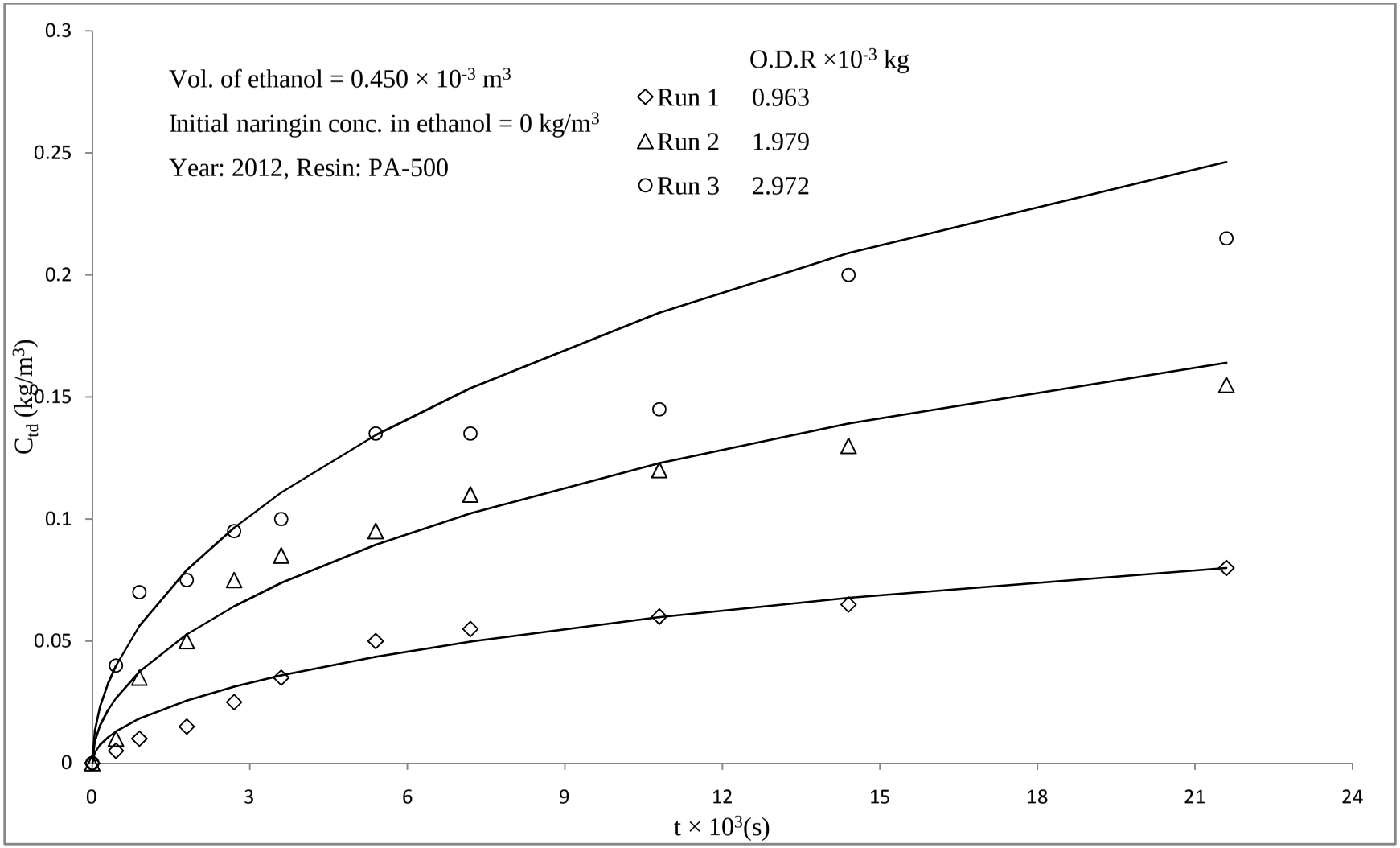

Figure 5.72: Desorption kinetic studies with naringin saturated resin PA-500 in ethanol: correlation of experimental data C_{td} *vs t* (system 5, year 2012)

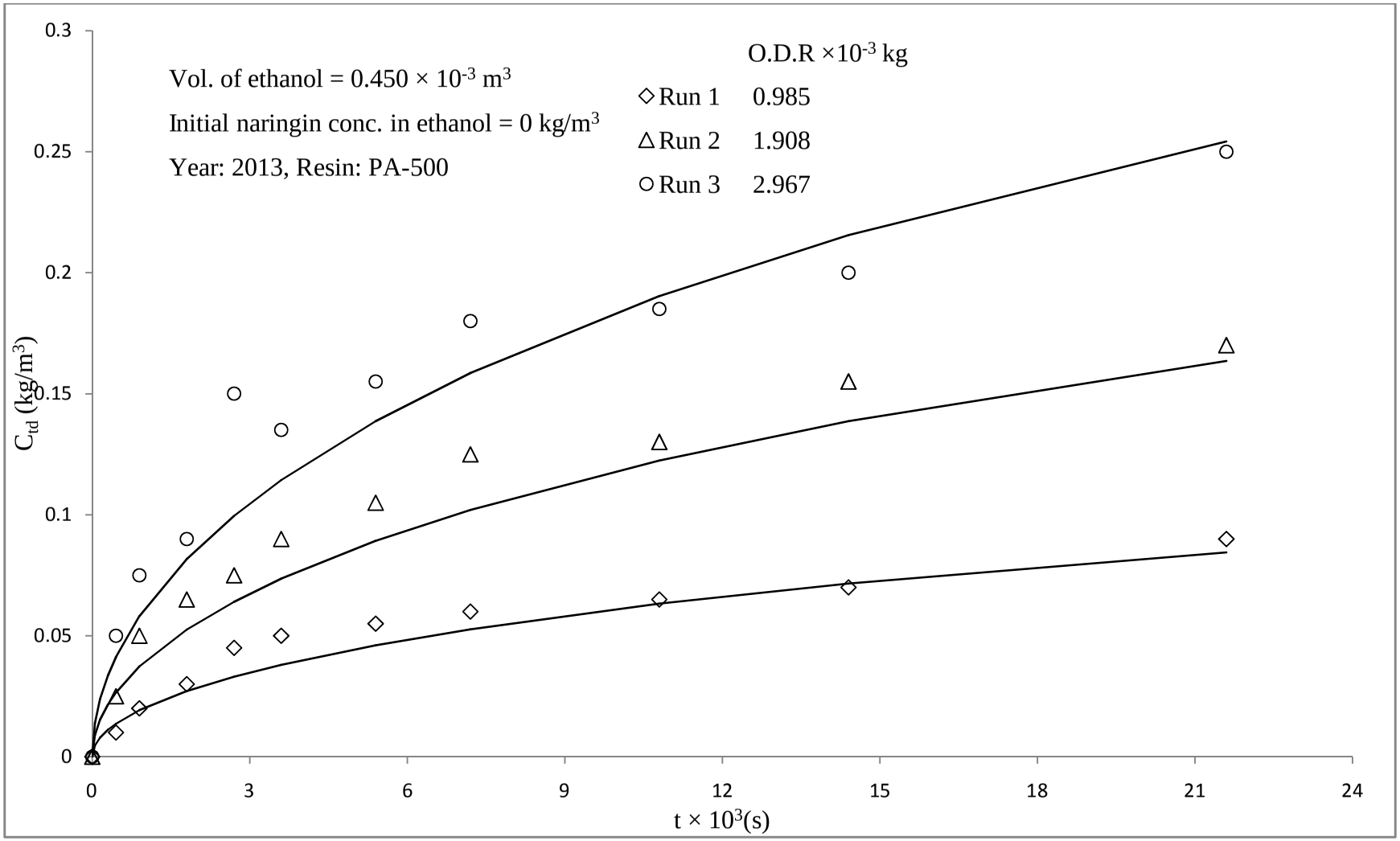

Figure 5.73 Desorption kinetic studies with naringin saturated resin PA-500 in ethanol: correlation of experimental data, C_{td} *vs t* (system 5, year 2013)

The summary of the statistical analysis of the predicted values from the model and experimental values is given in Table 5.51.

Table 5.51: Statistical analysis for predicted and experimental values of C_{td} (system 5)

Year	Run	Slope	R^2 C_{trep} vs. $C_{t\exp}$	t-Cri	t-Cal	Inference
2012	1	1.001	0.916	2.262	-1.374	NSD
	2	1.002	0.956	2.262	-0.255	NSD
	3	1.098	0.961	2.262	-1.990	NSD
2013	1	0.911	0.948	2.262	2.648	SD
	2	0.89	0.975	2.262	5.651	SD
	3	0.943	0.916	2.262	2.031	NSD

*NSD- No Significance difference, SD- Significance difference

From the above, it is evident that observed kinetic data studied could be correlated reasonably using Boyd's diffusivity model equation.

Comparison desorption kinetic data

The kinetics of naringin desorption from resin saturated with naringin to ethanol for the two different years with the same mass of resin has been compared, and it was shown in Figure 5.74. The rate of desorption of naringin in ethanol solution is almost same in both the years.

5.5.6. Desorption fixed bed column studies (System 5)

The desorption column studies were carried out in glass column as per the procedure described in the section 3.6.3 and presented in Figure 5.75. From the Figure 5.75, it is evident that the amount of naringin desorbed from resin saturated with naringin, obtained from adsorption column studies, in ethanol solution decreases with time. The data of column studies for naringin desorption with ethanol to recover naringin are given in Table F6.

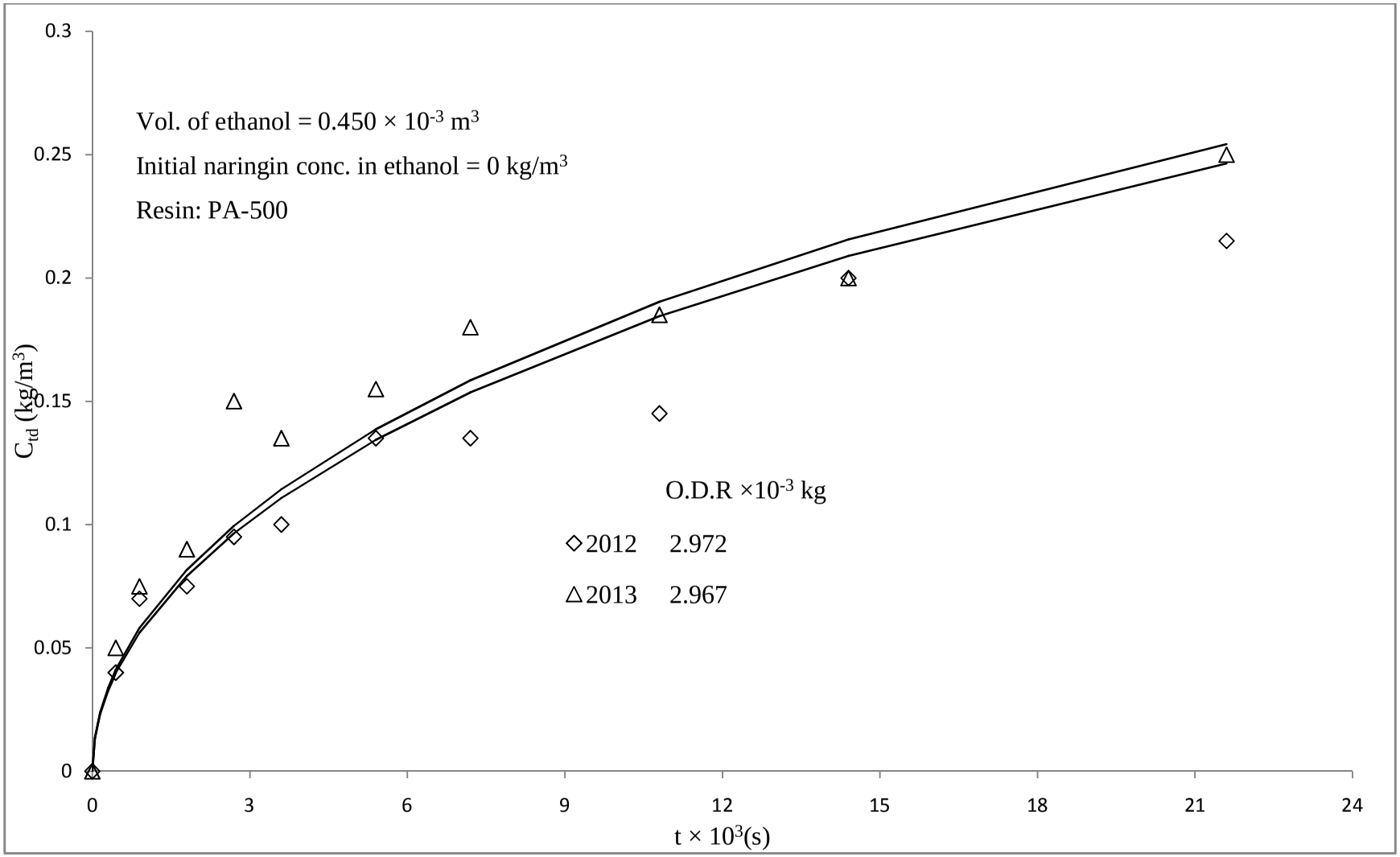

Figure 5.74: Comparison of desorption kinetic studies of naringin saturated resin PA-500 in ethanol with year (system 5), C_{td} *vs t*

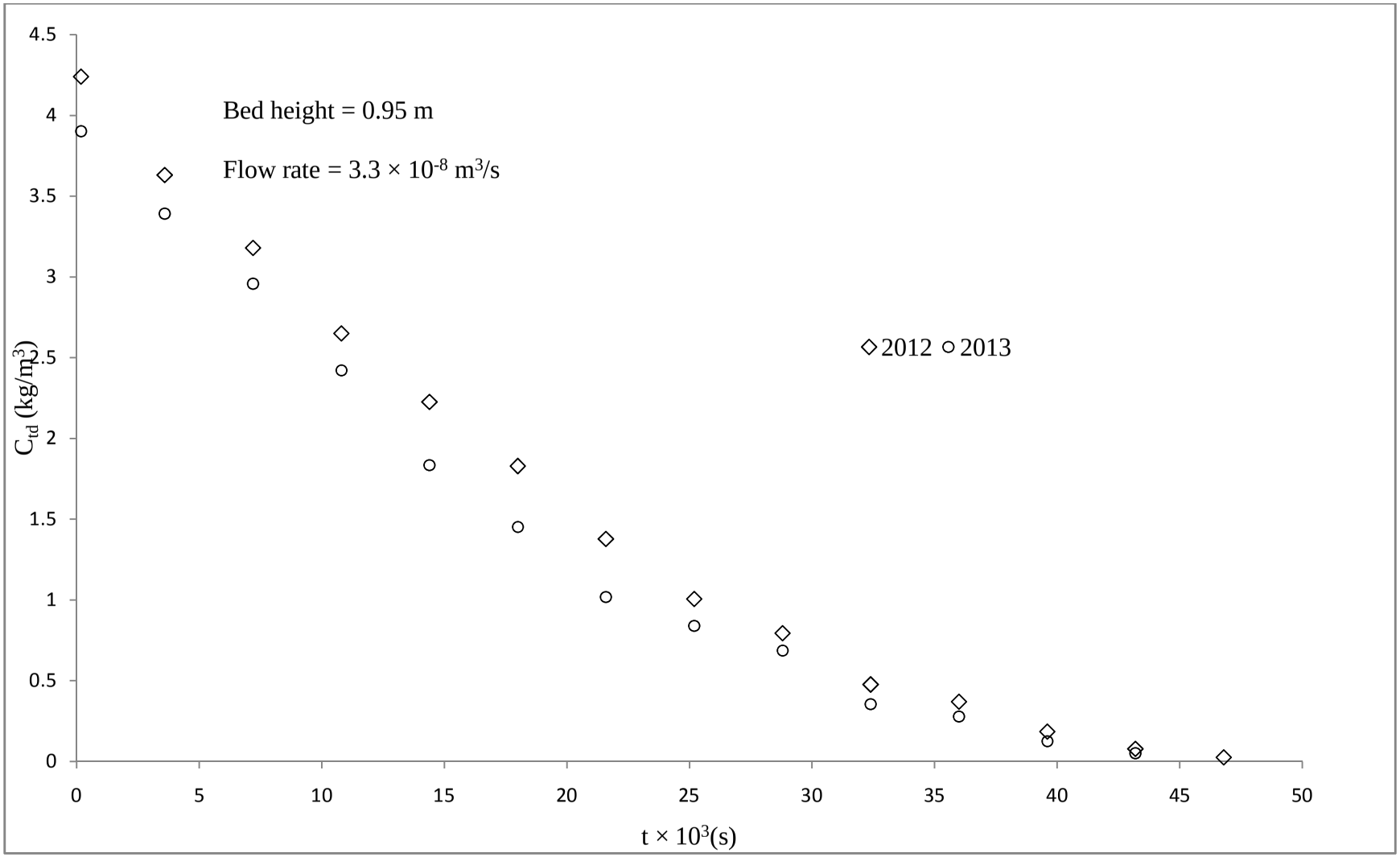

Figure 5.75: Column desorption studies from naringin saturated resin PA-500 into ethanol, C_{td} *vs* t (system 5)

From these desorption studies, it can be concluded that about 1300 ml of ethanol is sufficient for almost all the possible recoverable desorption of naringin from the resin PA-500 in a glass column of 14 mm ID filled up to the height 0.95 m (about 120 g naringin saturated resin (wet)). The amount of naringin desorbed in the column was found to be 1.93 and 1.71 g respectively for the years 2012 and 2013.

5.5.7. Purity and recovery of obtained Naringin and Pectin (System 5)

(A) Naringin recovery

Recovery and purity of naringin were calculated as per the procedure described in section 3.9 and are given in Table 5.52 for the years 2012 and 2013.

Table 5.52: Recovery of naringin from dry peels with resin PA-500

S.No	Year	Naringin Conc. in KPBW (kg/m^3)	Naringin obtained (g)	Purity (%)	Recovery (%)
1	2012	0.700	2.1	89.3	49.6
2	2013	0.650	1.9	88.6	49.0

(B) Pectin recovery and characterization

The recovery of pectin was calculated as per the procedure described in section 3.10. The obtained pectin was characterised, the values of different parameters determined are given in Table 5.53.

Table 5.53: Recovery of pectin from dry peels with resin PA-500

S. No	Year	Recovey (%)	Moisture (%)	Ash (%)	Equivalent weigh (mg/ml)	Methoxyl content (%)	Anhdrouronic acid (%)	DE (%)
1	2012	54.8	6.5	5.5	578.2	6.1	55.4	62.5
2	2013	58.7	5.5	6.1	613.5	4.9	50.1	55.5

5.6. Adsorption-Desorption studies for naringin with Dry peels on Resin PA-800 (system 6)

5.6.1. Adsorption equilibrium studies (System 6)

The adsorption equilibrium studies with kinnow peel boiled water were carried out as per the procedure described in the section 3.5.1. The data have been presented in Table G1 and Figure 5.76. The adsorption equilibrium experimental data could be correlated by using Langmuir adsorption isotherm and its parameters were evaluated and are shown in Table 5.54. It may be noted that the naringin concentration in solution (KPBW) was 0.700 and 0.650 kg/m^3 respectively in the years 2012 and 2013. The maximum amount of naringin that can be picked up by resin PA-800 from dry KPBW (calculated from Langmuir adsorption isotherm constants) was found to be 0.110 and 0.142 kg per kg of dry resin respectively for the years 2012 and 2013.

Table 5.54: Langmuir isotherm parameters for adsorption of naringin on resin PA-800 from dry KPBW

S.No	Year	Langmuir constants		
		A	b	R^2
1	2012	0.320	2.898	0.956
2	2013	0.207	1.442	0.869

5.6.2. Adsorption kinetic studies (System 6)

The adsorption kinetic studies were carried out as per the procedure described in the section 3.5.2.

The concentration of naringin in the solution as a function of time during adsorption for various amounts of resin is presented in Figures 5.77 and 5.78 for the years 2012 and 2013. The data obtained in these experiments are given in Tables G2 (a-b). It may be observed that the rate of change in concentration of a solution is more when the mass of the resin used is more.

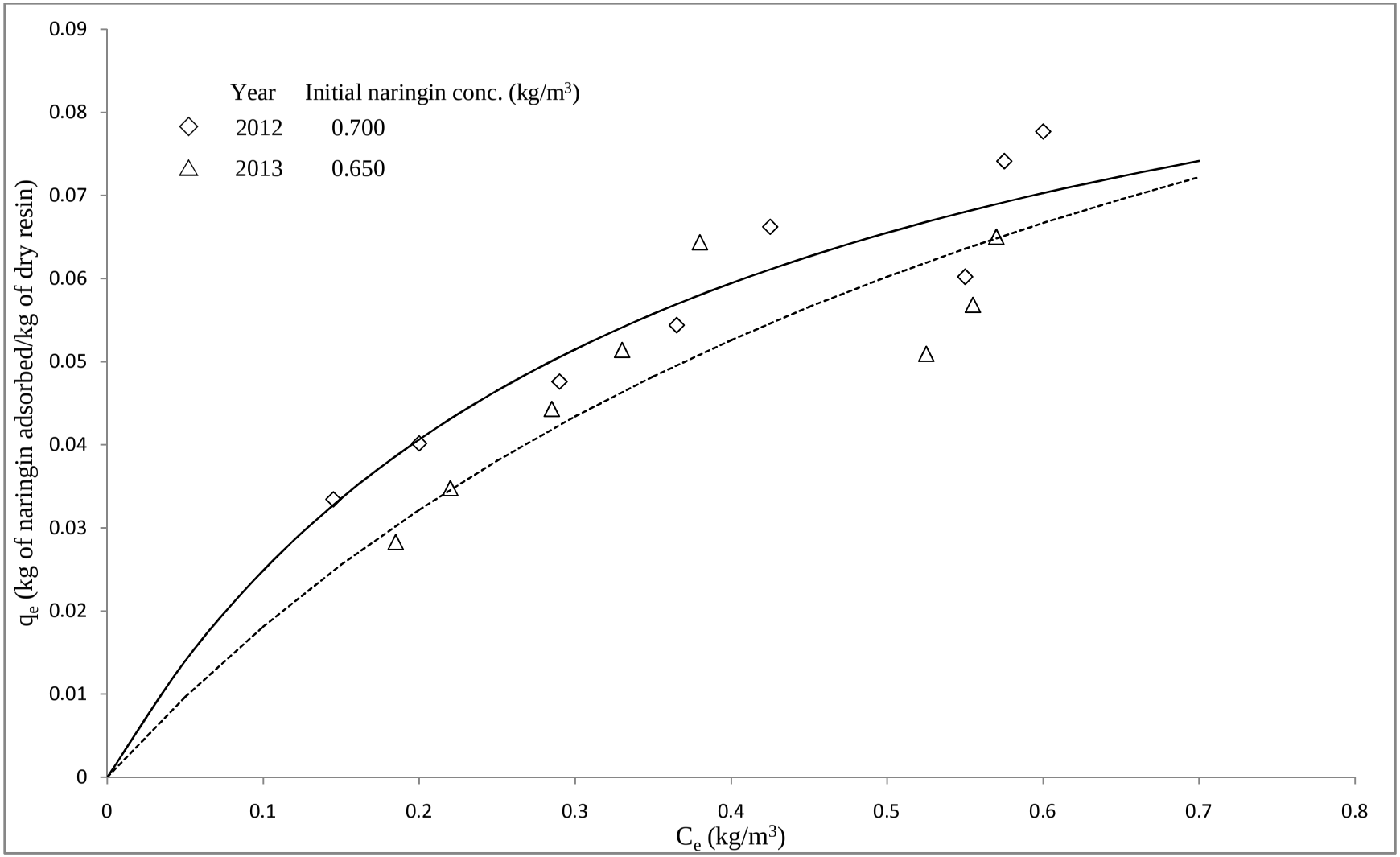

Figure 5.76: Adsorption equilibrium studies with dry KPBW on resin PA-800 in two years (system 6)

Modelling of adsorption kinetic data

The kinetic data have been analysed with the same approach (modified adsorption shell model) as discussed in the earlier for system 1. The values of different parameters viz. slopes of $F_n(t)$ vs t plots, K, β and ψ are tabulated below (Table 5.55) for all the runs of both the years.

Table 5.55: Modified adsorption shell model parameters for system 6

$D_P = 1.032\times10^{-10}\, m^2/s$, $\varepsilon = 0.39$, $R_p = 0.48\times10^{-3}$ m

Year	Run	C_o kg/m^3	q_e kg/m^3	Slope × 10^{-4} (s^{-1})	K	β	ψ	$\frac{D_c}{r_c^2}$ × 10^{-4} (s^{-1})
2012	1	0.700	75.64	2.51	236.6	503.7	4.66	4.45
	2	0.700	67.67	3.08	260.0	609.0	6.29	6.01
	3	0.700	55.02	3.36	230.7	478.2	6.08	5.81
	4	0.700	51.26	1.74	111.2	96.42	1.31	1.26
2013	1	0.665	68.49	2.49	229.5	473.1	4.49	4.29
	2	0.650	54.55	3.88	284.1	726.4	8.65	8.26
	3	0.650	51.42	4.30	296.8	791.3	10.0	9.55
	4	0.650	47.76	3.72	238.3	511.1	6.95	6.64

The generated C_t (with a representative value of ψ = 6.058) for all the runs are shown by smooth curves, and experimental data are given for comparison in Figures 5.77 and 5.78.

The data were tested for significance of the mean difference, paired observation by t -test at a 5% level of significance, and it was found that the experimental and predicted data for almost all the runs does not differ significantly. The summary of the statistical analysis values is given in Table 5.56.

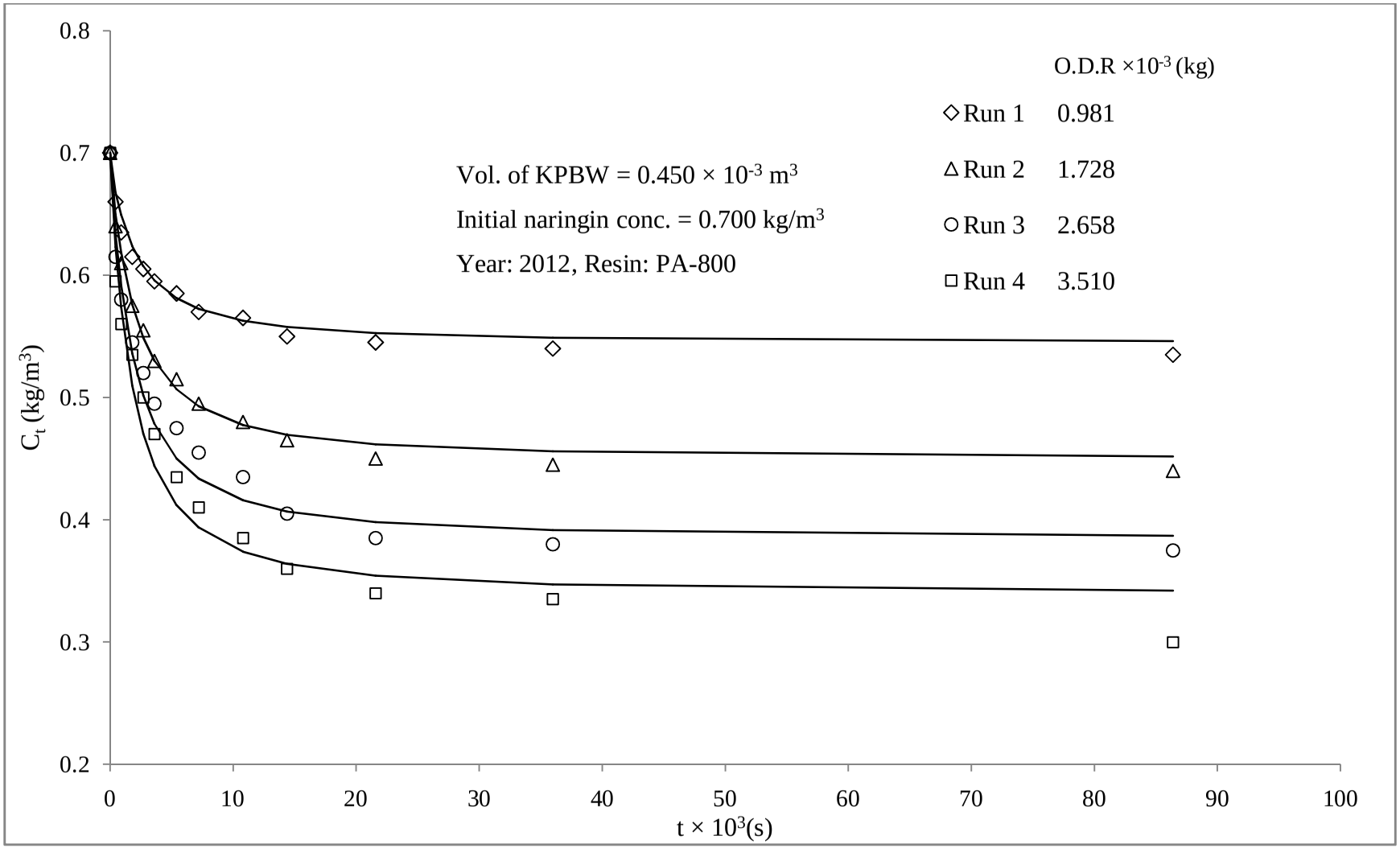

Figure 5.77: Adsorption of naringin on adsorbent PA-800 from dry KPBW: kinetic studies, correlation of experimental data, C_t *vs t* (system 6, year 2012)

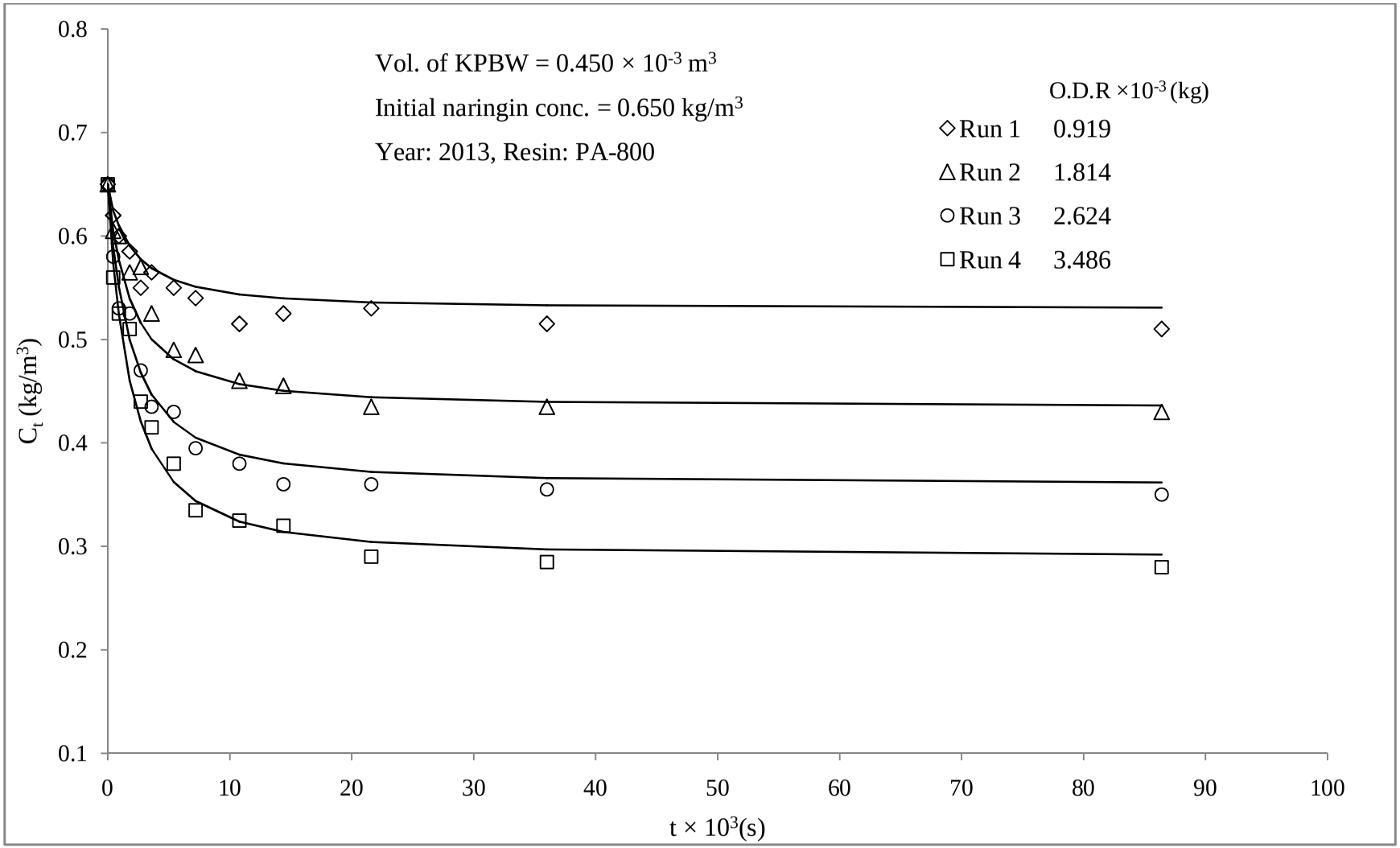

Figure 5.78: Adsorption of naringin on adsorbent PA-800 from dry KPBW: kinetic studies, correlation of experimental data, C_t *vs t* (system 6, year 2013)

Table 5.56: Statistical analysis for predicted and experimental values of C_t (system 6)

Year	Run	Slope C_{trep} vs. $C_{t\exp}$ passing through origin	R^2	t-Cri	t-Cal	Inference
2012	1	1.009	0.981	2.200	-3.455	SD
	2	1.006	0.987	2.200	-1.576	NSD
	3	0.992	0.96	2.200	0.723	NSD
	4	0.994	0.935	2.200	0.210	NSD
2013	1	1.023	0.91	2.200	-5.167	SD
	2	0.974	0.907	2.200	2.244	SD
	3	1.013	0.968	2.200	-1.744	NSD
	4	0.984	0.959	2.200	0.802	NSD

*NSD- No Significance difference, SD- Significance difference

From the above, it is evident that observed kinetic data could be correlated reasonably using modified adsorption shell model.

Comparison of adsorption kinetics:

The kinetics of adsorption of naringin from dry kinnow peel boiled water for two years with the same mass of resin have been compared, and it is shown in Figure 5.79, and the rate of adsorption is almost similar.

5.6.3. Fixed bed column adsorption studies (System 6)

The adsorption column studies were carried out as per the procedure described in the earlier section 3.5.3. The column studies of the different year's samples of KPBW is shown in Figure 5.80. From the Figure 5.80, it was observed that the first 7200 (s) the concentration of naringin in outgoing solution was almost zero for both the years. The adsorption column data are given in Table G3 (a-b). The various parameters of breakthrough curves are listed for the two years in Table 5.57.

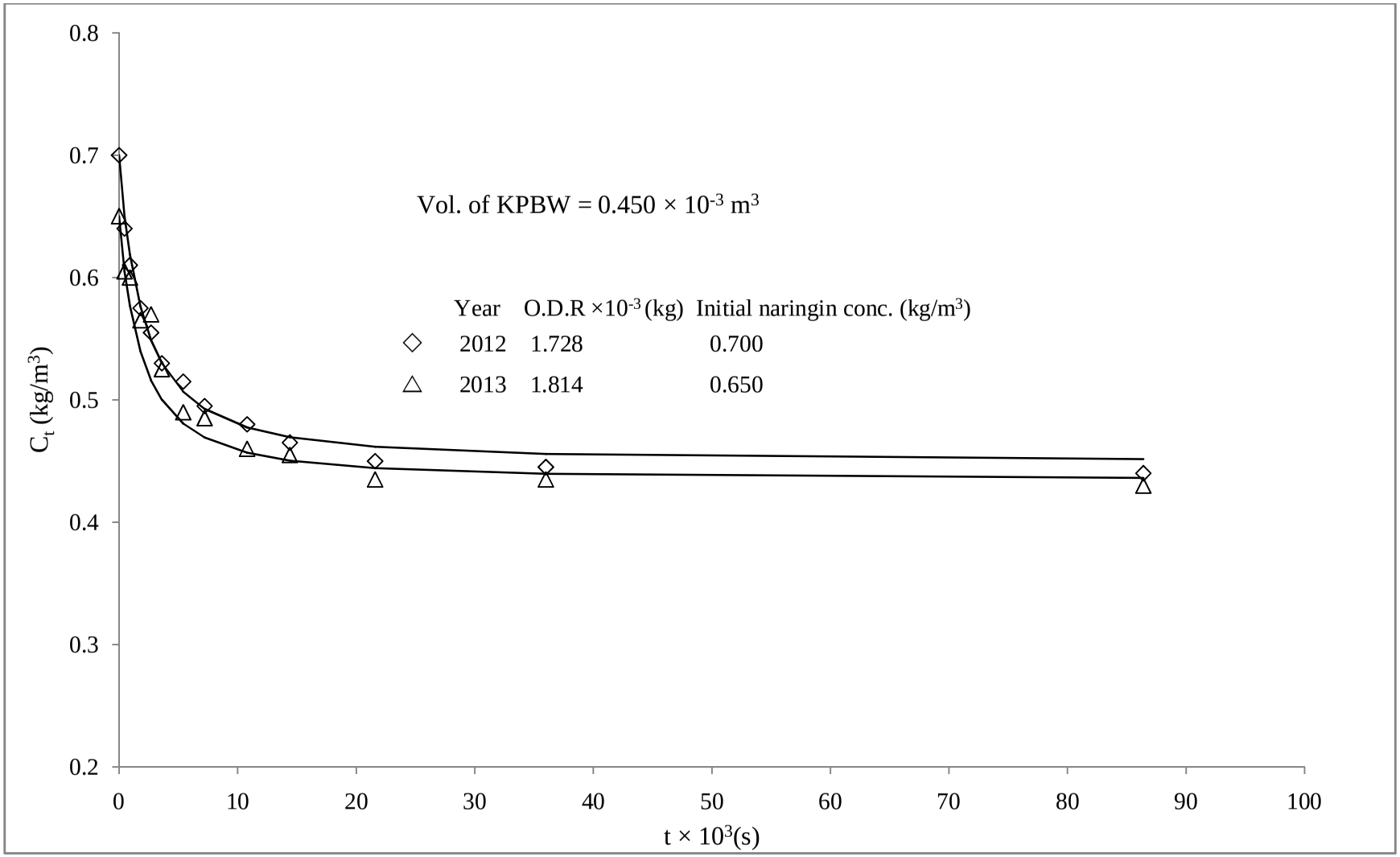

Figure 5.79: Comparison of naringin adsorption kinetic studies on the resin PA-800 from dry KPBW with year (system 6), C_t *vs t*

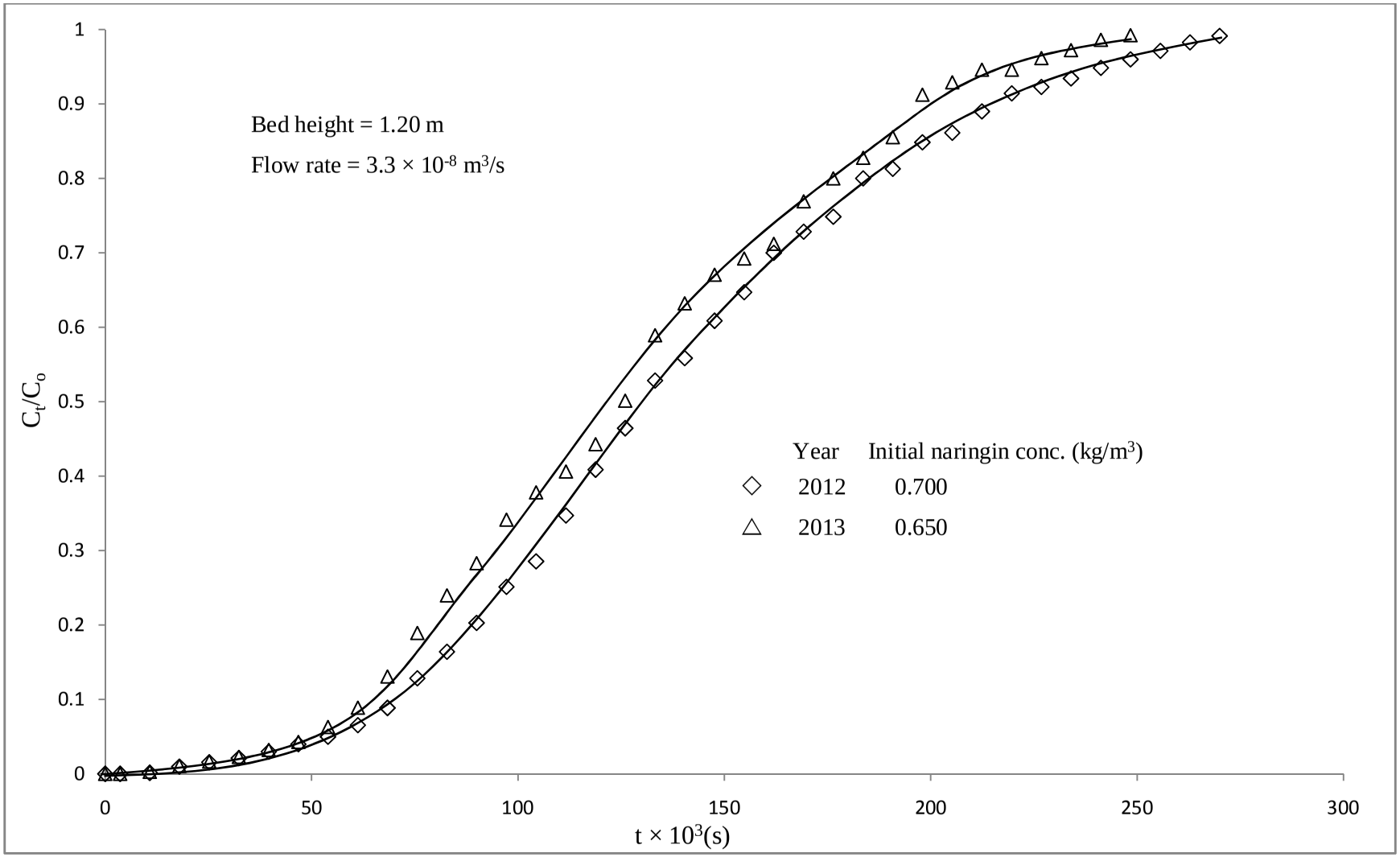

Figure 5.80: Adsorption of naringin on adsorbent PA-800 from dry KPBW: fixed bed column study (system 6)

Table 5.57: Parameters of breakthrough curves for adsorption of naringin on resin PA-800 from dry KPBW in a fixed-bed column for two years

Bed height = 1.20 m, Flow rate = 3.3×10^{-8} m^3/s

S.No	Year	C_o (kg/m^3)	$t_b \times 10^3$ (s)	$t_t \times 10^3$ (s)	q_{total} g	q_s kg/kg	H_{UNB} (m)	MTZ (m)
1	2012	0.700	57.6	136.1	3.68	0.071	0.692	0.724
2	2013	0.650	50.4	124.8	3.15	0.074	0.715	0.758

5.6.4. Desorption equilibrium studies (System 6)

The equilibrium studies of desorption of naringin into ethanol from naringin saturated resin were carried out as per the procedure described in the section 3.6.1.

The data have been presented in Table G4 and Figure 5.81. It is found that the desorption is favourable with ethanol but does not approach completion. The desorption equilibrium experimental data could be correlated with Freundlich adsorption isotherm and its parameters were evaluated and are presented in Table 5.58.

Table 5.58: Freundlich isotherm constants for desorption of naringin from naringin saturated resin PA-800 (dry peels)

S.No	Year	Freundlich constants		
		K_{fd}	n_d	R^2
1	2012	0.102	1.048	0.931
2	2013	0.072	1.526	0.908

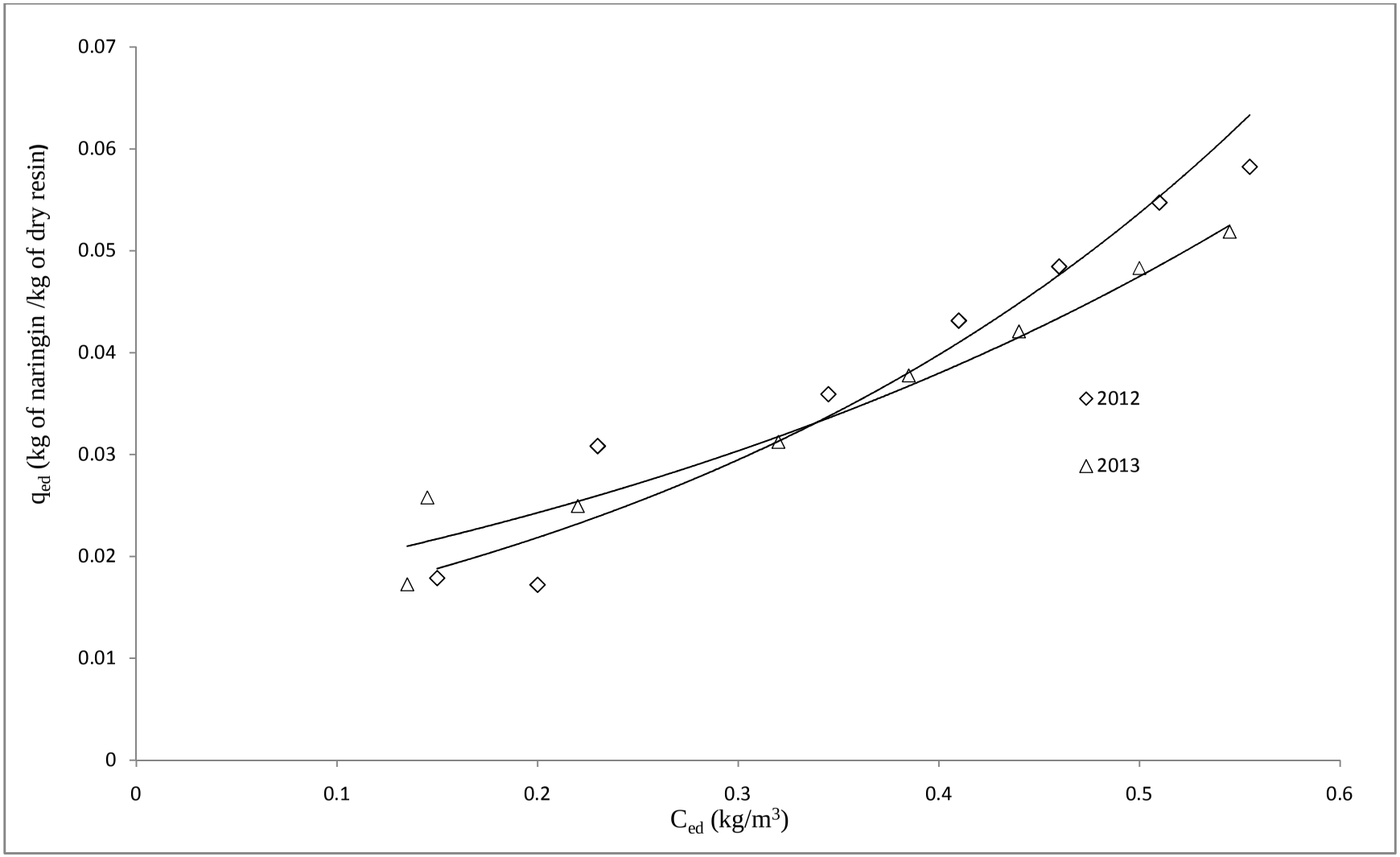

Figure 5.81: Desoption equilibrium studies from naringin saturated resin PA-800 to ethanol solution (system 6)

5.6.5. Desorption kinetic studies (System 6)

The kinetic studies of desorption of naringin into ethanol from naringin saturated resin were carried out as per the procedure described in the section 3.6.2 and, data are presented in Table G5 (a-b) and Figures 5.82 and 5.83.

Modelling of desorption kinetic data

The above data have been analysed with the same approach as done for System 1 (i.e., Boyd's diffusivity model equation).

The values of effective diffusivity D_{ed}, were estimated using linear plots of $\ln\left(1/1-u_d^2(t)\right)$ vs time (t) and given in Table 5.59. The average value of effective diffusivity D_{ed} is found to be 12.52×10^{-13} (m^2s^{-1}).

Table 5.59: Boyd's diffusivity model parameters for desorption of naringin from naringin saturated resin PA-800 (system 6)

S.No	Run	Year			
		2012		2013	
		$D_{ed}\times10^{-13}$ (m^2s^{-1})	R^2	$D_{ed}\times10^{-13}$ (m^2s^{-1})	R^2
1	1	13.3	0.950	13.7	0.964
2	2	13.0	0.990	12.0	0.983
3	3	11.3	0.980	11.6	0.979

The generated C_{td} (with a representative value of D_{ed} = $12.52\times10^{-13}\,m^2s^{-1}$) for all the runs are shown by smooth curves, and experimental data are given for comparison in Figures 5.82 and 5.83.

The data were tested for significance of the mean difference, paired observation by t -test at a 5% level of significance, and it was found that the experimental, as well as predicted data of almost all the runs, does not differ significantly.

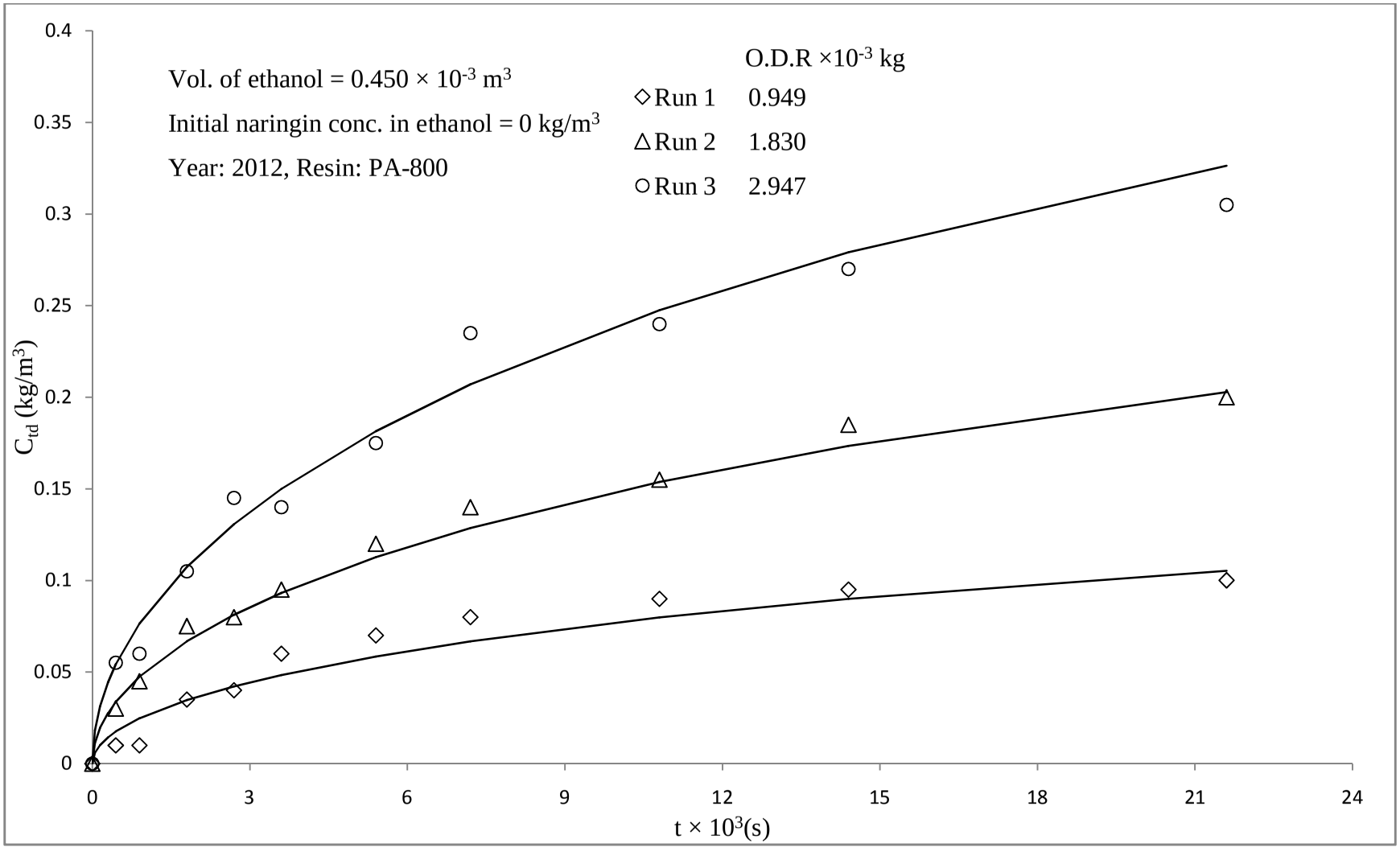

Figure 5.82: Desorption kinetic studies with naringin saturated resin PA-800 in ethanol: correlation of experimental data C_{td} *vs t* (system 6, year 2012)

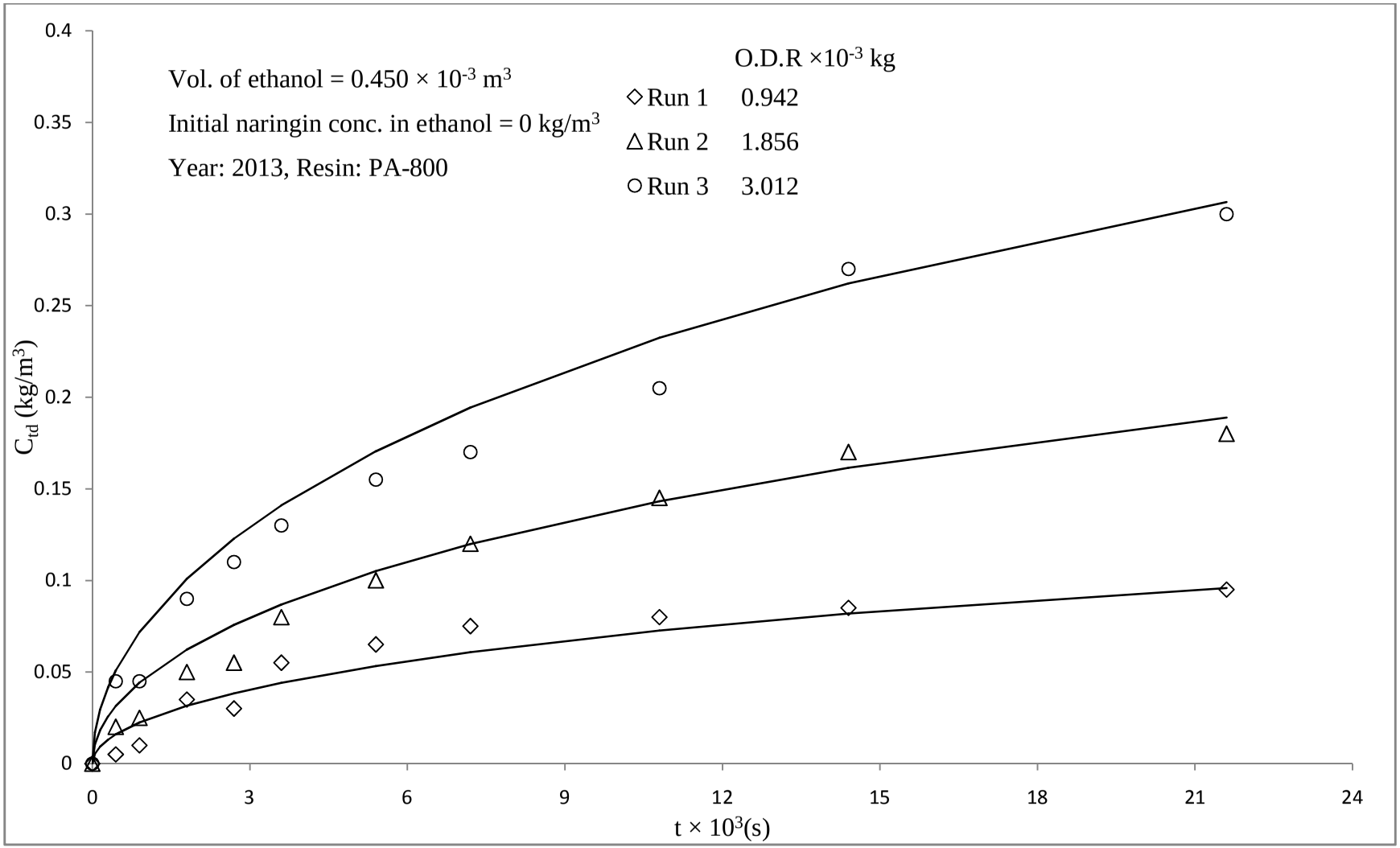

Figure 5.83: Desorption kinetic studies with naringin saturated resin PA-800 in ethanol: correlation of experimental data C_{td} *vs t* (system 6, year 2013)

The summary of the statistical analysis of the predicted values from the model and experimental values is given in Table 5.60.

Table 5.60: Statistical analysis for predicted and experimental values of C_{td} (system 6)

Run	Year	Slope	R^2 C_{trep} vs. $C_{t\exp}$	t-Cri	t-Cal	Inference
1	2012	0.929	0.911	2.262	0.750	NSD
2		0.969	0.99	2.262	1.669	NSD
3		1.016	0.973	2.262	-0.659	NSD
1	2013	0.923	0.893	2.262	0.587	NSD
2		1.028	0.949	2.262	-2.544	SD
3		1.057	0.97	2.262	-3.862	SD

*NSD- No Significance difference, SD- Significance difference

From the above, it is evident that observed kinetic data studied could be correlated reasonably using Boyd's diffusivity model equation.

Comparison of desorption kinetics:

The kinetics of naringin desorption from resin saturated with naringin to ethanol for the two different years with the same mass of resin has been compared, and it is shown in Figure 5.84. The kinetics of desorption of naringin into ethanol solution is almost same in both the years.

5.6.6. Desorption fixed bed column studies (System 6)

The desorption column studies were carried out in glass column as per the procedure described in the section 3.6.3 and presented in Figure 5.85. From the Figure 5.85, it is evident that the amount of naringin desorbed from resin saturated with naringin, obtained from adsorption column studies, in ethanol solution decreases with time. The data of naringin desorption column studies with ethanol to recover naringin are given in Table G6.

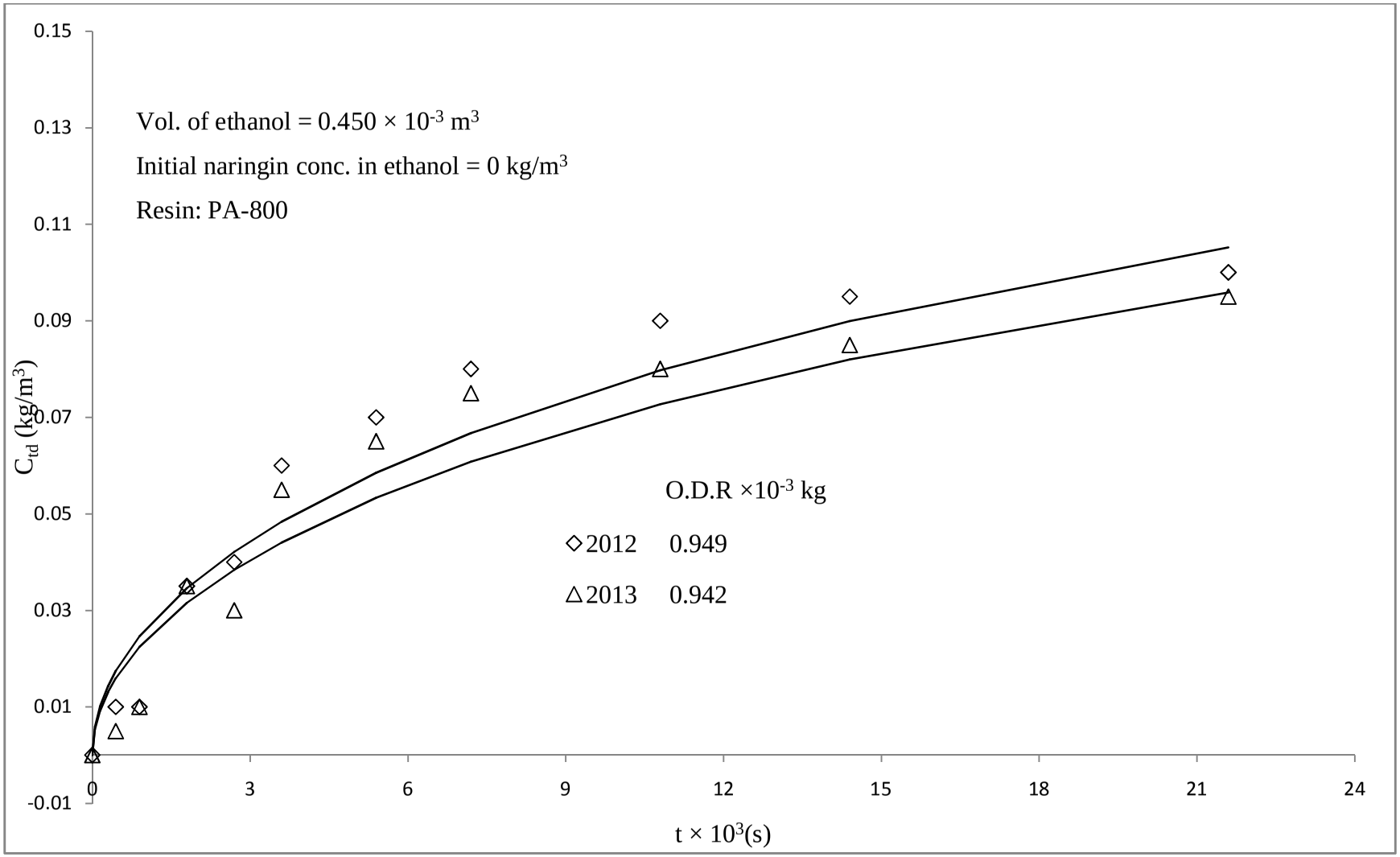

Figure 5.84: Comparison of desorption kinetic studies of naringin saturated resin PA-800 in ethanol with year (system 6), C_{td} *vs t*

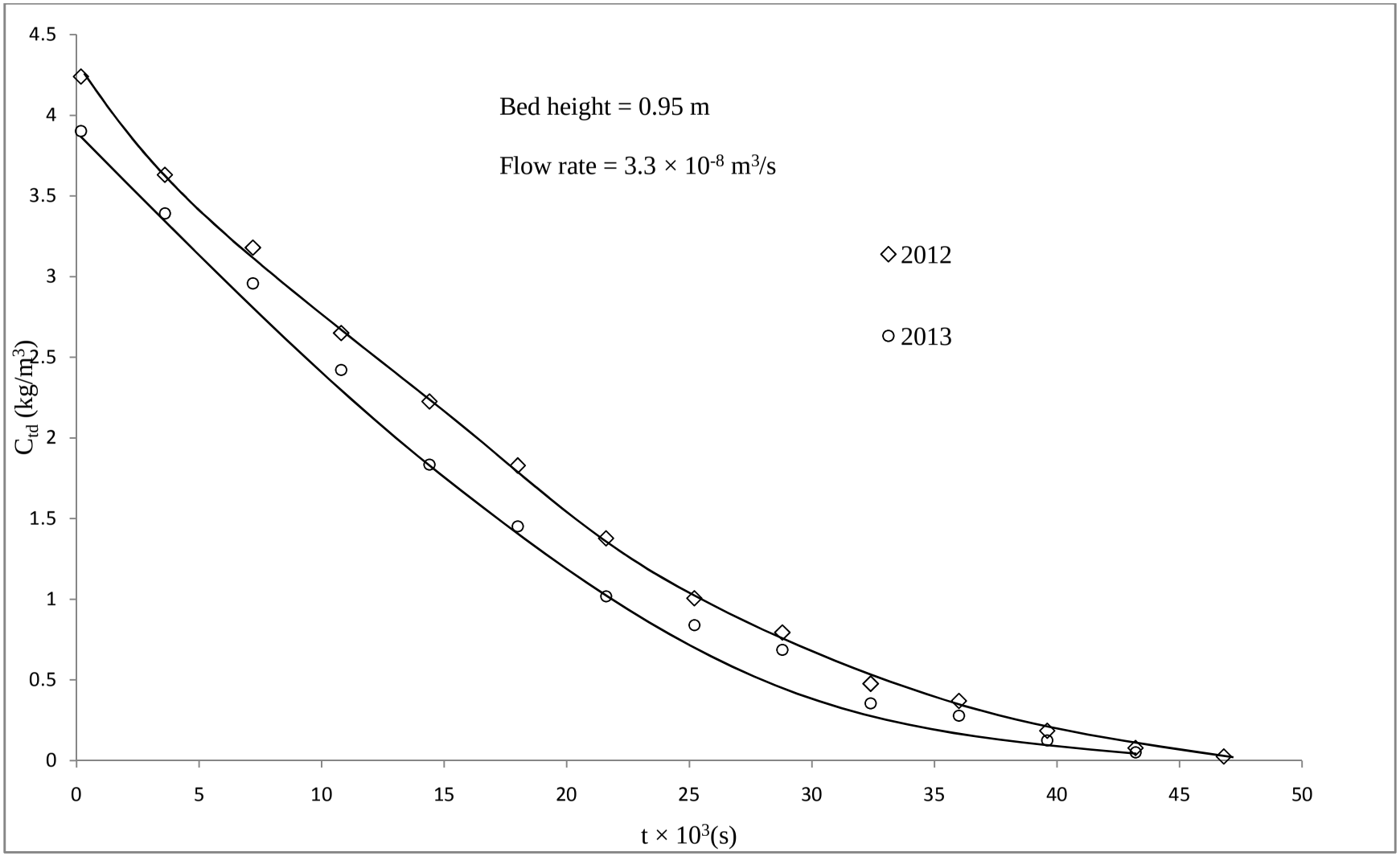

Figure 5.85: Column desorption studies from naringin saturated resin PA-800 into ethanol, C_{td} *vs t* (system 6)

From these desorption studies, it can be concluded that about 1500 ml of ethanol is sufficient for almost all the possible recoverable desorption of naringin from the resin PA-800 in a glass column of 14 mm ID filled up to the height 0.95 m (about 120 g naringin saturated resin (wet)). The amount of naringin desorbed in the column was found to be 2.32 and 2.06 g respectively for the years 2012 and 2013.

5.6.7. Purity and recovery of obtained Naringin and Pectin (System 6)

(A) Naringin recovery

Recovery and purity of naringin were calculated as per the procedure described in section 3.9 and are tabulated in Table 5.61 for the years 2012 and 2013.

Table 5.61: Recovery of naringin from dry peels with resin PA-800

S.No	Year	Naringin Conc. in KPBW (kg/m^3)	Naringin obtained (g)	Purity (%)	Recovery (%)
1	2012	0.700	2.4	87.5	50.0
2	2013	0.650	2.2	90.1	51.8

(B) Pectin recovery and characterization

The recovery of pectin was calculated as per the procedure described in section 3.10. The obtained pectin was characterised, the values of different parameters determined are given in Table 5.62.

Table 5.62: Recovery of pectin from dry peels with resin PA-800

S. No	Year	Recovey (%)	Moisture (%)	Ash (%)	Equivalent weigh (mg/ml)	Methoxyl content (%)	Andhrouronic acid (%)	DE (%)
1	2012	57.1	6.2	5.8	550.6	5.3	48.3	62.2
2	2013	58.3	5.9	6.9	601.2	5.5	57.8	54.0

5.7. Adsorption-Desorption studies of naringin with fresh peels on regenerated resin PA-500 (system 7)

5.7.1. Adsorption equilibrium studies (System 7)

The procedure to regenerate the used resin after desorption studies are described in section 3.8.

The adsorption equilibrium studies with kinnow peel boiled water were carried out as per the procedure mentioned in the section 3.5.1. The data have been presented in Table H1 (a) and Figure 5.86. The adsorption equilibrium experimental data could be correlated by using Langmuir adsorption isotherm and its constants a and b are found to be 0.171 and 1.603 respectively. It was found that the naringin concentration in solution (KPBW) was 0.800 kg/m^3. The maximum amount of naringin that can be picked up by regenerated resin PA-500 (calculated from Langmuir adsorption isotherm constants) was found to be 0.106 kg per kg of dry resin.

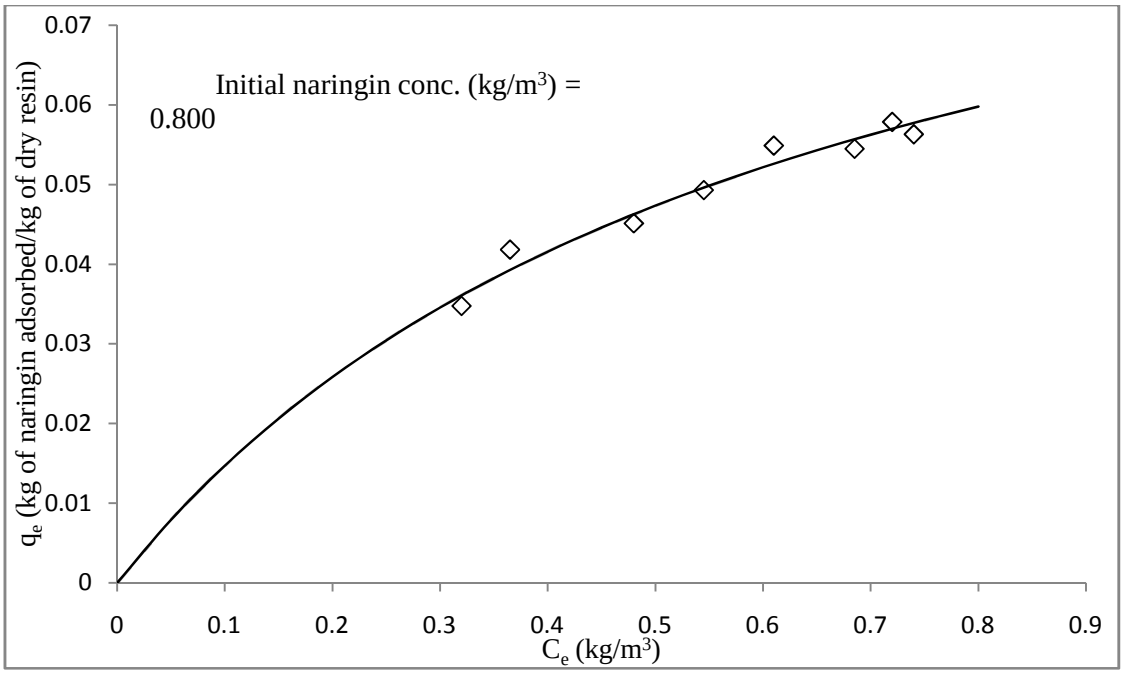

Figure 5.86: Adsorption equilibrium studies with fresh KPBW on regenerated resin PA-500 (system 7)

5.7.2. Adsorption kinetic studies (System 7)

The adsorption kinetic studies were carried out as per the procedure described in the section 3.5.2.

The concentration of naringin in the solution as a function of time during adsorption for various amounts of oven dried resin is presented in Figure 5.87. The data obtained in these experiments are given in Table H2 (a). It may be observed that the rate of change in concentration of a solution is more when the mass of the resin used is more.

Modelling of adsorption kinetic data

The kinetic data have been analysed with the same approach (modified adsorption shell model) as discussed in the earlier for system 1. The values of different parameters viz. slopes of $F_n(t)$ vs t plot, K, β and ψ are tabulated below (Table 5.63) for all the three runs.

Table 5.63: Modified adsorption shell model parameters for system 7

$D_P = 1.032\times10^{-10} m^2/s$, $\varepsilon = 0.39$, R_p = 0.375×10^{-3} m

Run	C_o kg/m^3	q_e kg/m^3	Slope × 10^{-4} (s^{-1})	K	β	ψ	$\frac{D_c}{r_c^2}$ × 10^{-4} (s^{-1})
1	0.800	53.15	1.64	58.12	18.54	0.27	0.43
2	0.800	39.37	2.05	53.79	14.96	0.30	0.47
3	0.800	37.75	4.19	105.2	84.54	1.79	2.80

The generated C_t (with a representative value of ψ = 0.791) for all the runs are shown by smooth curves, as well as experimental data are given for comparison in Figure 5.87. The data were tested for significance of the mean difference, paired observation by t -test at a 5% level of significance.

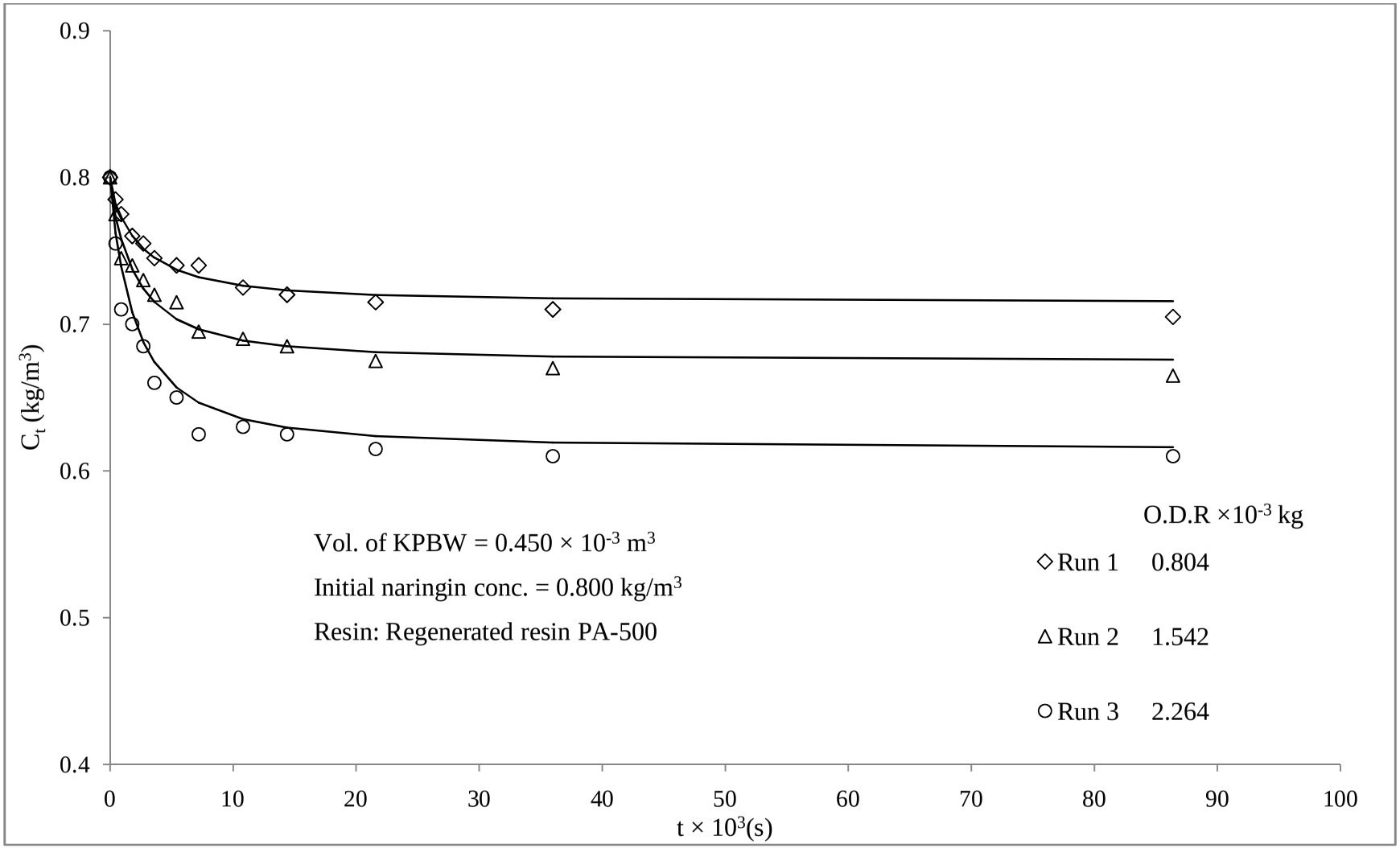

Figure 5.87: Adsorption of naringin on regenerated resin PA-500 from fresh KPBW: kinetic studies, correlation of experimental data, C_t *vs t* (system 7)

It was found that the experimental and predicted data for almost all the runs does not differ significantly. The summary of the statistical analysis values is given in Table 5.64.

Table 5.64: Statistical analysis for predicted and experimental values of C_t (system 7)

Run	Slope C_{trep} vs. $C_{t\exp}$ passing through origin	R^2	t-Cri	t-Cal	Inference
1	1.000	0.944	2.200	-0.470	NSD
2	1.001	0.949	2.200	-0.463	NSD
3	1.015	0.975	2.200	-4.626	SD

* NSD- No Significance difference, SD- Significance difference

From the above, it is evident that observed kinetic data could be correlated reasonably using modified adsorption shell model.

5.7.3. Fixed bed column adsorption studies (System 7)

The adsorption column study was carried out as per the procedure described in the section 3.5.3. The column study with the fresh peels on regenerated resin PA-500 is shown in Figure 5.88. From the Figure 5.88, it was observed that for the first 3600 (s) the concentration of naringin in outgoing solution was almost zero. The adsorption column data are given in Table H3 (a). The various parameters of the breakthrough curve are given in Table 5.65.

Table 5.65: Parameters of breakthrough curves for adsorption of naringin on regenerated resin PA-500 from KPBW in a fixed-bed column

Bed height = 1.20 m, Flow rate = 3.3×10^{-8} m^3/s

C_o (kg/m^3)	$t_b \times 10^3$ (s)	$t_t \times 10^3$ (s)	q_{total} g	q_s kg/kg	H_{UNB} (m)	MTZ (m)
0.800	43.2	129.9	3.46	0.058	0.801	0.848

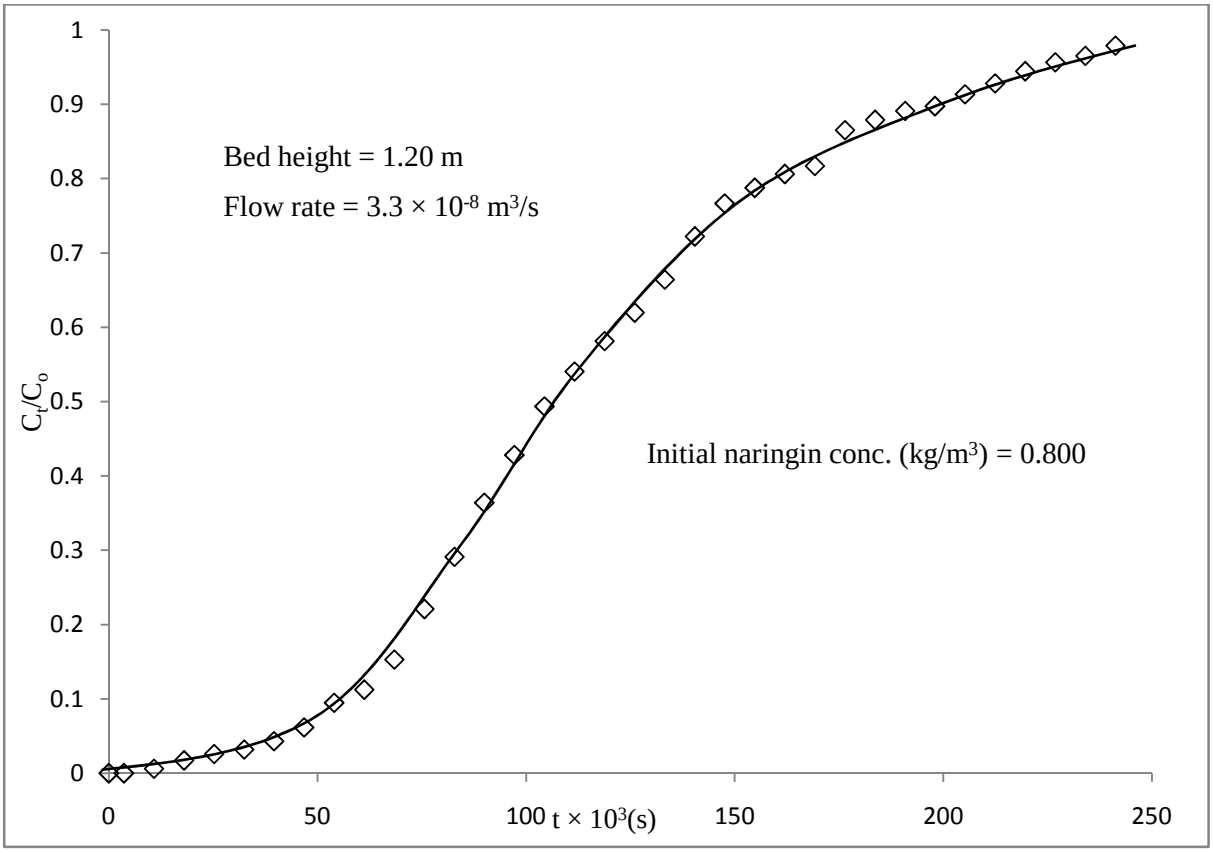

Figure 5.88: Adsorption of naringin on regenerated resin PA-500 from fresh KPBW: fixed bed column study (system 7)

5.7.4. Desorption equilibrium studies (System 7)

The equilibrium studies of desorption of naringin into ethanol from naringin saturated regenerated resin was carried out as per the procedure described in the section 3.6.1.

The data have been presented in Table H4 (a) and Figure 5.89. The desorption is favourable with ethanol but does not approach completion. The desorption equilibrium experimental data could be correlated with Freundlich adsorption isotherm and its constants K_{fd} and n_d are found to be 0.115 and 0.922 respectively.

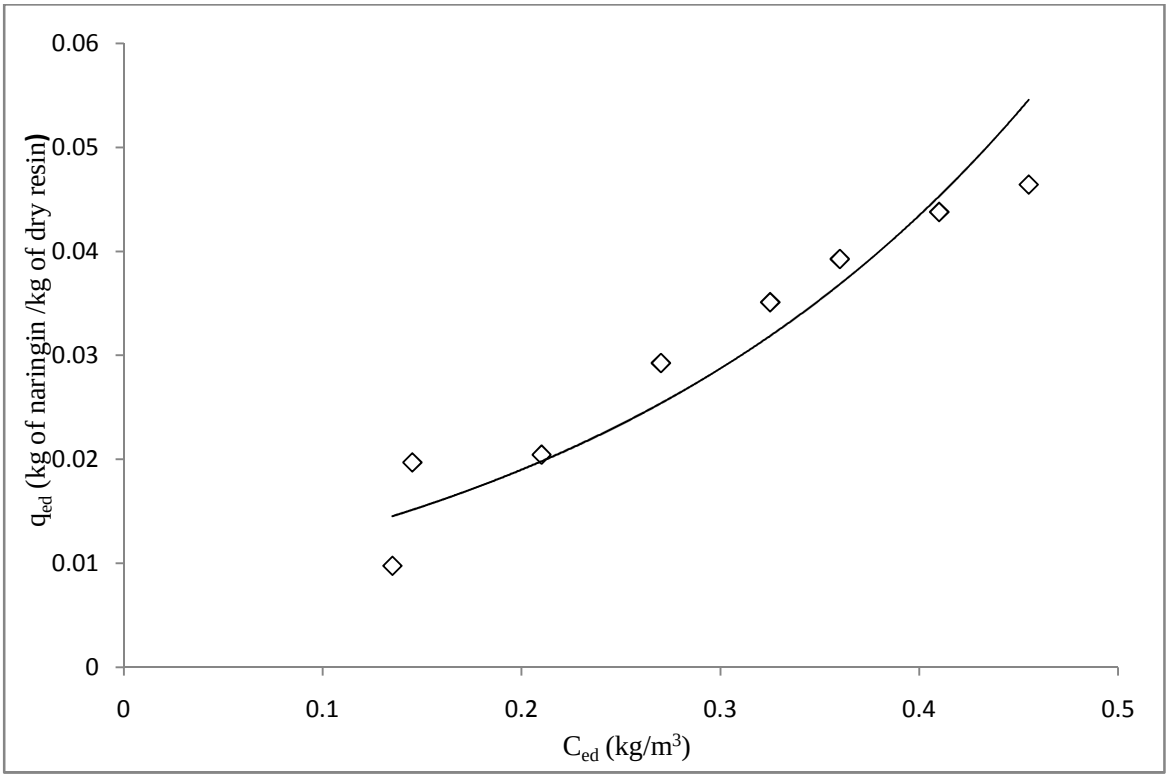

Figure 5.89: Desoption equilibrium studies from naringin saturated resin (regenerated) PA-500 to ethanol solution (system 7)

5.7.5. Desorption kinetic studies (System 7)

The kinetic studies of desorption of naringin into ethanol from naringin saturated resin was carried out as per the procedure described in the section 3.6.2 and, data is presented in Table H5 (a) and Figure 5.90.

Modelling of desorption kinetic data

The above data have been analysed with the same approach as done for System 1 (i.e., Boyd's diffusivity model equation).

The values of effective diffusivity D_{ed}, were estimated using linear plots of $\ln\left(1/1-u_d^2(t)\right)$ vs time (t) and presented in Table 5.66. The average value of effective diffusivity D_{ed} was found to be 13.71×10^{-13} (m^2s^{-1}).

The generated C_{td} (with a representative value of D_{ed} = $13.71\times10^{-13}\,m^2s^{-1}$) for all the runs are shown by smooth curves, and experimental data are given for comparison in Figure 5.90.

Table 5.66: Boyd's diffusivity model parameters for desorption of naringin from naringin saturated resin (regenerated) PA-500 (system 7)

S.No	Run	$D_{ed}\times10^{-13}(m^2s^{-1})$	R^2
1	1	14.9	0.968
2	2	13.0	0.984
3	3	13.0	0.925

The data were tested for significance of the mean difference, paired observation by t -test at a 5% level of significance, and it was found that the experimental and predicted data does not differ significantly of almost all the runs. The summary of the statistical analysis of the predicted values from the model and experimental values is given in Table 5.67.

Table 5.67: Statistical analysis for predicted and experimental values of C_{td} (system 7)

Run	Slope	R^2 C_{trep} vs. $C_{t\exp}$	t-Cri	t-Cal	Inference
1	0.931	0.926	2.262	0.758	NSD
2	1.003	0.953	2.262	-1.063	NSD
3	0.981	0.952	2.262	0.244	NSD

*NSD- No Significance difference, SD- Significance difference

From the above, it is evident that observed kinetic data could be correlated reasonably using Boyd's diffusivity model equation.

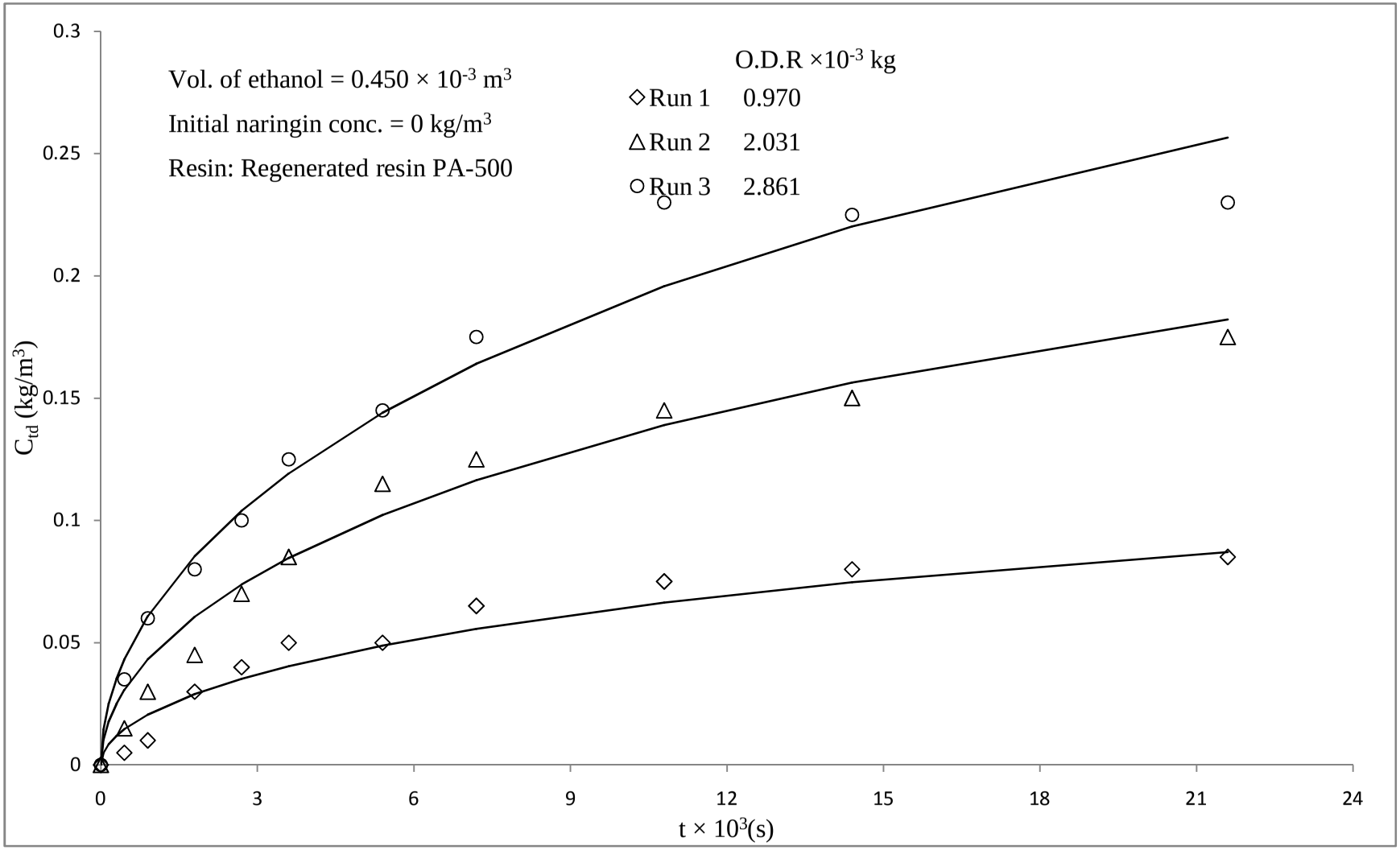

Figure 5.90: Desorption kinetic studies with naringin saturated resin (regenerated) PA-500 in ethanol: correlation of experimental data C_{td} *vs* t (system 7)

5.7.6. Desorption fixed bed column studies (System 7)

The desorption column study was carried out in a glass column as per the procedure described in the section 3.6.3 and, presented in Figure 5.91. From the Figure 5.91, it is evident that the amount of naringin desorbed from resin saturated with naringin, obtained from adsorption column studies, in ethanol solution decreases with time.

The data of column studies for naringin desorption with ethanol to recover naringin are given in Table H6 (a). From this desorption study, it can be concluded that about 1300 ml of ethanol is sufficient for almost all the possible recoverable desorption of naringin from the resin PA-500 in a glass column of 14 mm ID filled up to the height 0.95 m (about 120 g naringin saturated resin (wet)). The amount of naringin desorbed in the column was found to be 2.04 g.

5.7.7. Purity and recovery of obtained Naringin and Pectin (System 7)

(A) Naringin recovery

Recovery and purity of naringin were calculated as per the procedure described in section 3.9, and found to be 46.9 and 90.1%. The naringin obtained was 2.0 g.

(B) Pectin recovery and characterization

The recovery of pectin was calculated as per the procedure described in section 3.10. The obtained pectin was characterised, the values of different parameters determined are presented in Table 5.68.

Table 5.68: Recovery of pectin from fresh peels with regenerated resin PA-500

Recovey (%)	Moisture (%)	Ash (%)	Equivalent weigh (mg/ml)	Methoxyl content (%)	Anhdrouronic acid (%)	DE (%)
52.6	7.5	6.5	567.3	5.7	57.2	56.5

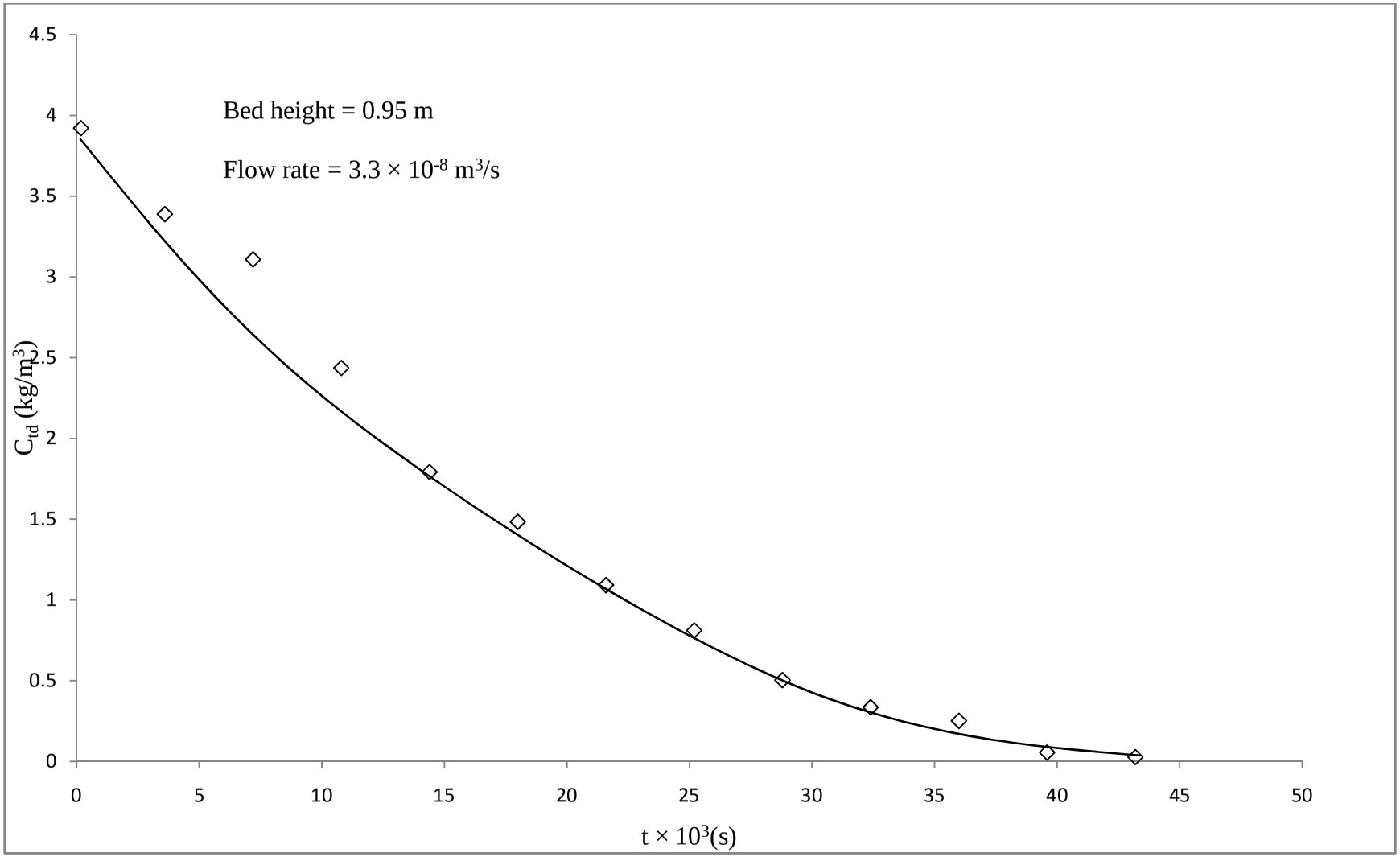

Figure 5.91: Column desorption studies from naringin saturated resin (regenerated) PA-500 into ethanol, C_{td} *vs t* (system 7)

5.8. Adsorption-Desorption studies of naringin with fresh peels on regenerated resin PA-800 (system 8)

5.8.1. Adsorption equilibrium studies (System 8)

The adsorption equilibrium studies with kinnow peel boiled water were carried out as per the procedure described in the section 3.5.1. The data have been presented in Table H1 (b) and Figure 5.92. The adsorption equilibrium experimental data could be correlated by using Langmuir adsorption isotherm and its constants a and b are found to be 0.188 and 1.452 respectively. It was found that the naringin concentration in solution (KPBW) was 0.800 kg/m^3. The maximum amount of naringin that can be picked up by regenerated resin PA-800 (calculated from Langmuir adsorption isotherm constants) was found to be 0.129 kg per kg of dry resin.

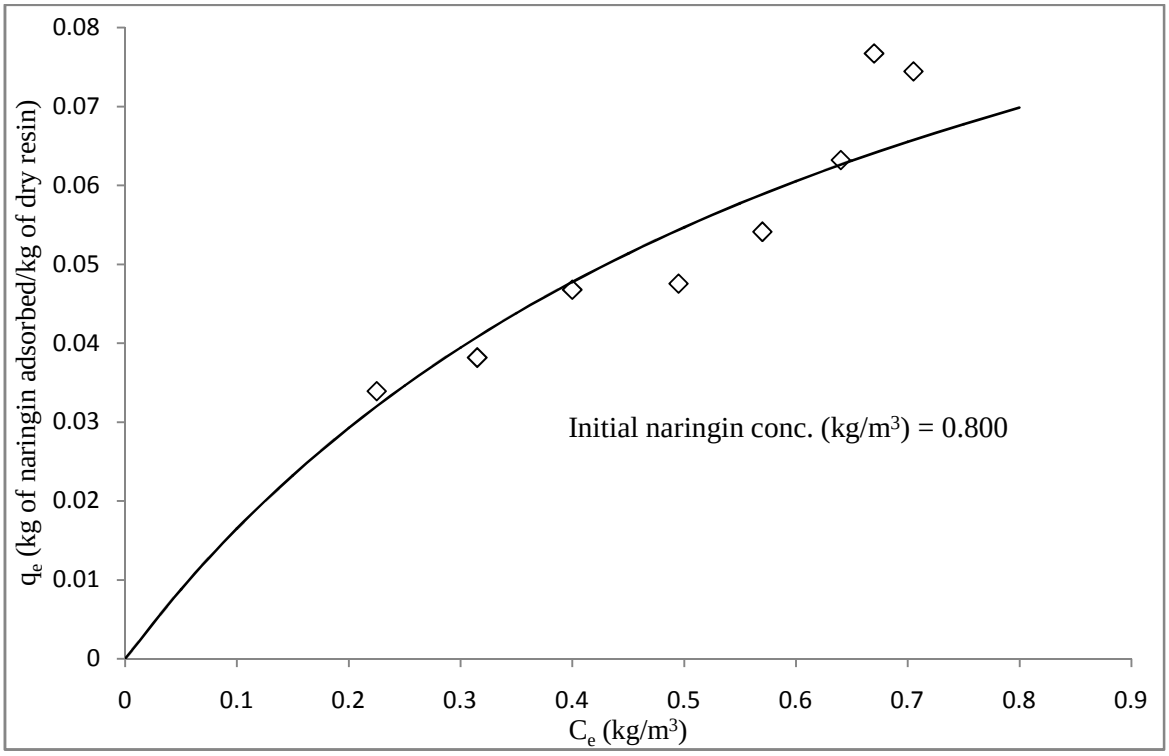

Figure 5.92: Adsorption equilibrium studies with fresh KPBW on regenerated resin PA-800 (system 8)

5.8.2. Adsorption kinetic studies (System 8)

The adsorption kinetic studies were carried out as per the procedure described in the section 3.5.2.

The concentration of naringin in the solution as a function of time during adsorption for various amounts of oven dried resin is presented in Figure 5.93. The data obtained in these experiments are given in Table H2 (b). It may be observed that the rate of change in concentration of a solution is more when the mass of the resin used is more.

Modelling of adsorption kinetic data

The kinetic data have been analyzed with the same approach (modified adsorption shell model) as discussed in the earlier for system 1. The values of different parameters viz. slopes of $F_n(t)$ vs t plot, K, β and ψ are tabulated below (Table 5.69) for all the four runs.

Table 5.69: Modified adsorption shell model parameters for system 8

$D_P = 1.032\times10^{-10} m^2/s$, $\varepsilon = 0.39$, R_p = 0.48×10^{-3} m

Run	C_o kg/m^3	q_e kg/m^3	Slope × 10^{-4} (s^{-1})	K	β	ψ	$\frac{D_c}{r_c^2}$ × 10^{-4} (s^{-1})
1	0.800	76.99	2.344	196.6	343.3	3.56	3.41
2	0.800	60.20	1.69	111.2	96.55	1.28	1.22
3	0.800	55.06	1.83	109.9	93.82	1.36	1.30
4	0.800	54.13	2.88	169.9	251.4	3.71	3.55

The generated C_t (with a representative value of ψ = 2.482) for all the runs are shown by smooth curves, and experimental data are given for comparison in Figure 5.93.

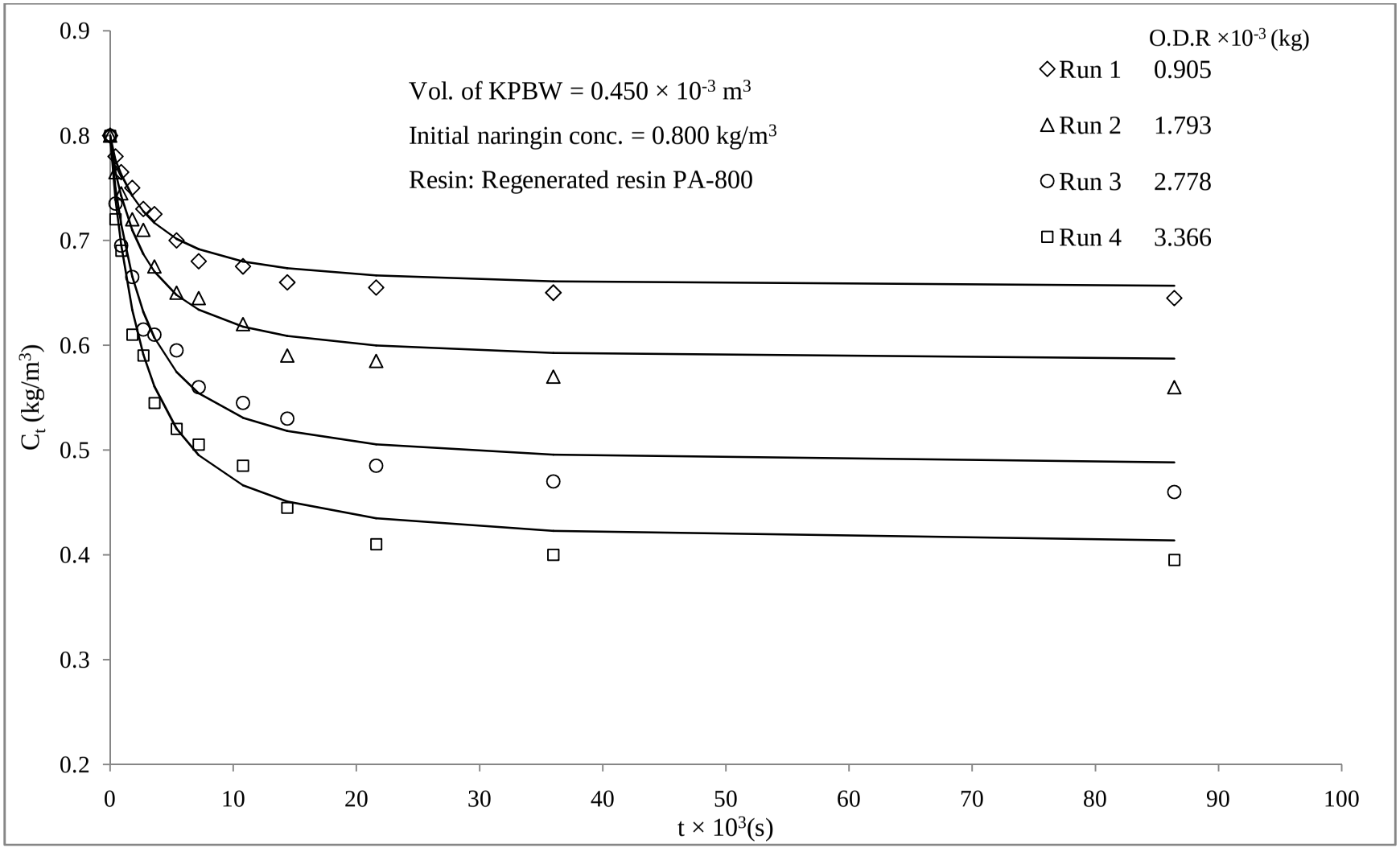

Figure 5.93: Adsorption of naringin on regenerated resin PA-800 from fresh KPBW: kinetic studies, correlation of experimental data, C_t *vs t* (system 8)

The data were tested for significance of the mean difference, paired observation by t -test at a 5% level of significance, and it was found that the experimental and predicted data of three out of the four runs do not differ significantly. The summary of the statistics analysis values is given in Table 5.7.

Table 5.70: Statistical analysis for predicted and experimental values of C_t (system 8)

Run	Slope C_{trep} vs. $C_{t\exp}$ passing through origin	R^2	t-Cri	t-Cal	Inference
1	1.004	0.957	2.200	-1.461	NSD
2	1.001	0.937	2.200	-0.497	NSD
3	1.009	0.962	2.200	-1.195	NSD
4	1.016	0.983	2.200	-2.233	SD

*NSD- No Significance difference, SD- Significance difference

From the table 5.70, it is evident that observed kinetic data studied could be correlated reasonably using modified adsorption shell model.

5.8.3. Fixed bed column adsorption studies (System 8)

The adsorption column study was carried out as per the procedure described in the section 3.5.3. The column study with the fresh peels on regenerated resin PA-800 is shown in Figure 5.94 and Table H3 (b). From the Figure 5.94, it was observed that for the first 7000 (s) the concentration of naringin in outgoing solution was almost zero. The various parameters of the breakthrough curve are presented in Table 5.71.

Table 5.71: Parameters of breakthrough curves for adsorption of naringin on regenerated resin PA-800 from KPBW in a fixed-bed column

Bed height = 1.20 m, Flow rate = 3.3×10^{-8} m^3/s

C_o (kg/m^3)	$t_b \times 10^3$ (s)	$t_t \times 10^3$ (s)	q_{total} (g)	q_s (kg/kg)	H_{UNB} (m)	MTZ (m)
0.800	50.4	140.2	3.74	0.065	0.768	0.808

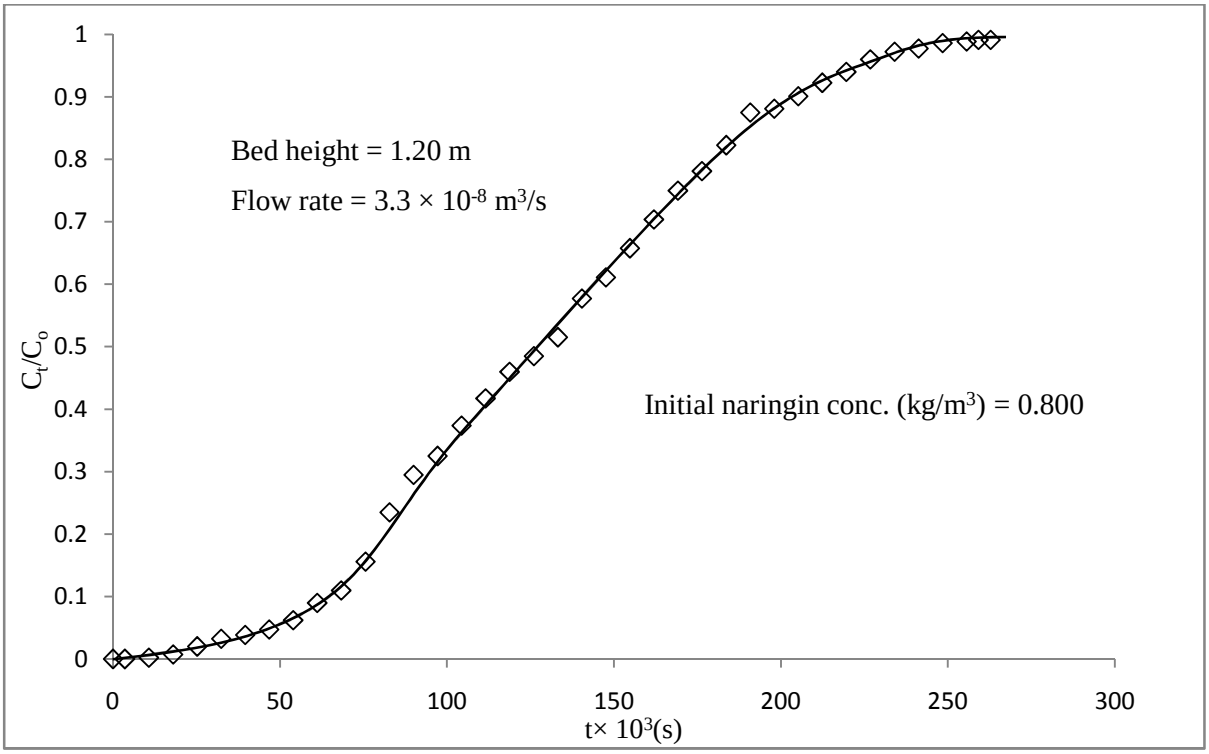

Figure 5.94: Adsorption of naringin on regenerated resin PA-800 from fresh KPBW: fixed bed column study (system 8)

5.8.4. Desorption equilibrium studies (System 8)

The equilibrium studies of desorption of naringin into ethanol from naringin saturated regenerated resin PA-800 was carried out as per the procedure described in the section 3.6.1. The data have been presented in Table H4 (b) and Figure 5.95. The desorption is favourable with ethanol but does not approach completion.

The desorption equilibrium experimental data could be correlated with Freundlich adsorption isotherm and its constants K_{fd} and n_d are found to be 0.101 and 1.164 respectively.

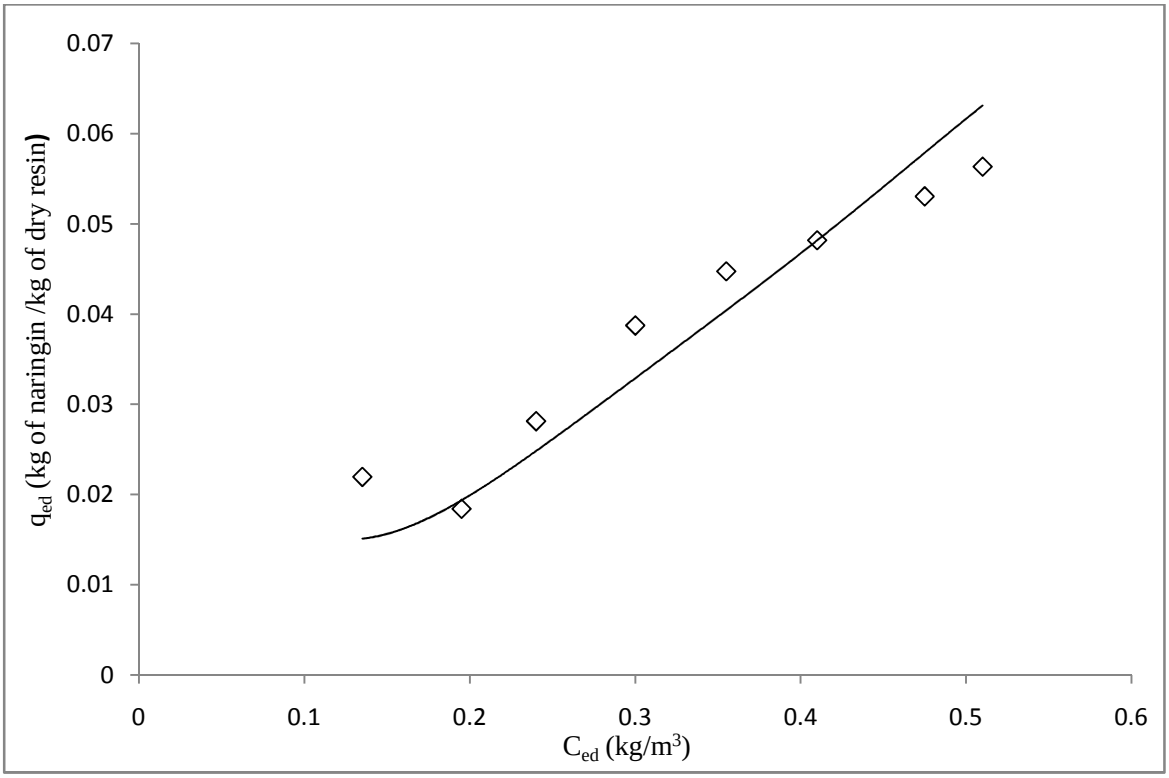

Figure 5.95: Desoption equilibrium studies from naringin saturated resin (regenerated) PA-800 to ethanol solution (system 8)

5.8.5. Desorption kinetic studies (System 8)

The kinetic studies of desorption of naringin into ethanol from naringin saturated resin was carried out as per the procedure described in the section 3.6.2, and data is presented in Table H5 (b) and Figure 5.96.

Modelling of desorption kinetic data

The above data have been analysed with the same approach as done for System 1 (i.e., Boyd's diffusivity model equation).

The values of effective diffusivity D_{ed}, were estimated using linear plots of $\ln\left(1/1-u_d^2(t)\right)$ vs time (t) and presented in Table 5.72. The average value of effective diffusivity D_{ed} is found to be 12.32×10^{-13} (m^2s^{-1}).

Table 5.72: Boyd's diffusivity model parameters for desorption of naringin from naringin saturated resin (regenerated) PA-800 (system 8)

S.No	Run	$D_{ed} \times 10^{-13} (m^2 s^{-1})$	R^2
1	1	13.5	0.924
2	2	12.3	0.947
3	3	11.1	0.955

The generated C_{td} (with a representative value of D_{ed} = $12.32 \times 10^{-13} m^2 s^{-1}$) for all the runs are shown by smooth curves as well as experimental data are given for comparison in Figure 5.96. The data were tested for significance of the mean difference, paired observation by t - test at a 5% level of significance, and it was found that the experimental and predicted data of two of the three runs do not differ significantly. The summary of the statistical analysis of the predicted values from the model and experimental values is given in Table 5.73.

Table 5.73: Statistical analysis for predicted and experimental values of C_{td} (system 8)

Run	Slope	R^2 (C_{trep} vs. $C_{t\exp}$)	t-Cri	t-Cal	Inference
1	0.888	0.918	2.262	2.793	SD
2	0.941	0.952	2.262	2.242	NSD
3	0.981	0.961	2.262	1.410	NSD

*NSD- No Significance difference, SD- Significance difference

From the above, it is evident that observed kinetic data could be correlated reasonably using Boyd's diffusivity model equation.

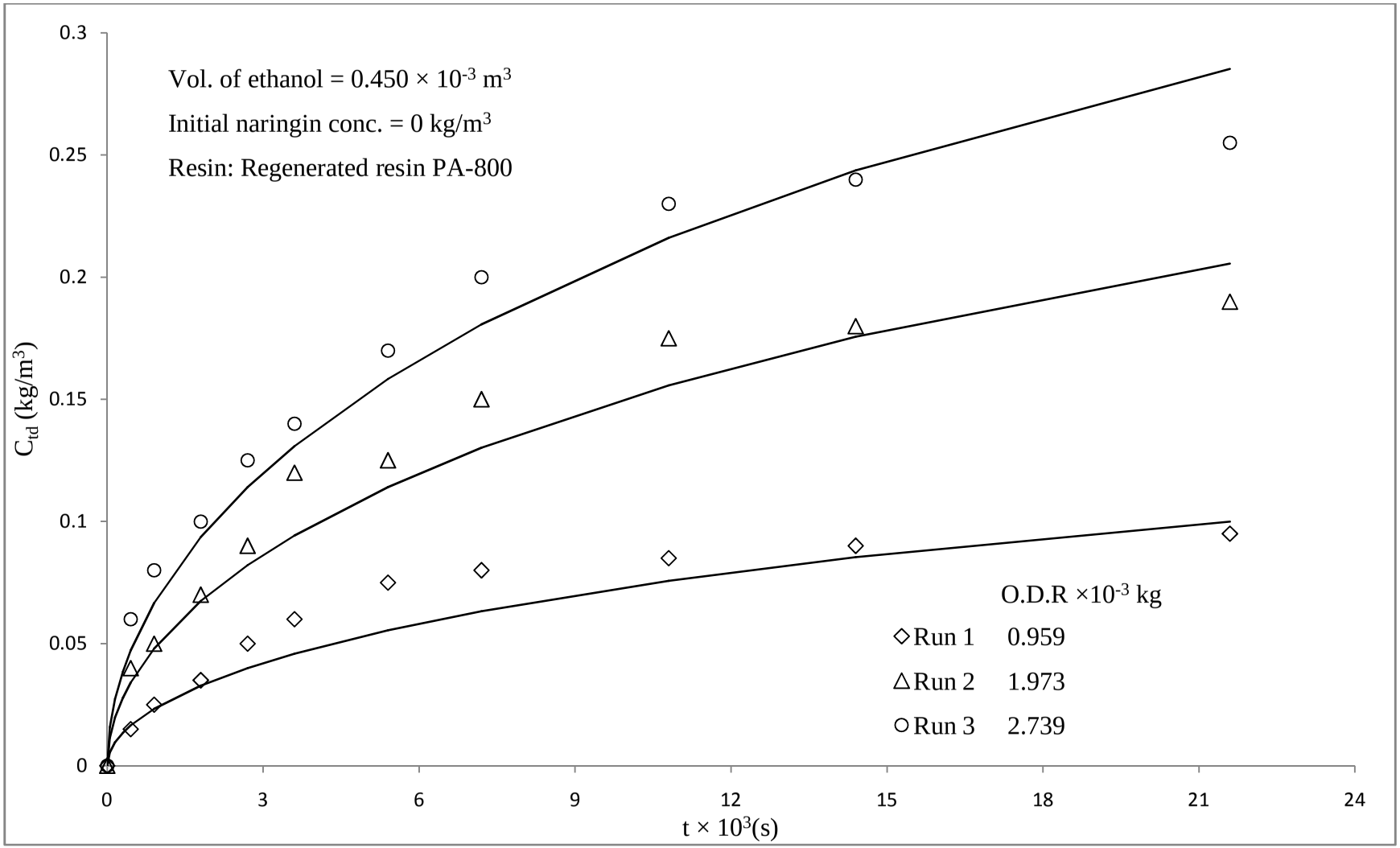

Figure 5.96: Desorption kinetic studies with naringin saturated resin (regenerated) PA-800 in ethanol: correlation of experimental data C_{td} *vs t* (system 8)

5.8.6. Desorption fixed bed column studies (System 8)

The desorption column studies were carried out in a glass column as per the procedure described in the section 3.6.3 and presented in Figure 5.97. From the Figure 5.97, it is evident that the amount of naringin desorbed from regenerated resin PA-800 saturated with naringin, obtained from adsorption column studies, in ethanol solution decreases with time. The data of naringin desorption column studies with ethanol to recover naringin are given in Table H6 (b). From this desorption study, it can be concluded that about 1200 ml of ethanol is sufficient for almost all the possible recoverable desorption of naringin from the resin PA-800 in a glass column of 14 mm ID filled up to the height 0.95 m (about 120 g naringin saturated resin (wet)). The amount of naringin desorbed in the column was found to be 2.29 g.

5.8.7. Purity and Recovery of obtained Naringin and Pectin(System 8)

(A) Naringin recovery

Recovery and purity of naringin were calculated as per the procedure described in section 3.9, and found to be 50.5 and 88.9%. The naringin obtained was 2.4 g.

(B) Pectin recovery and characterization

The recovery of pectin was calculated as per the procedure described in section 3.9. The obtained pectin was characterised, the values of different parameters determined are listed in Table 5.74.

Table 5.74: Recovery of pectin from fresh peels with regenerated resin PA-800

Recovey (%)	Moisture (%)	Ash (%)	Equivalent weigh (mg/ml)	Methoxyl content (%)	Anhdrouronic acid (%)	DE (%)
57.8	7.8	7.7	524.3	6.4	60.4	60.1

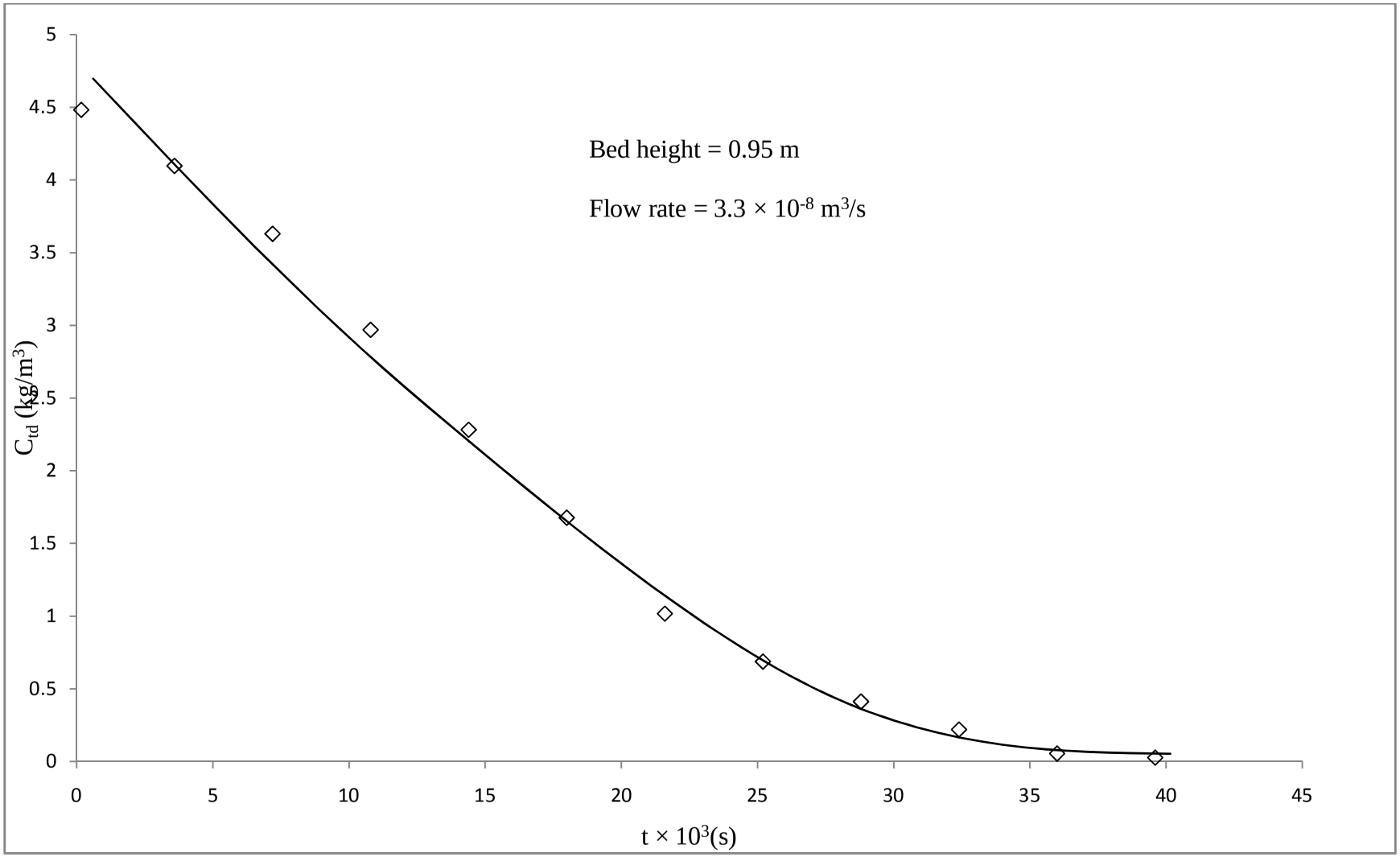

Figure 5.97: Column desorption studies from naringin saturated resin (regenerated) PA-800 into ethanol, C_{td} *vs t* (system 8)

5.9. Comparative studies

In six systems (system 1 to 6) data has been observed for 2 or 3 years. However, for comparison of systems, representative data has been taken and the years are not mentioned in the figures.

1. Adsorption equilibrium studies

(a) Comparison of fresh and regenerated resins with fresh peels

The adsorption equilibrium data of system 1 with 7 and system 2 with 8 have been compared in Figures 5.98 and 5.99 respectively. It is observed that adsorption of naringin on regenerated resins PA-500 (system 7) and PA-800 (system 8) is lower than the adsorption on corresponding fresh resins (systems 1 and 2).

(b) Comparison of different peels with resin PA-500 and PA-800

The adsorption equilibrium data of systems 1, 3 and 5 (with different peels and resin PA-500) have been compared in Figure 5.100. It is found that the naringin adsorption from dropped peels is more in comparison to fresh and dry peels.

The adsorption of naringin from different peels on resin PA-500 is in the order given below.

Dropped peels (system 3) > Fresh peels (system 1) > Dry peels (system 5)

The adsorption equilibrium data of systems 2, 4 and 6 have been compared in Figure 5.101. The naringin adsorption with dropped peels is the maximum among the three (fresh, dropped, and dry) peels. The adsorption of naringin with different peels on resin PA-800 is in the order

Dropped peels (system 4) > Fresh peels (system 2) > Dry peels (system 6)

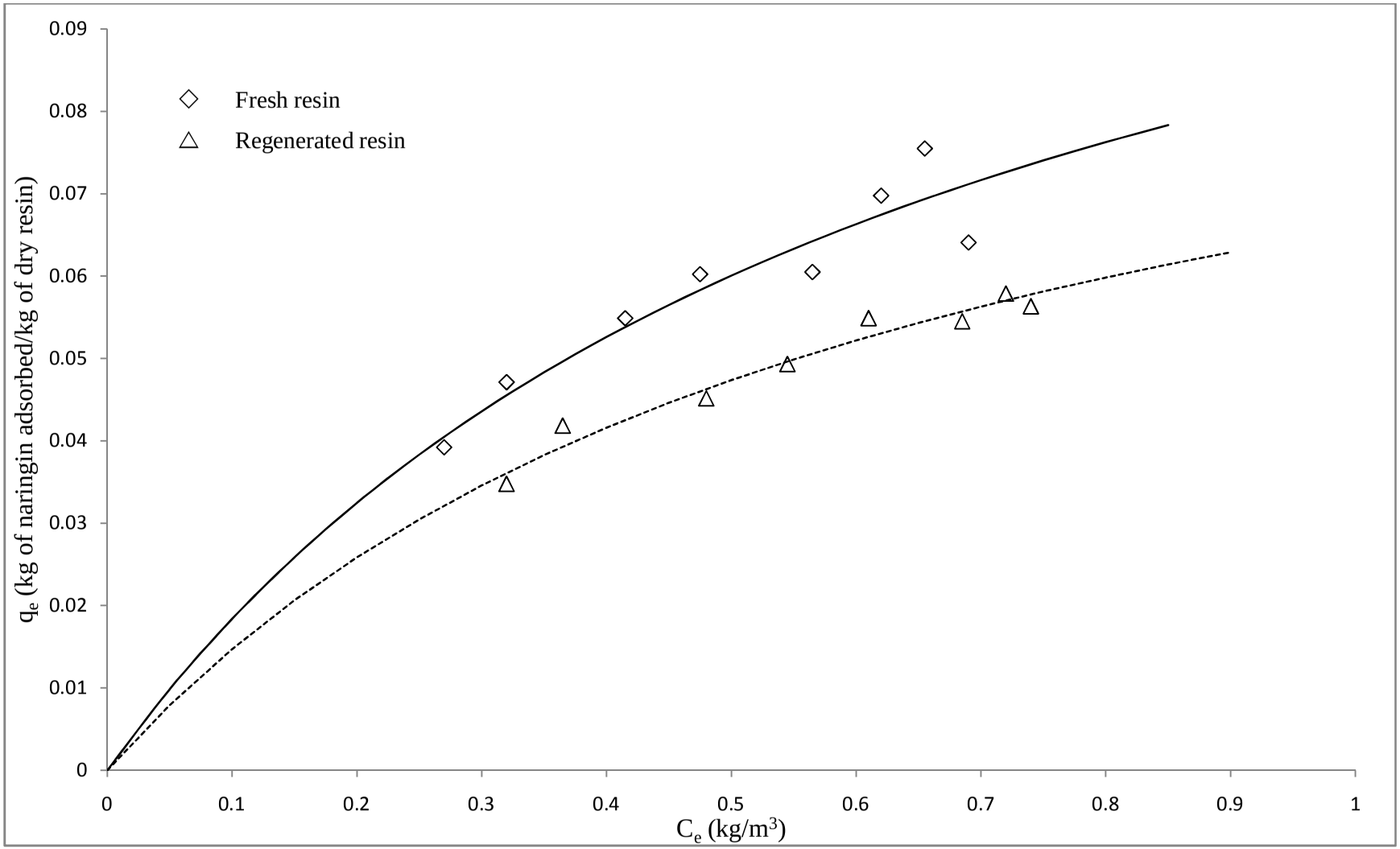

Figure 5.98: Adsorption of naringin on resin PA-500 and regenerated resin PA-500 from fresh KPBW: a comparison of equilibrium data of system 1 with 7

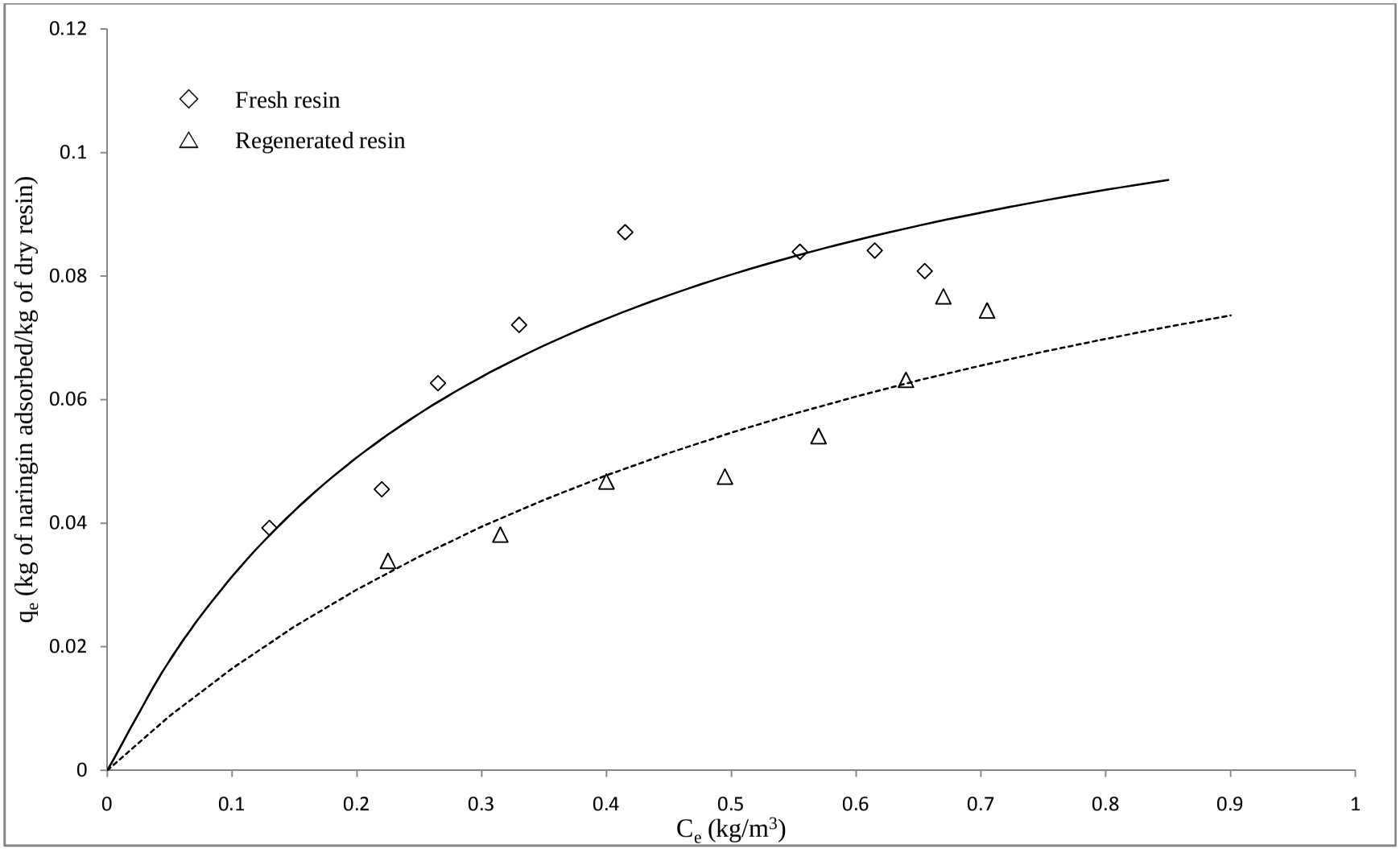

Figure 5.99: Adsorption of naringin on resin PA-800 and regenerated resin PA-800 from fresh KPBW: a comparison of equilibrium data of system 2 with 8

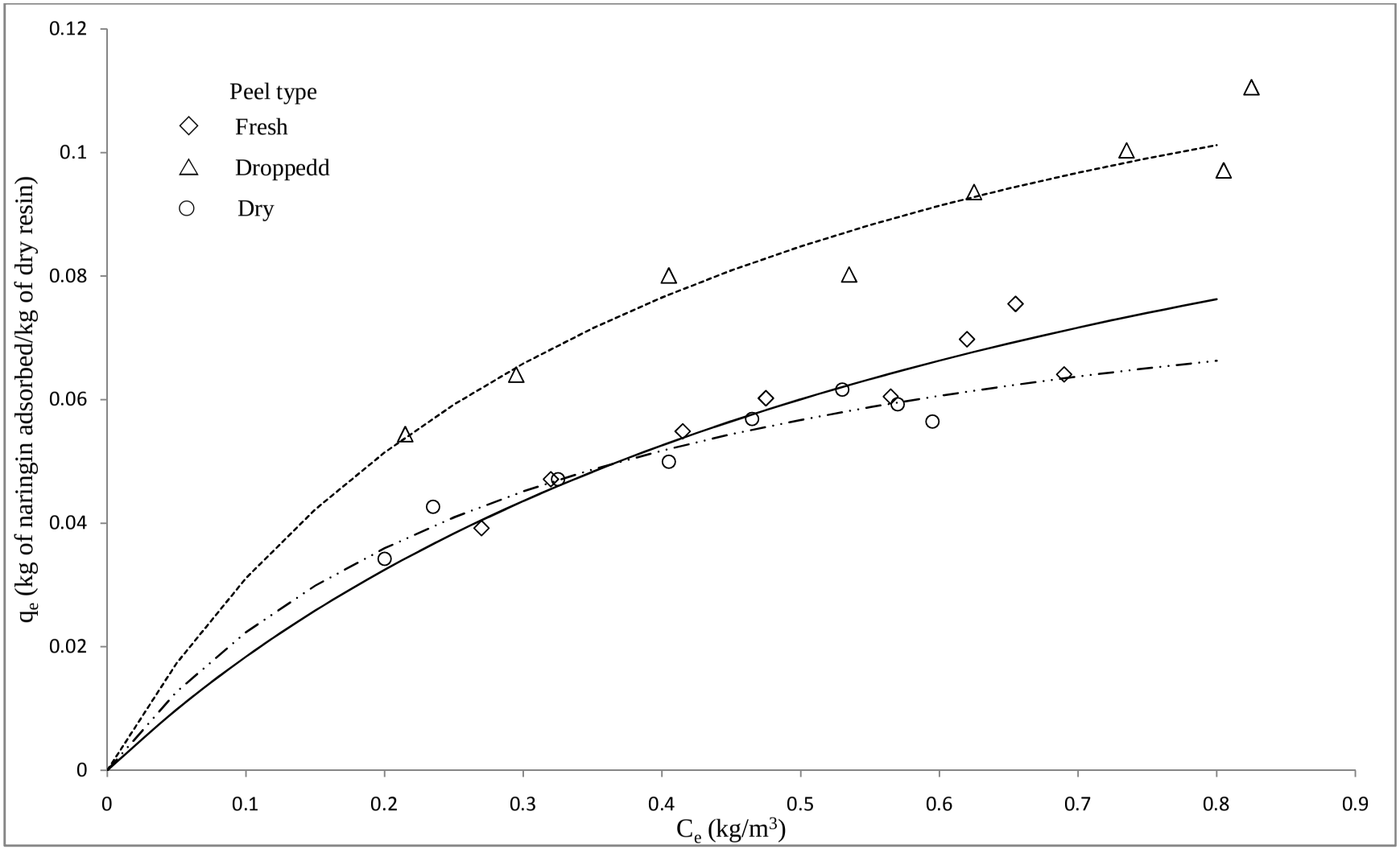

Figure 5.100: Adsorption of naringin on resin PA-500 from fresh, dropped and dry KPBW: a comparison of equilibrium data of systems 1,3, and 5

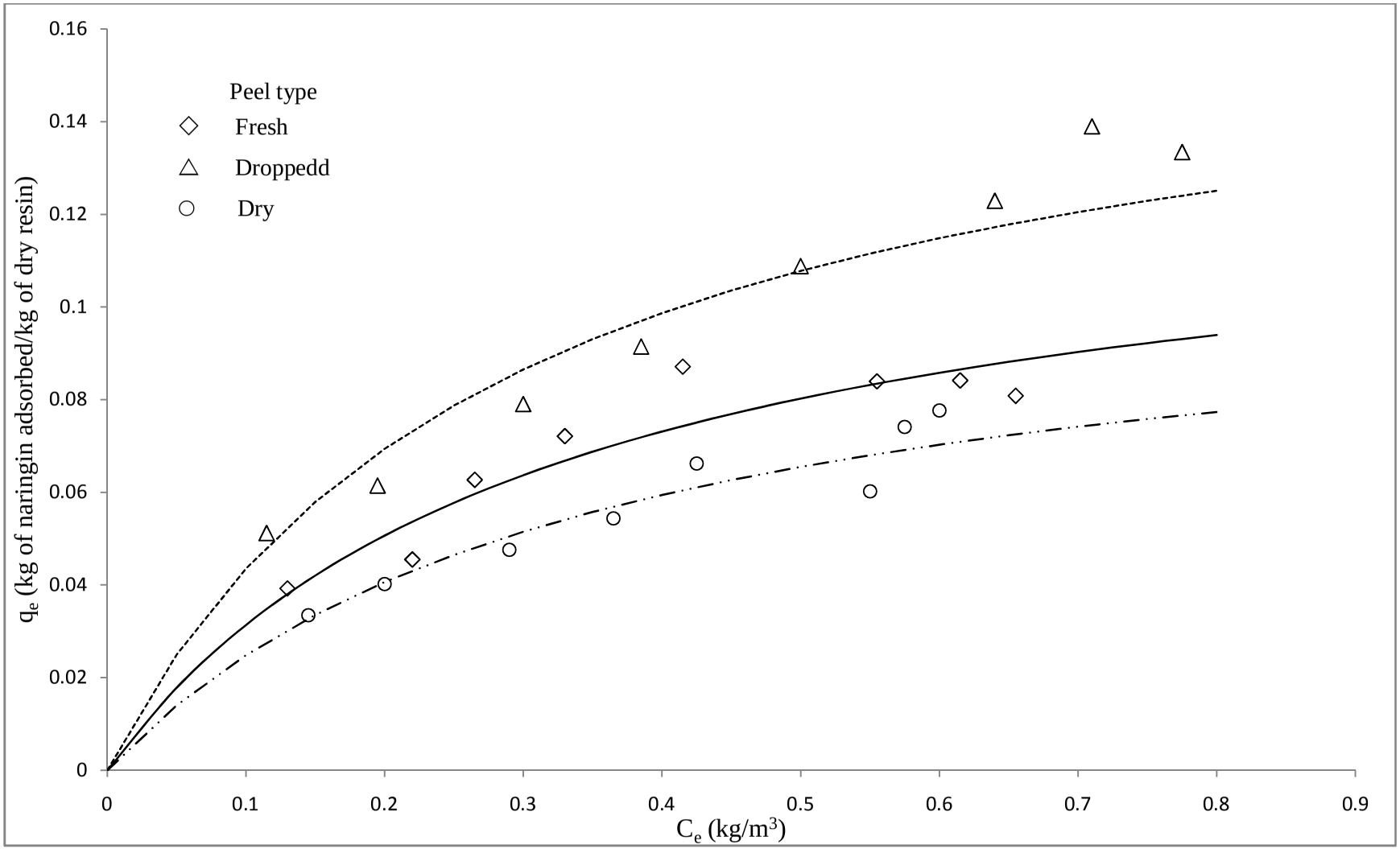

Figure 5.101: Adsorption of naringin on resin PA-800 from fresh, dropped and dry KPBW: a comparison of equilibrium data of systems 2, 4, and 6

The observation is similar with the both resin PA-500 and PA-800. It seems that the dropped peels contain the higher amount of naringin and lesser quantities of essential oils, where as fresh peels contain higher quantities of essentials oils. The essential oils are adsorbed on the resin and therefore decrease the adsorption of naringin (Kimball, 1991). Although it is likely most of the essential oils are vaporized during boiling, but some still remains.

During the drying process of peels and its storage the composition of the peel may have changed, this has affected the adsorption. Further, it might have been harder to essential oil come out from dry peel during boiling in water and oil content may be the maximum in KPBW; although not confirmed by experimentally. Also, KPBW, in this case, might contain tiny particulate of dry peel which reduced the adsorption sites and the total adsorption. Also, during storage, any other compound, which compete with naringin adsorption might have developed (although not confirmed) and thereby reduce adsorption. It is found that naringin adsorption is highest on both the resins with dropped peels among the three peels studied.

(c) Comparison of resins PA-500 and PA-800 with fresh, dropped and dry peels

The adsorption equilibrium data of system 1 with 2 (fresh peels with PA-500 and 800), system 3 with 4 (dropped peels with PA-500 and 800), and system 5 with 6 (dry peels with PA-500 and PA-800) have been compared in Figures 5.102 to 5.104 respectively. It was observed that the amount of naringin adsorbed on resin PA-800 is more in comparison to resin PA-500 in all three cases of peels.

It is attributed to the fact that the resin PA-800 has higher specific surface area. It may be noted that surface area of PA-500 and PA-800 is 500 and 800 m^2/g respectively.

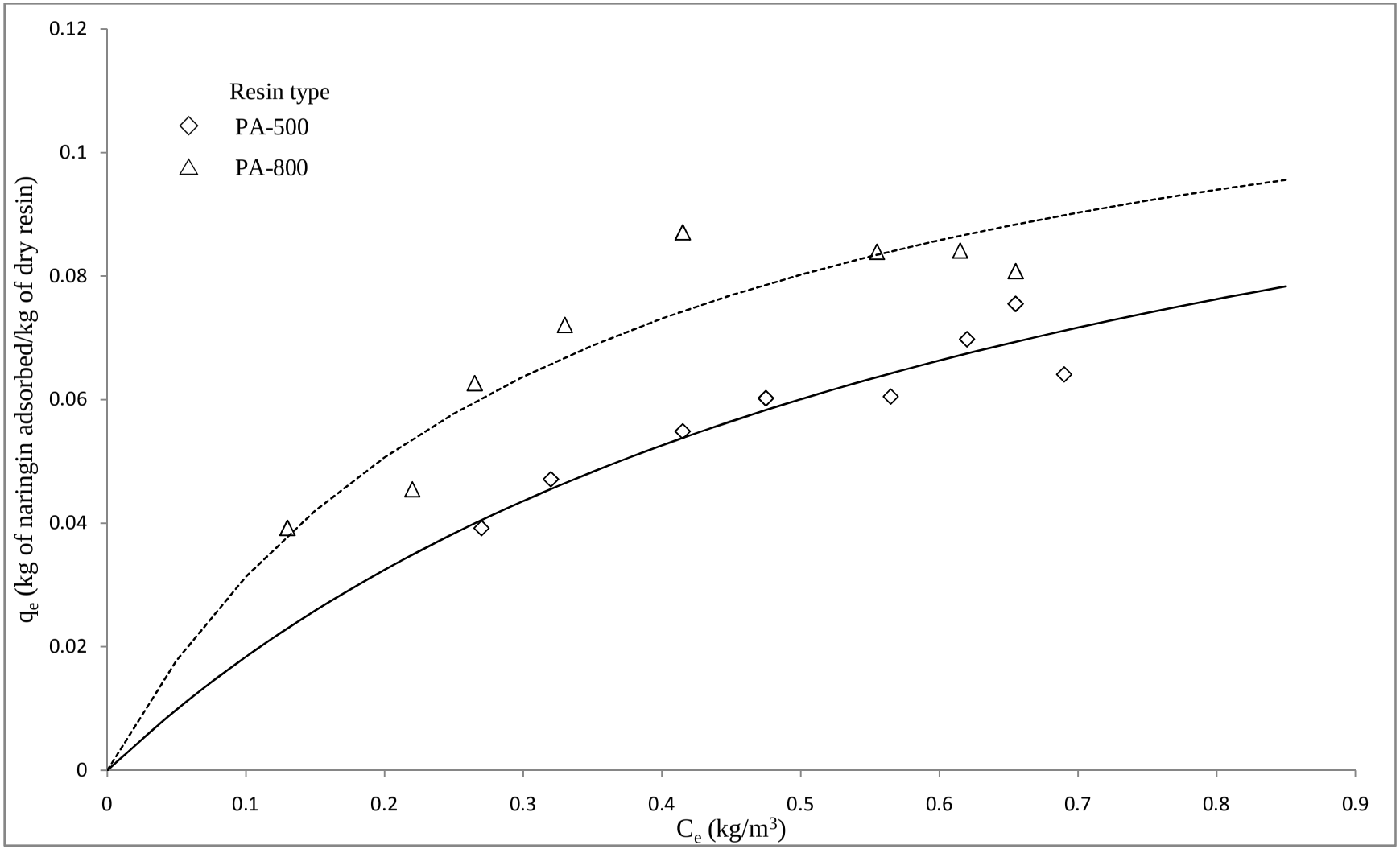

Figure 5.102: Adsorption of naringin on resins PA-500 and PA-800 from fresh KPBW: a comparison of equilibrium data of system 1 with 2

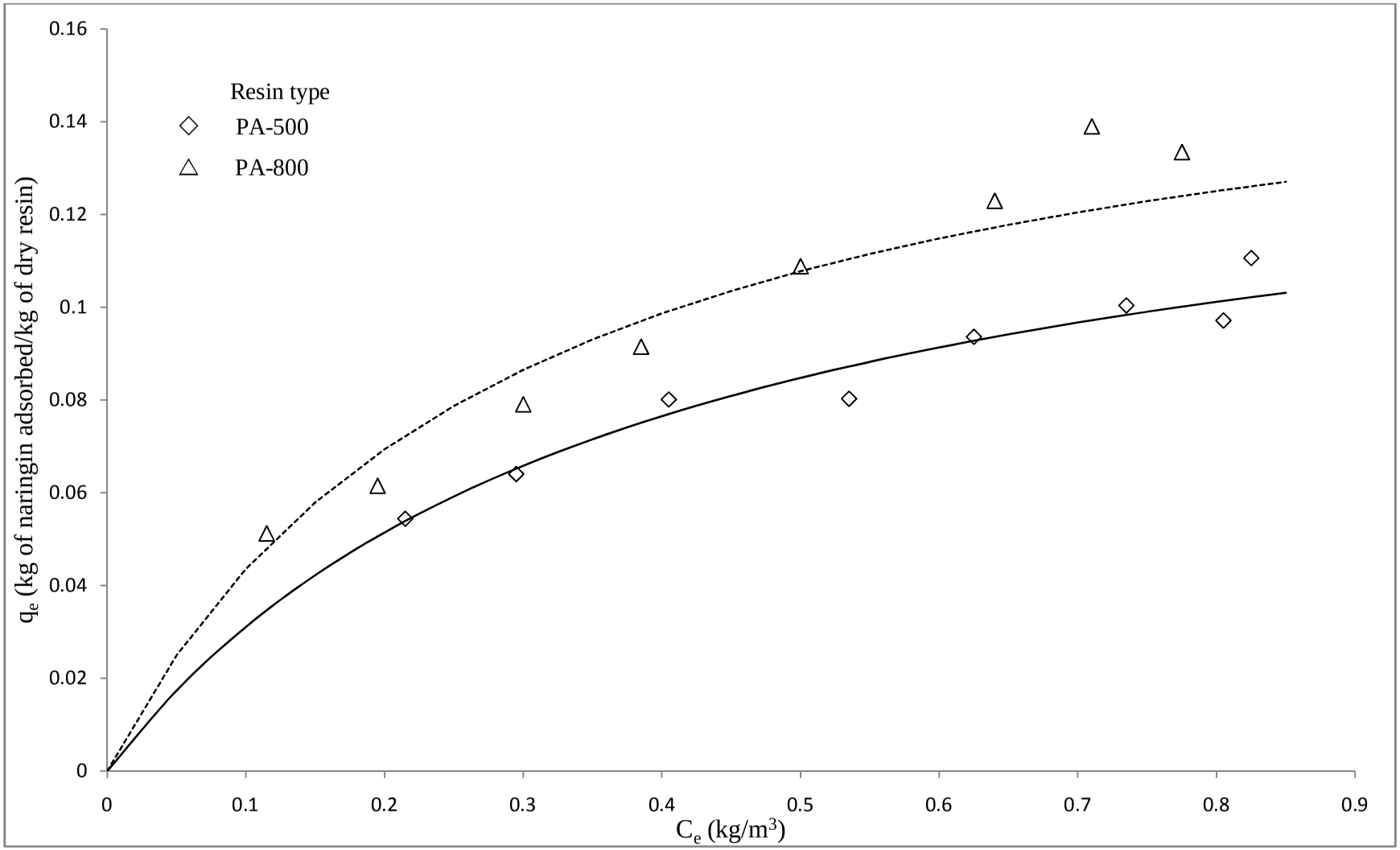

Figure 5.103: Adsorption of naringin on resins PA-500 and PA-800 from dropped KPBW: a comparison of equilibrium data of system 3 with 4

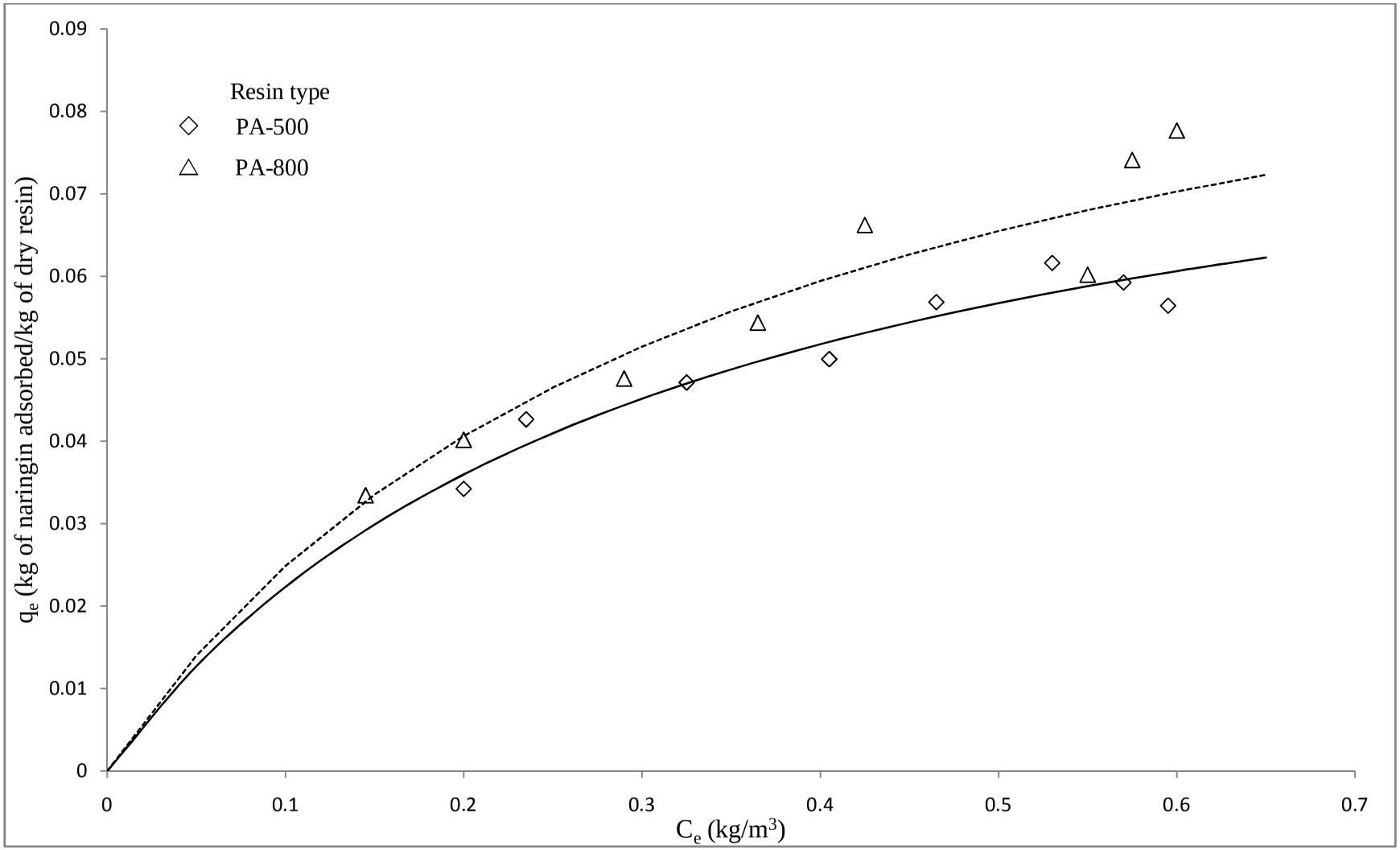

Figure 5.104: Adsorption of naringin on resins PA-500 and PA-800 from dry KPBW: a comparison of equilibrium data of system 5 with 6

Summary of comparison of adsorption of all the systems:

The adsorption of naringin on resins PA-500 and PA-800 with different peels and also on regenerated resins PA-500 and PA-800 from fresh peels, i.e., in all the eight systems in the order

Dropped peels with PA-800 (system 4) > Dropped peels with PA-500 (system 3) > Fresh peels with PA-800 (system 2) > Dry peels with PA-800 (system 6) > Fresh peels with PA 500 (system 1) > Dry peels with PA-500 (system 5) > Fresh peels with regenerated resin PA-800 (system 8) > Fresh peels with regenerated resin PA-500 (system 7)

2. Adsorption kinetic studies

(a) Comparison of fresh and regenerated resins with fresh peels

The adsorption kinetic data of system 1 with 7 and system 2 with 8 have been compared in Figures 5.105 and 5.106 respectively. It was observed that the rate of adsorption of naringin on regenerated resins PA-500 (system 7) and PA-800 (system 8) is lower than the corresponding fresh resins i.e. systems 1 and 2.

(b) Comparison of different peels with resin PA-500 and PA-800

The adsorption kinetic data of systems 1, 3 and 5 have been compared in Figure 5.107. Also, the adsorption kinetic data of systems 2, 4 and 6 have been compared in Figure 5.108. Amongst the three peels the adsorption rate for dropped peels is highest and for dry peels is lowest for both the resins.

The observations are explained by the fact that retained essential oils are least in dropped peel boiled water and hence maximum adsorption. Also, the composition changes in dry peel during storage of peels may have caused minimum adsorption rate among the three peels.

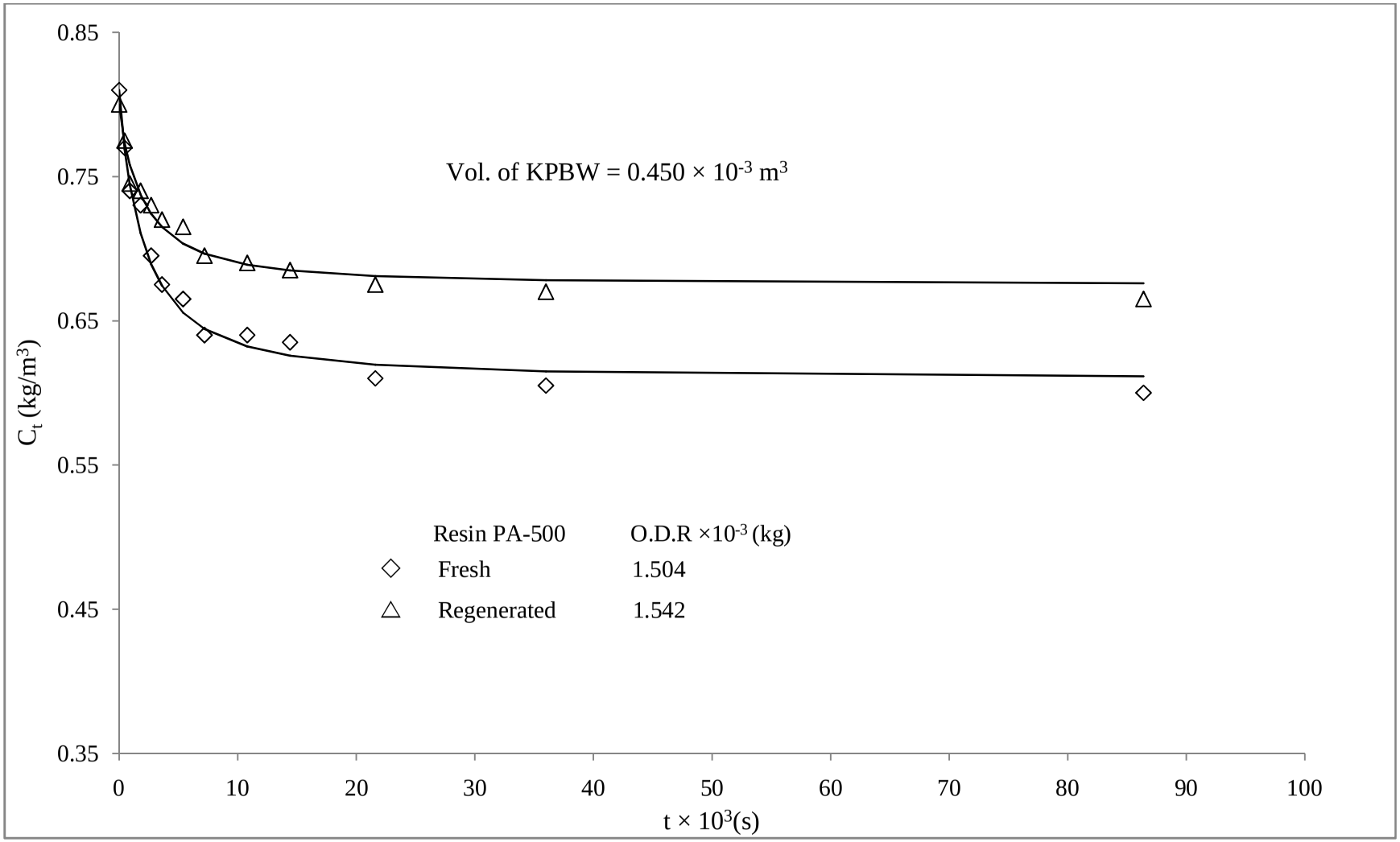

Figure 5.105: Adsorption of naringin on resin PA-500 and regenerated resin PA-500 from fresh KPBW: a comparison of kinetic data of systems 1 with 7

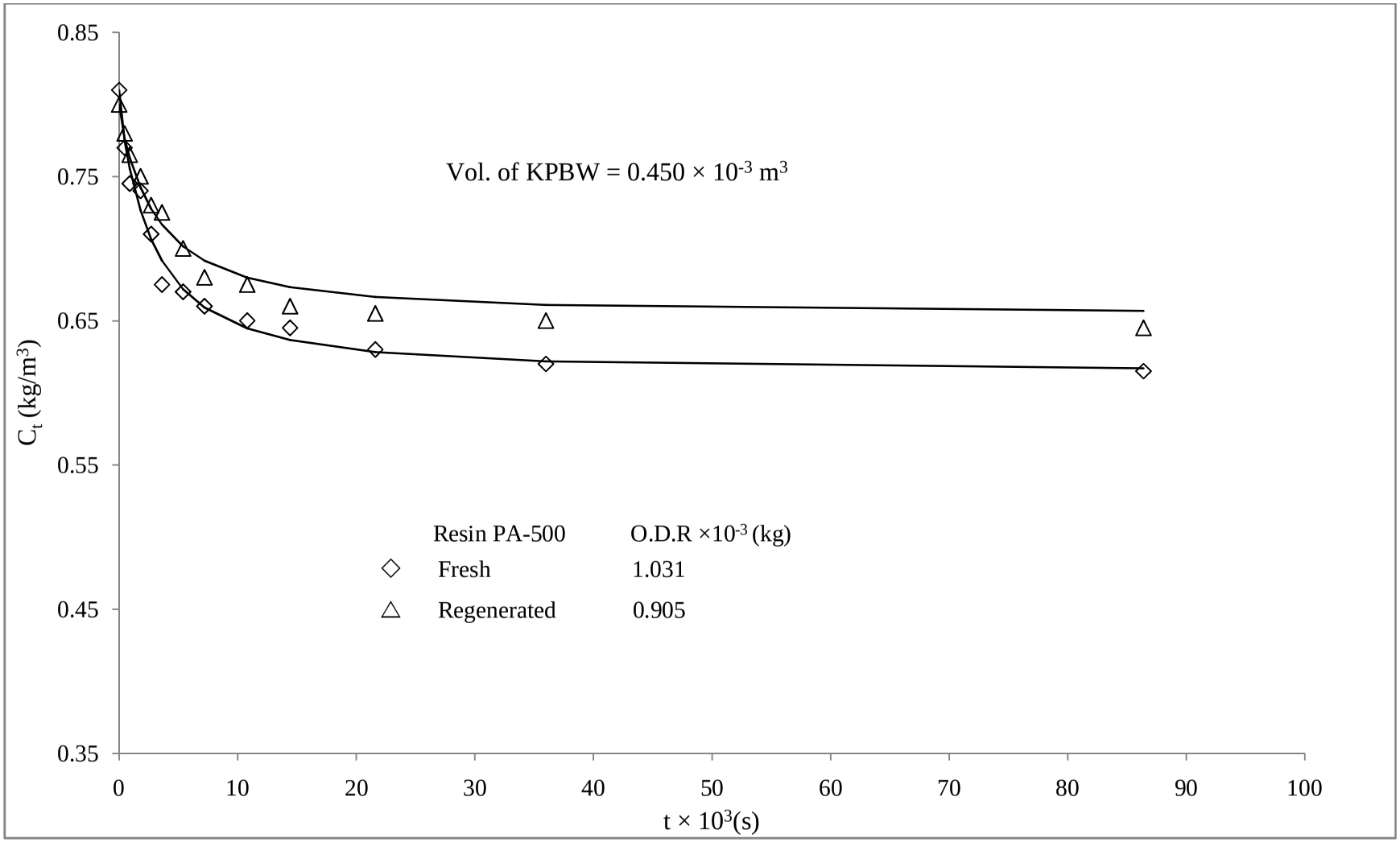

Figure 5.106: Adsorption of naringin on resin PA-800 and regenerated resin PA-800 from fresh KPBW: a comparison of kinetic data of systems 2 with 8

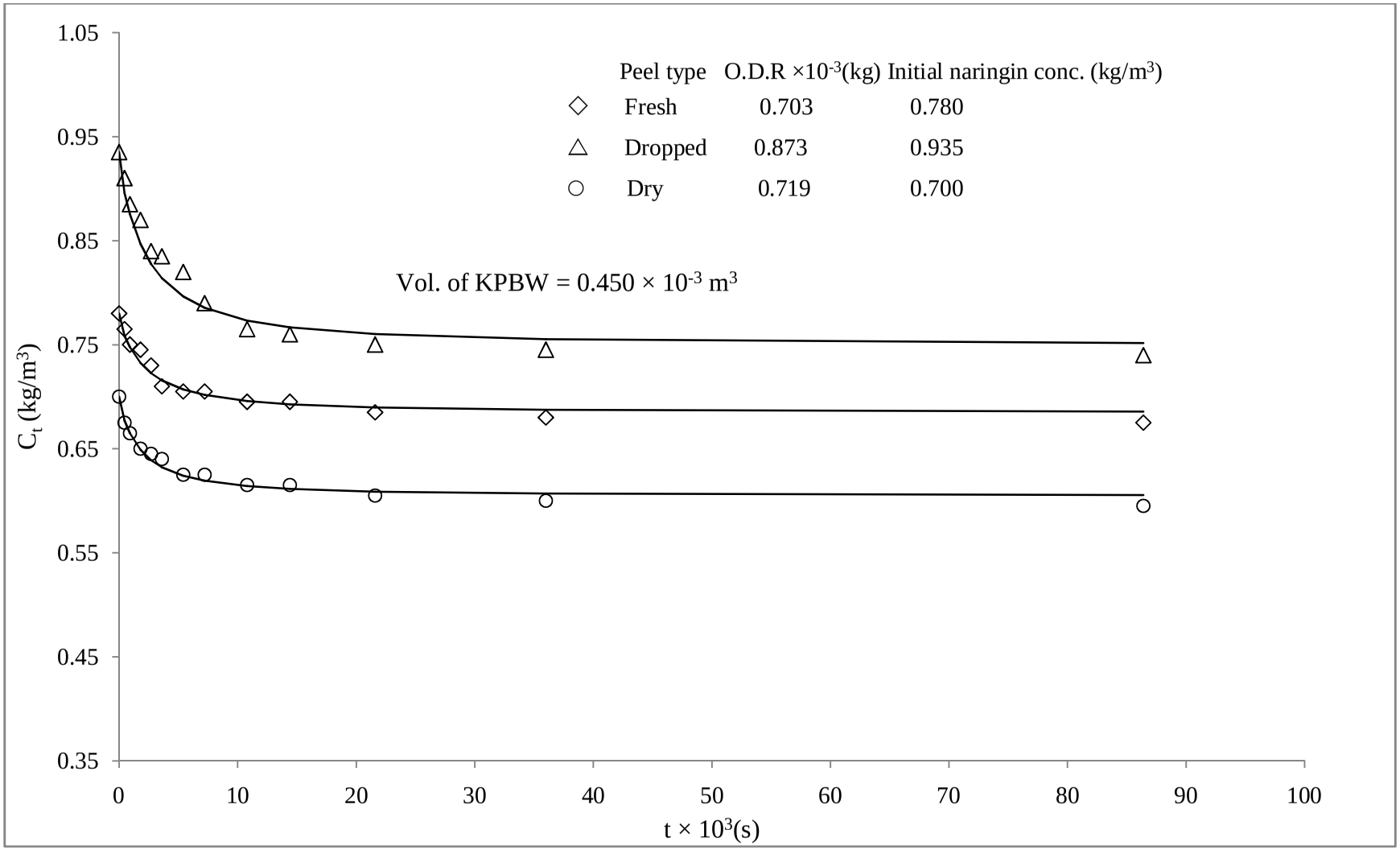

Figure 5.107: Adsorption of naringin on resin PA-500 from fresh, dropped and dry KPBW: a comparison of kinetic data, C_t *vs.* t of systems 1, 3, and 5

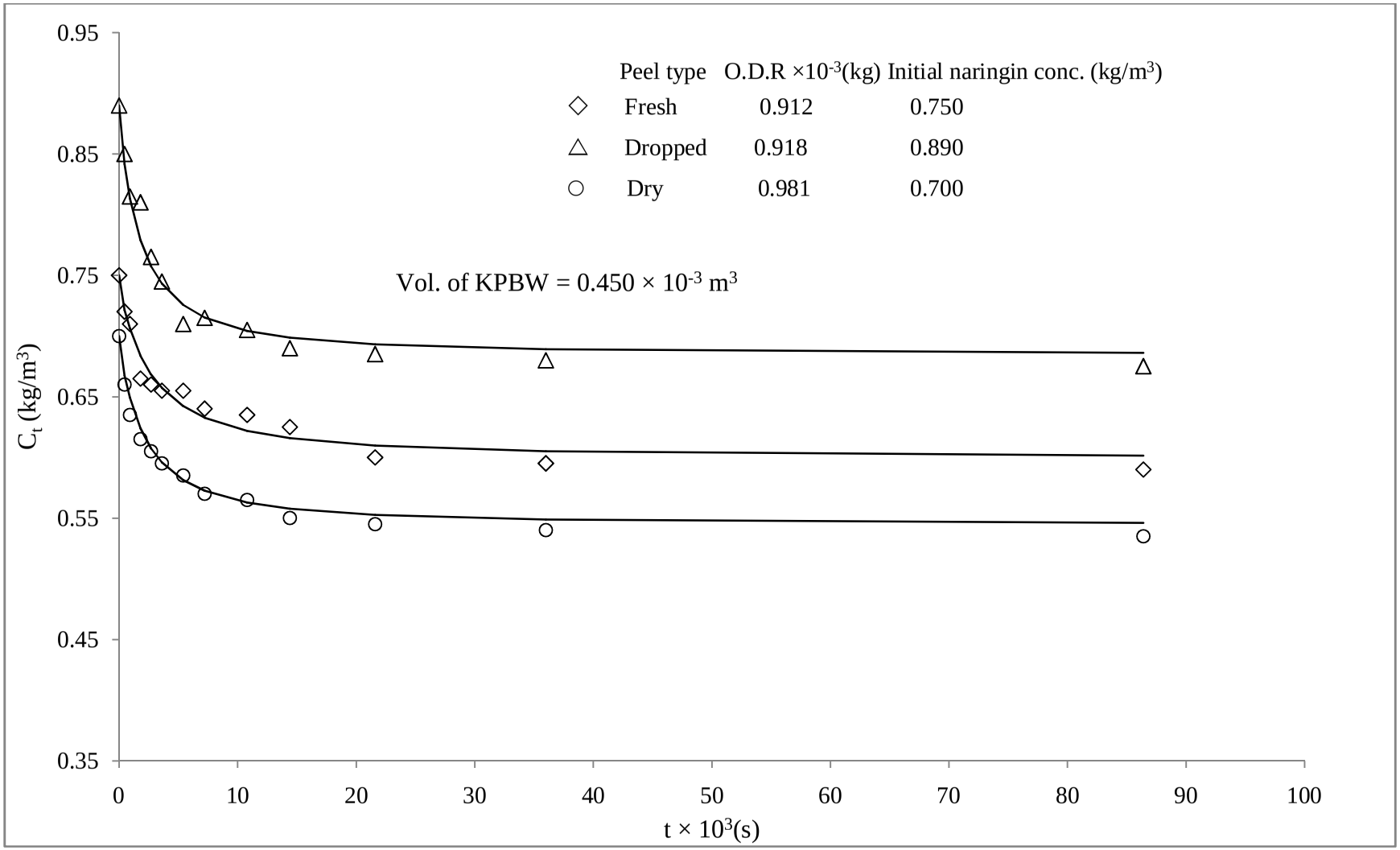

Figure 5.108: Adsorption of naringin on resin PA-800 from fresh, dropped and dry KPBW: a comparison of kinetic data, C_t *vs*. t of systems 2, 4, and 6

(c) Comparison of resins PA-500 and PA-800 with fresh, dropped, dry peels

The adsorption kinetic data of system 1 with 2 (fresh peels with PA-500 and 800), system 3 with 4 (dropped peels with PA-500 and 800), and system 5 with 6 (dry peels withPA-500 and PA-800) have been compared in Figures 5.109 to 5.111 respectively. It was observed that the rate of adsorption of naringin on resin PA-800 is more in comparison to resin PA-500 in all three cases of peels, it is because the resin PA-800 is having the higher specific surface area (800 m^2/g).

3. Fixed bed adsorption column studies

(a) Comparison of different peels with resin PA-500 and PA-800

The breakthrough curves obtained from column studies with resin PA-500 using fresh, dropped, and dry peels have been compared in Figure 5.112. It is observed that the breakthrough curves showed a typical "S" shape profile and the breakthrough curves were found to shift from left to right with dry, fresh, and dropped peels respectively.

The values of t_b and q_{total} decreased in the order dry, fresh, and dropped peels respectively. It was found that the unused bed height was minimum with dropped peels and maximum with dry peels. The reason for such observations seems to be the presence of essential oils in fresh peels and storage of dry peels, which may have affected the adsorption sites. The mass transfer zone is biggest for dry peels and smallest to dropped peels among the three peels.

The breakthrough curves of fresh, dropped, and dry peels have also been compared for studies with resin PA-800 and presented in Figure 5.113. The observations with PA-800 were similar to the resin PA-500 as described in preceding paragraph.

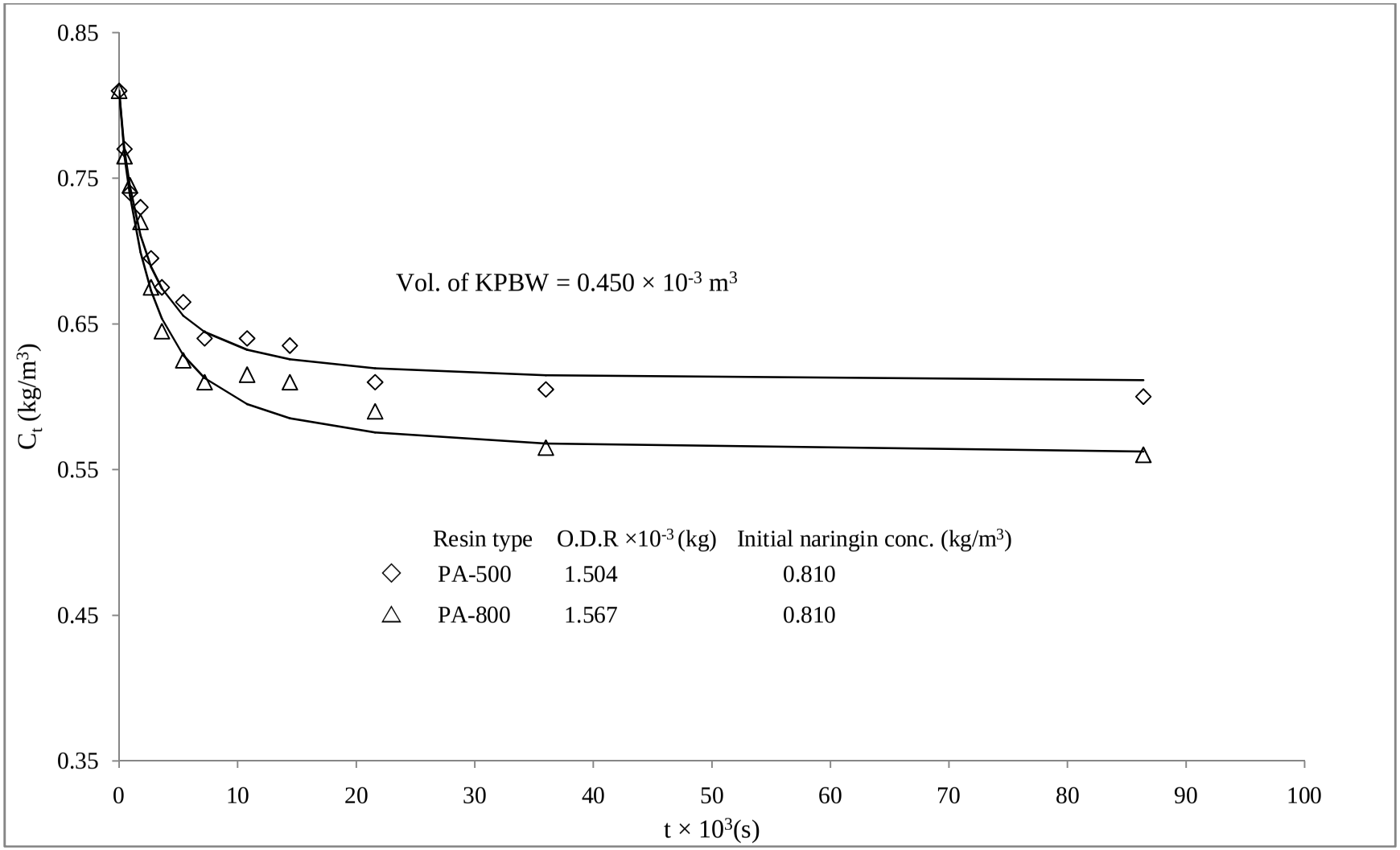

Figure 5.109: Adsorption of naringin on resins PA-500 and PA-800 from fresh KPBW: a comparison of kinetic data, C_t *vs.* t of system 1 with 2

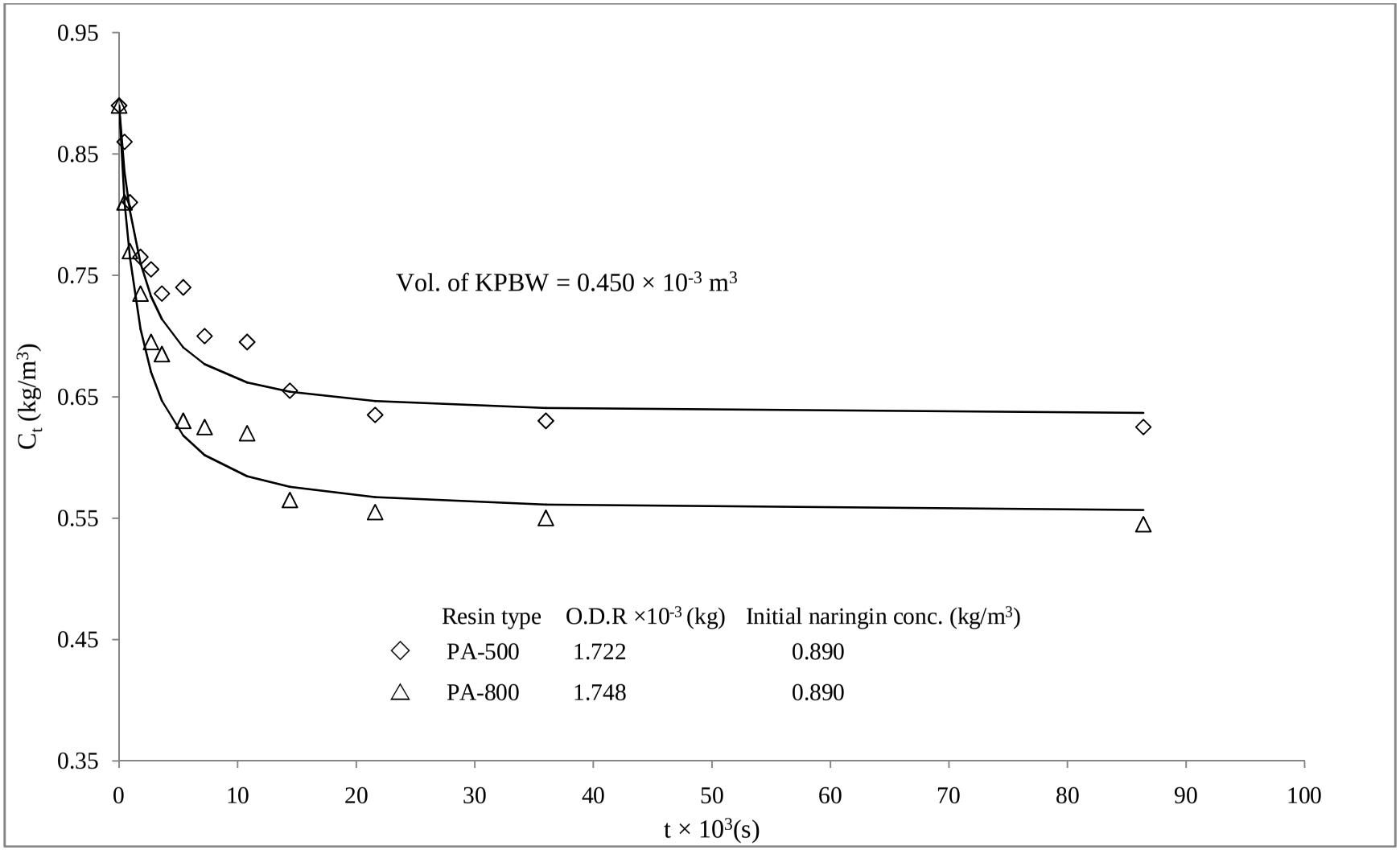

Figure 5.110: Adsorption of naringin on resins PA-500 and PA-800 from dropped KPBW: a comparison of kinetic data, C_t *vs.* t of system 3 with 4

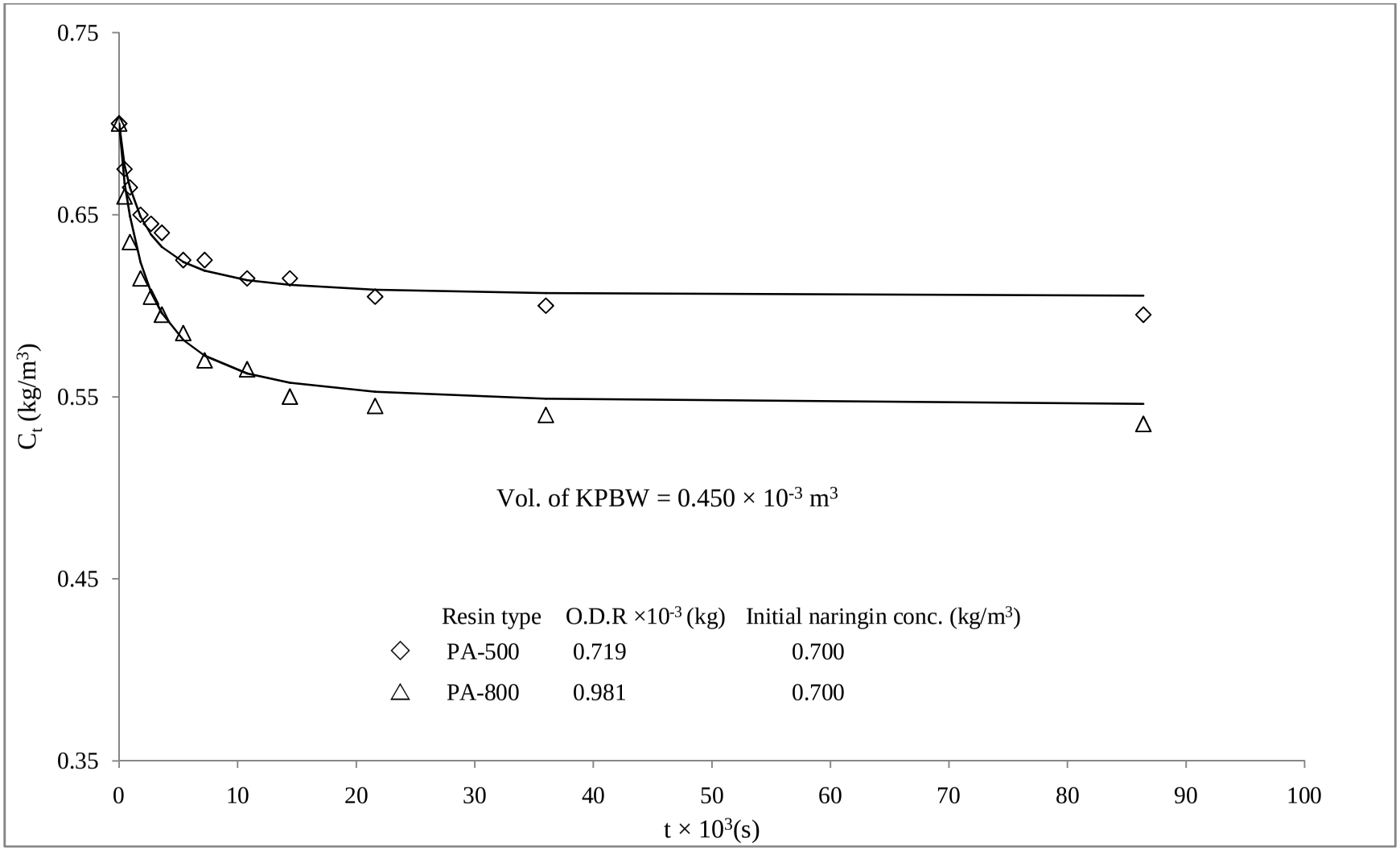

Figure 5.111: Adsorption of naringin on resins PA-500 and PA-800 from dry KPBW: a comparison of kinetic data, C_t *vs.* t of system 5 with 6

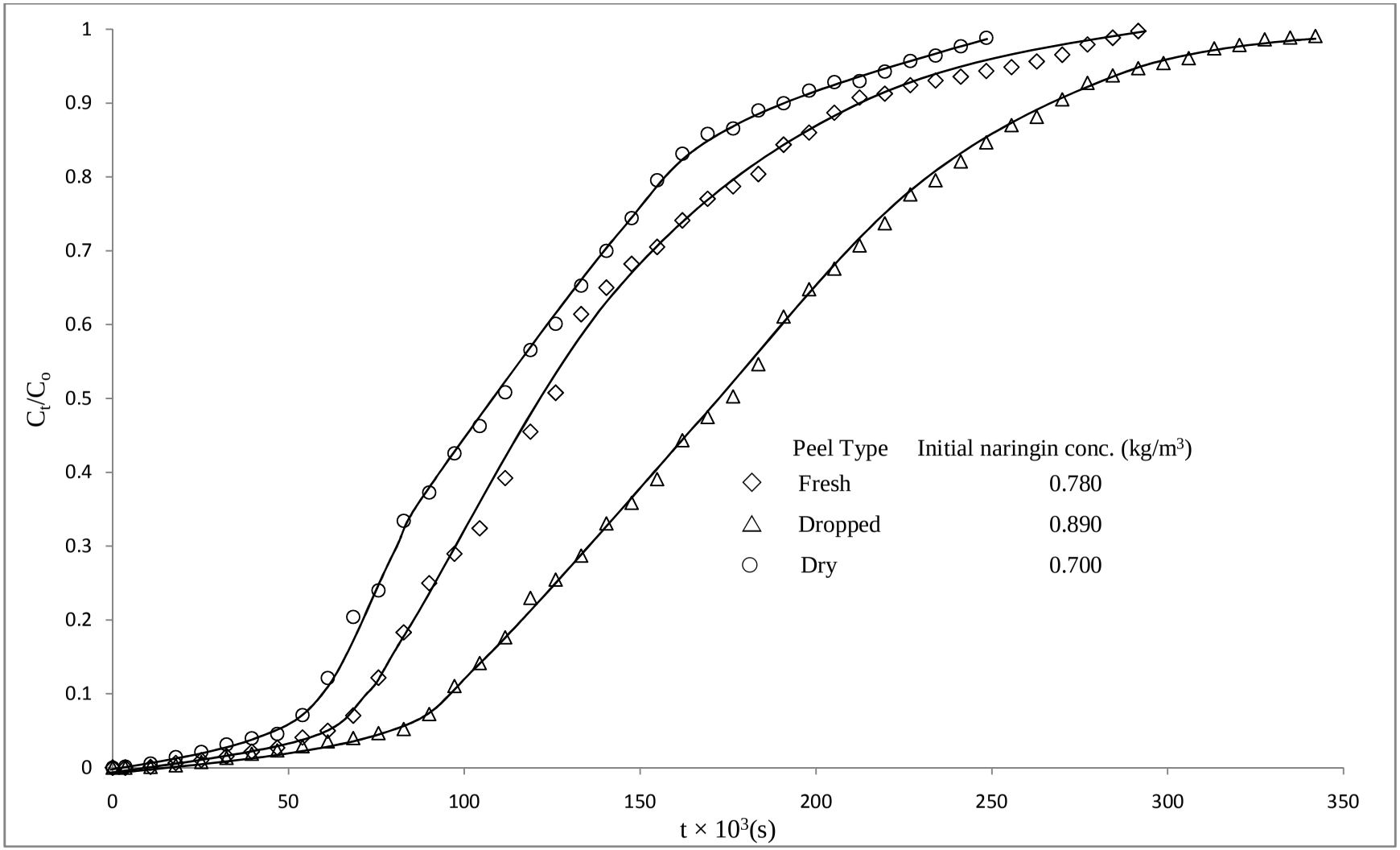

Figure 5.112: Adsorption of naringin on resin PA-500 from fresh, dropped and dry KPBW: a comparison of fixed bed column study of systems 1, 3, and 5

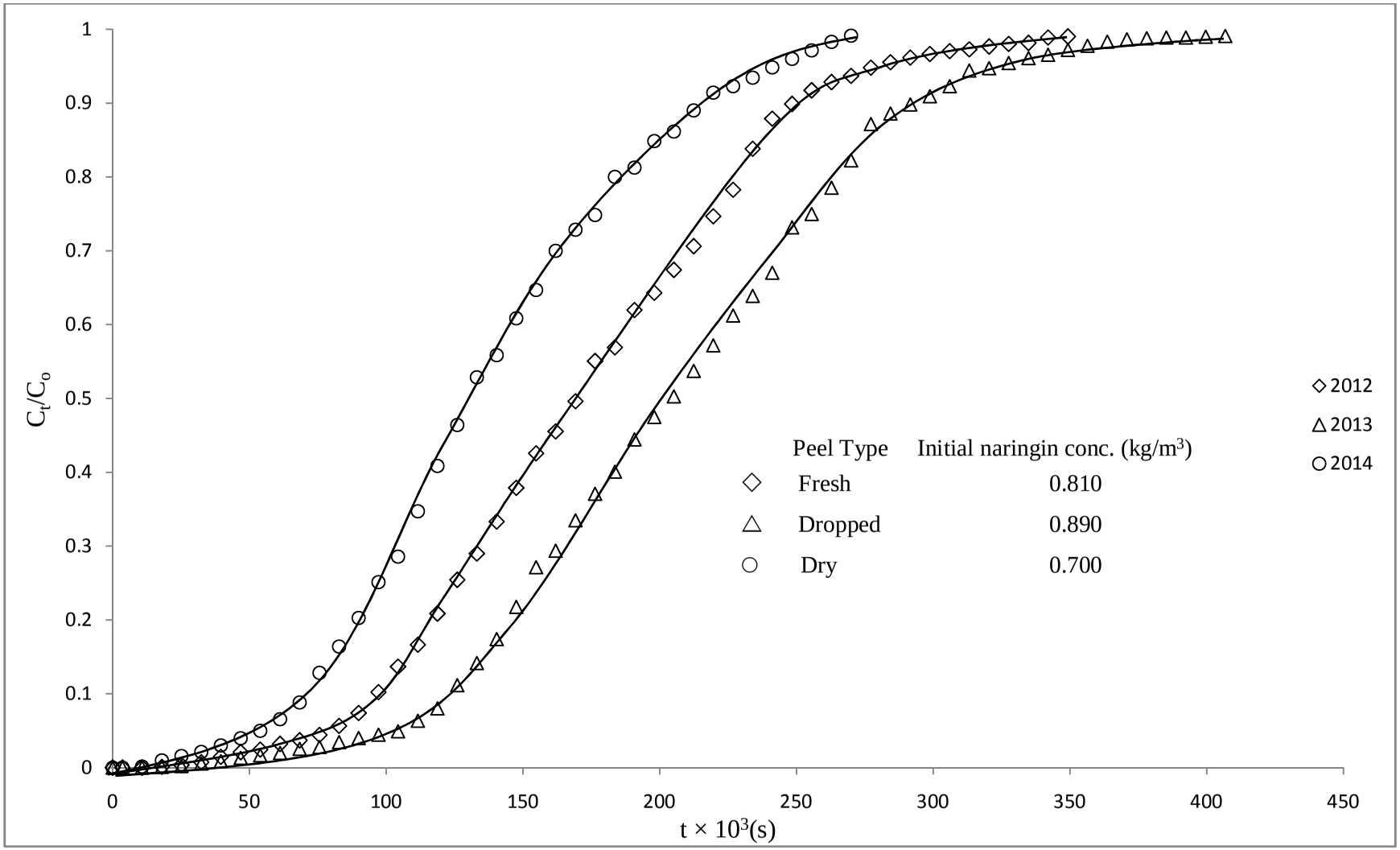

Figure 5.113: Adsorption of naringin on resin PA-800 from fresh, dropped and dry KPBW: a comparison of fixed bed column study of systems 2, 4, and 6

(b) Comparison of resins PA-500 and PA-800 with fresh, dropped, dry peels

The breakthrough curves for system 1 with 2 (fresh peels with PA-500 and 800) have been compared in Figure 5.114. It is observed that breakthrough and exhaustion time for resin PA-500 occurs earlier with fresh peels. The column was found to perform better with resin PA-800, which resulted in a longer breakthrough and exhaustion time.

The adsorption column data for system 3 with 4 (dropped peels with PA-500 and 800) and system 5 with 6 (dry peels with PA-500 and PA-800) have been compared in Figures 5.115 and 5.116 respectively. The observations with dropped and dry peels were found similar to as found with fresh peels.

4. Desorption equilibrium studies

(a) Comparison of different peels with resin PA-500 and PA-800

The equilibrium desorption curves of fresh, dropped, and dry peels for resin PA-500 (systems 1, 3 and, 5) have been compared in Figure 5.117. Although the initial content of naringin in the resin PA-500 was different in three peels also KPBW is a multi-component system; therefore comparison has limited validity. From the Figure 5.117, it was observed that the naringin desorption into ethanol from resin PA-500 is highest with dropped peels among the three peels.

The desorption of naringin into ethanol from resin PA-500 saturated with adsorbed naringin from KPBW with different peels is in the order

Dropped peels (system 3) > Fresh peels (system 1) > Dry peels (system 5)

The equilibrium desorption curves of fresh (system 2), dropped (system 4), and dry peels (system 6) with resin PA-800 have been compared in Figure 5.118. The desorption of naringin from resin PA-800 into ethanol with different peels is in the order given below.

Dropped peels (system 4) > Fresh peels (system 2) > Dry peels (system 6)

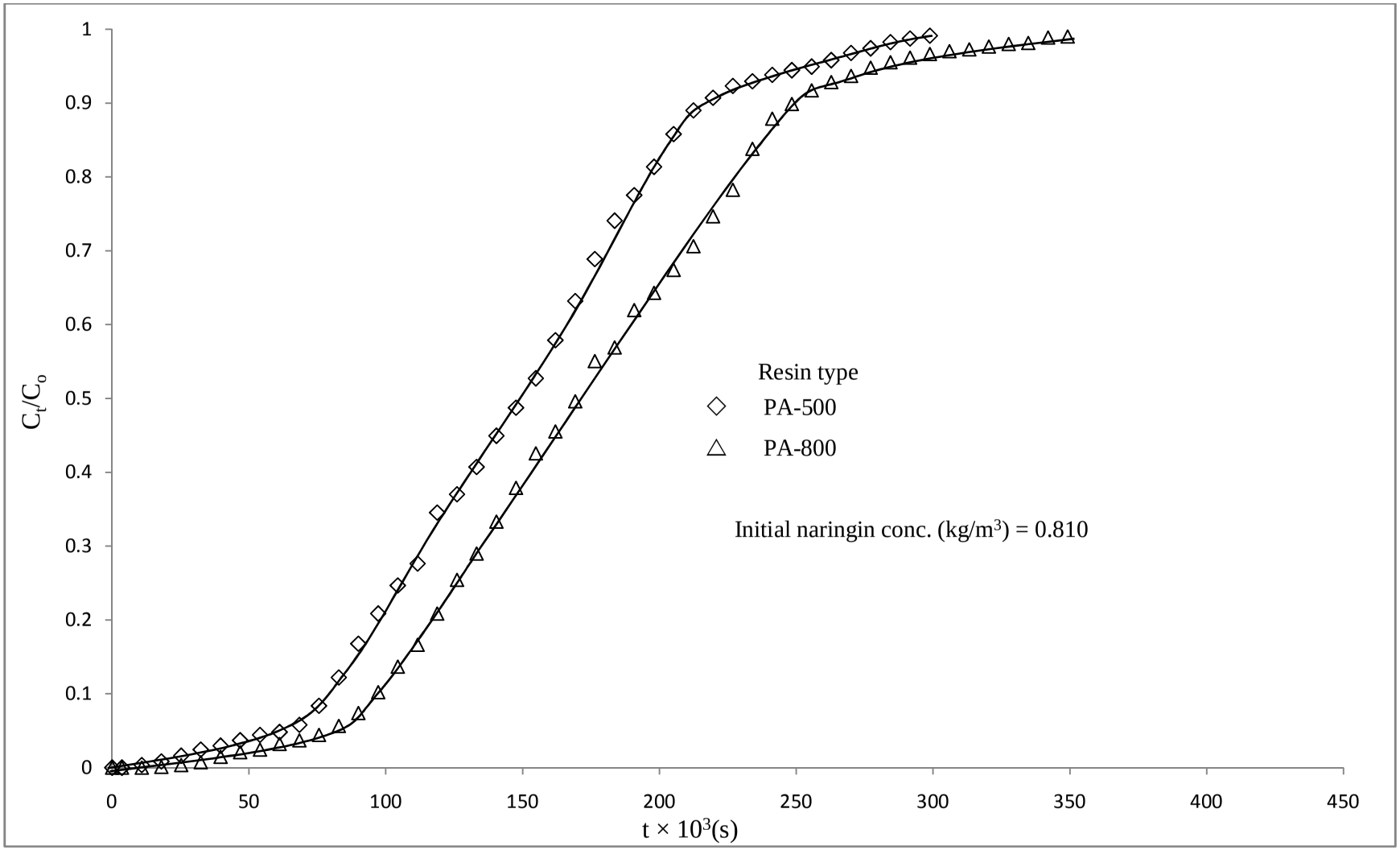

Figure 5.114: Adsorption of naringin on resins PA-500 and PA-800 from fresh KPBW: a comparison of fixed bed column study of system 1 with 2

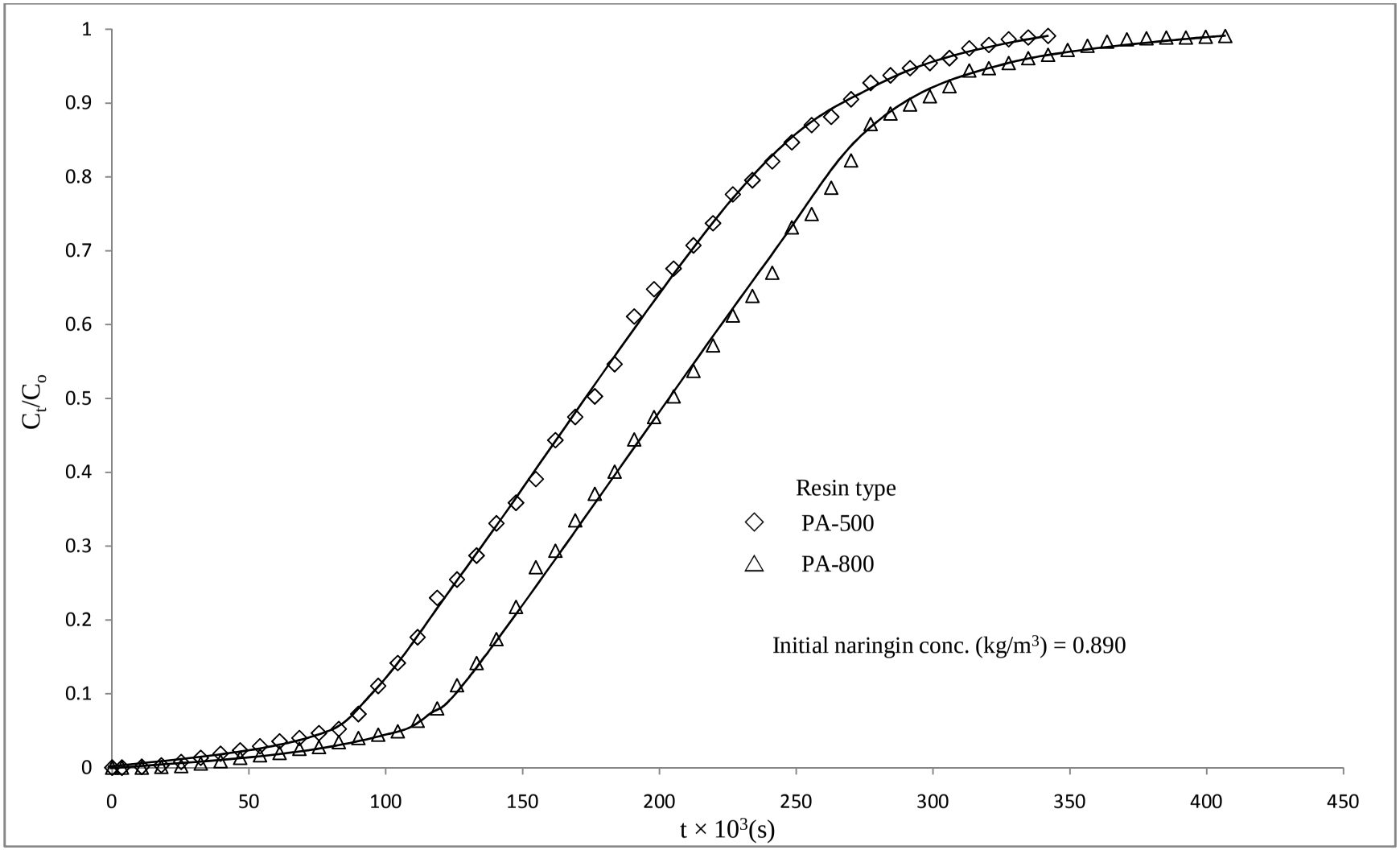

Figure 5.115: Adsorption of naringin on resins PA-500 and PA-800 from dropped KPBW: a comparison of fixed bed column study of system 3 with 4

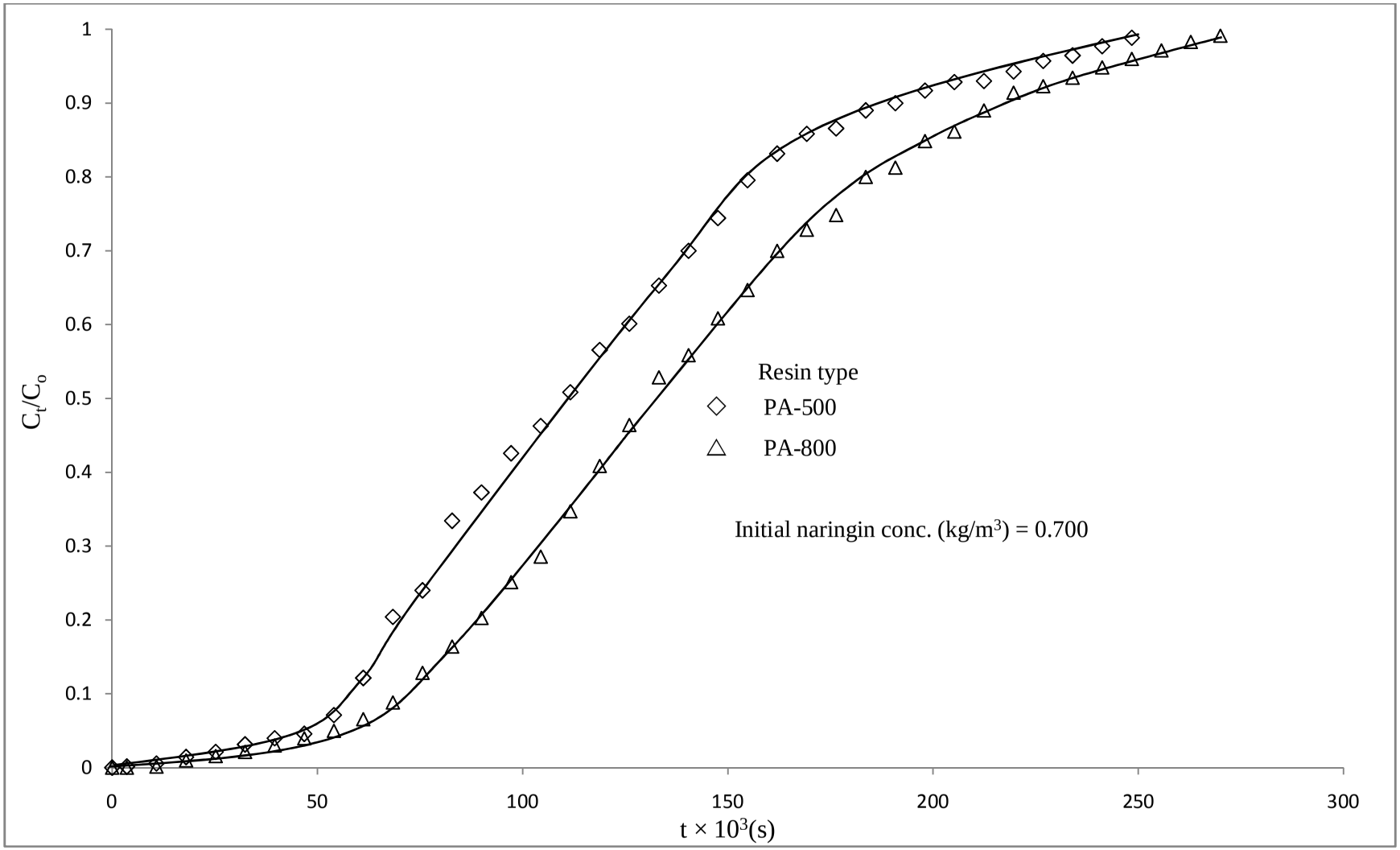

Figure 5.116: Adsorption of naringin on resins PA-500 and PA-800 from dry KPBW: a comparison of fixed bed column study of system 5 with 6

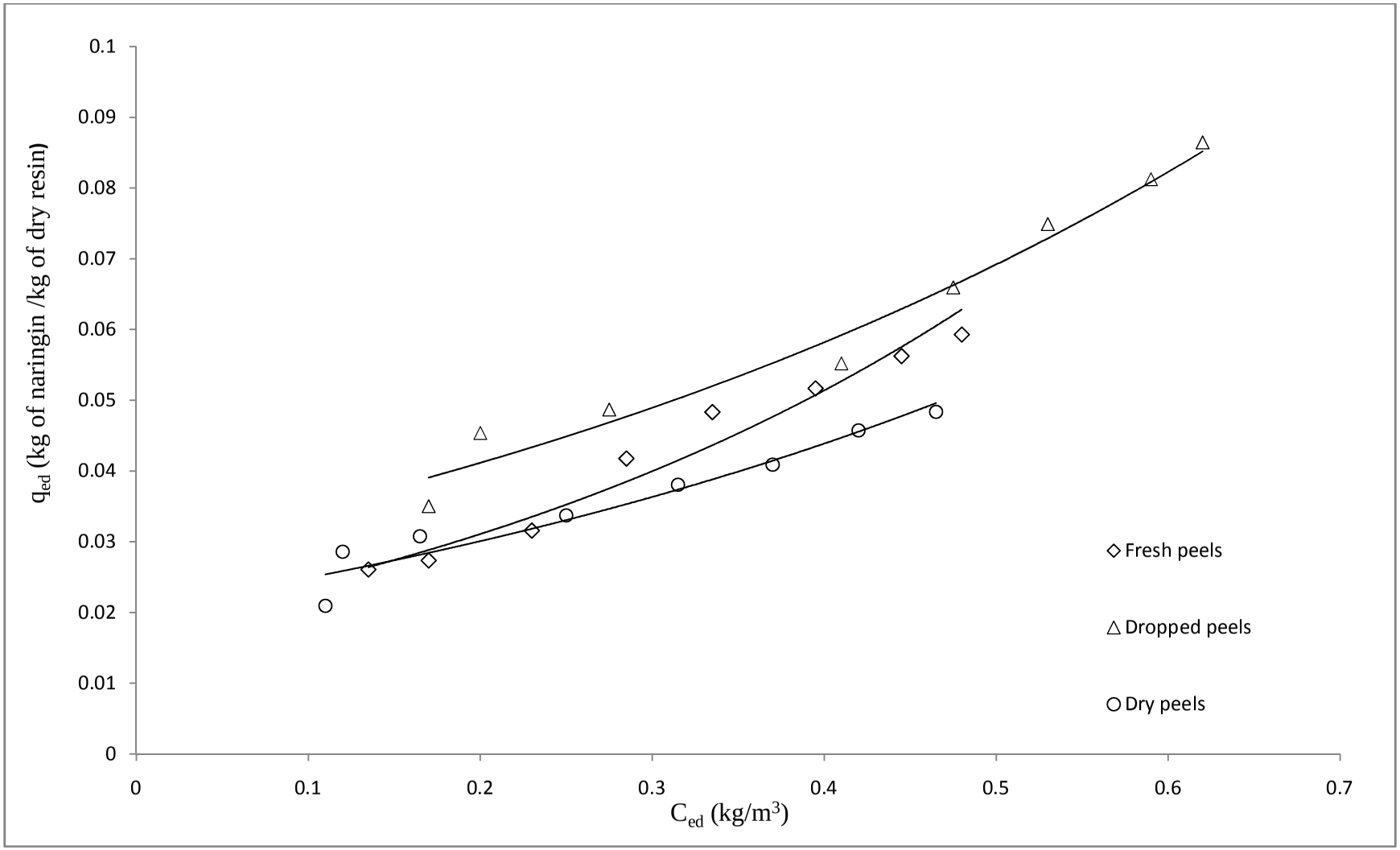

Figure 5.117: Desorption of naringin from naringin saturated resin PA-500 to ethanol: a comparison of equilibrium data (fresh, dropped and dry peels) of systems 1, 3, and 5

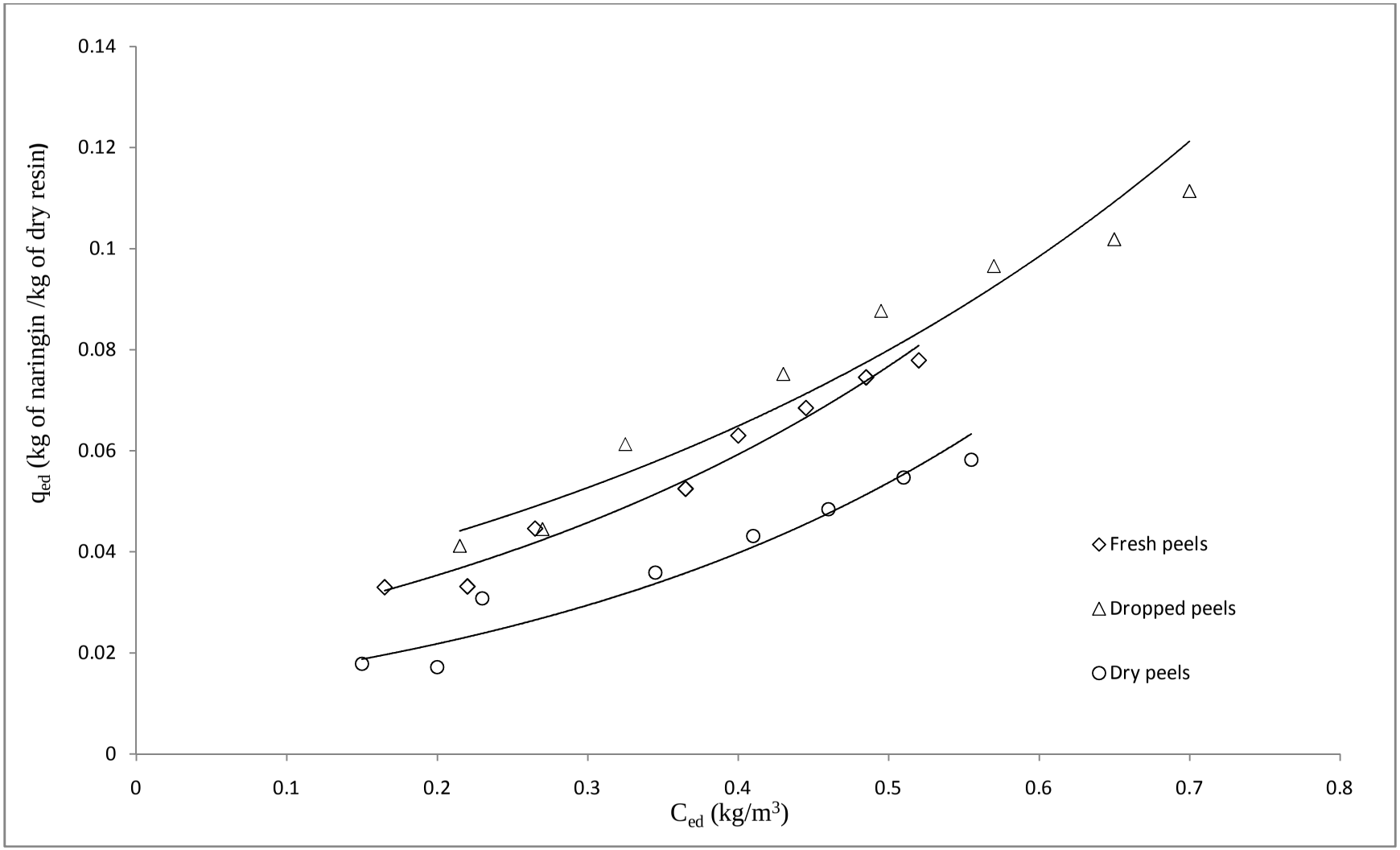

Figure 5.118: Desorption of naringin from naringin saturated resin PA-800 to ethanol: a comparison of equilibrium data (fresh, dropped and dry peels) of systems 2, 4, and 6

(b) Comparison of resins PA-500 and PA-800 with fresh, dropped, dry peels

The equilibrium desorption curves of system 1 with 2 (fresh peels with PA-500 and 800), system 3 with 4 (dropped peels with PA-500 and 800), and system 5 with 6 (dry peels withPA-500 and PA-800) have compared in Figures 5.119 to 5.121 respectively. It is observed that the naringin desorption into ethanol from resin PA-800 is higher than from resin PA-500 with all the three peels. The reason may be the higher amount of adsorbed naringin on PA-800 and higher specific surface area.

Summary of comparison of desorption equilibrium studies for all systems

The desorption of naringin from resins PA-500 and PA-800 into ethanol with different peels and also from regenerated resins PA-500 and PA-800 with fresh peels is in the order

Dropped peels with PA-800 (system 4) > Dropped peels with PA-500 (system 3) > Fresh peels with PA-800 (system 2) > Fresh peels with PA-500 (system 1) > Dry peels with PA 500 (system 5) > Dry peels with PA-800 (system 6) > Fresh peels with regenerated resin PA-800 (system 8) > Fresh peels with regenerated resin PA-500 (system 7)

5. Desorption kinetic studies

(a) Comparison of different peels with resin PA-500 and PA-800

The desorption kinetic data of systems 1, 3 and 5 have been compared in Figure 5.122. Desorption rate for dropped peels is fastest; this is in the order

Dropped peels > Fresh peels > Dry peels.

Although the initial content of naringin in the resin PA-500 samples are different since these have been obtained from adsorption column from KPBW of three peels; also KPBW is a multi-component system. Therefore comparison has limited validity.

The desorption kinetic data of systems 2, 4 and 6 have been compared in Figure 5.123. The observations with PA-800 were similar to as found with PA-500.

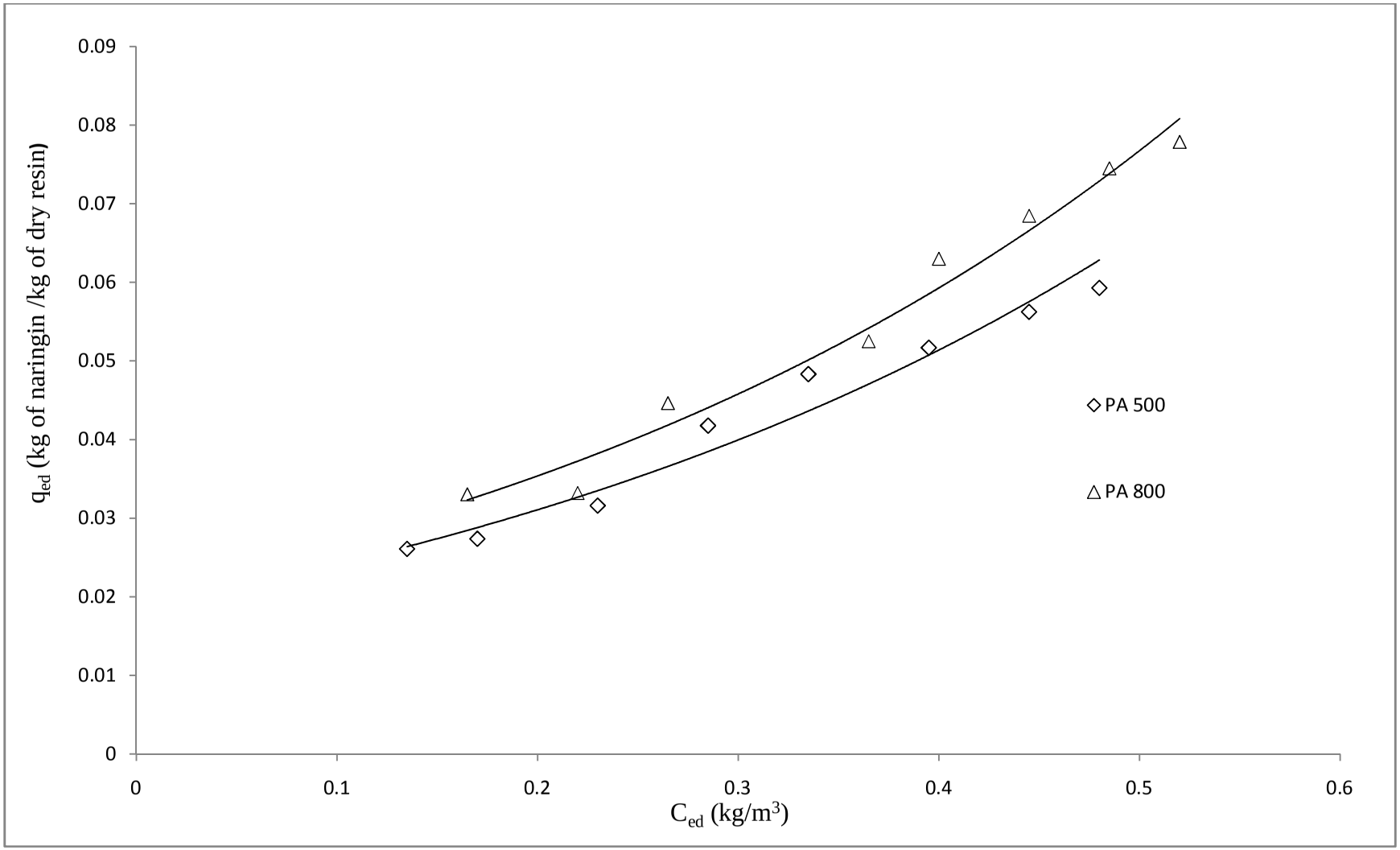

Figure 5.119: Desorption of naringin from naringin saturated resin PA-500 and PA-800 to ethanol: a comparison of equilibrium data (fresh peels) of system 1 with 2

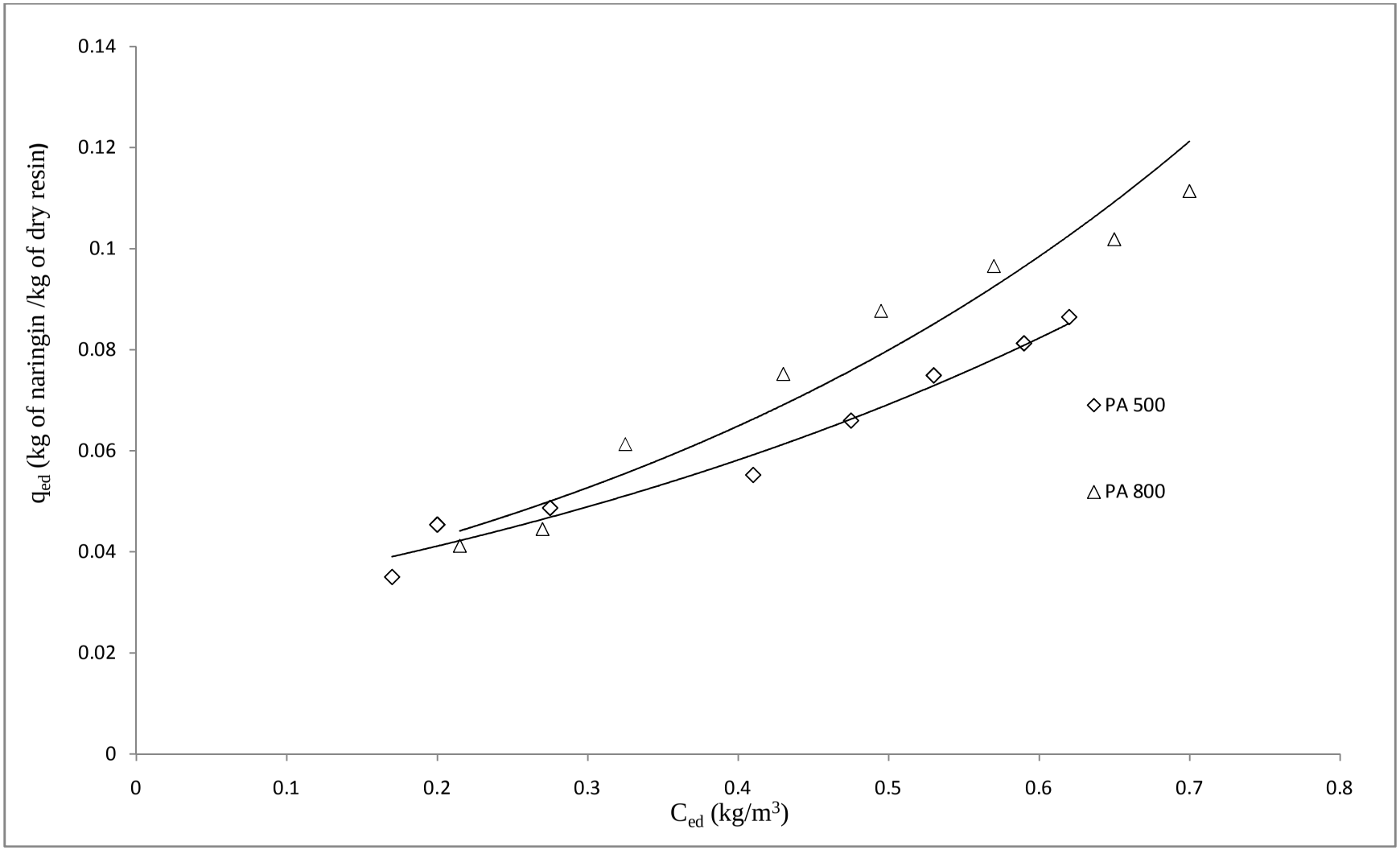

Figure 5.120: Desorption of naringin from naringin saturated resin PA-500 and PA-800 to ethanol: a comparison of equilibrium data (dropped peels) of system 3 with 4

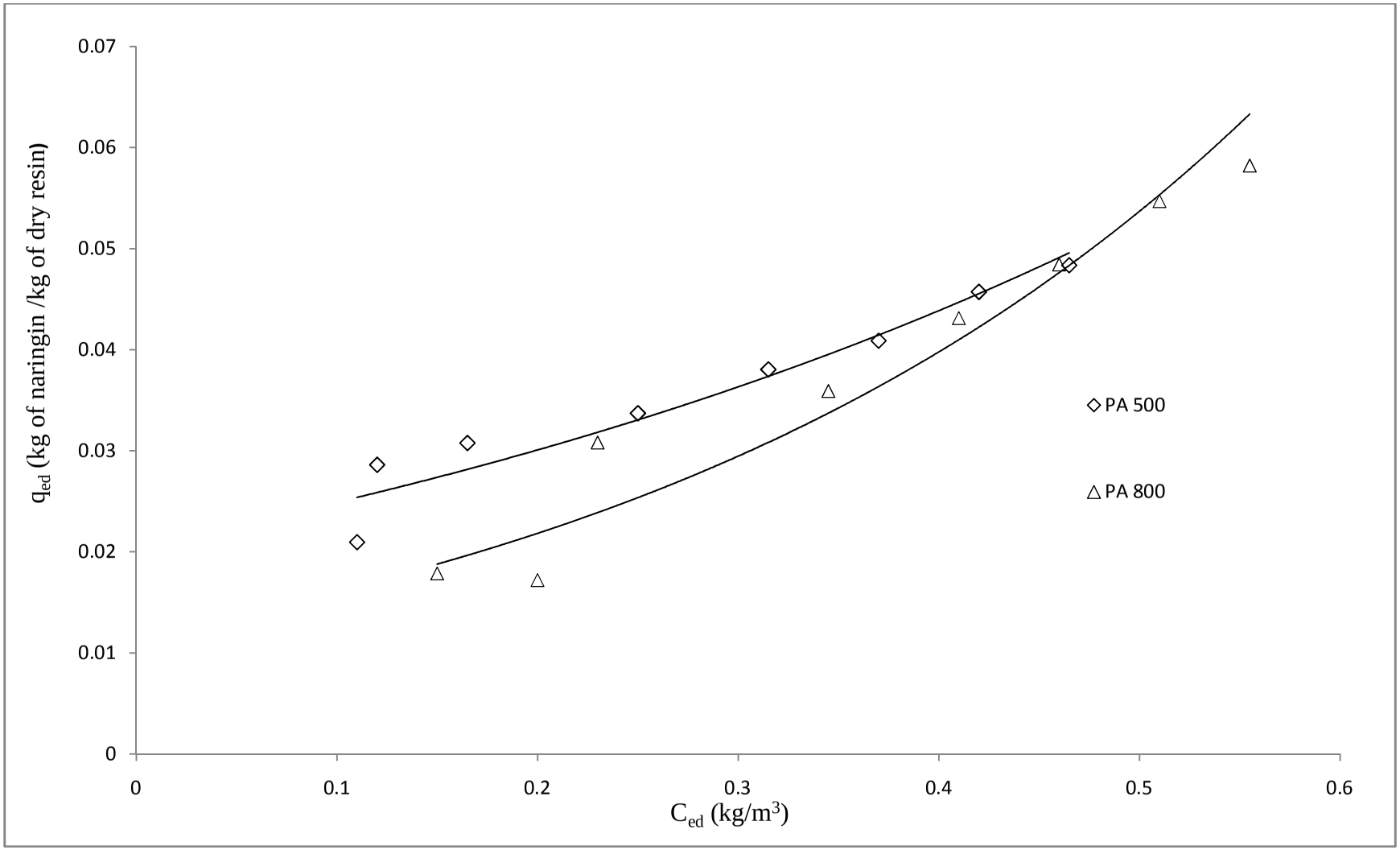

Figure 5.121: Desorption of naringin from naringin saturated resin PA-500 and PA-800 to ethanol: a comparison of equilibrium data (dry peels) of system 5 with 6

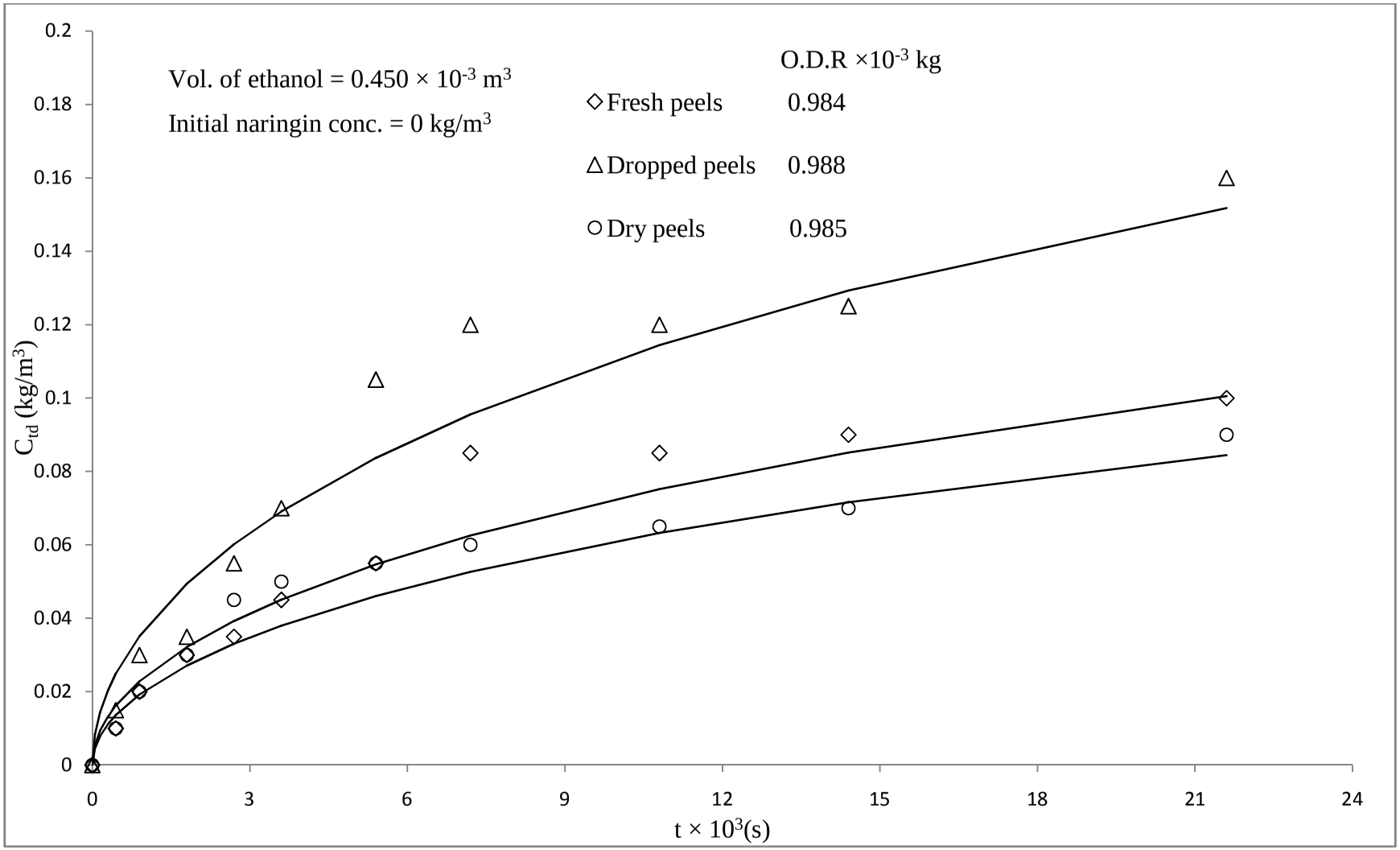

Figure 5.122: Desorption of naringin from naringin saturated resin PA-500 into ethanol: a comparison of kinetic data (fresh, dropped and dry peels) C_{td} *vs.* t of systems 1, 3, and 5

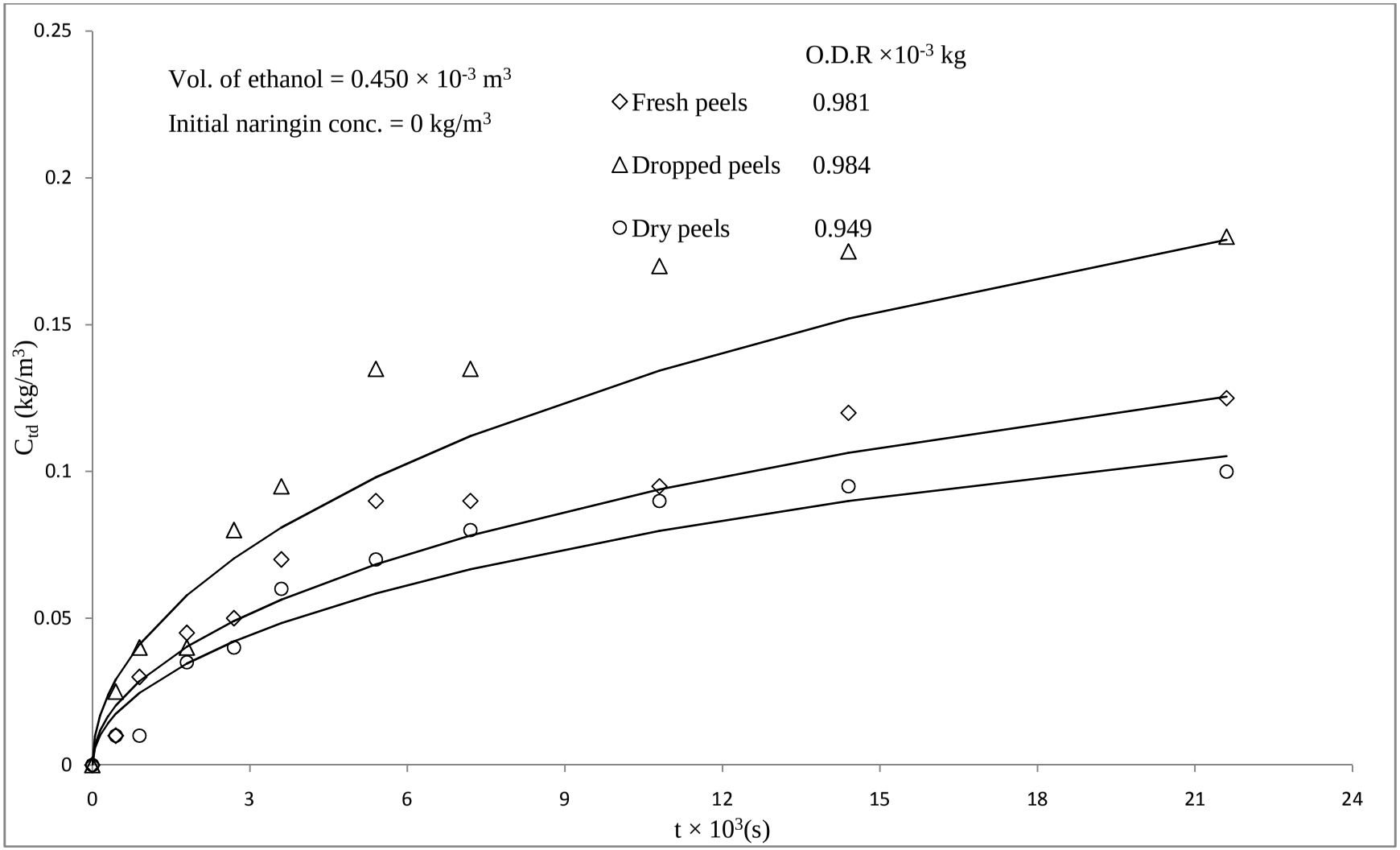

Figure 5.123: Desorption of naringin from naringin saturated resin PA-800 to ethanol: a comparison of kinetic data (fresh, dropped and dry peels) C_{td} *vs.* t of systems 2, 4, and 6

(b) Comparison of resins PA-500 and PA-800 with fresh, dropped, dry peels

The desorption kinetics data of system 1 with 2 (fresh peels with PA-500 and 800), system 3 with 4 (dropped peels with PA-500 and 800), and system 5 with 6 (dry peels withPA-500 and PA-800) have been compared in Figures 5.124 to 5.126 respectively. It was observed that the rate of desorption of naringin from resin PA-800 is faster when compared to resin PA-500 for all the three (fresh, dropped, and dry) peels. The observations may be due to the higher specific surface area for adsorption and availability of more amount of naringin per unit mass in PA-800.

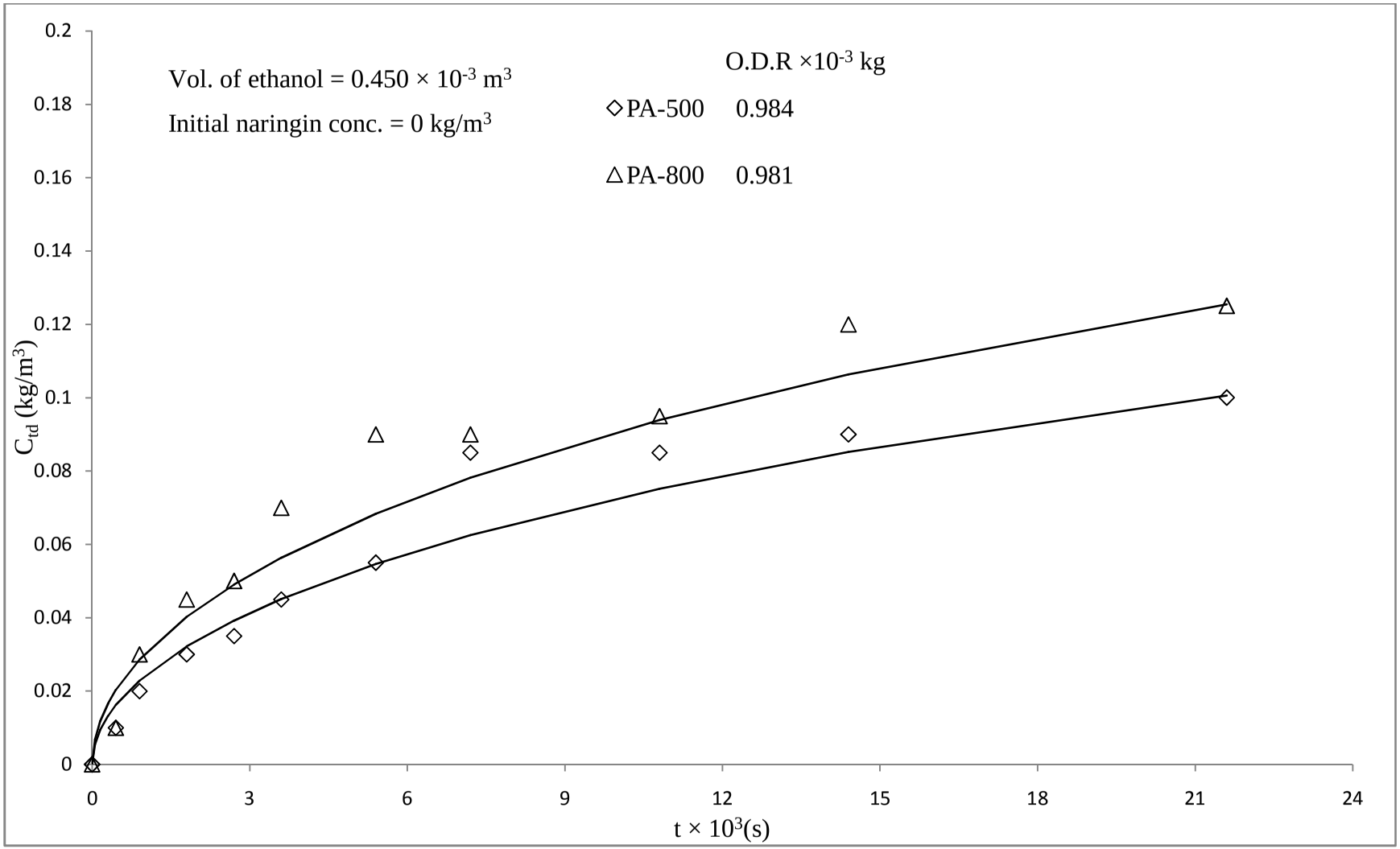

Figure 5.124: Desorption of naringin from naringin saturated resin PA-500 and PA-800 to ethanol: a comparison of kinetic data (fresh peels)

C_{td} *vs.* t of system 1 with 2

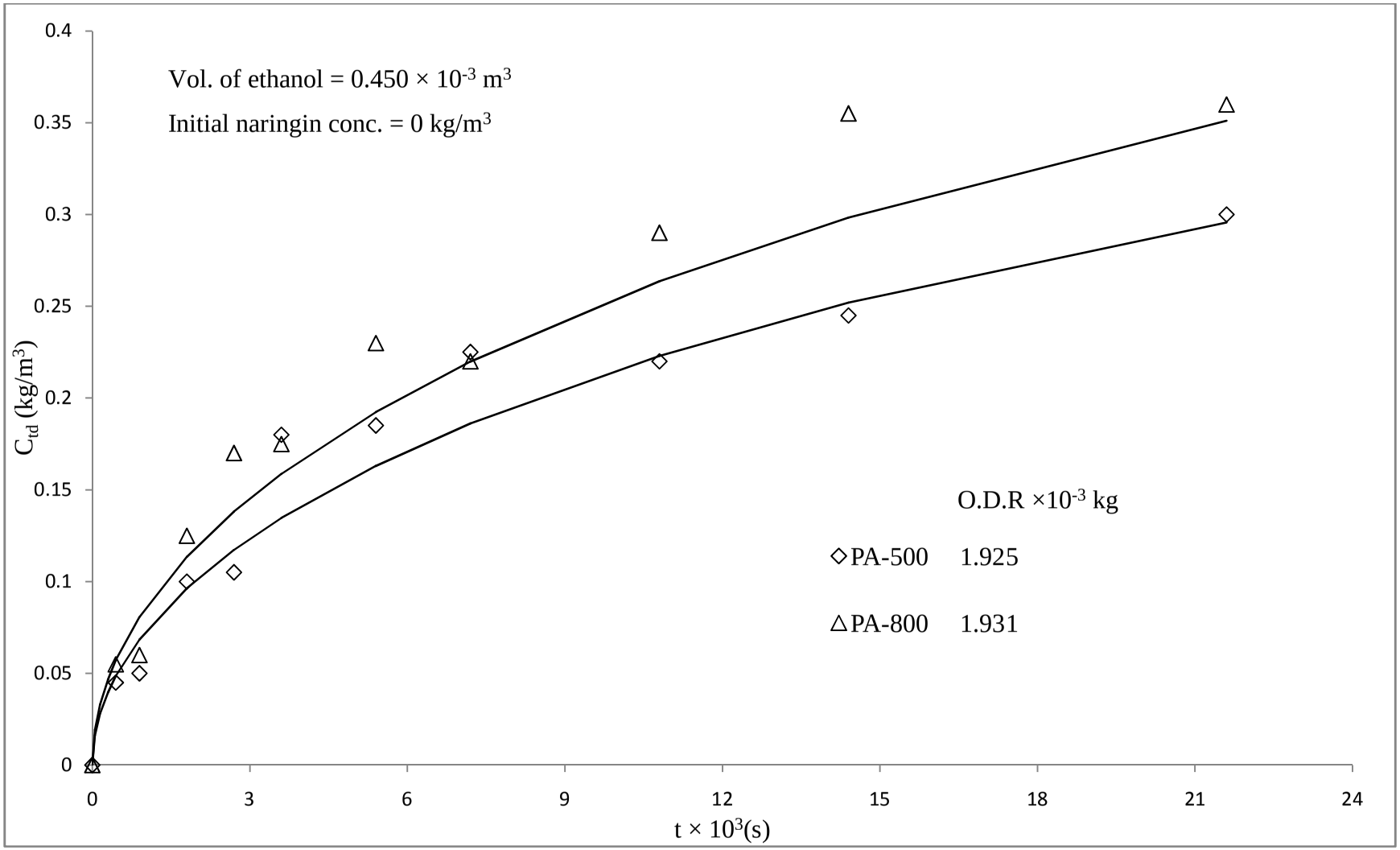

Figure 5.125: Desorption of naringin from naringin saturated resin PA-500 and PA-800 to ethanol: a comparison of kinetic data (dropped peels)

C_{td} *vs.* t of system 3 with 4

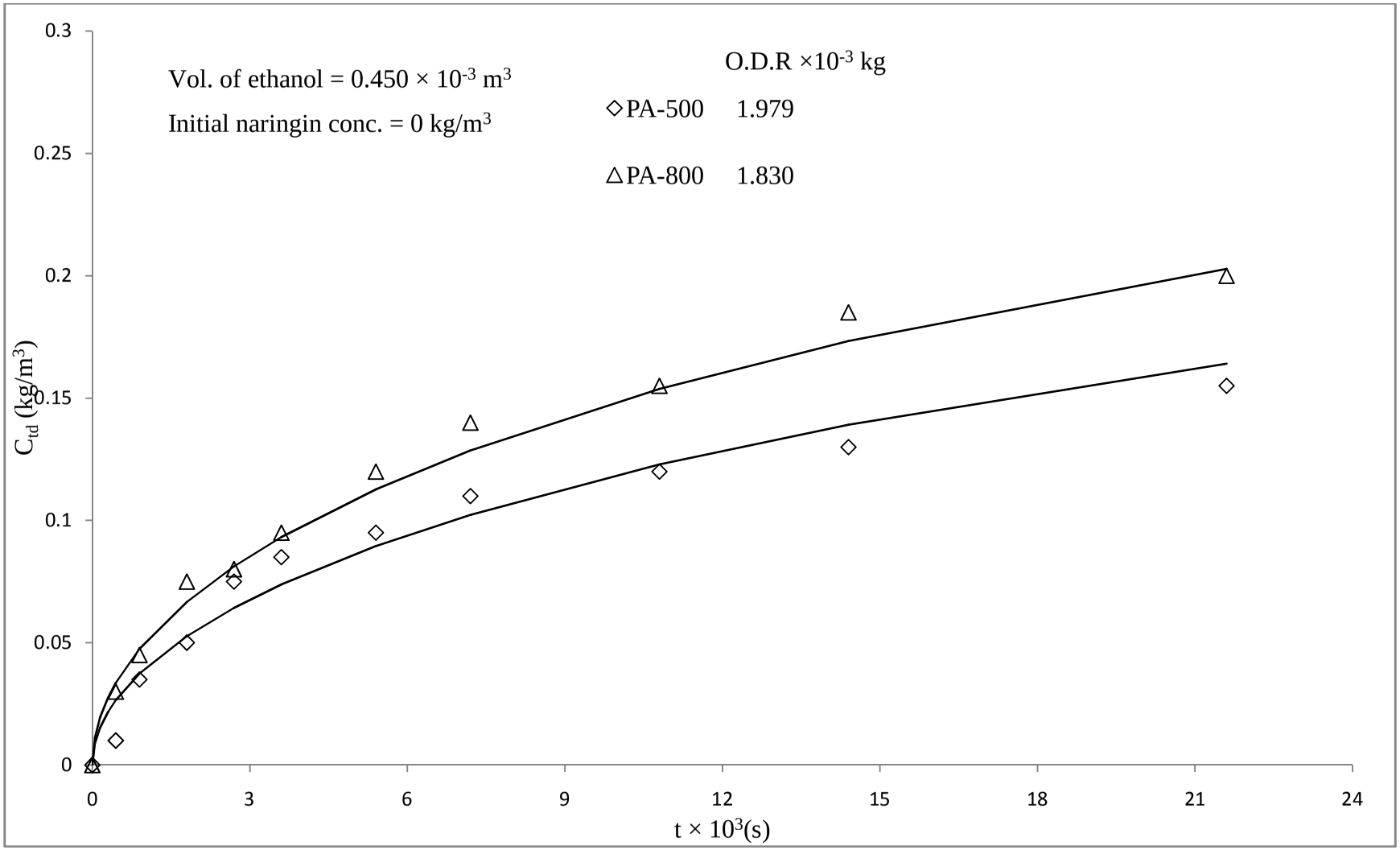

Figure 5.126: Desorption of naringin from naringin saturated resin PA-500 and PA-800 to ethanol: a comparison of kinetic data (dry peels)

C_{td} *vs.* t of system 5 with 6

6. Desorption fixed bed column studies

(a) Comparison of different peels with resin PA-500 and PA-800

The column desorption curves of systems 1, 3 and 5 (resin PA-500 with fresh, dropped, and dry peels) have been compared in Figure 5.127. Although the initial content of naringin in the resin PA-500 is different in the three cases; therefore comparison has limited validity. From the Figure 5.127, it was observed that the naringin desorption into ethanol from resin PA-500 is fastest with dropped peels followed by fresh and dry peels.

The column desorption curves of PA-800 with fresh, dropped, and dry peels have been compared in Figure 5.128. The observations are similar to as finding with resin PA-500 mentioned in preceding paragraph.

(b) Comparison of resins PA-500 and PA-800 with fresh, dropped, dry peels

The column desorption curves of system 1 with 2 (fresh peels with PA-500 and 800), system 3 with 4 (dropped peels with PA-500 and 800), and system 5 with 6 (dry peels with PA-500 and PA-800) have been compared in Figures 5.129 to 5.131 respectively. In all the three cases of peels, it is observed that the naringin desorption into ethanol from resin PA-800 is higher than with PA-500. The naringin adsorption on the resin PA-800 was more when compared to PA-500, i.e., more naringin concentration in solid phase also PA-800 has the higher specific surface area, these are possible reasons that desorption of naringin from PA-800 is more.

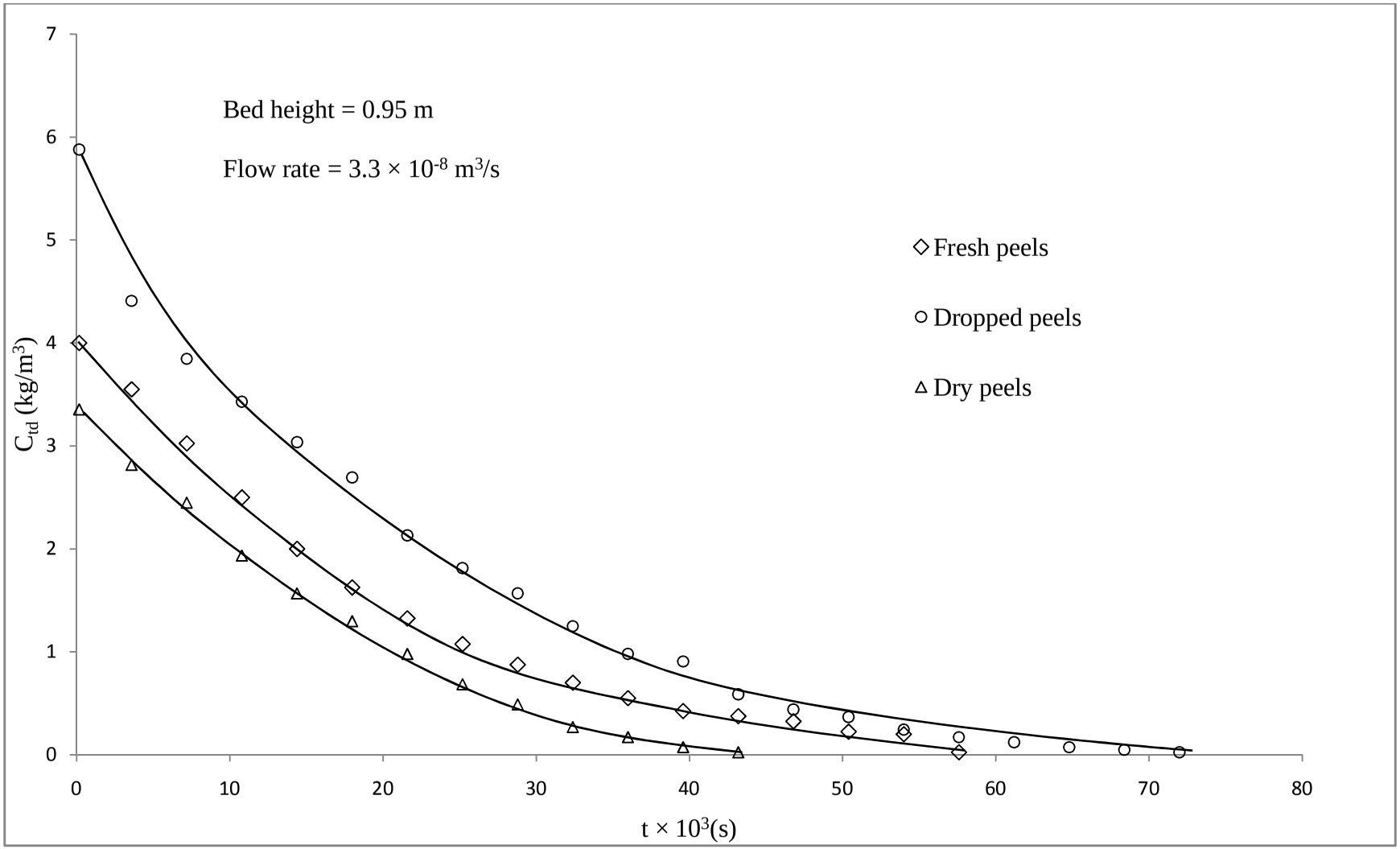

Figure 5.127: Desorption of naringin from naringin saturated resin PA-500 into ethanol: a comparison of column data (fresh, dropped, and dry peels) of systems 1, 3, and 5

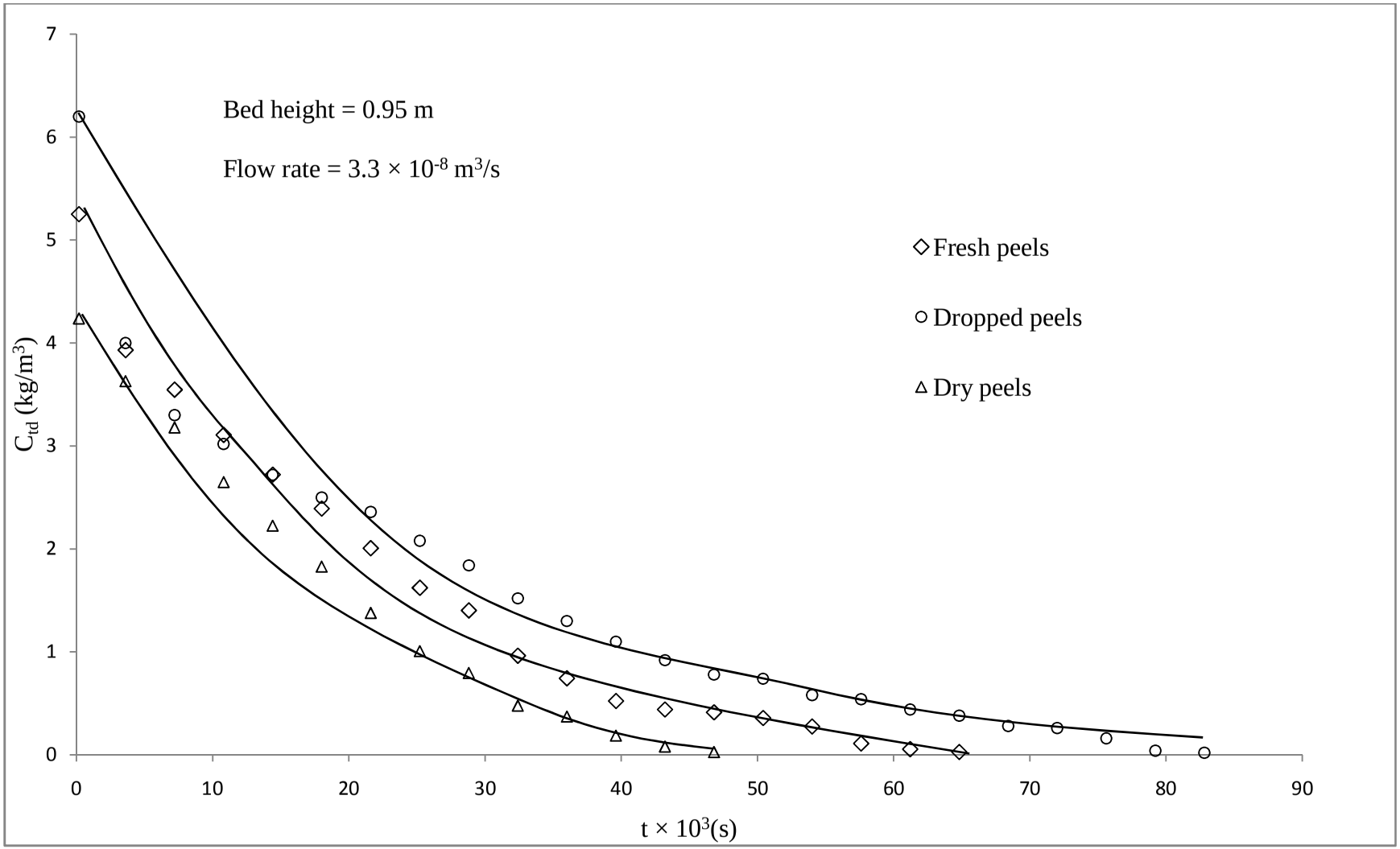

Figure 5.128: Desorption of naringin from naringin saturated resin PA-800 into ethanol: a comparison of column data (fresh, dropped, and dry peels) of systems 2, 4, and 6

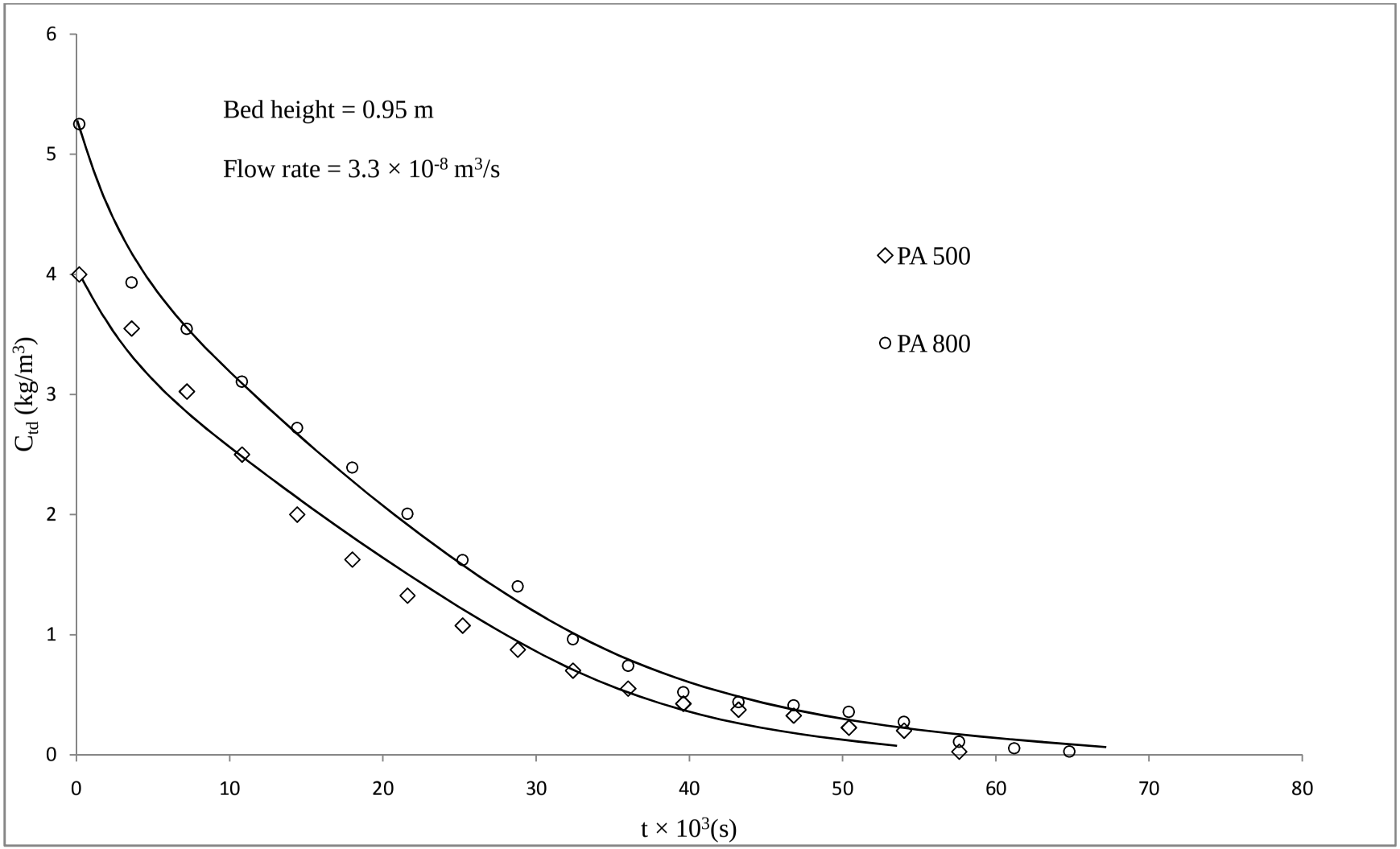

Figure 5.129: Desorption of naringin from naringin saturated resin PA-500 and PA-800 to ethanol: a comparison of column data (fresh peels) of system 1 with 2

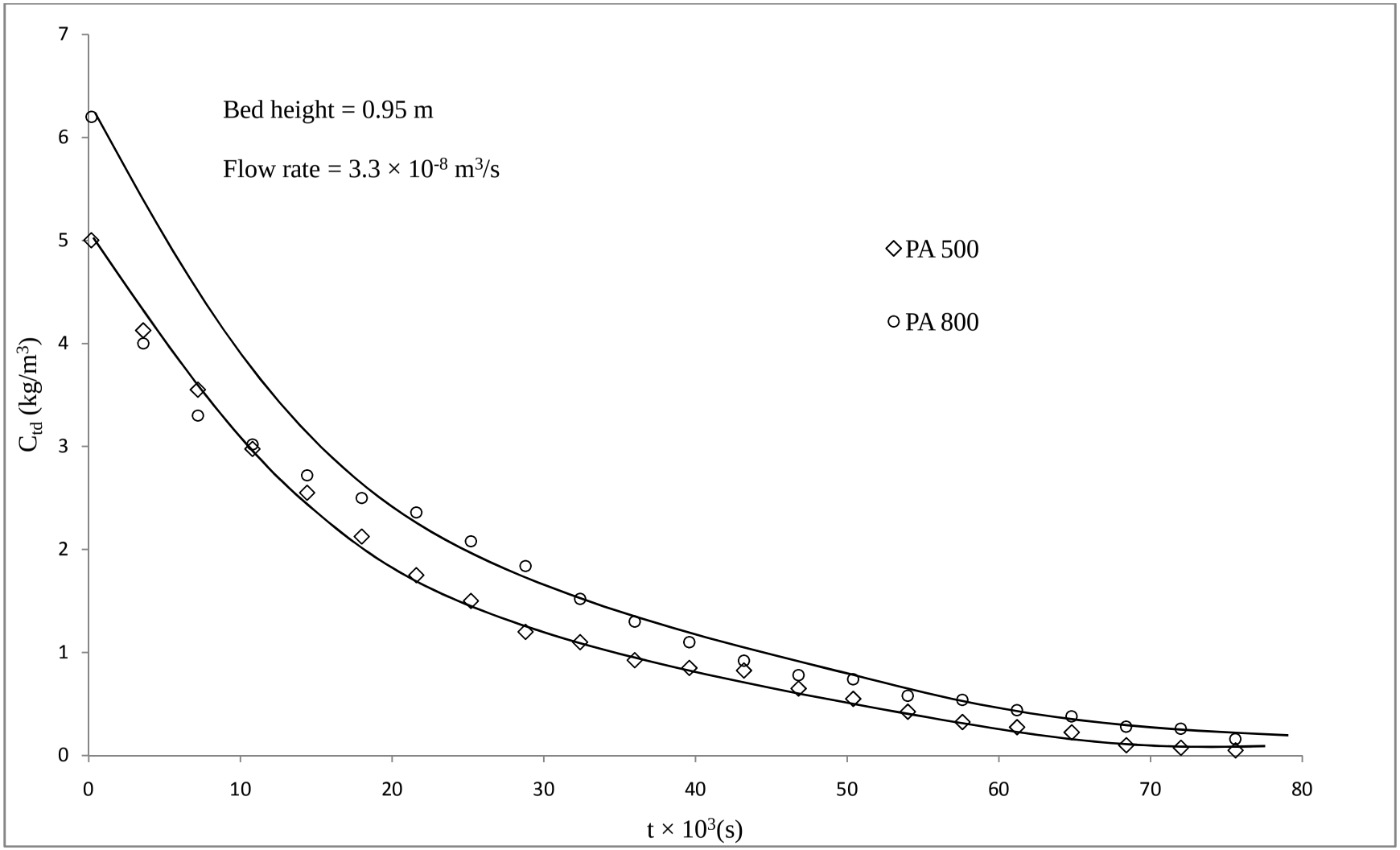

Figure 5.130: Desorption of naringin from naringin saturated resin PA-500 and PA-800 to ethanol: a comparison of column data (dropped peels) of system 3 with 4

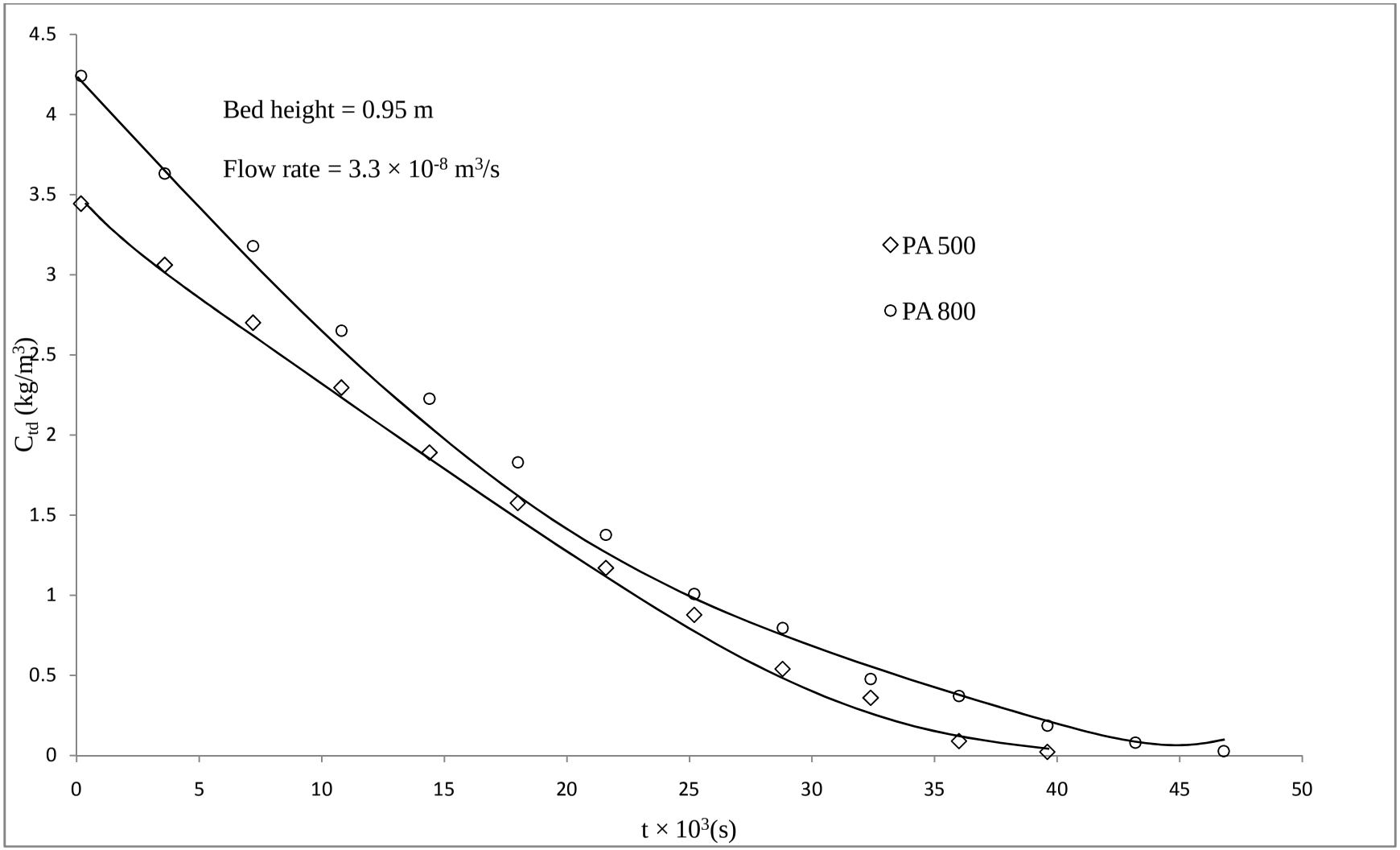

Figure 5.131: Desorption of naringin from naringin saturated resin PA-500 and PA-800 to ethanol: a comparison of column data (dry peels) of system 5 with 6

7. Recovery of naringin:

Recovery and purity of naringin are tabulated along with the values reported in the literature for recovery and purity of naringin from different citrus fruit peels and different methods in Table 5.75. Though the recovery is lesser than that obtained by using more sophisticated processes such as Ultrasonic or SC-CO_2 extraction, however, due to high purity of the product obtained, the simple adsorption-desorption method studied in the present work may be preferred due to lesser initial costs involved than that in these processes. High-quality naringin was achieved in this process which can be used as raw material for preparation of the sweetener (when naringin was treated with potassium hydroxide, it became a dihydrochalcone which was roughly 300-1800 times sweeter than sugar at threshold concentrations). The present adsorbent an Indigenous Resin is cheap relative to XAD-16, and it may be feasible to use the process even at small scale.

The FTIR was carried out to understand the impurities in pure naringin and presented in Fig. 5.132. Naringin has formula $C_{27}H_{32}O_{14}$ with different groups (side chain (CH_3, CH_2), In ring (C, CH, CH_2, Phenol) Non ring (-O, Ring -O- Ring, Ring >C=O, -OH alcohol).
FTIR spectra of naringin sample have characteristic peaks at 3385, 2913, 1631, 1373, 1204, 1061, 820.6 and 633.6 cm^{-1} corresponding to (O–H stretch, H–bonded), C–H stretch, N–H bend, C–H rock, C–O stretch, C–N stretch, C–Cl stretch, and –C≡C–H: C–H bend respectively. The presence of N-H bend corresponds to amines showing presence of protein. The presence of C-Cl stretch O-H stretch corresponds to hydrochloric acids and alcohols, phenols. The C-O stretch corresponds to alcohols, carboxylic acids, esters, and ethers. This indicated the presence of impurities such as limonin, pigments, proteins, citric acid, ethanol, etc. in naringin.

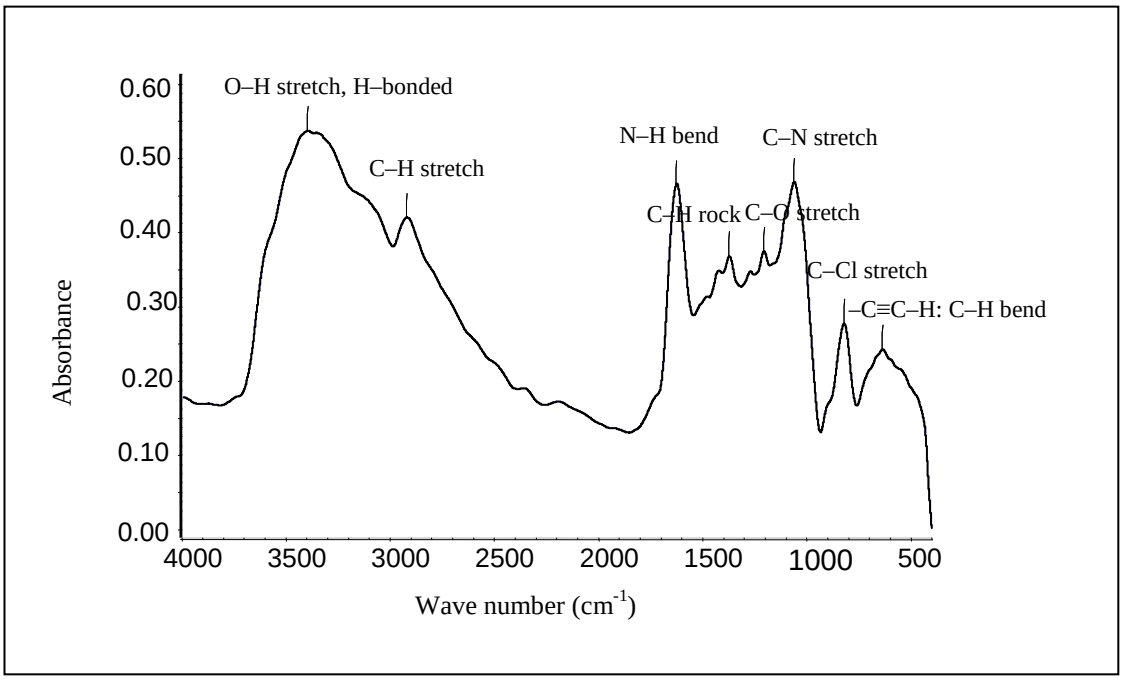

Figure 132: FTIR analysis of Naringin

8. Recovery of pectin:

The obtained pectin is a light brown powder solid. The yield of the pectin in the present study was 0.7 to 1.2 g/kg of wet peels. Recovery of pectin based on available in KPBW was 51-63%. The obtained pectin contained 60-72.5% anhydrouronic acid. Anhydrouronic acid content is reported 79.2% with Citrus depressa by Tamaki *et al.* (2008), 26.6% with citrus *unshiu* (Kara Mandarin) by Kurita *et al*. (2008), 74.2-88.5%, with Guanxi honey pomelo peel by Xiao-feng *et al*. (2011).

The methoxyl content was found to be 6-8%. Therefore pectin is a higher ester pectin (Kimball, 1991). The ash content in pectin was found in the range of 6-9%, and moisture content was 7-10%.

The degree of esterification (DE) was found to be 45-60%, whereas it was 54.23% when pectin was extracted from kinnow peels with HCl acid extraction by Singh and Dhillon (2007). \

As per the specifications of commercial pectin, the values of Anhydrouronic acid content ≥ 70%, DE for higher ester pectin ≥ 50%, total ash content ≤ 10%, loss on drying ≤ 12%

(Kimball, 1991). The values in pectin obtained are comparable with standard commercial pectin.

Table 5.75: Recovery and purity of Naringin in different methods with different fruits reported in literature

S.No	Name of the peel		Method of extraction	Recovery	Purity	Reference
1	Kinnow (*Citrus reticulata Blanco*) peels	Fresh	Adsorption followed by desorption	48-50%	92%	Present study
		Dropped		51-54%	92%	
		Dry		44-46%	93%	
2	Grapefruit (*Citrus paradisi Macf*.) seeds		$SC\text{-}CO_2$ extraction	0.2 mg/g	--	Yu et al. (2007)
3	*Citrus junos* peels		$SC\text{-}CO_2$ extraction	50-60%	--	Suetsugu et al. (2013)
4	*Citrus paradise* peel		$SC\text{-}CO_2$ extraction	14.2 %	--	Giannuzzo et al. (2003)
5	Bergamot peel		Solvent extraction	1.66 - 3.80 %	95%	Tripodo et al. (2007)
6	Pomelo (*Citrus grandis*) peel		Solvent extraction	2-3%	98%	Sudto et al. (2009)
7	*Citrus grandis* Tomentosa peels		Ultrasonic extraction	82%	--	Kong et al. (2013)
8	Pomelo peel		Ultrasonic extraction	--	78%	Tang et al (2011)
9	Bergamot peels		Adsorption followed by desorption	93%		Calvarano et al (1996)
10	Shaddock peels		Adsorption followed by desorption	--	--	Jiang et al. (2006)

Discussion of naringin adsorption from KPBW and desorption into ethanol:

Adsorption equilibrium studies

The equilibrium behavior of adsorption of naringin on the resins PA-500 and PA-800 from KPBW obtained from all the three type of peels also on regenerated reins PA-500 and PA-800 from fresh peels i.e., all the systems (1 to 8) could be described satisfactorily by the Langmuir adsorption isotherm. The mean free energy of adsorption was estimated using the Dubinin–Radushkevich isotherm constants and was in the range of 2-4 (kJ mol^{-1}) signifying the occurrence of physical adsorption (Barkakati *et al.* 2010), which is true in our case as adsorption is on the neutral resin.

The equilibrium data for naringin adsorbed on resins PA-500 and PA-800 are compared. It is observed that the amount of naringin adsorbed on the resin PA-800 is more compared to PA-500; it is attributed to the resin PA-800 having more surface area compared to PA-500. The equilibrium data of PA-500 and PA-800 for different years are compared. It is observed that the equilibrium data are very close to each other the variation is due to composition changes. It appears that adsorption equilibrium is not significantly affected by the concentration of naringin in KPBW.

Naringin adsorbed by the unit mass of adsorbent at fixed equilibrium concentration in KPBW in below Table 5.76.

Table 5.76: Values of q_e at fixed C_e for all systems (1 to 8)

System, C_e kg/m^3	1	2	3	4	5	6	7	8
0.200	0.0324	0.0506	0.0514	0.0693	0.0359	0.0406	0.0258	0.0292
0.300	0.0435	0.0636	0.0658	0.0865	0.0451	0.0514	0.0345	0.0394

For a given concentration of naringin in KPBW (solution) C_e, the amounts of naringin in adsorbent q_e for different systems are in the order

Dropped peels with PA-800 (system 4) > Dropped peels with PA-500 (system 3) > Fresh peels with PA-800 (system 2) > Dry peels with PA-800 (system 6) > Fresh peels with PA 500 (system 1) > Dry peels with PA-500 (system 5) > Fresh peels with regenerated resin PA-800 (system 8) > Fresh peels with regenerated resin PA-500 (system 7)

The representative correlating equations for equilibrium are summarized in below in Table 5.77.

Table 5.77: Representative correlating equations for Adsorption equilibrium for all systems (1 to 8)

S.No	System No	Name of the system	Correlating equation
1	1	Fresh peels with resin PA-500	$q_e = \frac{0.211C_e}{1 + 1.528C_e}$
2	2	Fresh peels with resin PA-800	$q_e = \frac{0.411C_e}{1 + 3.135C_e}$
3	3	Dropped peels with resin PA-500	$q_e = \frac{0.392C_e}{1 + 2.630C_e}$
4	4	Dropped peels with resin PA-800	$q_e = \frac{0.584C_e}{1 + 3.423C_e}$
5	5	Dry peels with resin PA-500	$q_e = \frac{0.294C_e}{1 + 3.193C_e}$
6	6	Dry peels with resin PA-800	$q_e = \frac{0.320C_e}{1 + 2.898C_e}$
7	7	Fresh peels with regenerated resin PA-500	$q_e = \frac{0.170C_e}{1 + 1.603C_e}$
8	8	Fresh peels with regenerated resin PA-800	$q_e = \frac{0.118C_e}{1 + 1.452C_e}$

Adsorption Kinetic studies:

The kinetic data for adsorption of naringin for all the systems studied could be correlated satisfactorily in terms of modified adsorption shell model; however, during the early period, the model predicts slightly lower take up of naringin as compared to the experimental values. From the correlating procedure one can predict concentration history of naringin change with time from initial conditions viz the concentration of solution, the ratio of the amount of adsorbent to the volume of solution and adsorption equilibrium correlation, without further experimentation. This is useful to determine optimal time of contact required for adsorption design calculations in a batch or column. The representative values of modified adsorption shell model parameters ψ and D_c / r_c^2 for all systems (1 to 8) are summarized below in Table 5.78.

Table 5.78: Representative modified adsorption shell model parameters ψ and D_c / r_c^2 for all systems (1 to 8)

System	No. of experiment	Representative value of ψ	D_c / r_c^2 ($\times 10^{-4}$) s^{-1}
1	12	1.57	2.46
2	12	3.44	3.32
3	8	1.73	2.71
4	7	8.89	8.50
5	8	2.55	3.99
6	8	6.05	5.78
7	3	0.79	1.24
8	4	2.48	2.37

Fixed bed adsorption column studies

Variations of parameters were investigated as adsorbent bed height and feed flow rate to evaluate adsorption capacity, H_{UNB} and MTZ of the column. It was found that the maximum amount of naringin was achieved at a flow rate of 3.3×10^{-8} m^3/s and bed height 1.20 m

The representative values of the parameter at the above flow rate and height are summarized in below in Table 5.79.

Table 5.79: Representative values of fixed bed column parameters for all systems (1 to 8)

System	$t_b \times 10^3$ (s)	$t_t \times 10^3$ (s)	q_{total} g	q_s kg/kg	H_{UNB} (m)	MTZ (m)
1	64.0	161.8	4.20	0.076	0.72	0.73
2	72.0	157.5	3.93	0.088	0.65	0.67
3	93.6	185.5	5.78	0.104	0.59	0.61
4	118.8	215.1	6.70	0.124	0.53	0.54
5	49.6	127.9	2.77	0.060	0.73	0.77
6	57.6	136.1	3.68	0.071	0.69	0.72
7	43.2	129.9	3.46	0.058	0.80	0.84
8	50.4	140.2	3.74	0.065	0.76	0.80

Desorption of naringin in ethanol:

Equilibrium studies: Naringin retained at equilibrium in adsorbent q_{ed} and concentrations in ethanol C_{ed} are compared at fix value of C_{ed} are given below in Table 5.80.

Table 5.80: Value of q_{ed} at fixed C_{ed} for all systems (1 to 8)

System C_{ed} kg/m^3	1	2	3	4	5	6	7	8
0.200	0.0319	0.0348	0.0405	0.0378	0.0317	0.0219	0.0202	0.019
0.300	0.0425	0.0486	0.0519	0.0539	0.0383	0.0323	0.0314	0.032

It may be noted that lesser value of q_{ed} for same C_{ed}, corresponds to more desorption.

The values of q_{ed} found in the following order

Dropped peels with PA-800 (system 4) > Dropped peels with PA-500 (system 3) > Fresh peels with PA-800 (system 2) > Fresh peels with PA-500 (system 1) > Dry peels with PA 500 (system 5) > Dry peels with PA-800 (system 6) > Fresh peels with regenerated resin PA-800 (system 8) > Fresh peels with regenerated resin PA-500 (system 7)

Kinetic studies: The kinetic data were correlated by Boyd's diffusivity model (Boyd *et al.* 1947) equation. The values of the parameter (Boyd's effective diffusivity) for all systems are summarized in Table 5.81 given below.

Table 5.81: Representative values of Boyd's effective diffusivity for all systems (1 to 8)

System	No. of experiments	Representative value of $D_{ed} \times 10^{-13}$ ($m^2 s^{-1}$)
1	9	9.75
2	9	9.99
3	6	11.4
4	6	10.6
5	6	10.1
6	6	12.5
7	3	13.7
8	3	12.3

Conclusions:

The aim of the present study was to recover naringin and pectin from fresh, dropped, dry kinnow peels for their valorization and value addition. In the present, study naringin could be recovered with sufficient purity from peels. The pectin was also recovered with sufficient purity by precipitating it from outgoing solution of naringin adsorption column as a by-product.

Naringin adsorption from KPBW equilibrium, kinetic and column studies data has been obtained and correlated. Naringin elution in ethanol from naringin saturated resin equilibrium, kinetic and column studied data has been collected and correlated. Thus, the useful data required for scale-up of the process for recovery of naringin followed by pectin has been collated.

Summary of products obtained from 1 kg peel:

The naringin and pectin obtained from 1 kg of kinnow peels (wet basis) are

S.No	Type of peel	g Naringin/kg of peel		g Pectin/kg of peel	
		PA-500	PA-800	PA-500	PA-800
1	Fresh	3.0	3.1	1.1	1.10
2	Dropped	3.7	3.9	0.6	0.66
3	Dry	1.8	2.0	0.7	0.91

The present study is the first of its kind for recovery of both naringin and pectin from kinnow peels. By the recovery of naringin and pectin from kinnow peels, it may solve the environmental waste problems as well as add value to citrus fruit waste and benefit kinnow growers and the country as well. The process described in the thesis can be used for scaling

up of the process to a pilot scale or commercial level thereby making the process more cost effective.

Possible sources of errors in handling of data of adsorption of naringin

Equilibrium studies

The q_e is calculated from C_e .The calculated q_e will be higher with lower value of C_e and will be lower for the higher value of C_e , thus deviating from real value. The percentage error will be depending on the value of C_o and C_e . The maximum error in the term $(C_o - C_e)$ may occur is 20 ppm.

Kinetic studies

The value of q_t calculated will be affected in a similar fashion as discussed in equilibrium studies. The reason is $(C_o - C_t)$ term, in which an error of 20 ppm may occur and may affect adversely results especially with a lower initial concentration of naringin.